Effect of cigarette smoke extract and hypoxia on vasoactive gene expression and mediator release in human pulmonary artery smooth muscle and endothelial cells

Abdullah Abdulghani M Alqarni MSRT, RRT, RRT-NPS

Supervisors: Prof. Linhua Pang and Prof. Alan Knox

Division of Respiratory Medicine

Thesis submitted to the University of Nottingham for the degree of Doctor of Philosophy in Respiratory Medicine

School of Medicine

The University of Nottingham
March 2020

Acknowledgements

I would like to take this opportunity to thank several individuals who contributed in some way to the work described in this thesis.

I express my deepest gratitude to my primary supervisor, Professor Linhua Pang, for allowing me to grow as a research scientist in his group. In addition to the weekly supervisory meetings, the door to Professor Linhua Pang's office was always open whenever I had a question about my research project or writing. This PhD thesis would not have been completed without his endless guidance, support, and assistance. I am very thankful for his helpful advice and constant encouragement in the last four years. My sincerest gratitude also goes to Professor Alan Knox, my secondary supervisor, for all the educational and insightful weekly divisional meetings and for his support and encouragement.

I would also like to thank everyone in the division of respiratory medicine at Nottingham University Hospital NHS Trust - City Campus. My special thanks go to Dr Oliver Brand, Dr Alice Pasini, and Ms Mazengarb Lisa for their help during my first months in the lab. In addition, I am grateful to the staff in the division of stroke for providing the hypoxia incubator. I also thank the King Abdulaziz University and Saudi cultural bureau in the UK for the support and funding, as well as for giving me the opportunity to go further in my education.

To my mother and father, thank you for always believing in me and for all the sacrifices you made to help me achieve my goals. To my wife (Ahlam) and daughter (Reema), words can not express how grateful I am for your unconditional love and support, as well as for your caring and understanding during tough times when all hope seemed lost.

Conference presentations and awards

Accepted abstracts for presentations at national and international meetings

Abdullah Alqarni, Oliver Brand, Alice Pasini, Abdulrhman Alghamdi, Wael Alshehri, Mushabbab Alahmari, Linhua Pang. Role of vasoactive mediators on cigarette smoke extract (CSE)-induced proliferation in human pulmonary artery smooth muscle cells (hPASMCs). Accepted for poster presentation at the European Respiratory Society International Congress, Madrid, Spain, 2019.

Abdulrhman Alghamdi, Amanda Tatler, **Abdullah Alqarni**, Mushabab Alahmari, Wael Alshehri, Linhua Pang. Cigarette smoke extract (CSE) reduces the anti-inflammatory effect of Fluticasone in human airway smooth muscle cells (HASMCs). Accepted for poster presentation at the European Respiratory Society International Congress, Madrid, Spain, 2019.

Wael Alshehri, A Tatler, **A Alqarni**, Mushabbab Alahmari, Abdulrhman Alghamdi, L Pang. Effect of cigarette smoke extracts (CSE) and e-cigarette vapour extracts (ECVE) on the production of cytokines and chemokines in human airway smooth muscle cells (HASMCs). Accepted for poster presentation at the European Respiratory Society International Congress, Madrid, Spain, 2019.

A Alqarni, O Brand, P Alice, M Alshehri, L Pang. Effect of electronic cigarette extraction on vasoactive gene expression in human pulmonary artery smooth muscle and endothelial cells. Accepted for oral presentation at the British Thoracic Society Winter Meeting, London, 2018.

Abdullah Alqarni, Oliver Brand, Alice Pasini, Mohammed Alshehri, Linhua Pang. Effect of e-cigarette vapour extraction on vasoactive gene expression in human pulmonary artery smooth muscle and endothelial cells. Accepted for poster presentation at the European Respiratory Society International Congress, Paris, France, 2018.

A Alqarni, O Brand, A Pasini, M Alshehri, L Pang. Cigarette smoke- and hypoxia-induced imbalanced vasoactive gene expression in human pulmonary artery endothelial and smooth muscle cells. Accepted for poster presentation at the British Thoracic Society Winter Meeting, London, 2017.

M Alshehri, O Brand, **A Alqarni**, A Pasini, L Pang. Cigarettes smoke extract induces inflammatory gene expression in human bronchial epithelial cells. Accepted for poster presentation at the British Thoracic Society Winter Meeting, London, 2017.

Mohammed Alshehri, Oliver Brand, **Abdullah Alqarni**, Alice Pasini, Linhua Pang. RAGE Partially Mediates Cigarettes Smoke Extract induced Cytokine and Chemokine Production in Human Bronchial Epithelial Cells. Accepted for poster presentation at the European Respiratory Society International Congress, Paris, France, 2018.

Mohammed Alshehri, Oliver Brand, **Abdullah Alqarni**, Alice Pasini, Linhua Pang. The Effect of Cordycepin and Simvastatin on Cigarettes Smoke Extract Induced Cytokine and Chemokine Production in Human Bronchial Epithelial Cells. Accepted for poster presentation at the European Respiratory Society International Congress, Paris, France, 2018.

Abdullah Alqarni, Oliver Brand, Alice Pasini, Linhua Pang. Cigarette smoke- and hypoxia-induced imbalanced vasoactive gene expression in human pulmonary artery smooth muscle cells. Accepted for poster presentation at the European Respiratory Society International Congress, Milan, Italy, 2017.

Awards

- The National Institute for Health Research Nottingham Biomedical Research Centre travel award winner for the European Respiratory Society International Congress, Madrid, Spain, 2019.
- The British Association for Lung Research travel award winner for the British Thoracic Society Winter Meeting, London, 2018.
- An excellence award from Royal Embassy of Saudi Arabia Cultural Bureau, 2017 and 2018.

Abbreviations

A

AA	Arachidonic acid
AChE	Acetylcholinesterase
ATS	American Thoracic Society

B

β2M	βeta-2-Microglobulin
BCA	Bicinchoninic acid
BSA	Bovine serum albumin

C

cAMP	Cyclic adenosine monophosphate
CCK-8	Cell counting kit-8
CDC	Centres for Disease Control and Prevention
cDNA	Complementary DNA
cGMP	Cyclic guanosine monophosphate
COPD	Chronic obstructive pulmonary disease
COX	Cyclooxygenase
COX-1	Cyclooxygenase-1
COX-2	Cyclooxygenase-2
cPGES	Cytosolic prostaglandin E synthase.
CS	Cigarette smoke
CSE	Cigarette smoke extract
C_T	Cycle threshold

D

DAN	2, 3-diaminonaphthalene
DMEM	Dulbecco's modified eagles medium
DMEM-	DMEM with 0.5% FBS
DMEM+	DMEM with 20% FBS
DMSO	Dimethyl sulfoxide
DNase	Deoxyribonuclease
dNTP	Deoxynucleotide triphosphate
dsDNA	Double-stranded DNA

E

E-cig	E-cigarette
ECL	Enhanced chemi-luminescence
ECVE	E-cig vapour extract
eNOS	Endothelial NOS synthase
ERS	European Respiratory Society
ET-A	Endothelin A
ET-B	Endothelin B
ET-1	Endothelin-1

F

FBS	Foetal bovine serum
FDA	Food and Drug Administration
FEV_1	Forced expiratory volume (in one second)
FVC	Forced vital capacity
FW	Forward

G

GAPDH	Glyceraldehyde-3-phosphate dehydrogenase
GOLD	Global Initiative for Chronic Obstructive Lung Disease

H

HEPES-BSS	HEPES-buffered balanced salt solution
HRP	Horseradish peroxidase

I

IC50	Half-maximal inhibitory concentration
IL-1β	Interleukin-1β
IL-6	Interleukin-6
IL-8	Interleukin-8
IL-10	Interleukin-10
iNOS	Inducible nitric oxide synthase

L

LS-ECGM	Low-serum endothelial cell growth medium

M

mPAP	Mean pulmonary artery pressure
mPGES-1	Microsomal prostaglandin E synthase-1
mPGES-2	Microsomal prostaglandin E synthase-2
mRNA	Messenger RNA
MTT	3-(4,5-dimethylthiazol-2-yl)-2,5-diphenyltetrazolium bromide

N

+/-n	With and without nicotine
NADPH	Nicotinamide adenine dinucleotide phosphate
NaOH	Sodium hydroxide
nNOS	Neuronal nitric oxide synthase

NSAIDs	Non-steroidal anti-inflammatory drugs

P

PAECs	Pulmonary artery endothelial cells
PAH	Pulmonary arterial hypertension
PAP	Pulmonary artery pressure
PARP1	Poly [ADP-ribose] polymerase 1
PASMCs	Pulmonary artery smooth muscle cells
PBS	Phosphate buffered saline
PCWP	Pulmonary capillary wedge pressure
PFT	Pulmonary function test
PGs	Prostaglandins
PGD_2	Prostaglandin D_2
PGDS	Prostaglandin D synthase
PGE_2	Prostaglandin E_2
PDE5	Phosphodiesterase 5
PGF_2	Prostaglandin F_2
PGFS	Prostaglandin F synthase
PGH_2	Prostaglandin H_2
PGI_2	Prostaglandin I_2
PGIS	Prostaglandin I synthase
PS	Phosphatidylserine
PVDF	Polyvinylidene fluoride
PVR	Pulmonary vascular resistance

R

RHC	Right heart catheterization

RIPA	Radio-immunoprecipitation assay
RT	Reverse transcription
RT-qPCR	reverse transcription-quantitative polymerase chain reaction
RV	Reverse

S

SAHA	Suberanilohydroxamic acid
SDS-PAGE	Sodium dodecyl sulphate polyacrylamide gel electrophoresis
SEM	Standard error of the mean

T

TBS-T	Tris buffered saline plus tween 20
TGF-β1	Transforming growth factor-β1
TNS	Trypsin neutralization solution
TX	Thromboxane
TXA_2	Thromboxane A_2
TXAS	Thromboxane synthase
TXB_2	Thromboxane B_2

V

VEGF	Vascular endothelial growth factor

W

WHO	World Health Organization
WST-1	Water-soluble tetrazolium-1
WST-8	Water-soluble tetrazolium-8

Abstract

Background: Pulmonary hypertension is a common and serious complication of COPD. Studies suggest that hypoxia and cigarette smoke (CS) can cause vascular remodelling in COPD as a result of cell proliferation; however, the underlying cause is not fully understood. In addition, it is suggested that the use of e-cig may lead to vascular diseases, but no data are available on what effect e-cig may have on dysfunction of pulmonary artery smooth muscle cells (PASMCs) and pulmonary artery endothelial cells (PAECs). Thus, we hypothesise that cigarette smoke extract (CSE) and hypoxia can induce imbalanced vasoactive gene expression and mediator release, and then contribute to cell proliferation and apoptosis. Furthermore, e-cig vapour extract with and without nicotine ($ECVE^{-/+n}$) may have similar effects as CSE.

Methods: Western blotting and real-time RT-PCR were used to assess the protein and mRNA expression of vasoactive genes, respectively. ELISA was used to assess the prostanoids and endothelin production. Nitric oxide levels were assessed by nitrate/nitrite assay. WST-1 and CCK-8 assays were used to assess cell proliferation.

Results: We found that CSE induced cyclooxygenase-2 (COX-2) and thromboxane synthase (TXAS) and reduced prostaglandin (PG) I synthase at mRNA levels in PASMCs and PAECs. CSE treatment reduced PGI synthase protein expression and PGI_2 production in PASMCs (but not in PAECs). Interestingly, CSE had the ability to reduce and increase microsomal prostaglandin E synthase-1 (mPGES-1) protein expression/PGE_2 production in PASMCs and PAECs, respectively. Despite the undetected TXAS protein expression, CSE increased thromboxane A_2 (TXA_2) production in both cell types, likely as a result of the increased COX-2 protein expression. Although hypoxia induced COX-2 mRNA expression in PASMCs (but in PAECs), it had no effect on the mRNA levels of PGIS and TXAS in both cell types. We also demonstrated that hypoxia induced TXA_2, PGE_2, and PGI_2 production as a result of the upregulated TXAS and COX-2 and unchanged PGIS protein expression in PASMCs. Interestingly, hypoxia had no effect on the protein expression of TXAS

and COX-2 and the production of PGI_2 and PGE_2 in PAECs, but it induced the production of TXA_2. Both CSE and hypoxia had no effect on endothelial nitric oxide synthase (eNOS) mRNA expression, but reduced eNOS protein expression/nitric oxide production in PAECs. Although hypoxia failed to affect mRNA endothelin-1 levels and endothelin production in both cell types, CSE increased mRNA endothelin-1 levels and reduced endothelin production in PAECs (but not in PASMCs). Intriguingly, hypoxia did not enhance CSE-induced effects and $ECVE^{+/-n}$ had no similar effects as CSE. The results also showed CSE-induced proliferation of both cell types and hypoxia-induced proliferation of PASMCs were inhibited by the stable PGI_2 analogue, selective COX-2 inhibitor and TXA_2 receptor antagonist and nitric oxide donor (but not by mPGES-1 inhibitor and ET-A and ET-B receptor antagonist), whereas hypoxia-induced PAEC proliferation was only reduced by nitric oxide donor. Although hypoxia failed to cause apoptosis, CSE induced apoptosis only in PAECs and this was unlikely mediated by altered release of vasoactive mediators.

Conclusion: Our results suggest that CSE (but not $ECVE^{+/-n}$) and hypoxia to a lesser extent can induce imbalanced vasoactive gene expression and mediator release; however, it is unlikely that hypoxia can further amplify CSE-induced effects. The CSE- and hypoxia-induced imbalanced release of vasoactive mediators (particularly prostanoids (e.g. TXA_2) and nitric oxide) may be critically involved in the contribution to vascular remodelling via the induction of cell proliferation. These data provide new insights into our understanding of CS- and hypoxia-induced vascular remodelling and may represent a potential therapeutic target for pulmonary hypertension in COPD.

Table of Contents

Acknowledgements ..... **I**

Conference presentations and awards ..... **II**

Abbreviations ..... **IV**

Abstract ..... **VI**

List of figures ..... **XXII**

List of tables ..... **XXXI**

1. Introduction **1**

1.1 Pulmonary hypertension 1

1.1.1 Definition and classification of pulmonary hypertension 1

1.1.2 Pulmonary hypertension in COPD 5

1.1.2.1 Clinical evaluation of pulmonary hypertension in COPD 7

1.1.2.2 Prevalence and impact 8

1.1.2.3 Treatment 10

1.2 Pathophysiology of COPD-associated pulmonary hypertension 13

1.2.1 Pulmonary vasoconstriction 15

1.2.2 Endothelial dysfunction 15

1.2.3 Pulmonary vascular remodelling 17

1.2.3.1 Role of pulmonary artery smooth muscle cells 20

1.2.3.2 Role of pulmonary artery endothelial cells 21

1.2.4 Hypoxia 23

1.2.5 Cigarette smoke 24

1.2.6 Hypoxia and cigarette smoke 24

1.2.7 Inflammation 25

1.3 Imbalanced vasoactive gene expression and mediator release in COPD-associated pulmonary hypertension 28

1.3.1 eNOS/nitric oxide 28

1.3.2 Role of prostanoids and their synthases in COPD-associated pulmonary hypertension 31

1.3.2.1 COX-2 34

1.3.2.2 mPGES-1 and PGE_2 36

1.3.2.3 PGIS and PGI_2 38

1.3.2.4 TXAS and TXA_2 42

1.3.3 Endothelin 45

1.3.4 Electronic cigarette 49

1.4 Summary 53

1.5 Hypothesis and aims 54

1.5.1 Hypothesis 54

1.5.2 Aims 54

2. Materials and methods 57

2.1 Introduction 58

2.2 Cell culture 58

2.2.1 Culture conditions 58

2.2.2 Maintenance of cultured cells 58

2.2.2.1 Pulmonary artery smooth muscle cells 58
2.2.2.2 Pulmonary artery endothelial cells.....59
2.2.3 Cell sub-culture.....59
2.2.3.1 Pulmonary artery smooth muscle cells 59
2.2.3.2 Pulmonary artery endothelial cells.....59
2.2.4 Cell counting.....60
2.2.5 Cryopreservation of cells 60
2.3 Cigarette extract preparation.....61
2.3.1 Cigarette smoke extract.....61
2.3.2 E-Cigarette vapour extract 61
2.4 Cell treatment.....62
2.4.1 CSE treatment under normoxic and hypoxic conditions 62
2.4.1.1 Pulmonary artery smooth muscle cells 62
2.4.1.2 Pulmonary artery endothelial cells.....63
2.4.2 ECVE treatment.....64
2.4.2.1 Pulmonary artery smooth muscle cells 64
2.4.2.2 Pulmonary artery endothelial cells.....64
2.4.3 Effect of drugs.....64
2.5 Drug preparation 65
2.5.1 Celecoxib 65
2.5.2 Beraprost sodium 65

2.5.3 Daltroban....65
2.5.4 PF-03549184....66
2.5.5 Sodium nitroprusside dihydrate....66
2.5.6 Bosentan hydrate....66
2.6 Cell lysate preparation....67
2.7 Bicinchoninic acid protein assay....67
2.8 Western blotting analysis....67
2.8.1 Principle....67
2.8.2 SDS-PAGE....68
2.8.3 Protein transfer....69
2.8.4 Blocking and antibody incubation....69
2.8.5 Protein detection....70
2.9 Real-time reverse transcription-quantitative polymerase chain reaction analysis....71
2.9.1 Principle....71
2.9.2 Total RNA isolation....71
2.9.3 RNA quantification....72
2.9.4 RT....73
2.9.5 Primer specificity....74
2.9.6 qPCR....74
2.10 Mediator release analysis....76
2.10.1 PGE_2....76

2.10.1.1 Assay principle....76
2.10.1.2 Method....77
2.10.2 PGI_2....78
2.10.2.1 Assay principle....78
2.10.2.2 Method....80
2.10.3 TXA_2....81
2.10.3.1 Assay principle....81
2.10.3.2 Method....82
2.10.4 Nitric oxide....83
2.10.4.1 Assay principle....83
2.10.4.2 Method....84
2.10.5 Endothelin....85
2.10.5.1 Assay principle....85
2.10.5.2 Method....85
2.11 Cell proliferation analysis....86
2.11.1 Cell proliferation reagent WST-1....87
2.11.1.1 Assay principle....87
2.11.1.2 Method....87
2.11.2 CCK-8....88
2.11.2.1 Assay principle....88
2.11.2.2 Method....88

2.12 Apoptosis analysis 89
2.12.1 Annexin v human ELISA kit 89
2.12.1.1 Assay principle 89
2.12.1.2 Method 90
2.12.2 Apoptosis western blot cocktail biomarkers 91
2.12.2.1 Assay principle 91
2.12.2.2 Method 92
2.13 Cell viability 92
2.14 Statistical analysis 93
Chapter 3. Effect of CSE on vasoactive gene expression and mediator release in human PASMCs and PAECs 94
3.1 Introduction 95
3.2 Aims 96
3.3 Materials and methods 97
3.3.1 Cigarette smoke extract preparation 97
3.3.2 Cell treatment 97
3.3.2.1 Pulmonary artery smooth muscle cells 97
3.3.2.2 Pulmonary artery endothelial cells 97
3.3.3 RT-qPCR 98
3.3.4 Western blotting 98
3.3.5 ELISA 98
3.3.6 Nitrate/nitrite assay 98

3.4 Results 99

3.4.1 Effect of CSE on the mRNA and protein expression of COX-2 and PGE_2 production in human PASMCs and PAECs 99

3.4.2 Effect of CSE on the protein expression of mPGES-1 in human PASMCs and PAECs 107

3.4.3 Effect of CSE on the mRNA and protein expression of PGIS and PGI_2 production in human PASMCs and PAECs 110

3.4.4 Effect of CSE on the mRNA and protein expression of TXAS and TXA_2 production in human PASMCs and PAECs 117

3.4.5 Effect of CSE on the PGI_2/TXA_2 ratio in human PASMCs and PAECs 124

3.4.6 Effect of CSE on the mRNA and protein expression of eNOS and nitric oxide release in human PASMCs and PAECs 126

3.4.7 Effect of CSE on the mRNA expression of endothelin-1 and production of endothelin in human PASMCs and PAECs 132

3.5 Discussion 136

3.5.1 CSE and prostanoids 138

3.5.1.1 Human pulmonary artery smooth muscle cells 138

3.5.1.2 Human pulmonary artery endothelial cells 145

3.5.2 CSE and eNOS/nitric oxide 150

3.5.3 CSE and endothelin 151

Chapter 4. Effect of hypoxia alone and in combination with CSE on vasoactive gene expression and mediator release in human PASMCs and PAECs 155

4.1 Introduction 156

4.2 Aims 156

4.3 Materials and methods 158

4.3.1 Cigarette smoke extract preparation 158

4.3.2 Cell treatment 158

4.3.2.1 Pulmonary artery smooth muscle cells 158

4.3.2.2 Pulmonary artery endothelial cells 158

4.3.3 RT-qPCR 158

4.3.4 Western blotting 159

4.3.5 ELISA 159

4.3.6 Nitrate/nitrite assay 159

4.4 Results 160

4.4.1 Effect of hypoxia alone and in combination with CSE on the mRNA and protein expression of COX-2 and PGE_2 production in human PASMCs and PAECs 160

4.4.2 Effect of hypoxia alone and in combination with CSE on the mRNA and protein expression of PGIS and PGI_2 production in human PASMCs and PAECs 168

4.4.3 Effect of hypoxia alone and in combination with CSE on the mRNA and protein expression of TXAS and TXA_2 production in human PASMCs and PAECs 175

4.4.4 Effect of hypoxia alone and in combination with CSE on the PGI_2/TXA_2 ratio in human PASMCs and PAECs 181

4.4.5 Effect of hypoxia alone and in combination with CSE on the mRNA and protein expression of eNOS and nitric oxide production in human PASMCs and PAECs 183

4.4.6 Effect of hypoxia alone and in combination with CSE on the mRNA expression of endothelin-1 and the production of endothelin in human PASMCs and PAECs 188

4.5 Discussion 192

4.5.1 Hypoxia and prostanoids 194

4.5.1.1 Human pulmonary artery smooth muscle cells 194

4.5.1.2 Human pulmonary artery endothelial cells 199

4.5.2 Hypoxia and eNOS/nitric oxide 203

4.5.3 Hypoxia and endothelin 204

Chapter 5. Effect of ECVE with and without nicotine on vasoactive gene expression and mediator release in human PASMCs and PAECs 207

5.1 Introduction 208

5.2 Aims 209

5.3 Materials and methods 210

5.3.1 ECVE preparation 210

5.3.2 Cell treatment 210

5.3.2.1 Pulmonary artery smooth muscle cells 210

5.3.2.2 Pulmonary artery endothelial cells 210

5.3.3 RT-qPCR 210

5.3.4 Western blotting 211

5.3.5 ELISA 211

5.3.6 Nitrate/nitrite assay 211

5.4 Results 212

5.4.1 Effect of $ECVE^{+/-n}$ on the mRNA and protein expression of COX-2 and PGE_2 production in human PASMCs and PAECs 212

5.4.2 Effect of $ECVE^{+/-n}$ on the mRNA and protein expression of PGIS and PGI_2 production in human PASMCs and PAECs 218

5.4.3 Effect of $ECVE^{+/-n}$ on the expression of TXAS and TXA_2 production in human PASMCs and PAECs 223

5.4.4 Effect of $ECVE^{+/-n}$ on the mRNA and protein expression of eNOS and nitric oxide production in human PAECs 226

5.4.5 Effect of $ECVE^{+/-n}$ on the mRNA expression of endothelin-1 and endothelin production in human PASMCs and PAECs 231

5.5 Discussion 234

Chapter 6. The role of the altered release of individual vasoactive mediator in CSE- and hypoxia-induced proliferation and apoptosis of human PASMCs and PAECs 241

6.1 Introduction 242

6.2 Aims 244

6.3 Materials and methods 245

6.3.1 CSE treatment under normoxic and hypoxic conditions 245

6.3.2 Effect of drugs 245

6.3.3 Cell proliferation analysis 245

6.3.4 Apoptosis analysis 246

6.4 Results 247

6.4.1 Effect of CSE on proliferation of human PASMCs and PAECs 247

6.4.2 Effect of hypoxia on proliferation of human PASMCs and PAECs 249

6.4.3 Effect of hypoxia and CSE in combination on proliferation of human PASMCs and PAECs 251

6.4.4 Effect of celecoxib on CSE-induced proliferation of human PASMCs and PAECs 254

6.4.5 Effect of celecoxib on hypoxia-induced proliferation of human PASMCs and PAECs 257

6.4.6 Effect of celecoxib on hypoxia in combination with CSE-induced proliferation of human PASMCs and PAECs 259

6.4.7 Effect of beraprost sodium on CSE-induced proliferation of human PASMCs and PAECs 261

6.4.8 Effect of beraprost sodium on hypoxia-induced proliferation of human PASMCs and PAECs 263

6.4.9 Effect of beraprost sodium on hypoxia in combination with CSE-induced proliferation of human PASMCs and PAECs 265

6.4.10 Effect of daltroban on CSE-induced proliferation of human PASMCs and PAECs 267

6.4.11 Effect of daltroban on hypoxia-induced proliferation of human PASMCs and PAECs 270

6.4.12 Effect of daltroban on hypoxia in combination with CSE-induced proliferation of human PASMCs and PAECs.....272

6.4.13 Effect of PF-03549184 on CSE-induced proliferation of human PASMCs and PAECs.....274

6.4.14 Effect of PF-03549184 on hypoxia-induced proliferation of human PASMCs and PAECs.....276

6.4.15 Effect of PF-03549184 on hypoxia in combination with CSE-induced proliferation of human PASMCs and PAECs.....278

6.4.16 Effect of sodium nitroprusside on CSE-induced proliferation of human PASMCs and PAECs.....280

6.4.17 Effect of sodium nitroprusside on hypoxia-induced proliferation of human PASMCs and PAECs.....282

6.4.18 Effect of sodium nitroprusside on hypoxia in combination with CSE-induced proliferation of human PASMCs and PAECs.....284

6.4.19 Effect of bosentan on CSE-, hypoxia- and hypoxia in combination with CSE-induced proliferation of human PAECs.....286

6.4.20 Effect of CSE and hypoxia alone or in combination on pro/cleaved caspase 3 levels in human PASMCs and PAECs.....289

6.4.21 Effect of CSE, hypoxia and hypoxia in combination with CSE on cleaved PARP1 levels in human PASMCs and PAECs.....292

6.4.22 Effect of drugs targeting prostanoid and sodium nitroprusside on CSE-induced cleaved PARP1 levels in human PAECs.....295

6.4.23 Effect of CSE, hypoxia and hypoxia in combination with CSE on annexin v in human PAECs 297

6.5 Discussion 299

6.5.1 CSE and hypoxia effect on PASMC and PAEC proliferation 302

6.5.1.1 The role of prostanoids in CSE- and hypoxia-induced PASMC proliferation 303

6.5.1.2 The role of prostanoids in CSE- and hypoxia-induced PAEC proliferation 306

6.5.1.3 The role of nitric oxide and endothelin in CSE- and hypoxia-induced PASMC and PAEC proliferation 308

6.5.2 CSE and hypoxia effect on PASMC and PAEC apoptosis 309

Chapter 7. General discussion, limitations, future directions and conclusions .313

7.1 General discussion 314

7.2 Limitations of the current studies 317

7.3 Future directions 320

7.4 Concluding remarks 320

Chapter 8. Appendix 322

8.1 Cell viability 323

8.1.1 Effect of CSE on the cell viability of human PASMCs and PAECs 323

8.1.2 Effect of hypoxia alone and in combination with CSE on the cell viability of human PASMCs and PAECs 325

8.1.3 Effect of $ECVE^{+/-n}$ on the cell viability of human PASMCs and PAECs. 327

8.2 Housekeeping gene β2M.....329

8.2.1 Effect of CSE on the mRNA of housekeeping gene β2M in human PASMCs and PAECs.....329

8.2.2 Effect of hypoxia alone and in combination with CSE on the mRNA of housekeeping gene β2M in human PASMCs and PAECs.....331

8.2.3 Effect of $ECVE^{+/-n}$ on the mRNA of housekeeping gene β2M in human PASMCs and PAECs.....333

8.3 Direct correlation of human PASMCs with WST-1 assay 335

8.4 Materials 337

8.5 Reagents.....337

8.6 Antibodies.....338

8.7 Kits.....338

8.8 Drugs.....338

8.9 Buffer recipes.....339

8.10 Cell culture medium recipes 341

8.11 CSE and ECVE Materials.....341

Chapter 9. References.....343

List of figures

Figure 1.1 Established vasomotor pathways targeted by current and emerging therapies in PAH. 12

Figure 1.2 Possible underlying mechanisms contributing to pulmonary hypertension in COPD. 14

Figure 1.3 Pulmonary muscular artery from a patient with COPD. 19

Figure 1.4 Arachidonic acid metabolism 33

Figure 1.5 Schematic diagram of hypothesis. 56

Figure 3.1 Effect of CSE on the mRNA expression of COX-2 in human PASMCs. 101

Figure 3.2 Effect of CSE on the mRNA expression of COX-2 in human PAECs. ... 101

Figure 3.3 Effect of CSE on the protein expression of COX-2 in human PASMCs. 103

Figure 3.4 Effect of CSE on the protein expression of COX-2 in human PAECs. ... 104

Figure 3.5 Effect of CSE on PGE_2 production in human PASMCs. 106

Figure 3.6 Effect of CSE on PGE_2 production in human PAECs. 106

Figure 3.7 Effect of CSE on the protein expression of mPGES-1 in human PASMCs. 108

Figure 3.8 Effect of CSE on the protein expression of mPGES-1 in human PAECs. 109

Figure 3.9 Effect of CSE on the mRNA expression of PGIS in human PASMCs. ... 111

Figure 3.10 Effect of CSE on the mRNA expression of PGIS in human PAECs. 111

Figure 3.11 Effect of CSE on the protein expression of PGIS in human PASMCs. . 113

Figure 3.12 Effect of CSE on the protein expression of PGIS in human PAECs. 114

Figure 3.13 Effect of CSE on 6-keto $PGF_{1\alpha}$ production in human PASMCs. 116

Figure 3.14 Effect of CSE on 6-keto $PGF_{1\alpha}$ production in human PAECs. 116

Figure 3.15 Effect of CSE on the mRNA expression of TXAS in human PASMCs.119
Figure 3.16 Effect of CSE on the mRNA expression of TXAS in human PAECs....119
Figure 3.17 Effect of CSE on the protein expression of TXAS in human PASMCs and PAECs.....122
Figure 3.18 Effect of CSE on TXB_2 production in human PASMCs.....123
Figure 3.19 Effect of CSE on TXB_2 production in human PAECs. 123
Figure 3.20 Effect of CSE on PGI_2/TXA_2 ratio in human PASMCs.....125
Figure 3.21 Effect of CSE on PGI_2/TXA_2 ratio in human PAECs. 125
Figure 3.22 Effect of CSE on the mRNA expression of eNOS in human PAECs. ...128
Figure 3.23 Effect of CSE on the protein expression of eNOS in human PASMCs. 129
Figure 3.24 Effect of CSE on the protein expression of eNOS in human PAECs. ...130
Figure 3.25 Effect of CSE on total nitrate/nitrite level in human PAECs. 131
Figure 3.26 Effect of CSE on the mRNA expression of endothelin-1 in human PASMCs. 134
Figure 3.27 Effect of CSE on the mRNA expression of endothelin-1 in human PAECs.....134
Figure 3.28 Effect of CSE on endothelin production in human PASMCs. 135
Figure 3.29 Effect of CSE on endothelin production in human PAECs.....135

Figure 4.1 Effect of hypoxia and hypoxia+CSE on the mRNA expression of COX-2 in human PASMCs. 162
Figure 4.2 Effect of hypoxia and hypoxia+CSE on the mRNA expression of COX-2 in human PAECs.....162
Figure 4.3 Effect of hypoxia and hypoxia+CSE on the protein expression of COX-2 in human PASMCs.....164

Figure 4.4 Effect of hypoxia and hypoxia+CSE on the protein expression of COX-2 in human PAECs. 165
Figure 4.5 Effect of hypoxia and hypoxia+CSE on PGE_2 production in human PASMCs. 167
Figure 4.6 Effect of hypoxia and hypoxia+CSE on PGE_2 production in human PAECs. 167
Figure 4.7 Effect of hypoxia and hypoxia+CSE on the mRNA expression of PGIS in human PASMCs 169
Figure 4.8 Effect of hypoxia and hypoxia+CSE on the mRNA expression of PGIS in human PAECs. 169
Figure 4.9 Effect of hypoxia and hypoxia+CSE on the protein expression of PGIS in human PASMCs 171
Figure 4.10 Effect of hypoxia and hypoxia+CSE on the protein expression of PGIS in human PAECs. 172
Figure 4.11 Effect of hypoxia and hypoxia+CSE on 6-keto $PGF_{1\alpha}$ production in human PASMCs 174
Figure 4.12 Effect of hypoxia and hypoxia+CSE on 6-keto $PGF_{1\alpha}$ production in human PAECs. 174
Figure 4.13 Effect of hypoxia and hypoxia+CSE on the mRNA expression of TXAS in human PASMCs. 176
Figure 4.14 Effect of hypoxia and hypoxia+CSE on the mRNA expression of TXAS in human PAECs. 176
Figure 4.15 Effect of hypoxia and hypoxia+CSE on the protein expression of TXAS in human PASMCs and PAECs. 178

Figure 4.16 Effect of hypoxia and hypoxia+CSE on TXB_2 production in human PASMCs. 180
Figure 4.17 Effect of hypoxia and hypoxia+CSE on TXB_2 production in human PAECs. 180
Figure 4.18 Effect of hypoxia and hypoxia+CSE on the PGI_2/TXA_2 ratio in human PASMCs. 182
Figure 4.19 Effect of hypoxia and hypoxia+CSE on the PGI_2/TXA_2 ratio in human PAECs. 182
Figure 4.20 Effect of hypoxia and hypoxia+CSE on the mRNA expression of eNOS in human PAECs. 185
Figure 4.21 Effect of hypoxia and hypoxia+CSE on the protein expression of eNOS in human PAECs. 186
Figure 4.22 Effect of hypoxia and hypoxia+CSE on total nitrate/nitrite level in human PAECs. 187
Figure 4.23 Effect of hypoxia and hypoxia+CSE on the mRNA expression of endothelin-1 in human PASMCs. 190
Figure 4.24 Effect of hypoxia and hypoxia+CSE on the mRNA expression of endothelin-1 in human PAECs 190
Figure 4.25 Effect of hypoxia and hypoxia+CSE on endothelin production in human PASMCs. 191
Figure 4.26 Effect of hypoxia and hypoxia+CSE on endothelin production in human PAECs. 191

Figure 5.1 Effect of $ECVE^{+/-n}$ on the mRNA expression of COX-2 in human PASMCs. 213

Figure 5.2 Effect of $ECVE^{+/-n}$ on the mRNA expression of COX-2 in human PAECs. 213

Figure 5.3 Effect of $ECVE^{+/-n}$ on the protein expression of COX-2 in human PASMCs. 214

Figure 5.4 Effect of $ECVE^{+/-n}$ on the protein expression of COX-2 in human PAECs 215

Figure 5.5 Effect of $ECVE^{+/-n}$ on PGE_2 production in human PASMCs. 217

Figure 5.6 Effect of $ECVE^{+/-n}$ on PGE_2 production in human PAECs. 217

Figure 5.7 Effect of $ECVE^{+/-n}$ on the mRNA expression of PGIS in human PASMCs. 219

Figure 5.8 Effect of $ECVE^{+/-n}$ on the mRNA expression of PGIS in human PAECs. 219

Figure 5.9 Effect of $ECVE^{+/-n}$ on the protein expression of PGIS in human PASMCs. 220

Figure 5.10 Effect of $ECVE^{+/-n}$ on 6-keto $PGF_{1\alpha}$ production in human PASMCs. ...222

Figure 5.11 Effect of $ECVE^{+/-n}$ on 6-keto $PGF_{1\alpha}$ production in human PAECs. 222

Figure 5.12 Effect of $ECVE^{+/-n}$ on the mRNA expression of TXAS in human PASMCs. 224

Figure 5.13 Effect of $ECVE^{+/-n}$ on the mRNA expression of TXAS in human PAECs. 224

Figure 5.14 Effect of $ECVE^{+/-n}$ on TXB_2 production in human PASMCs. 225

Figure 5.15 Effect of $ECVE^{+/-n}$ on TXB_2 production in human PAECs. 225

Figure 5.16 Effect of $ECVE^{+/-n}$ on the mRNA expression of eNOS in human PAECs. 228

Figure 5.17 Effect of ECVE$^{+/-n}$ on the protein expression of eNOS in human PAECs. 229

Figure 5.18 Effect of ECVE$^{+/-n}$ on total nitrate/nitrite level in human PAECs.....230

Figure 5.19 Effect of ECVE$^{+/-n}$ on the mRNA expression of endothelin-1 in human PASMCs. 232

Figure 5.20 Effect of ECVE$^{+/-n}$ on the mRNA expression of endothelin-1 in human PAECs.....232

Figure 5.21 Effect of ECVE$^{+/-n}$ on endothelin production in human PASMCs.....233

Figure 5.22 Effect of ECVE$^{+/-n}$ on endothelin production in human PAECs. 233

Figure 6.1 Effect of CSE on proliferation of human PASMCs. 248

Figure 6.2 Effect of CSE on proliferation of human PAECs.....248

Figure 6.3 Effect of hypoxia on proliferation of human PASMCs.....250

Figure 6.4 Effect of hypoxia on proliferation of human PAECs. 250

Figure 6.5 Effect of CSE, hypoxia and hypoxia+CSE on proliferation of human PASMCs. 253

Figure 6.6 Effect of CSE, hypoxia and hypoxia+CSE on proliferation of human PAECs.....253

Figure 6.7 Effect of celecoxib on CSE-induced proliferation of human PASMCs. ..256

Figure 6.8 Effect of celecoxib on CSE-induced proliferation of human PAECs. 256

Figure 6.9 Effect of celecoxib on hypoxia-induced proliferation of human PASMCs. 258

Figure 6.10 Effect of celecoxib on hypoxia-induced proliferation of human PAECs. 258

Figure 6.11 Effect of celecoxib on hypoxia+CSE-induced proliferation of human PASMCs. 260

Figure 6.12 Effect of celecoxib on hypoxia+CSE-induced proliferation of human PAECs. 260
Figure 6.13 Effect of beraprost sodium on CSE-induced proliferation of human PASMCs. 262
Figure 6.14 Effect of beraprost sodium on CSE-induced proliferation of human PAECs. 262
Figure 6.15 Effect of beraprost sodium on hypoxia-induced proliferation of human PASMCs. 264
Figure 6.16 Effect of beraprost sodium on hypoxia-induced proliferation of human PAECs. 264
Figure 6.17 Effect of beraprost sodium on hypoxia+CSE-induced proliferation of human PASMCs 266
Figure 6.18 Effect of beraprost sodium on hypoxia+CSE-induced proliferation of human PAECs. 266
Figure 6.19 Effect of daltroban on CSE-induced proliferation of human PASMCs. 269
Figure 6.20 Effect of daltroban on CSE-induced proliferation of human PAECs. 269
Figure 6.21 Effect of daltroban on hypoxia-induced proliferation of human PASMCs. 271
Figure 6.22 Effect of daltroban on hypoxia-induced proliferation of human PAECs. 271
Figure 6.23 Effect of daltroban on hypoxia+CSE-induced proliferation of human PASMCs. 273
Figure 6.24 Effect of daltroban on hypoxia+CSE-induced proliferation of human PAECs. 273

Figure 6.25 Effect of PF-03549184 on CSE-induced proliferation of human PASMCs. 275
Figure 6.26 Effect of PF-03549184 on CSE-induced proliferation of human PAECs. 275
Figure 6.27 Effect of PF-03549184 on hypoxia-induced proliferation of human PASMCs. 277
Figure 6.28 Effect of PF-03549184 on hypoxia-induced proliferation of human PAECs. 277
Figure 6.29 Effect of PF-03549184 on hypoxia+CSE-induced proliferation of human PASMCs. 279
Figure 6.30 Effect of PF-03549184 on hypoxia+CSE-induced proliferation of human PAECs. 279
Figure 6.31 Effect of sodium nitroprusside on CSE-induced proliferation of human PASMCs. 281
Figure 6.32 Effect of sodium nitroprusside on CSE-induced proliferation of human PAECs. 281
Figure 6.33 Effect of sodium nitroprusside on hypoxia-induced proliferation of human PASMCs. 283
Figure 6.34 Effect of sodium nitroprusside on hypoxia-induced proliferation of human PAECs. 283
Figure 6.35 Effect of sodium nitroprusside on hypoxia+CSE-induced proliferation of human PASMCs.....285
Figure 6.36 Effect of sodium nitroprusside on hypoxia+CSE-induced proliferation of human PAECs. 285
Figure 6.37 Effect of bosentan on CSE-induced proliferation of human PAECs. 287

Figure 6.38 Effect of bosentan on hypoxia-induced proliferation of human PAECs. 287
Figure 6.39 Effect of bosentan on hypoxia+CSE-induced proliferation of human PAECs. 288
Figure 6.40 Effect of CSE, hypoxia and hypoxia+CSE on pro/cleaved caspase 3 in human PASMCs.....290
Figure 6.41 Effect of CSE, hypoxia and hypoxia+CSE on pro/cleaved caspase 3 in human PAECs. 291
Figure 6.42 Effect of CSE, hypoxia and hypoxia+CSE on cleaved PARP1 in human PASMCs. 293
Figure 6.43 Effect of CSE, hypoxia and hypoxia+CSE on cleaved PARP1 in human PAECs. 294
Figure 6.44 Effect of drugs targeting prostanoid and sodium nitroprusside on CSE-induced cleaved PARP1 in human PAECs. 296

List of tables

Table 1.1 Updated classification of pulmonary hypertension. 4

Table 2.1 A summary of the volume of components used to prepare RT master mix. 73

Table 2.2 A summary of thermal profile of RT reaction. 74

Table 2.3 A summary of the volume of components used to prepare qPCR reaction. 74

Table 2.4 FW and RV primer sequences for the target and housekeeping genes. 75

Table 2.5 A summary of thermal profile of the qPCR reaction. 75

Table 2.6 Cross reactivity of PGE_2 ELISA kit-monoclonal.....77

Table 2.7 Cross reactivity of 6-keto $PGF_{1\alpha}$ ELISA kit. 79

Table 2.8 Cross reactivity of TXB_2 ELISA kit. 81

Table 3.1 A summary table of the findings of Chapter 3.....137

Table 4.1 A summary table of the findings of Chapter 4.....193

Table 5.1 A summary table of the findings of Chapter 5.....235

Table 6.1 A summary table of the findings of Chapter 6.....300

Table 6.2 A summary table of the findings of Chapter 6.....301

1. Introduction

1.1 Pulmonary hypertension

1.1.1 Definition and classification of pulmonary hypertension

Pulmonary hypertension is a haemodynamic and pathophysiologic disease that is characterised by an elevation of blood pressure within the pulmonary artery and increased pulmonary vascular resistance. This eventually leads to right ventricular failure and death unless diagnosed early and treated appropriately (Bazan and Fares, 2015, Barst, 2008, Galie et al., 2016). Haemodynamically, pulmonary hypertension has been defined as a mean pulmonary artery pressure (mPAP) of more than 25 mmHg at rest and 30 mmHg during exercise; pulmonary capillary wedge pressure (PCWP) of less than 15 mmHg; and pulmonary vascular resistance (PVR) of less than 3 Wood units as assessed by right heart catheterisation (RHC) (Abman et al., 2015, Galie et al., 2016).

Based on symptoms and physical examinations, clinical suspicion is required to diagnose patients with pulmonary hypertension (Galie et al., 2016). Although the symptoms and signs of pulmonary hypertension are non-specific, the initial clinical presentations of pulmonary hypertension are normally induced by exertion, including shortness of breath, fatigue, weakness, angina, and syncope (Galie et al., 2016). These clinical presentations can vary widely, depending on the underlying cause of pulmonary hypertension (Galie et al., 2016). For this reason, pulmonary hypertension has been classified by the World Health Organization (WHO) based on similarities in pathophysiologic mechanisms, clinical features, and treatment strategies to standardise the diagnosis of the disease.

As rapid advancements in imaging methods, pharmacologic management, and molecular medicine have been developed (Foshat and Boroumand, 2017), WHO classification of pulmonary hypertension has undergone several modifications. These changes have been implemented at four meetings held in Evian in 1998 (Fishman, 2001), Venice in 2003 (Simonneau et al., 2004), Dana Point in 2008 (Simonneau, 2009), and Nice in 2013 (Simonneau et al., 2013).

The Evian classification was not only widely used in clinical practice but also used by researchers and drug agencies. A consensus of the general scheme of the Evian classification of pulmonary hypertension was maintained, and no major modifications were made at either the third or fourth WHO meetings. However, five years later, the previous clinical classification of pulmonary hypertension was updated and slightly modified at the fifth meeting held in 2013 in Nice, France. This was completed according to the published clinical and experimental data, as the general philosophy was to maintain the five main groups of disorders that cause pulmonary hypertension. These were classified as follows: pulmonary arterial hypertension (PAH) (group 1), pulmonary hypertension due to left heart disease (group 2), pulmonary hypertension due to lung diseases and/or hypoxia (group 3), chronic thromboembolic pulmonary hypertension (group 4), and pulmonary hypertension with unclear multifactorial mechanisms (group 5) (Table 1.1) (Dunlap and Weyer, 2016). This most recent classification grouped pulmonary hypertension into five different categories based on clinical presentations, haemodynamic features, and specific therapeutic interventions. However, the mechanisms involved in pulmonary artery remodelling for these conditions are not fully understood. Further studies are needed to classify pulmonary hypertension more

effectively based on its underlying causes, in addition to the current classification and management strategies.

Table 1.1 Updated classification of pulmonary hypertension.

Classification	*Targeted treatment available?*
Group 1*: Pulmonary arterial hypertension	Yes
Including idiopathic, heritable, and HIV-associated; systemic sclerosis and other connective tissue disease; congenital heart disease; schistosomiasis; drug- and toxin-induced	
Group 2: Pulmonary hypertension due to left heart disease	No
Including systolic and diastolic dysfunction and valvular heart disease	
Group 3: Pulmonary hypertension due to lung diseases and/or hypoxia	No
Including chronic obstructive pulmonary disease, sleep-disordered breathing, and interstitial lung disease	
Group 4: Chronic thromboembolic pulmonary hypertension	Yes
Group 5: Multifactorial pulmonary hypertension	No
Including metabolic, systemic, and hematologic disorders (sickle cell disease), and others	

HIV = human immunodeficiency virus.

**—Also includes 1′ (pulmonary venoocclusive disease and/or pulmonary capillary hemangiomatosis) and 1″ (persistent pulmonary hypertension of the newborn).*

Adopted from (Dunlap and Weyer, 2016)

1.1.2 Pulmonary hypertension in COPD

Pulmonary hypertension due to lung diseases and/or hypoxia was classified as group 3 by the WHO in the most recent meeting in 2013. According to the updated classification, pulmonary hypertension associated with disorders of the respiratory system include: 1) chronic obstructive pulmonary disease (COPD), 2) interstitial lung disease, 3) other pulmonary diseases with a mixed restrictive and obstructive pattern, 4) sleep-disordered breathing, 5) alveolar hypoventilation disorders, 6) chronic exposure to high altitude, and 7) developmental lung diseases. COPD is considered the most frequent underlying lung disease in WHO group 3 pulmonary hypertension and is associated with a decrease in functional capacity and survival (Opitz and Ulrich, 2018).

COPD has been defined by the American Thoracic Society (ATS) and the European Respiratory Society (ERS) (Celli et al., 2015, Rodriguez-Roisin et al., 2017) as ‘a preventable and treatable disease state characterised by airflow limitation that is not fully reversible. The airflow limitation is usually progressive and associated with an abnormal inflammatory response of the lungs to noxious particles or gases, primarily caused by cigarette smoking. Although COPD affects the lungs, it also produces significant systemic consequences’ (Celli et al., 2015). In addition to the ATS/ERS definition, the Global Initiative for Chronic Obstructive Lung Disease (GOLD) defined COPD as ‘a common, preventable and treatable disease that is characterized by persistent respiratory symptoms and airflow limitation that is due to airway and/or alveolar abnormalities usually caused by significant exposure to noxious particles or gases’ (Rodriguez-Roisin et al., 2017). Both definitions note that COPD is a preventable and treatable disease, characterised by a progressive airflow limitation that is not fully

reversible, and is associated with an abnormal inflammatory response of the lung to noxious particles or gases, particularly cigarette smoking.

Patients with COPD typically present with dyspnoea, a persistent cough with or without sputum production, and a history of exposure to environmental risk factors, including cigarette smoking. To confirm the diagnosis of COPD, a post-bronchodilator forced expiratory volume (in 1 s) to forced vital capacity (FEV_1/FVC) ratio is assessed by spirometry. An FEV_1/FVC ratio of <70% confirms the existence of irreversible airflow limitation, while the severity of COPD can be determined by measuring FEV_1 (Perez-Padilla et al., 2009).

COPD has become the fourth leading cause of morbidity and mortality worldwide and is expected to be the third most likely cause of death in the coming years (Ho et al., 2019). It affected 384 million people in 2010, with a global prevalence of 11.7%. More than 3 million people died of COPD in 2012, despite the fact that COPD is frequently under-diagnosed and under-treated (Viegi et al., 2007, Mannino, 2006, Koblizek et al., 2016). Approximately 50% of COPD cases are under-diagnosed (Koblizek et al., 2016), and an evaluation for comorbidities in COPD (such as cardiovascular diseases) is not part of the guidelines and is not routinely performed in clinical practice (John et al., 2016). Therefore, COPD patients suffer from this condition for years and die either from the disease or its complications (Koblizek et al., 2016). The most common and serious complication of COPD (which can lead to early death) is cardiovascular disease, particularly pulmonary hypertension (Zakynthinos et al., 2011, Mannino et al., 2015). Pulmonary hypertension in patients with COPD is associated with increased mortality and morbidity (Smith and Wrobel, 2014) and is characterised by pulmonary

vasoconstriction and vascular remodelling, including dysfunction and proliferation of pulmonary artery cells.

1.1.2.1 Clinical evaluation of pulmonary hypertension in COPD

The physical signs and symptoms of COPD patients are associated with an increased risk of acute exacerbations when pulmonary hypertension subsequently develops (Shujaat et al., 2012). This affects both mortality and quality of life (Galie et al., 2016). Consequently, a double hospitalisation rate is seen in patients with COPD-associated pulmonary hypertension. Clinically, it is difficult to distinguish between the physical signs and symptoms of COPD with and without pulmonary hypertension at the early or mid-stages. This is because the initial signs and symptoms of pulmonary hypertension in COPD (such as dyspnoea, shortness of breath, and fatigue) are similar to those seen with COPD patients (Weitzenblum et al., 2013). Therefore, further clinical assessments are needed to identify pulmonary hypertension in COPD.

Although cardiac auscultations, electrocardiograms, and transthoracic echocardiographies are routinely performed to estimate haemodynamic measurements when the presence of pulmonary hypertension is suspected, these non-invasive methods have been shown to be inaccurate in diagnosing pulmonary hypertension in patients with COPD. Furthermore, even normal findings assessed by these non-invasive methods do not exclude the existence of pulmonary hypertension (Galie et al., 2016, Fisher et al., 2009, Chaouat et al., 2005, Arcasoy et al., 2003). Currently, pulmonary hypertension can only be confirmed by invasively assessing the haemodynamic status using right heart catheterisation (RHC). RHC remains the gold standard method to confirm a diagnosis of

pulmonary hypertension (mPAP ≥ 25 mmHg) (Galie et al., 2016, Nathan et al., 2019, Weitzenblum et al., 1981).

Once the presence of pulmonary hypertension is confirmed (with no pervious history of COPD), pulmonary function tests, arterial blood gases, 6-minute walking tests (6MWTs), and cardiopulmonary exercise testing can be performed to identify the underlying causes. Pulmonary abnormalities in COPD-associated pulmonary hypertension include irreversible airflow obstruction (a post-bronchodilator FEV_1/FVC ratio of <70) combined with decreased lung diffusion capacity for carbon monoxide (DLCO) (<40% of predicted), decreased arterial oxygen pressure (PaO_2), increased arterial carbon dioxide pressure ($PaCO_2$), and limited maximal exercise capacity.

Although the development of pulmonary hypertension due to COPD is associated with haemodynamic and pulmonary abnormalities, the physical signs and symptoms are difficult to identify, and early clinical suspicion together with invasive procedures are needed to diagnose the disease. Therefore, understanding the molecular mechanisms involved in its development would not only lead to a novel therapeutic approach, but could also identify non-invasive biological biomarkers associated with future pulmonary vascular remodelling in COPD, which may help in early diagnosis and intervention.

1.1.2.2 Prevalence and impact

The development of pulmonary hypertension is a common complication of COPD, and is defined by an increase of pulmonary artery pressure (PAP) (invasively confirmed by RHC). Currently, its prevalence is not precisely known, due to the expensive and invasive method required to confirm the diagnosis of pulmonary hypertension in COPD patients (Gologanu et al., 2013). Moreover, this invasive

procedure can not be performed frequently in clinical practice in individuals with mild and moderate COPD, as it is associated with an increased risk of serious complications (Chaouat et al., 2008, Arcasoy et al., 2003, Gologanu et al., 2013). The determination of the prevalence of pulmonary hypertension in COPD has been affected by the inaccuracy of the non-invasive diagnostic method for determining its presence. Furthermore, there are differences in defining pulmonary hypertension and difficulties in performing invasive procedures in stable COPD patients due to ethical concerns and possible complications (Chaouat et al., 2008). Consequently, only hospitalised subjects are accessible for investigations.

Previous studies have reported that the prevalence of pulmonary hypertension in patients with COPD varies between 20.5% and 90.8% (Burrows et al., 1972, Weitzenblum et al., 1981, Weitzenblum et al., 1984, Oswald-Mammosser et al., 1991, Scharf et al., 2002, Arcasoy et al., 2003, Chaouat et al., 2005, Thabut et al., 2005, Katiyar and Khare, 2018). This inconsistent and inaccurate estimate may be due to the severity level of the disease and the differences in methods used to measure PAP (echocardiography versus RHC). In addition to the differences in the methods used, it has been shown that the measurement of PAP by the use of non-invasive methods (such as echocardiography) can be affected by pulmonary hyperinflation seen in patients with COPD (Arcasoy et al., 2003, Fisher et al., 2007, Peinado et al., 2008).

In view of all these factors, it is likely that the number of COPD patients with pulmonary hypertension is high, although the precise prevalence of pulmonary hypertension in COPD patients remains unclear. Thus, further studies are needed to identify other diagnostic tools (such as cellular biomarkers) that may be involved in the

development of pulmonary hypertension in COPD, which may then pave the way for identification of therapeutic targets.

1.1.2.3 Treatment

The difficulties in routinely assessing PAP in patients with lung diseases, together with poor understanding of the underlying mechanisms of the development of pulmonary hypertension due to lung diseases (group 3 pulmonary hypertension) have resulted in the absence of specific and approved therapies (Grimminger et al., 2016, Galie et al., 2016). Thus, it is well known that clinicians have no choice but to use so-called PAH (group 1 pulmonary hypertension) drugs to treat other forms of pulmonary hypertension, although these drugs are not recommended, due to lack of studies and no proven benefits (Galie et al., 2016, Yerly et al., 2016, Humbert et al., 2014, Hoeper, 2008, Stolz et al., 2008, Rietema et al., 2008).

The past decade has seen rapid development in the treatment of PAH (Bai et al., 2011). Recently, supportive therapy (oral anticoagulants, diuretics, O_2, and digoxin) together with specific pulmonary vasodilator drugs targeting endothelin, prostacyclin (also called prostaglandin I_2 (PGI_2), and nitric oxide pathways (Figure 1.1) (Galie et al., 2016, Yerly et al., 2016) have shown significant improvements in patients with PAH (Galie et al., 2016, Jyothula and Safdar, 2009). The current approved specific therapies for PAH are nitric oxide donors (e.g. sodium nitroprusside and riociguat) and phosphodiesterase 5 (PDE5) inhibitors (sildenafil, tadalafil and vardenafil); PGI_2 analogues and PGI_2 receptor agonists (epoprostenol, beraprost sodium, iloprost, treprostinil, and selexipag); and endothelin receptor antagonists (bosentan, ambrisentan and macitentane) (Galie et al., 2016, Yerly et al., 2016). Although it has long been

thought that the use of all three categories of drugs approved for PAH can be ineffective and may impair gas exchange caused by the inhibition of hypoxic pulmonary vasoconstriction in patients with group 3 pulmonary hypertension (Agusti et al., 1990), there is still insufficient data to support this assumption (Abman et al., 2015, Barbera and Blanco, 2009). Thus, a greater understanding of the role of nitric oxide, PGI_2, and endothelin pathways in the development of COPD-associated pulmonary hypertension is needed to assess the efficacy of the targeted therapies, and to develop new effective therapies for the treatment of COPD-associated pulmonary hypertension.

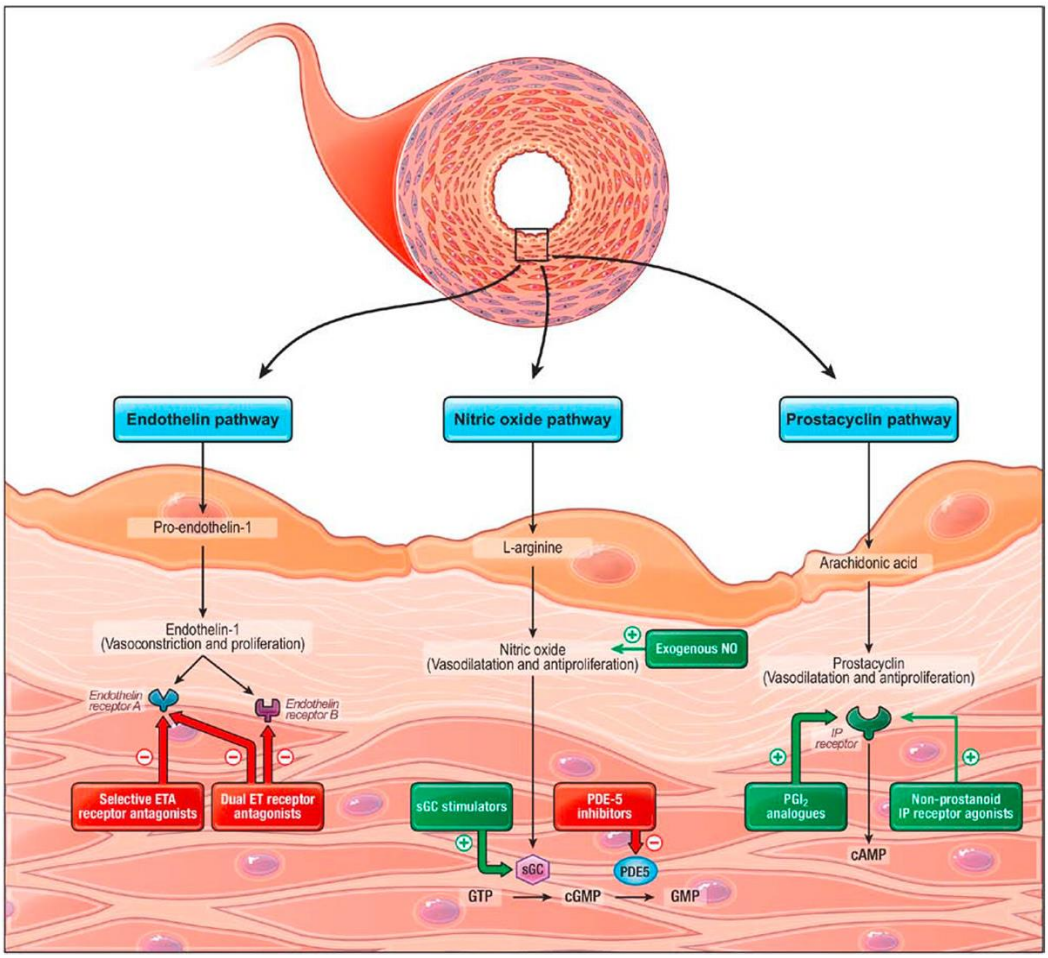


Figure 1.1 Established vasomotor pathways targeted by current and emerging therapies in PAH.
The three major pathways (endothelin, nitric oxide, and prostacyclin) involved in the regulation of pulmonary vasomotor tone are shown. These pathways represent the targets of all currently approved PAH therapies. Endothelial dysfunction results in decreased production of endogenous vasodilatory mediators (nitric oxide and prostacyclin) and the upregulation of endothelin-1, which promotes vasoconstriction and smooth muscle cell proliferation. The endothelin-1 pathway can be blocked by either selective or non-selective endothelin-1 receptor antagonists; the nitric oxide pathway can be manipulated by direct administration of exogenous nitric oxide, inhibition of phosphodiesterase type-5, or stimulation of soluble guanylate cyclase; and the prostacyclin pathway can be enhanced by the administration of prostanoid analogues or non-prostanoid IP receptor agonists. Endothelin (ET), Endothelin type A (ETA), prostaglandin I_2 receptor (IP), nitric oxide (NO), pulmonary arterial hypertension (PAH), phosphodiesterase type 5 (PDE-5), soluble guanylate cyclase (sGC). Adopted from (Humbert et al., 2014).

1.2 Pathophysiology of COPD-associated pulmonary hypertension

The hallmark of all forms of pulmonary hypertension is thought to be pulmonary artery vasoconstriction and remodelling of the pulmonary vessel wall, including dysfunction and proliferation of pulmonary artery cells. Although the pathophysiological mechanisms of COPD in pulmonary hypertension are not fully understood, it is suspected that pulmonary hypertension complicating COPD occurs as a consequence of the combined effects of inflammation, cigarette smoke (CS), and hypoxia, which could then lead to elevated PVR and eventually contribute to pulmonary hypertension in COPD patients (Figure 1.2) (Chaouat et al., 2008).

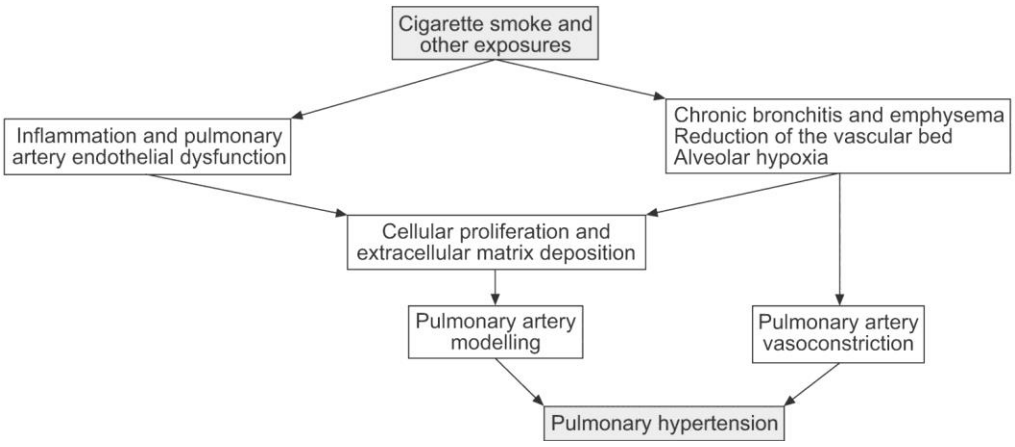


Figure 1.2 Possible underlying mechanisms contributing to pulmonary hypertension in COPD.
Noxious particles or gases, particularly CS, can cause pulmonary inflammation, endothelial dysfunction, chronic alveolar hypoxia, loss of pulmonary capillaries in chronic bronchitis, and emphysema. These pathophysiological changes may ultimately contribute to pulmonary hypertension in COPD due to pulmonary artery vasoconstriction and pulmonary artery remodelling as a result of proliferation of pulmonary artery cells. Adapted from (Chaouat et al., 2008).

1.2.1 Pulmonary vasoconstriction

Pulmonary artery vasoconstriction induced by alveolar hypoxia is a reflex contraction of pulmonary artery smooth muscle cells (PASMCs). This hypoxic pulmonary vasoconstriction is a vasoprotective response to hypoxia to maintain ventilation-perfusion balance, as blood flow in the pulmonary arteries of COPD patients is shifted from hypoxic alveoli toward normoxic alveoli to help minimise ventilation-perfusion mismatch. As the disease progresses, persistent hypoxia (resulting from inadequate delivery of oxygen to the tissues) is thought to lead to elevated PVR and pulmonary hypertension in COPD (Shujaat et al., 2012).

Over the past two decades, substantially more information has become available and the traditional view that suggests the elevated PVR in COPD can only be a result of hypoxic pulmonary vasoconstriction has been challenged (Scharf et al., 2002). Recent evidence shows that endothelial dysfunction (driven by CS, inflammation, and chronic hypoxia in COPD) also plays a key role in the cause of pulmonary vasoconstriction and pulmonary vascular remodelling in COPD patients (Bogaard, 2017, Peinado et al., 2002). This suggests that CS can be the primary driver of pulmonary vascular remodelling in COPD (Wright et al., 2005) (Figure 1.2), although hypoxia is definitely known to induce pulmonary vascular remodelling. Today, the exact mechanistic basis of CS and hypoxia, either individually or in combination, on the induction of pulmonary artery dysfunction and remodelling in COPD is still unclear.

1.2.2 Endothelial dysfunction

Pulmonary hypertension is characterised by endothelial dysfunction and pulmonary artery remodelling as consequence of cell proliferation (Giaid et al., 1993). It

has long been known that endothelial cells maintain the balance between vasodilator (nitric oxide and PGI_2) and vasoconstrictor (thromboxane A_2 (TXA_2), and endothelin-1) mediators and prevent PASMC proliferation. Endothelial dysfunction leads to a shift in the endothelium toward increased vasoconstrictor mediators, and eventually contributes to pulmonary hypertension. An imbalance with reduced PGI_2 and increased TXA_2 has been observed in PAH patients (Christman et al., 1992). Similarly, reduced prostaglandin I synthase (PGIS) expression and PGI_2 production (Chen et al., 2012) and increased TXA_2 production (Davi et al., 1997) have been reported in smokers and ex-smokers with COPD. In addition to the opposing effects of the mediators PGI_2 and TXA_2 in vascular cells (Norel, 2007), previous studies have also reported that reduced nitric oxide and increased endothelin-1 is a characteristic of endothelial dysfunction, and can be an important indicator of pulmonary artery remodelling (Bourque et al., 2011). Reduced expression of endothelial nitric oxide synthase (eNOS) (Giaid and Saleh, 1995) and increased endothelin-1 expression (Giaid et al., 1993) have been demonstrated in patients with PAH and non-COPD related pulmonary hypertension.

Preliminary evidence suggests that CS and chronic hypoxia can stimulate PASMC proliferation, which may be critical for pulmonary artery remodelling in COPD-associated pulmonary hypertension. However, the effect of CS and hypoxia on the vasoactive gene expression and mediator release, and the contribution of pulmonary artery endothelial cell (PAEC) dysfunction and particularly PASMC dysfunction to pulmonary artery remodelling in COPD remain unclear. Accordingly, understanding the synergistic or additive effects of chronic hypoxia-and CS-induced pulmonary vascular remodelling in COPD is of great importance.

1.2.3 Pulmonary vascular remodelling

Pulmonary vascular remodelling refers to the key structural changes in the vascular wall that eventually contribute to elevated PAP by increasing PVR in all forms of pulmonary hypertension, including COPD-associated pulmonary hypertension (Wright et al., 1992, Santos et al., 2002). Pulmonary vascular abnormalities have been attributed to the proliferation of endothelial, smooth muscle, and fibroblast cells, which are cellular components of the three layers of pulmonary vascular wall: intima, media, and adventitia, respectively (Pak et al., 2007).

The intima is composed predominantly of endothelial cells, and plays an important role in regulating the vascular tone and controlling cell growth. Thickness of the intima layer has been associated with endothelial dysfunction in the pulmonary arteries of COPD patients, which may initiate the process of vascular remodelling (Peinado et al., 1998). In addition, medial wall thickening, caused by proliferative smooth muscle cells, has been observed in patients with COPD (Sakao et al., 2014). More importantly, histochemical and immunohistochemical studies performed in the vasculature of patients with COPD have shown increased number of smooth muscle cells (but not fibroblasts) in the enlarged intima as a result of staining the intimal layer by specific smooth muscle cell and fibroblast markers (Santos et al., 2002, Peinado et al., 1998, Barbera et al., 2003). The proliferation of smooth muscle cells observed in the thickened intima of patients with COPD occurred in an inward direction, thus reducing the vascular lumen (Figure 1.3) (Barbera et al., 2003). This suggests that PASMCs play an important role, in addition to PAECs, in the development of COPD-associated pulmonary hypertension.

Although the key signalling pathways involved in the remodelling process are unknown, the pathophysiological changes reported in the innermost two layers of pulmonary artery in COPD, the media and intima, are believed to occur as a result of PASMC proliferation due to PAEC dysfunction (Santos et al., 2002, Peinado et al., 1998). Therefore, PASMCs and PAECs are considered the two key cell types that play a major role in the pathophysiology of COPD-associated pulmonary hypertension.

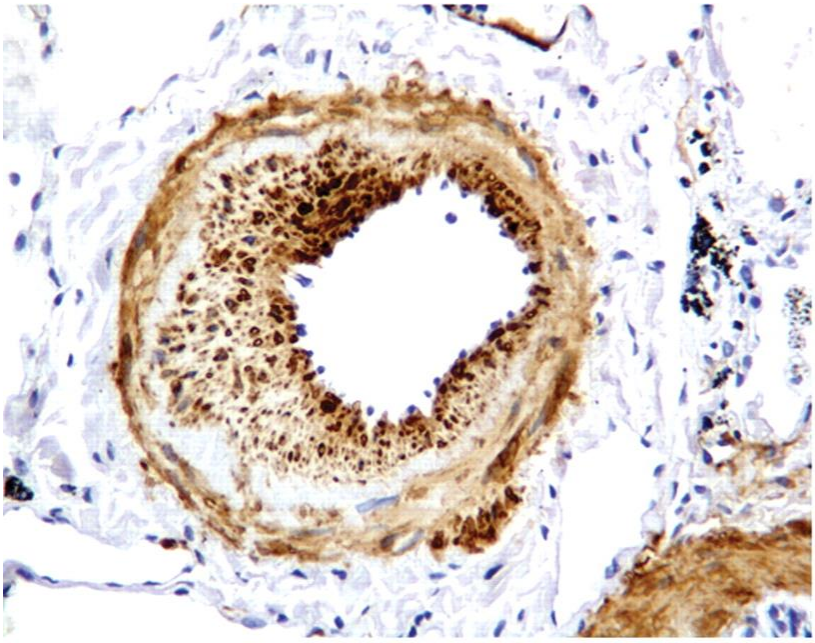


Figure 1.3 Pulmonary muscular artery from a patient with COPD.
Immunostaining with monoclonal antibody against α-smooth muscle actin, marker of smooth muscle cells, shows abundant proliferation of smooth muscle cells in the intima. Note: the prominent intimal thickening and the luminal narrowing. Adopted from (Barbera et al., 2003)

1.2.3.1 Role of pulmonary artery smooth muscle cells

Pulmonary hypertension is the end result of pulmonary artery vasoconstriction and remodelling of the pulmonary vessel wall. Pulmonary artery vasoconstriction is considered to be a consequence of PASMC contraction, while pulmonary vascular remodelling is associated with increased proliferation of pulmonary artery cells including PASMCs (Makino et al., 2011). Excessive PASMC proliferation is known to lead to thickness of the middle layer of the pulmonary vascular wall in all forms of pulmonary hypertension, including COPD-associated pulmonary hypertension (Stenmark et al., 2018, Santos et al., 2002, Barbera et al., 2003).

Increased proliferation of PASMCs as a consequence of endothelial dysfunction is believed to be an important contributor to pulmonary vascular remodelling in patients with COPD (Sakao et al., 2014). Vascular endothelial cells are considered the main source for the production of vasoactive mediator release. When released, endothelial cells also participate in regulating the proliferation of PASMCs by diffusing the production of the vasoactive mediators into PASMCs, where these mediators can induce proliferative or anti-proliferative effects. However, the possible role of PASMC synthetic functions on the imbalance between the extent of vasodilation/anti-proliferation and vasoconstriction/proliferation in COPD-associated pulmonary hypertension has not been previously explored. It has long been recognised that chronic hypoxia is a strong stimulus for vascular remodelling (Pak et al., 2007) and can directly enhance PASMC proliferation in both human (Raghavan et al., 2012) and animal models (Walker et al., 2016). This view is supported by Sakao et al. (2014), who found that the abnormality of pulmonary vascular in COPD patients is associated with the degree of hypoxemia, suggesting

hypoxia plays a key role in the induction of media enlargement of the pulmonary arteries, thereby contributing to the development of pulmonary hypertension in COPD. Furthermore, structural changes in the pulmonary arteries, including PASMC proliferation, which eventually leads to medial hypertrophy, have also been noted in smokers with no airway obstruction (Santos et al., 2002). This suggests that CS may lead directly to pulmonary vascular remodelling by stimulating the proliferation of PASMCs. Convincingly, it has been shown that the effect of CS extract (CSE) can induce proliferation of both human and rat PASMCs (Xiang et al., 2010, Xing et al., 2012). However, CSE effect on the induction of imbalanced vasoactive gene expression and mediator release in PASMCs and the potential contribution of this imbalance to PASMC proliferation have not been studied.

Together, these observations suggest that hypoxia and CS play a pathogenic role in vascular remodelling in COPD by inducing PASMC proliferation. However, the role of PASMC synthetic functions leading to CS- and hypoxia-induced cell proliferation in COPD remains unknown. Given the fact that PASMCs constitute a prominent part in remodelled vasculature, it is important to understand the role of PASMC dysfunction in the physiopathology of COPD-associated pulmonary hypertension.

1.2.3.2 Role of pulmonary artery endothelial cells

PAECs are located in the intimal layer of pulmonary arteries that line the vascular lumen and play a key role in controlling cell growth and regulating vascular tone. Apoptosis-resistant and hyper-proliferative PAECs have been reported in patients with PAH (Masri et al., 2007). It has also been shown that vascular endothelial growth factor (VEGF) receptor inhibitor in combination with chronic hypoxia can cause vascular

endothelial cells apoptosis. This initial apoptosis is followed by proliferative vascular endothelial cells in rat models of pulmonary hypertension (Taraseviciene-Stewart et al., 2001), suggesting that the emergence of apoptosis-resistant proliferating vascular endothelial cells may play an important role in vascular remodelling and the development of pulmonary hypertension. This is also supported by a more recent study showing that the initial apoptosis, induced by VEGF receptor inhibitor, is followed by increased proliferation of apoptosis-resistant human pulmonary microvascular endothelial cells (Sakao et al., 2005). The accumulative evidence suggests that proliferative PAECs play a role in the pulmonary vascular remodelling in PAH. However, whether PAEC proliferation plays a role in the development of COPD-associated vascular remodelling and pulmonary hypertension is largely unknown.

It is a widely held view that CS and hypoxia play a critical role in the contribution to vascular remodelling, resulting in pulmonary hypertension in patients with COPD. Human PAECs exposed to hypoxia have been shown to induce cell proliferation (Dabral et al., 2016), suggesting that the hyper-proliferative apoptosis-resistant endothelial cells induced by hypoxia may lead to vascular remodelling in COPD. In addition, thickness of the inner layer in the lumen of the pulmonary arteries and vascular remodelling are observed in COPD and smokers without COPD (Santos et al., 2002), indicating that CS can initiate vascular remodelling, eventually leading to pulmonary hypertension. However, there are a limited amount of experimental data on the effect of CSE on human PAEC apoptosis and proliferation. Human experimental studies reported that CSE treatment can induce apoptosis in human umbilical vein endothelial cells (Shi et al., 2017) and in human pulmonary microvascular endothelial cells (Nana-Sinkam et al.,

2007). Furthermore, an increased apoptosis rate has been observed in human lung tissue from COPD patients with a smoking history compared with non-smoking controls (Shi et al., 2017). However, the effect of CSE on human PAEC apoptosis and proliferation has not been explored. Therefore, it is important to understand the biological causes involved in vascular remodelling, including PAEC dysfunction, apoptosis, and proliferation, in order to develop targeted therapies for COPD-associated pulmonary hypertension.

1.2.4 Hypoxia

It has been reported that pulmonary vascular remodelling is observed in pulmonary vessels of COPD patients with hypoxemia (Wang et al., 2018). It has also been suggested that the degree of pulmonary hypertension in COPD is directly related to the severity of hypoxemia, and the alteration of pulmonary vessels in COPD at a late stage of the disease is thought to result from chronic hypoxia (Sakao et al., 2014), indicating that hypoxia is an important contributor to vascular remodelling in COPD. This is supported by human and animal experimental studies that demonstrate induction of PASMC proliferation in response to hypoxia. For example, hypoxia has been shown to induce proliferation of human PASMCs (Wang et al., 2018, Yu and Hales, 2011, Raghavan et al., 2012) and rat PASMCs (Li et al., 2016). Similarly, experimental studies have also shown that hypoxia can induce proliferation of human PAECs (Porter et al., 2014, Dabral et al., 2016). However, there are conflicting data with regards to the direct effect of hypoxia on the proliferation of PAECs in human and animal experimental models. It has been shown that hypoxia alone does not stimulate proliferation of PAECs in human experimental models of hypoxia-induced pulmonary hypertension, as well as in hypoxic models of mice and rats (Yu and Hales, 2011). These rather contradictory

observations may be due to methodological factors such as differences in exposure time and oxygen concentrations. Although the most recent data suggest that hypoxia is a direct stimulus of PASMC and PAEC proliferation, the underlying cause that leads to hypoxia-induced proliferation of PASMCs and PAECs is unclear.

1.2.5 Cigarette smoke

CS is considered the most common etiological factor in developing COPD (MacNee, 2005). Although its role in COPD-associated pulmonary hypertension is not well characterised, the traditional view that pulmonary hypertension in COPD is secondary to chronic hypoxia and emphysema is challenged by clinical and experimental evidence (Wright et al., 2006). Apparent vascular remodelling has been demonstrated in "healthy" smokers and patients with mild-to-moderate COPD, despite the fact that pulmonary hypertension is usually diagnosed in patients with advanced COPD (Barbera and Blanco, 2009). Furthermore, thickness of vascular layers has been observed in patients with COPD and smokers with no sign of airway obstruction (Santos et al., 2002, Wright et al., 1983, Naeije and Barbera, 2001), suggesting CS plays an important role in vascular remodelling in COPD. These findings are in agreement with human and animal experimental studies showing that CSE directly stimulates proliferation of human PASMCs (Xiang et al., 2010), which ultimately contributes to pulmonary vascular remodelling. However, CSE effect on PAEC proliferation and the possible contribution of PASMC and PAEC dysfunction in this process remain to be explored.

1.2.6 Hypoxia and cigarette smoke

CS and chronic hypoxia are known to be associated with the remodelling of pulmonary vessels in pulmonary hypertension. Chronic hypoxia is a common cause of

pulmonary hypertension and pulmonary vascular remodelling (Wang et al., 2018, Pak et al., 2007). In recent years, it has been thought that factors other than chronic hypoxia (such as CS) could contribute to vascular abnormalities. Vascular remodelling and pulmonary hypertension preceding emphysema have been detected in healthy smokers with no signs of airway obstruction (Santos et al., 2002). This has also been noted in animals chronically exposed to CS (Wright and Churg, 1991, Wright et al., 2006). Interestingly, more prominent remodelling in the pulmonary arteries is present in animals exposed to CS and hypoxia, in comparison to either CS or hypoxia alone (Ferrer et al., 2011). These observations support the idea that CS can initiate vascular remodelling, which may be further amplified by chronic hypoxia in advanced COPD. However, the exact role of hypoxia+CS-induced vascular changes remains unknown. Accordingly, more studies are needed to assess the similarities and differences between both exposures, either individually or in combination, in human PASMCs and PAECs.

1.2.7 Inflammation

Pulmonary vascular remodelling in patients with COPD is the main cause of increase in PAP and is believed to be a consequence of CS, hypoxia, and chronic lung inflammation (Chaouat et al., 2008, Zakynthinos et al., 2011). Although the potential role of inflammation in COPD-associated pulmonary hypertension and the pathways involved are unknown, it is a widely held view that inflammatory cytokines play a key role in the vascular changes seen in patients with COPD. It has been reported that elevated tumor necrosis factor alpha (TNF-α), interleukin-10 (IL-10), interleukin-8 (IL-8), interleukin-1β (IL-1β) (Soon et al., 2010), and interleukin-6 (IL-6) (Humbert et al., 1995) are found in PAH patients and experimental models of PAH. Among these cytokines, the main

inflammatory mediator involved in the vascular remodelling process in PAH is the pro-inflammatory cytokine IL-6 (Humbert et al., 1995, Selimovic et al., 2009, Tuder et al., 2001). This could be because an IL-6 increase in vascular cells has the potential to contribute to the activation of growth factors (e.g. VEGF and transforming growth factor-β1 (TGF-β1)), which is associated with increased proliferation of both PASMCs and PAECs, leading to vascular remodelling and development of pulmonary hypertension. Similarly, levels of plasma IL-6 are found to be higher in patients with pulmonary hypertension in COPD compared with COPD patients with no pulmonary hypertension. This elevation of IL-6 is associated with increased PAP in patients with pulmonary hypertension in COPD (Chaouat et al., 2009, Eddahibi et al., 2006), suggesting that inflammation, most likely involving IL-6, could lead to increased PVR, PAP, and ultimately, could contribute to vascular remodelling by inducing PASMC proliferation (Steiner et al., 2009).

Furthermore, several *in vitro* studies have thus far linked the inflammatory mediators with key enzymes involved in prostanoid biosynthesis, particularly cyclooxygenase-2 (COX-2)/prostaglandin and inducible nitric oxide synthase (iNOS or NOS2) pathways in human vascular cells. iNOS is one of the nitric oxide synthase (NOS) isoforms and is induced in response to inflammation. The inflammatory stimulus IL-1β induces the expression of iNOS in cultured rat aortic vascular smooth muscle (Hirokawa et al., 1994) and in human PASMCs (Yang et al., 2002). Importantly, increased protein and mRNA expression of iNOS has been associated with pulmonary vascular remodelling and the development of hypoxic pulmonary hypertension in neonatal rats (Wang et al., 2013). In addition, the inhibition of iNOS expression has been shown to

prevent chronic hypoxic pulmonary hypertension in the rat model (Hampl et al., 2006). These observations suggest that the pulmonary vascular iNOS induction in response to inflammatory stimuli and hypoxic stress may participate in the development of pulmonary hypertension. It has also been reported that COX-2 expression is induced in response to inflammatory stimulus IL-1β, as well as after hypoxia exposure in human aortic smooth muscle cells and umbilical vein endothelial cells (Camacho et al., 2011). This is consistent with our previous findings showing that bradykinin, TGF-β1, IL-1β, and hypoxia are all inducers of COX-2/prostaglandin E_2 (PGE_2) in human PASMCs. Furthermore, increased PGE_2 production is prevented by the use of the cyclooxygenase (COX) inhibitor indomethacin and the COX-2 inhibitor NS-398 (Bradbury et al., 2002). Interestingly, IL-1β stimulation under both normoxic and hypoxic conditions enhanced PGIS expression and PGI_2 in both human aortic smooth muscle cells and umbilical vein endothelial cells (Camacho et al., 2011), as well as in rat PASMCs following IL-1β treatment (Itoh et al., 2003). Endogenous PGI_2 and PGE_2 increased by inflammatory mediators and hypoxia as a result of COX-2 induction suggests that PGI_2 and PGE_2 may have an adaptive response to hypoxic stress and inflammatory injuries in vascular cells. Non-steroidal anti-inflammatory drugs (NSAIDs) are widely used for their anti-inflammatory properties, and have been shown to be effective in blocking prostaglandins production by inhibiting inflammatory mediators-induced COX-2 expression. However, there is increasing concern that suppression of COX-2-derived cardio-protective prostaglandins, particularly PGI_2 could lead to increased cardiovascular risk. Much remains to be elucidated about the role of the inflammatory mediators and COX-2

pathway in COPD-associated pulmonary hypertension and the cardiovascular safety of NSAIDs use.

1.3 Imbalanced vasoactive gene expression and mediator release in COPD-associated pulmonary hypertension

Pulmonary vascular remodelling, as a consequence of PASMC and PAEC proliferation, is an important pathological feature of most forms of pulmonary hypertension (Sakao et al., 2010). Although there is still no specific marker for pulmonary vascular remodelling in all forms of pulmonary hypertension, targeting mediators of vascular dysfunction has been shown to be effective in reversing vascular remodelling in group 1 pulmonary hypertension. Early evidence suggests that an imbalance of reduced anti-proliferative mediators as opposed to increased proliferative mediators may be critical for the aberrant PASMC proliferation caused by CS and chronic hypoxia in COPD-associated pulmonary hypertension (Zakynthinos et al., 2011). However, the extent of the imbalance, the role of the imbalanced individual mediator in vascular remodelling, the contribution of PAECs (particularly PASMCs) in this process, and the effect of CSE and hypoxia on the imbalance have not been explored.

1.3.1 eNOS/nitric oxide

Nitric oxide, a potent pulmonary vasodilator, anti-proliferative mediator, and endothelial-1 synthesis inhibitor (Labonte et al., 2008), is generated by NOS in vasculature. NOS is known to have three different isoforms named according to their roles: neuronal nitric oxide synthase (nNOS or NOS1), iNOS or NOS2, and eNOS or NOS3 (Umar and van der Laarse, 2010). nNOS is constitutively expressed in neuronal cells and skeletal muscle, while iNOS is induced at sites of inflammation in response to

inflammatory mediators (e.g. TNF-α and IL-1β) in many cell types (Newby et al., 1992). eNOS is constitutively expressed in vascular endothelial cells and is considered the main source of nitric oxide production in the pulmonary circulation system (Coggins and Bloch, 2007). After being produced by eNOS, nitric oxide is known to activate soluble guanylyl cyclase (sGC), the primary receptor for nitric oxide, resulting in the formation of the second messenger cyclic guanosine monophosphate (cGMP), which causes vasorelaxation and inhibits PASMC proliferation by decreasing the intracellular calcium concentration (Barbera and Blanco, 2009).

Deficiency of eNOS expression has been reported in the pulmonary arteries of smokers (Barbera et al., 2001), in the lung tissues of patients with PAH and non-COPD related pulmonary hypertension (Giaid and Saleh, 1995), as well as in lung homogenates of guinea pigs exposed to CS (Ferrer et al., 2011). Furthermore, levels of nitric oxide in the plasma of guinea pigs exposed to CS (Ferrer et al., 2011) and in CSE-treated human PAECs (Milara et al., 2010) are decreased. In addition, hypoxia, a pathological stimulus leading to vascular remodelling in COPD (Pak et al., 2007), has been shown to reduce eNOS expression and nitric oxide production in the lungs of piglets exposed to chronic hypoxia (Fike et al., 1998), as well as in human saphenous vein endothelial cells (Takemoto et al., 2002). Although there is limited information in the literature concerning the effect of hypoxia and CSE on eNOS expression and nitric oxide production in human vascular cells, studies so far suggest an association of reduced nitric oxide bioavailability with pulmonary hypertension development and a role for reduced eNOS expression in CS- and hypoxia-induced vascular remodelling. However, the underlying cause and role

of CS-induced effects and the synergies between CS and hypoxia in vascular remodelling in COPD remain unclear.

Given the fact that dysfunction of nitric oxide bioavailability limits nitric oxide-mediated protective effects in vascular cells, the direct replacement of nitric oxide by stimulating sGC together with the inhibition of the cGMP-degrading enzyme phosphodiesterase type 5 (PDE5) has been widely studied in PAH and has been shown to result in anti-proliferative and vasodilatory effects in the pulmonary arteries of patients with PAH (Tonelli et al., 2013, Humbert et al., 2014, Jeremy et al., 1999). Recent preclinical evidence showed that treatment with sGC stimulator riociguat for three months (following eight months of CS exposure) can reduce pulmonary vascular remodelling and mean vessel wall thickness, and fully reverse pulmonary hypertension in a mouse model of CS-induced pulmonary hypertension (Pichl et al., 2019). Similarly, treatment with riociguat has been reported to decrease PVR in retrospective analysis of seven patients with COPD-associated pulmonary hypertension (Pichl et al., 2019).

In addition to the beneficial effect of sGC stimulator, the use of the PDE5 inhibitor sildenafil was demonstrated to prevent CS-induced pulmonary hypertension in a guinea-pig model by reducing PAP (Dominguez-Fandos et al., 2015). Sildenafil has also been shown to return PAP to normal levels, to attenuate vascular remodelling, and prevent hypoxia-induced pulmonary hypertension in a rat model (Sebkhi et al., 2003). Although the long-term effect of sildenafil on pulmonary haemodynamics in patients with COPD is unknown, treatment with sildenafil significantly increases plasma cGMP levels, reduces PAP increase in healthy volunteers breathing 11% O_2, and attenuates pulmonary vascular remodelling in mice exposed to hypoxia (Zhao et al., 2001). In

addition, sildenafil has been reported to produce significant vasodilation in pulmonary circulation and improve pulmonary haemodynamics by reducing PAP and PVR in patients with COPD-associated pulmonary hypertension (Blanco et al., 2010). However, no improvement in exercise capacity has been observed with the use of sildenafil in COPD-related pulmonary hypertension (Rietema et al., 2008, Lederer et al., 2012, Blanco et al., 2013). The apparent absence of a beneficial effect on exercise capacity could be because PDE5 inhibitors possibly worsen gas exchange (Lederer et al., 2012) as consequence of the inhibition of pulmonary hypoxic vasoconstriction (Zhao et al., 2001). For this reason, these vasodilator drugs are currently not approved for the treatment of pulmonary hypertension in COPD (Galie et al., 2016), although there is insufficient evidence to support this theory.

Given the small number of studies available that have assessed the role of eNOS expression and the release of nitric oxide in the development of COPD-associated pulmonary hypertension, the potential usefulness of targeting the nitric oxide pathway in the treatment of pulmonary hypertension associated with COPD needs further attention. Furthermore, an enhanced understanding of the pathway may lead to a targeted therapy worthy of investigation for the treatment of pulmonary hypertension in COPD.

1.3.2 Role of prostanoids and their synthases in COPD-associated pulmonary hypertension

Arachidonic acid (AA) and its metabolite pathway play a key role in the homeostasis of vascular smooth muscle and endothelial cells. Abnormalities in this pathway have been shown to be associated with vascular remodelling and pulmonary hypertension (Chida and Voelkel, 1996, Gomberg-Maitland and Olschewski, 2008).

Vasoactive prostanoids, including prostaglandins (PGs) and thromboxane (TX) are the major metabolites of AA and are formed by COX or prostaglandin G/H synthase. The synthesis of PGs and TX involves the hydrolysis of cellular phospholipids via the action of phospholipase A_2 (PLA_2) enzyme to produce free AA. AA is converted to unstable prostaglandin H_2 (PGH_2) by COX activity, and then to main prostanoids PGI_2, TXA_2, PGD_2, PGE_2 and PGF_2 via their respective synthases PGIS, thromboxane A synthase (TXAS), prostaglandin D synthase (PGDS), prostaglandin E_2 synthases (PGESs) and prostaglandin F synthase (PGFS) (Figure 1.3) (Profit and Chrisp, 2007, Bradbury et al., 2002). Currently, there are nine known prostanoid receptors expressed in different cell types, namely IP for PGI_2, TP for TXA_2, DP_{1-2} for PGD_2, EP_{1-4} for PGE_2, and FP for PGF_2. Activation of these receptors leads to a wide variety of biological effects, particularly vasodilation or vasoconstriction in vascular cells. IP, $EP_{2/4}$ and DP_{1-2} receptors are considered relaxant receptors, while the activation of contractile receptors (TP, $EP_{1/3}$, and FP) is known to induce vasoconstriction (Lang and Gaine, 2015).

There are no reports to date showing the involvement of PGF_2 and PGD_2 in pulmonary vascular remodelling in all forms of pulmonary hypertension. Conversely, PGI_2, TXA_2, and PGE_2 play an important role in maintaining balance in cardiovascular homeostasis (Majed and Khalil, 2012). Although PGI_2/TXA_2 imbalance (Christman et al., 1992) and PGE_2 deficiency (Fan et al., 2018) have been implicated in the development of PAH, studies to date do not provide clear evidence about the role of these vasoactive prostanoids (PGI_2, TXA_2, and PGE_2) in the development of pulmonary hypertension in COPD.

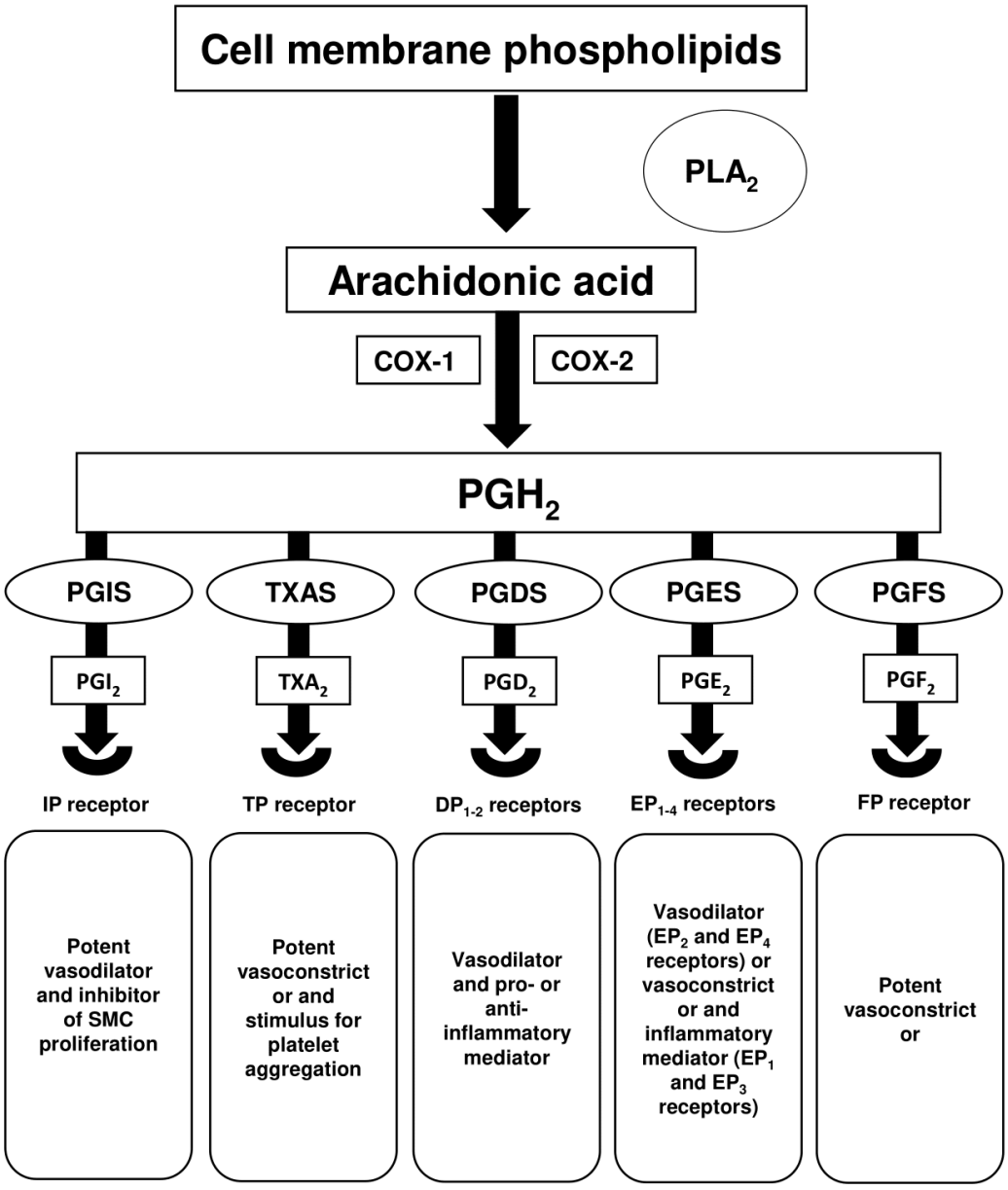


Figure 1.4 Arachidonic acid metabolism
Hydrolysis of cell membrane phospholipids via phospholipase A_2 (PLA_2) releases arachidonic acid (AA), which is then converted by cyclooxygenase-1 (COX-1) and cyclooxygenase-2 (COX-2) to the intermediate prostaglandin H_2 (PGH_2). PGH_2 is converted to multiple prostanoids; prostacyclin (PGI_2), thromboxane A_2 (TXA_2), prostaglandin D_2 (PGD_2), prostaglandin E_2 (PGE_2), and prostaglandin F_2 (PGF_2) via their respective synthases; prostaglandin I synthase (PGIS), thromboxane A synthase (TXAS), prostaglandin D synthase (PGDS), prostaglandin E_2 synthases (PGESs), and prostaglandin F synthase (PGFS).

1.3.2.1 COX-2

There are two isoforms of COX: cyclooxygenase-1 (COX-1) and COX-2. COX-1 is expressed constitutively in many cells and serves as a housekeeping gene, while COX-2 is a highly inducible gene, and its expression is increased in response to inflammation (Smith et al., 2000, DuBois et al., 1994, Subbaramaiah et al., 1996, Sheng et al., 1998). In addition to the role of COX-2 induction in both inflammation and airway remodelling in COPD (Chen et al., 2008), it has long been suggested that COX-2 upregulation is involved in pulmonary vascular remodelling (Chida and Voelkel, 1996). Recently, increased COX-2 protein expression has been reported in both vascular endothelial cells in lung tissues of patients with COPD and CSE-treated human umbilical vein endothelial cells (Shi et al., 2017). CSE treatment has also been shown to induce mRNA expression of COX-2 in human pulmonary microvascular endothelial cells (Nana-Sinkam et al., 2007). Importantly, the COX-2 expression upregulation following CSE stimulation in human umbilical vein endothelial cells and in patients with COPD is associated with an increased cell apoptosis rate (Shi et al., 2017). Interestingly, complete inhibition of COX-2 by the selective COX-2 inhibitor celecoxib further induces human umbilical vein endothelial cell apoptosis, caused by CSE, suggesting that COX-2 may have a protective effect against CSE-induced cell apoptosis. To date, the research on CSE effect on COX-2 has been primarily focussed on the role of COX-2 in CSE-induced endothelial cell apoptosis. However, no studies have comprehensively investigated the effect of CSE on COX-2 expression in human PAECs and particularly in vascular smooth muscle cells, including human PASMCs. In addition, it is largely unknown whether CSE effect on

COX-2 expression in human PASMCs and PAECs has a role in cell functions other than umbilical vein endothelial cell apoptosis, which may be important in vascular remodelling in COPD-pulmonary hypertension.

Besides the effect of CS on COX-2 expression, hypoxia (a key stimulus for vascular remodelling in pulmonary hypertension) has also been reported to induce COX-2 expression in human PASMCs (Bradbury et al., 2002), in rat lungs (Chida and Voelkel, 1996), in human umbilical vein epithelial cells (Bradbury et al., 2002), and in human umbilical vein endothelial cells (Zhao et al., 2012, Schmedtje et al., 1997). Although the use of selective COX-2 inhibitor has been shown to increase endothelin-1 release in human PASMCs (Wort et al., 2002), it has been demonstrated that selective inhibition of COX-2 induction can prevent hypoxic pulmonary vasoconstriction (Kylhammar and Radegran, 2012), the development of pulmonary hypertension in a rat model (Rakotoniaina et al., 2008) and chronic hypoxia-induced pulmonary hypertension in new-born pigs (Fike et al., 2005). It has also been reported that the use of selective COX-2 inhibitor can completely block hypoxia-induced proliferation of human umbilical vein endothelial cells (Zhao et al., 2012). These findings suggest the anti-proliferative effect of COX-2 inhibitor in umbilical vein endothelial cells is likely via the inhibition of prostanoid production. Nevertheless, more studies are needed to determine whether the increase in the expression of COX-2 and the production of its downstream vasoactive prostanoid mediators and cell proliferation by hypoxia observed in human umbilical vein endothelial cells exist in human PAECs, the major regulators of vascular function in pulmonary hypertension. In addition, COX-2 induction in response to hypoxia in experimental human and animal studies may represent an important mechanism by which

aortic smooth muscle cells can increase their capacity for prostanoid production (Camacho et al., 2011). However, the hypoxia effect on COX-2 downstream prostanoid production and the possible contribution of this effect on hypoxia-induced the functional properties of PASMCs in vascular remodelling is unknown.

Collectively, the induction of COX-2 in CS-and hypoxia-treated vascular cells (as well as in the lungs of COPD patients and smokers) suggests a potentially critical role of its downstream vasoactive prostanoid products in vascular remodelling in COPD-associated pulmonary hypertension. It is therefore necessary to understand the effect of CSE and hypoxia, either individually or in combination, on the expression of COX-2 and its downstream vasoactive prostanoid synthases, and on the release of vasoactive prostanoids in human PASMCs and PAECs, as well as the subsequent impact on cell proliferation and apoptosis.

1.3.2.2 mPGES-1 and PGE_2

PGE_2 is a known inflammatory mediator (Yin et al., 2018) and plays a role in regulating blood pressure in pulmonary circulation (Swan and Breyer, 2011). PGE_2 is mainly formed via the metabolism of AA by COX-1 and COX-2. The free AA is converted into PGE_2 via COX enzymes and terminal PGESs. Three different types of PGES may be involved in regulating PGE_2 production: microsomal prostaglandin E synthase-1 (mPGES-1), microsomal prostaglandin E synthase-2 (mPGES-2), and cytosolic PGE_2 synthase (cPGES). mPGES-2 and cPGES are constitutively expressed in several tissues and are known to have a housekeeping role (Murakami et al., 2003), whereas mPGES-1 is expressed at relatively low basal levels and acts as the terminal enzyme downstream of COX enzymes in producing PGE_2 from PGH_2 (Yang and Chen,

2016). Among the three different types of PGES, studies have shown that mPGES-1 is the key enzyme for induced PGE_2 (Sasaki et al., 2015, Chen et al., 2013, Martin and Jones, 2017, Lundequist et al., 2010). Although it is believed that mPGES-1 may have inflammatory effects (Yin et al., 2017) and deletion of mPGES-1 in the vasculature can be a potential novel target for development of anti-inflammatory drugs (Yin et al., 2018), the role of mPGES-1 in vascular remodelling in smokers and all forms of pulmonary hypertension (including COPD-associated pulmonary hypertension) and the effect of CSE and hypoxia on mPGES-1 expression in human vascular cells are largely unknown.

PGE_2 is commonly identified as a pro-inflammatory mediator and has been shown to be involved in the pathogenesis of COPD (Dagouassat et al., 2013) and in vascular diseases (Gomez et al., 2013), via acting on four specific G-protein-coupled receptors in various cell types: EP_1, EP_2, EP_3, and EP_4. PGE_2 production in the vascular cells may lead to either vasodilation or vasoconstriction, depending on its binding receptors (Yang and Chen, 2016). It is suggested that the stimulation of EP_2 and EP_4 receptors could lead to vasodilation by increasing intracellular cyclic adenosine monophosphate (cAMP) concentrations. Vasoconstriction is mediated via the activation of EP_1 and EP_3 receptors by increasing intracellular calcium and decreasing intracellular cAMP concentrations, respectively (Fan et al., 2018). Recently, it has been reported that circulating levels of PGE_2 are reduced in a chronic hypoxia rat model of pulmonary hypertension and in patients with PAH (Fan et al., 2018). Convincingly, the use of highly selective EP_2 receptor agonist butaprost has been shown to cause a significant reduction in proliferation of human PASMCs derived from patients with PAH (Patel et al., 2018). These observations suggest that PGE_2 can induce a vasodilatory/anti-proliferative effect via EP_2

in human PASMCs; however, the potential role of PGE_2 in vascular remodelling in COPD-associated pulmonary hypertension has not been studied.

The effect of CS on mPGES-1 and PGE_2 in human vascular cells (including PASMCs and PAECs) has not been explored. However, hypoxia has been reported to induce PGE_2 in human PASMCs (Bradbury et al., 2002). Hypoxia has also been shown to induce PGE_2 production in human umbilical vein endothelial cells (Zhao et al., 2012). Importantly, exogenous PGE_2 and hypoxia can stimulate proliferation of human umbilical vein endothelial cells, and this cell proliferation can be inhibited by the combined $EP_{1/2}$ receptor antagonist AH6809 (Zhao et al., 2012). These observations suggest that PGE_2 may modulate vascular remodelling via $EP_{1/2}$ receptors. However, whether hypoxia affects PGE_2 production in human PAECs, and whether PGE_2 can play the same role in hypoxia-induced proliferation of PAECs are both unknown.

Taken together, the role of the mPGES-1/PGE_2 pathway in vascular abnormalities in pulmonary hypertension remains controversial, due to the capability of PGE_2 and its receptors to either induce or suppress vasodilatory/anti-proliferative and vasoconstrictive/proliferative effects. To date, the effect of CSE either as a single factor or in combination with hypoxia on mPGES-1 expression and PGE_2 production in human PASMCs and PAECs, and the potential contribution of PGE_2 to CS- and hypoxia-induced vascular remodelling have not been determined.

1.3.2.3 PGIS and PGI_2

PGI_2, also called prostacyclin, a potent vasodilator and an inhibitor of PASMC proliferation, was first reported in 1976 by Needleman and Vane (Needleman et al., 1976). PGI_2 is a downstream product from the sequential enzymatic actions of COX and

PGIS and is considered the predominant prostanoid in vasculature. Within the lungs, PGI_2 is primarily produced in vascular smooth muscle and endothelial cells (Kawabe et al., 2010, Liou et al., 2000) and is quickly transformed by non-enzymatic procedures to a latent hydrolysis item, 6-keto-$PGF_{1\alpha}$ (Wu and Liou, 2005). PGI_2 acts on the IP receptor to induce vasodilatory and anti-proliferative effects as a result of increased intracellular cAMP concentrations.

PGI_2 plays a key role in maintaining local vascular tone. It has been reported that urinary metabolites of PGI_2 are decreased in PAH patients (Christman et al., 1992). In addition, reduced PGIS expression has been observed in the lung tissue of patients with PAH. Importantly, this deficiency of PGIS expression is associated with vascular remodelling (Tuder et al., 1999), suggesting that reduced PGIS expression and PGI_2 release may serve as markers for dysfunction of pulmonary artery cells and vascular remodelling in patients with PAH. In addition to the importance of PGIS/PGI_2 in group 1 pulmonary hypertension, reduced PGIS/PGI_2 has also been reported in the lungs of smokers with COPD, as well as in CSE-treated human umbilical vein endothelial cells (Chen et al., 2012). The study also showed that umbilical vein endothelial cell stimulation with CSE can induce apoptosis, whilst the use of the PGI_2 analogue beraprost sodium prevents CSE-induced cell apoptosis (Chen et al., 2012). The findings of the same group also demonstrated decreased PGI_2 production and induced apoptosis in the lungs of CSE-treated emphysematous rats (Chen et al., 2009), suggesting that the deficiency of PGI_2 in CSE-treated umbilical vein endothelial cells may contribute to cell apoptosis and vascular remodelling. This view is supported by another research group, who showed a downregulation of PGIS mRNA and protein expression and a reduction of PGI_2

production in lung tissue extracts from patients with emphysema (Nana-Sinkam et al., 2007). Consistently, CSE treatment has been shown to reduce the mRNA expression of PGIS in primary human pulmonary microvascular endothelial cells (Nana-Sinkam et al., 2007). These observations suggest PGI_2 may play a crucial role in CSE-induced vascular cell dysfunction and remodelling in COPD. However, the effect of CSE on PGIS expression and PGI_2 release and its contribution to cell apoptosis and proliferation of human PASMCs and PAECs remain to be investigated.

Hypoxia has been demonstrated to induce protective effects by further inducing the constitutively expressed PGIS in human aortic smooth muscle cells and human umbilical vein endothelial cells (Camacho et al., 2011), as well as increasing PGI_2 production in human aortic smooth muscle cells (Camacho et al., 2011) and in human PASMCs (Yang et al., 2002). Although hypoxia can also increase the mRNA expression of PGIS and the stable metabolite of PGI_2 in mice chronically exposed to hypoxia (Camacho et al., 2011), increased PGIS expression and PGI_2 production following the use of PGIS gene transfer has been shown to attenuate medial thickening of small pulmonary arteries and improve hypoxic pulmonary hypertension in a mouse model (Kawakami et al., 2007). Consistently, PGIS overexpression by gene transfer has been reported to provide protection against the development of hypoxic pulmonary hypertension, and to help prevent pulmonary vascular remodelling in a transgenic mouse model (Geraci et al., 1999). In addition, it has been demonstrated that PGI_2 analogue beraprost sodium can inhibit hypoxia-induced human PASMC proliferation (Kadowaki et al., 2007). The ability of PASMCs to produce more PGI_2 following hypoxia exposure, and the role of PGI_2 analogue in preventing proliferation of PASMCs induced by hypoxia, provide early

evidence of the protective effect of PGI_2 in hypoxia-induced vascular remodelling. However, hypoxia effect on PGIS expression and PGI_2 production in human PAECs is unknown. In addition, the effect of hypoxia on the mRNA and protein expression of PGIS in human PASMCs and the contribution of hypoxia effect on PGIS expression and PGI_2 production to the functions of both human PASMCs and PAECs remain to be investigated.

The deficiency of endogenous prostacyclin represents the rationale for targeting the prostacyclin pathway for the treatment of patients with PAH (Gomberg-Maitland and Olschewski, 2008). It is suggested that exogenous and endogenous PGI_2 can induce the relaxation of vascular smooth muscle and inhibit platelet activation (Barst, 2007). Currently, PGI_2 analogues and PGI_2 receptor agonists are used as part of the clinical management for treatment of patients with PAH and have been shown to improve exercise capacity, symptoms, and haemodynamics, although the mortality rate associated with PAH has not been significantly reduced with long-term use (Sitbon et al., 2014, Simonneau et al., 2002, Simonneau et al., 2012, Olschewski et al., 2002, Galie et al., 2002, Hiremath et al., 2010). The significant improvements in signs and symptoms of patients with PAH after administration of PGI_2 analogues and PGI_2 receptor agonists are likely due to the inhibition of smooth muscle cell proliferation and vasodilating effects on pulmonary arteries (Barst, 2007). However, the efficacy of such treatment in patients with pulmonary hypertension in COPD is still unknown due to lack of studies. To the best of our knowledge, only one study has been conducted by Archer and colleagues (1996) to evaluate the effect of PGI_2 analogue in treating mechanically ventilated patients with COPD-associated pulmonary hypertension. Although PVR was initially improved in

the first 24 h, the long-term effect of PGI_2 analogue use in patients with COPD-associated pulmonary hypertension receiving mechanical ventilation was not found to be beneficial (Archer et al., 1996). The life-threatening nature of respiratory failure in these patients with advanced COPD, in addition to the fact that PGI_2 is unstable and degrades quickly, may explain the ineffectiveness of PGI_2 observed in treating such patients. More studies are needed to assess the role of PGI_2 in COPD-associated pulmonary hypertension and the efficacy of PGI_2 analogues and PGI_2 receptor agonists use to treat patients with pulmonary hypertension in stable COPD.

Collectively, human experimental evidence demonstrates an association between reduced PGI_2 and increased cell apoptosis in the lungs of COPD patients and in CSE-treated umbilical vein endothelial cells. In contrast, hypoxia has been shown to induce PGIS/PGI_2, demonstrating an adaptive response to hypoxic stress in vascular cells. Most studies to date suggest a key role for PGIS/PGI_2 in contributing to umbilical vein endothelial cell dysfunction and apoptosis. However, no studies have investigated the effect of CSE, either as a single factor or in combination with hypoxia, on mRNA and protein expression PGIS and PGI_2 production in human PASMCs and PAECs (the two key cell types that play important roles in the development of pulmonary hypertension). Furthermore, how this effect contributes to the proliferation and apoptosis of PASMCs and PAECs has not been explored.

1.3.2.4 TXAS and TXA_2

TXA_2, named after its role in thrombosis, is a potent vasoconstrictor, platelet aggregator, and proliferative mediator with opposing effects to the vasoprotective PGI_2 in regulating vascular tone (Wilson et al., 2004, Ruan et al., 2010). Together with PGI_2,

TXA_2 plays an important role in maintaining homeostatic balance in pulmonary circulation. TXA_2 is one of the downstream products from COX-2 activity and its production is mediated by the enzyme TXAS. TXA_2 is unstable and rapidly converted to the inactive metabolite, thromboxane B_2 (TXB_2) (Ellis et al., 1976). After being produced by TXAS, TXA_2 binds to the TP receptor, stimulates the activation of platelet aggregation, and causes pulmonary vasoconstriction as a consequence of intracellular calcium concentration increase (Chen, 2018, Touyz et al., 2018). Traditionally, platelets were considered the only cellular source of TXA_2. It is now known that TXA_2 is produced in a variety of cells including vascular smooth muscle and endothelial cells.

The balance between vasoconstrictive TXA_2 and vasoprotective PGI_2 is important in the homeostasis of vascular function. It has been reported that the balance between these two vasoactive mediators in patients with PAH is shifted away from PGI_2 towards TXA_2 (Rubin and Badesch, 2005, Badesch et al., 2004, Jones et al., 1995, Christman et al., 1992). Although the role of TXA_2 in COPD-associated pulmonary hypertension is unknown, previous studies suggest CS is a major contributing factor to TXA_2 increase in COPD. Elevated levels of TXA_2 have been reported in the urine of smokers and ex-smokers COPD patients, compared with healthy subjects (Davi et al., 1997). In addition, it has been demonstrated that TXA_2 is increased in both bronchoalveolar lavage fluid and the lung tissue of rat models exposed to CS (An et al., 2013). Consistent with this animal study, CSE has been shown to induce TXA_2 levels in human PAECs (Milara et al., 2010), suggesting that TXA_2 is a key feature of endothelial dysfunction, induced by CS. However, the effect of CSE on TXAS/TXA_2 in human PASMCs and its contribution to PAEC and PASMC apoptosis and proliferation are largely unknown. In addition, the

effect of TXA_2 receptor blockers on CS-induced vascular remodelling in human vascular cells has not been explored.

Like CS, hypoxia can induce pulmonary vasoconstriction and vascular remodelling. However, the involvement of TXA_2 in this process is not understood. It has been reported that TXA_2 levels are increased in arterial and venous plasma of hypoxic rats (Su and Jin, 1989). Increased TXA_2 contributes to pulmonary artery constriction in piglet models of hypoxia-induced pulmonary hypertension. Furthermore, the use of a COX-2 inhibitor diminishes the production of downstream COX-2-dependent constrictors, TXA_2, without adversely affecting other prostanoid production, including PGI_2 release (Fike et al., 2005). Concordant with this, using selective COX-2 inhibitors and selective TP receptor antagonists reduces hyperresponsiveness of pulmonary arteries from mice exposed to chronic hypoxia, through blocking TXA_2-TP receptor signalling (Delannoy et al., 2010). In addition, the use of TXAS inhibitor has been shown to blunt the development of hypoxia-induced pulmonary hypertension in a neonatal piglet model (Hirenallur et al., 2012). Although these *in vivo* data suggest that the induction of TXA_2 production by hypoxia is of critical importance in pulmonary hypertension, there are no cellular studies on the effect of hypoxia on TXAS expression and TXA_2 production in human PAECs and PASMCs. In addition, whether TXAS expression and TXA_2 production effect plays a role in hypoxia-induced vascular remodelling is largely unknown.

As increased TXA_2 has been implicated in the pathogenesis of PAH (Christman et al., 1992), blocking the enhanced TXA_2 effect could restore PGI_2/TXA_2 balance and lead to a therapeutic approach for the treatment of patients with PAH (Kawut et al., 2011,

Robbins et al., 2006). The use of PGI_2 analogues to compensate for the loss of PGI_2 production in patients with PAH has been clinically approved and has demonstrated significant improvements in the symptoms of PAH (Galie et al., 2016). Although early evidence from preclinical animal studies suggests that the inhibition of TXA_2 by synthase inhibition or receptor antagonism can be effective for hypoxic pulmonary hypertension (Delannoy et al., 2010, Hirenallur et al., 2012), TXAS inhibitor and TXA_2 receptor antagonist are not clinically approved for the treatment of patients with PAH and other forms of pulmonary hypertension, due to lack of any evidence for their efficacy.

Taken together, limited data suggest that TXAS-derived TXA_2 may play a key role in the development of COPD-associated pulmonary hypertension. However, it is unclear whether CSE and hypoxia in combination (or each as a single factor) affect the expression of TXAS and the production of TXA_2 in human PASMCs and PAECs and whether TXAS-derived TXA_2 plays a role in CSE- and hypoxia-induced vascular cell proliferation, thereby contributing to vascular remodelling. Interestingly, targeting TXA_2 is not currently used as a therapeutic target for patients with all forms of pulmonary hypertension, including group 3 pulmonary hypertension, due to lack of evidence. More research will need to be conducted to determine the effect of CS and hypoxia on PGI_2 and TXA_2 production downstream of COX-2 and the efficacy of compensating for PGI_2 and blocking TXA_2 effect in preventing CS- and hypoxia-induced proliferation of PAECs and PASMCs.

1.3.3 Endothelin

Endothelin is known as a potent vasoconstrictor and proliferative mediator and was first identified by Yanagisawa and colleagues in 1988 (Yanagisawa et al., 1988). The

initial endothelin gene product, prepro-endothelin is cleaved by endopeptidase to pro-endothelin or big endothelin. The big endothelin is subsequently converted into endothelin isoforms via a specific enzyme, called an endothelin-converting enzyme. There are three different isoforms of endothelin: endothelin-1, endothelin-2, and endothelin-3. Endothelin-1 is a 21-amino acid peptide and is found mainly in the cardiovascular system (Compeer et al., 2012). Endothelin-2 differs from endothelin-1 by only two amino acids, shows similar endothelin pharmacology to endothelin-1, and is found primarily in the myocardium, kidney, and placental tissues (Fagan et al., 2001). Endothelin-3 is found mainly in the nervous system, differs by six amino acids from endothelin-1, and is considered a weaker vasoconstrictor when compared with endothelin-1 (Fagan et al., 2001, Bondurand et al., 2018).

Endothelin, latterly named endothelin-1, is the most studied peptide of the endothelin family. Although the primary source of endothelin-1 is considered to be endothelial cells (Yanagisawa et al., 1988), numerous cell types (e.g PASMCs) can release this peptide *in vitro* upon stimulation with TGF-β1 and pro-inflammatory mediators (Kowalczyk et al., 2015, Markewitz et al., 2001). Once produced, endothelin-1 then binds to either an endothelin-A (ET-A) or endothelin-B (ET-B) receptors (Galie et al., 2004, Galie et al., 2016). ET-B is most often found in vascular endothelial cells, while vascular smooth muscle cells can express both ET-A and ET-B receptors (Fagan et al., 2001). Activation of the ET-B receptor in pulmonary vascular endothelial cells can promote vasodilation by enhancing the release of nitric oxide (Hirata et al., 1993, Rubin and Badesch, 2005). However, the activation of ET-A and ET-B receptors in vascular

smooth muscle cells can lead to vasoconstriction (Xiong et al., 2018, Fukuroda et al., 1994).

Elevated endothelin-1 levels in plasma and lung tissues have been shown to be associated with the pathogenesis of various types of pulmonary hypertension, particularly groups 1 and 2 (Giaid et al., 1993, Stewart et al., 1991), suggesting endothelin-1 may play a role in the development of other types of pulmonary hypertension, such as COPD-associated pulmonary hypertension. However, previous studies investigating the role of endothelin-1 on smokers and patients with COPD have been inconsistent and contradictory. Although it has been reported that the levels of endothelin-1 are unchanged in the lung tissue samples of smokers compared with those of non-smokers (Barbera et al., 2001), increased ET-A and ET-B receptors expression has been observed in pulmonary arteries from smokers and COPD patients (Milara et al., 2012). In addition, an *in vitro* study has shown that CSE induces endothelin-1 mRNA expression and endothelin-1 secretion in both bovine and human PAECs (Lee et al., 2001). It also been reported that CSE induces endothelin release and ET-B receptor protein and mRNA expression in human PAECs (Milara et al., 2010). The same group has also shown that the use of bosentan (an ET-A and ET-B receptors antagonist) can inhibit CSE-induced endothelin receptors expression and CSE-induced proliferation of human PASMCs (Milara et al., 2012).

In addition to CS, hypoxia plays a key role in the development of pulmonary hypertension in COPD (Sakao et al., 2014). However, the contribution of endothelin-1 in this process remains unclear, as results from studies in cultured cells are conflicting. For example, hypoxia induces endothelin-1 mRNA expression in human PAECs (Zhang et

al., 2009) and in human pulmonary microvascular endothelial cells (Minchenko and Caro, 2000), whereas hypoxia reduces endothelin-1 production in cultured rat lung endothelial cells (Markewitz et al., 1995). Interestingly, CS has been shown to reduce plasma levels of endothelin-1 under hypoxic conditions in guinea pigs, although CS and hypoxia individually have been shown to induce plasma levels of endothelin-1 (Ferrer et al., 2011). Thus, there is a need for further *in vitro* investigations to improve our understanding of the effect of CS and hypoxia, either individually or in combination, on the endothelin pathway and the impact of the possible effect in pulmonary vascular remodelling in COPD.

Clinically, the use of bosentan has been shown to foster significant improvement in exercise capacity and haemodynamics in patients with PAH (Galie et al., 2003, Galie et al., 2008, Channick et al., 2001, Rubin et al., 2002). This is supported by *in vitro* studies showing that the stimulation of ET-A and ET-B receptors by endothelin-1 treatment in human PASMCs can promote the proliferation of the cells, and may eventually contribute to vascular remodelling and pulmonary hypertension (Davie et al., 2002). Bosentan has also been shown to inhibit the proliferation of human PASMCs from PAH patients (Kunichika et al., 2004). These observations suggest that targeting ET-A and ET-B receptors may be a promising therapeutic target for the treatment of PAH. Although the use of bosentan has failed clinically to improve exercise capacity, and hypoxaemia has become progressively worse in COPD without severe pulmonary hypertension (Stolz et al., 2008), it has been suggested that the use of bosentan to treat patients with severe or very severe COPD-associated pulmonary hypertension can be beneficial (Valerio et al., 2009).

Taken together, evidence from *in vitro* studies showing the inhibitory effect of ET-A and ET-B receptors antagonist on CSE-induced proliferation of human PASMCs suggests that there may be an important role for the endothelin pathway in CS-induced vascular remodelling in COPD-associated pulmonary hypertension. However, the effect of hypoxia with or without CSE on endothelin release in human PASMCs and PAECs has not been explored. In addition, the contribution of this possible effect to the function of PASMCs and PAECs is yet to be identified.

1.3.4 Electronic cigarette

Conventional cigarette smoking is the leading cause of COPD. As approximately 90% of patients with COPD have some form of smoking history, including cigarette smoking (Kamal et al., 2015), it is becoming increasingly clear that progression of COPD can be prevented in the early stages by smoking cessation (Abman et al., 2015, Hersh et al., 2004). Importantly, the discontinuation of cigarette smoking has been shown to reduce the risk of developing cardiovascular diseases. Thus, patients with COPD are encouraged to quit smoking.

Electronic cigarette (e-cig), invented in 2007, are devices that heat a flavoured or unflavoured liquid (with or without nicotine) to aid smokers in quitting (Morjaria et al., 2017). It has been suggested that the use of e-cig may aid smokers with COPD to quit, consequently reducing the annual rate of COPD exacerbation (Polosa et al., 2016). Based on these considerations, e-cig use is perceived as a safer alternative to conventional cigarette smoking. However, the Centers for Disease Control and Prevention (CDC) recently recommended that users of e-cig should consider refraining from their use. In particular, youths, young adults, or women who are pregnant are recommended to never

use e-cig or vaping products (Siegel et al., 2019). These recommendations are in response to a recent preliminary report of 53 cases in which e-cig or vaping product use-associated lung injury (EVALI) has been identified in Illinois and Wisconsinin, USA in July 2019 (Layden et al., 2019). Following this report, the CDC together with the U.S. Food and Drug Administration (FDA), and other U.S. clinical and public health partners commenced a multistate outbreak investigation of EVALI. As of November 05, 2019, 39 deaths have been confirmed and 2,051 cases of EVALI have been reported by the CDC. However, to date, the underlying cause of EVALI and e-cig substances responsible for the development of EVALI have not been identified due to limited data.

A number of cellular studies have shown that e-cig use may have pro-inflammatory effects in some cell types within the airway. Recently, a study conducted by our group has shown that unflavoured e-cig vapour extract (ECVE) with or without nicotine increases Th2 cytokine interleukin-13 (IL-13) production in human airway smooth muscle cells compared with untreated cells (unpublished observation). Furthermore, it has been reported that human neutrophils exposed to flavoured ECVE with or without nicotine (24 mg/ml, 0 mg/ml total nicotine, respectively) can produce higher levels of matrix metalloproteinase-9 and IL-8 than unstimulated human neutrophils (Higham et al., 2016). The same group has also demonstrated that flavoured ECVE treatment (24 mg/ml total nicotine) causes an increase in the release of IL-6 in cultured human airway epithelial cells compared with untreated cells (Higham et al., 2018). Moreover, primary human airway smooth muscle cells from COPD patients have been shown to produce more IL-8 in response to flavoured ECVE treatment with or without nicotine (18 mg/ml, 0 mg/ml total nicotine, respectively) compared with non-

COPD cells (Bozier et al., 2019). Although it is unknown whether this observed effect is associated with the flavouring in e-cig fluids, the overall observation suggests that ECVE may induce inflammation in cultured cell types of the airway from healthy subjects and patients with COPD. However, to date there has been a lack of any studies assessing the contribution of e-cig use to PASMC and PAEC dysfunction and proliferation.

Endothelial dysfunction plays a key role in the development of pulmonary hypertension. The effect of e-cig use on markers of oxidative stress has been recently assessed in 40 healthy subjects (20 smokers and 20 non-smokers). All subjects were asked to use an e-cig with nicotine for one week after smoking traditional cigarettes. An impairment in endothelial function biomarkers (including an increase in serum levels of NOX2-derived peptide and 8-iso PGF2α, and a decrease in serum levels of nitric oxide) was observed following use of the e-cig in both groups, compared with the baseline and pre-use of the e-cig (Carnevale et al., 2016). In addition, the use of the e-cig appears to be associated with signs of possible vascular changes, as e-cig use causes a rapid increase in the circulating endothelial progenitor cells in the blood of healthy volunteers before endothelial progenitor cells returned to baseline within 1 h of e-cig use (Antoniewicz et al., 2016). In addition, an increase in aortic stiffness and blood pressure has been observed in young cigarette smokers (Vlachopoulos et al., 2016). In line with these observations, it has recently been suggested that nicotine-free inhalation from e-cig use in thirty-one healthy never-smokers can lead to acute endothelial dysfunction, impaired microvascular function, and acute aortic stiffening (Caporale et al., 2019). These clinical studies suggest e-cig use may cause cardiovascular diseases by inducing endothelial dysfunction. However, no data are available on what effect e-cig use with and without the

presence of nicotine may have on human PASMC and PAEC dysfunction. Thus, there is a need to understand the possible effect of e-cig use on the induction of an imbalance between excessive vasoconstrictor and deficient vasodilators in vascular cells.

1.4 Summary

Pulmonary hypertension is a common and serious complication of COPD, characterised by pulmonary vasoconstriction and pulmonary vascular remodelling, including endothelial dysfunction and aberrant PASMC proliferation. Endothelial dysfunction is physiologically characterised by the imbalance between vasodilation and vasoconstriction. It is known that endothelial cells maintain the balance between vasodilator (nitric oxide and PGI_2) and vasoconstrictor (TXA_2 and endothelin-1) mediators and prevent PASMC proliferation. An imbalance with reduced vasodilators and increased vasoconstrictors plays an important role in the development of vascular remodelling in patients with PAH (Christman et al., 1992, Chester and Yacoub, 2014, Stewart et al., 1991). Studies suggest that CS and chronic hypoxia may cause pulmonary vascular remodelling in COPD patients (Sakao et al., 2014, Santos et al., 2002). Preliminary evidence suggests that altered release of vasoactive mediators may also play a role in vascular remodelling in guinea pig model of CS- and hypoxia-induced COPD (Ferrer et al., 2011). In addition, it has recently been suggested that e-cig use may also impair endothelial function (Caporale et al., 2019). However, the possible roles of PAECs, particularly PASMCs, on the vasoactive mediator imbalance in response to CSE, e-cig use, and hypoxia, and how the imbalance may affect cell function (e.g. proliferation), leading to vascular remodelling remain unknown.

1.5 Hypothesis and aims

1.5.1 Hypothesis

We hypothesised that: 1) CSE and hypoxia induce an imbalance between excessive vasoconstrictor and proliferative gene expression and mediator release, and deficient vasodilator and anti-proliferative gene expression and mediator release in human PASMCs and PAECs; 2) The imbalanced vasoactive gene expression and mediator release contribute to aberrant human PASMC and PAEC apoptosis and proliferation, leading to vascular remodelling and pulmonary hypertension in COPD; 3) ECVE may have similar effects as CSE on the induction of imbalanced vasoactive gene expression and mediator release, which then contributes to human PASMC and PAEC apoptosis and proliferation (Figure 1.4).

1.5.2 Aims

The aims of the study were as follows:

- To assess whether CSE can induce imbalanced vasoactive gene expression and mediator release (COX-2, mPGES-1/PGE_2, PGIS/PGI_2, TXAS/TXA_2, eNOS/nitric oxide and endothelin) in human PASMCs and PAECs.
- To evaluate whether hypoxia can cause imbalanced vasoactive gene expression and mediator release in human PASMCs and PAECs, and to investigate whether there is a synergetic or additive effect between CSE and hypoxia.
- To evaluate whether ECVE has similar effects as CSE on the induction of imbalanced vasoactive gene expression and mediator release in human PASMCs and PAECs.

- To examine whether CSE and hypoxia can induce proliferation and apoptosis of human PASMCs and PAECs.
- To assess the role of the altered release of individual vasoactive mediator in CSE- and hypoxia-induced proliferation and apoptosis of human PASMCs and PAECs.

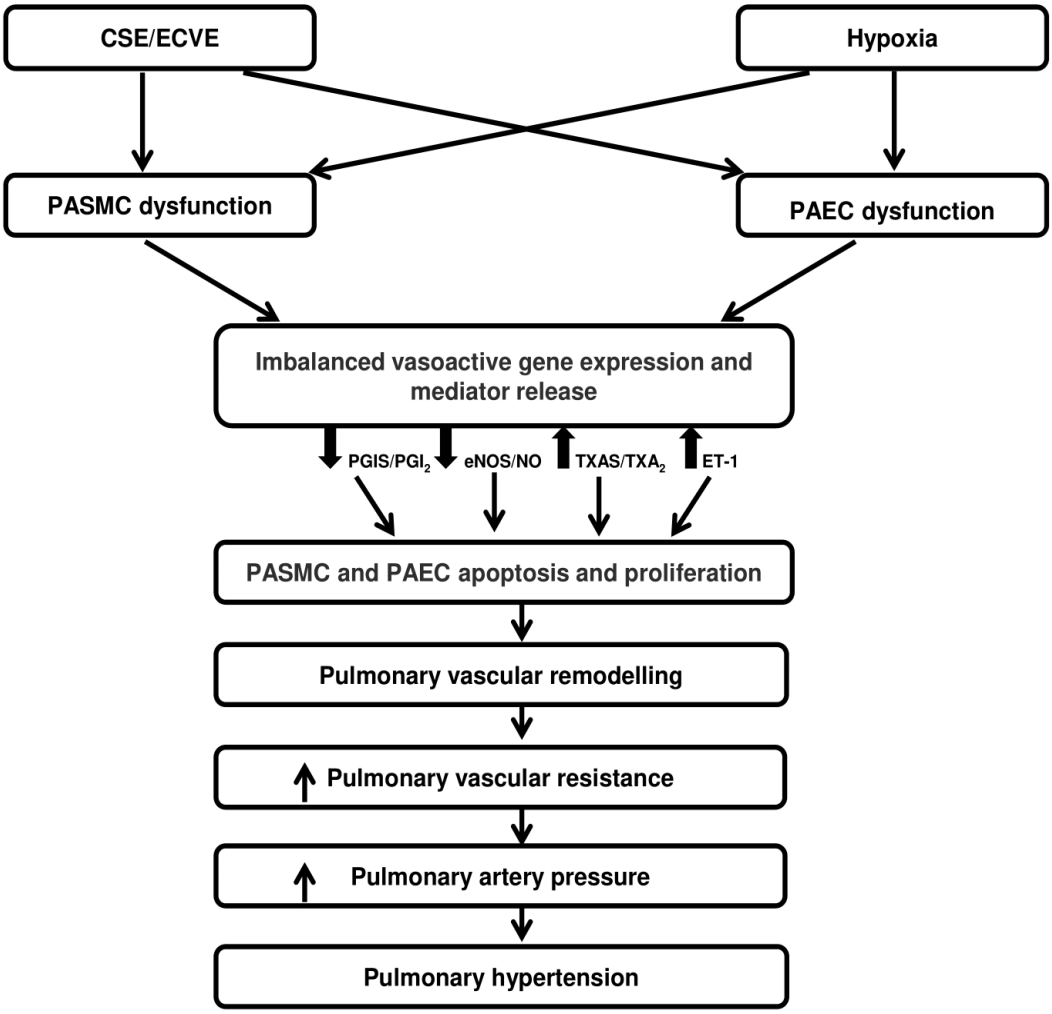


Figure 1.5 Schematic diagram of hypothesis.
This is a schematic diagram to present our proposed hypothesis. Cigarette smoke extract (CSE), e-cigarette vapour extract (ECVE) and hypoxia induce human pulmonary artery smooth muscle cell (PASMC) and pulmonary artery endothelial cell (PAEC) dysfunction. Dysfunction of pulmonary artery cells can cause an imbalance of vasoactive gene expression and mediator release. This imbalance then leads to PASMC and PAEC apoptosis and proliferation, pulmonary vascular remodelling, increased pulmonary vascular resistance, increased pulmonary artery pressure and eventually contributes to pulmonary hypertension. prostaglandin I synthase (PGIS), prostaglandin I_2 (PGI_2), Endothelial nitric oxide synthase (eNOS), Nitric oxide (NO), Thromboxane A synthase (TXAS), Thromboxane A_2 (TXA_2), Endothelin-1 (ET-1).

2. Materials and methods

2.1 Introduction

In this Chapter, the general methods used in this thesis are described. All materials, reagents, kits, buffer and media recipes are listed in the Appendix.

2.2 Cell culture

2.2.1 Culture conditions

All culture mediums and supplements were prepared and maintained according to the instructions of the manufacturer (Appendix 8.10). The cultured cells were maintained in a humidified cell culture incubator, gassed with 21% O_2, 5% CO_2, and 74% N_2 at 37°C. Furthermore, these were checked frequently for bacteria, yeast, or fungi contaminations. The cell culture medium was routinely changed until the cells reached 90%-100% confluence.

2.2.2 Maintenance of cultured cells

2.2.2.1 Pulmonary artery smooth muscle cells

Human PASMCs from three different healthy donors were purchased from (Thermo Fisher Scientific, USA), (Cell Applications, USA), and (Lonza Group, Switzerland). The cells were received at passage 3, sub-cultured according to the instructions of the manufacturer, and used at passage 6. The cells were seeded in cell culture plates at a density of 10,000 cells per cm^2 and maintained in Dulbecco's Modified Eagles Medium (DMEM) with 20% foetal bovine serum (FBS) (DMEM+) (Appendix 8.10) at 37°C, 5% CO_2 in a humidified cell culture incubator until approximately 90% confluence was achieved. Prior to all experiments, human PASMCs were classified as being free from mycoplasma infection.

2.2.2.2 Pulmonary artery endothelial cells

Human PAECs, isolated from the main pulmonary artery of a healthy donor, were obtained from (Promocell, Germany). The cells were received at passage 3, sub-cultured according to the instructions of the supplier, and used at passage 8. The cells were seeded in cell culture plates at a density of 10,000 cells per cm^2 and maintained in a ready-to-use low-serum endothelial cell growth medium (LS-ECGM) (Promocell) (Appendix 8.10) at 37°C and 5% CO_2 in a humidified cell culture incubator until 100% confluence was achieved. Prior to any experiments, human PAECs were classified as being free from mycoplasma infection.

2.2.3 Cell sub-culture

2.2.3.1 Pulmonary artery smooth muscle cells

Early passage cells were seeded in T-225 cm^2 flasks for 7-10 days with the medium being changed every other day until 100% confluence was achieved. Cells were washed with 1× phosphate buffered saline (PBS) and then incubated with 10 ml Trypsin-EDTA solution at 37°C for 5 min. After checking the cells under the microscope to ensure that the detachment occurred, an equal amount of DMEM+ (1:1 ratio) was added to the flask to neutralise trypsiniation. Next, the cells were collected, centrifuged at 1100 rpm for 5 min, and the pellet was re-suspended in fresh DMEM+. Finally, the cells were counted and either frozen in cell freezing solution or seeded into new cell culture flasks for the next passage.

2.2.3.2 Pulmonary artery endothelial cells

The detach kit (Promocell) was used in routine sub-culturing of PAECs. The kit consists of three components: HEPES-buffered balanced salt solution (HEPES-BSS),

Trypsin-EDTA solution, and trypsin neutralisation solution (TNS). Cells were seeded in T-225 cm^2 flasks for 7-10 days with the medium being changed every other day until 100% confluence was achieved. The fully confluent cells were washed with HEPES-BSS and then incubated with 10 ml Trypsin-EDTA solution at 37°C for 5 min. After detachment occurred, an equal amount of TNS (1:1 ratio) was added to the flask to inactivate trypsinisation. Next, the cells were collected, centrifuged at 1100 rpm for 5 min, and then the pellet was re-suspended in fresh LS-ECGM. Finally, the cells were counted and either frozen in cell freezing solution or seeded into new cell culture flasks for the next passage.

2.2.4 Cell counting

In *in vitro* studies, counting cells is often necessary to ensure reproducibility and accuracy (Ongena et al., 2010). Thus, cell counting was performed regularly before seeding cells using a light microscope and an improved Neubauer haemocytometer. To differentiate between live and dead cells, trypan blue was added to the cell suspension (1:1 ratio) and mixed thoroughly. Subsequently, 10 µl of this mix was placed under the coverslip on the haemocytometer and the number of cells in each of the large four squares was counted, including cells lying on the left and top margin of each square. To determine the number of cells per ml, the total number of cells in all four large squares of the hemocytometer was averaged and multiplied by a dilution factor and 10^4.

2.2.5 Cryopreservation of cells

After counting the cells, cell suspension was centrifuged at 1100 rpm for 5 min and the pellet was re-suspended in cell freezing solution (containing 90% FBS and 10% DMSO) for human PASMCs, and in ready-to-use freezing medium (Cryo-SFM) for

human PAECs (supplied by Promocell). The suspended cells were aliquoted in 1 ml cryogenic vials (1 million per ml) and stored at -80°C freezer overnight in a Nunc Cryo freezing container (Thermo Fisher Scientific), containing 100% isopropyl alcohol to freeze cells slowly at a rate of 1°C per min. The cells were then transferred to liquid nitrogen for long-term storage until required.

2.3 Cigarette extract preparation

2.3.1 Cigarette smoke extract

Aqueous CSE from 3R4F research-grade cigarettes (Kentucky Tobacco Research and Development Center, University of Kentucky, USA) (Appendix, section 8.11) was prepared under standardised conditions by bubbling the smoke from two cigarettes into 20 ml DMEM with 0.5% FBS (DMEM-) (Appendix, section 8.10) for human PASMCs or 20 ml LS-ECGM for human PAECs at 1 cigarette per min. The smoke was drawn through the medium using a vacuum pump (Charles Austen Pumps, UK) with a constant pressure of 0.2 bars to achieve a static burning rate. After the resulting CSE was filtered through a 0.22 μm pore size filter, the absorbance at 320 nm was used to measure CSE strength (1.5 =100%) prior to preparation of the desired concentrations using a spectrophotometer (Cecil Instruments, UK) to ensure reproducibility and desired strength (Volpi et al., 2011). For all experiments, the fresh aqueous CSE was made on the day of the experiment and used immediately after preparation.

2.3.2 E-cigarette vapour extract

Flavourless e-cig liquid with and without nicotine ($^{+/-n}$) consisting of 50% propylene glycol/vegetable glycerin mix and the e-cig delivery system used in this study

were obtained commercially from fully licensed and FDA compliant stores, Vapor Vapes and SmokTech, respectively (Appendix, section 8.11).

ECVE was prepared in the same way as CSE from 6 ml of e-cig liquid $^{+/-n}$ (0.24 mg/ml nicotine, with the total nicotine being the same as two cigarettes used for CSE) under standardised conditions by bubbling the vapour into 20 ml DMEM- or 20 ml LS-ECGM at 3 s per puff. The vapour was drawn through the medium using a vacuum pump (Charles Austen Pumps, UK) with a constant vaping at 40 W, ≤ 37°C, and a vacuum pressure of 0.2 bars to achieve a steady vaping rate and to ensure reproducibility. Similar to CSE, the absorbance at 320 nm was initially used to measure ECVE strength using a spectrophotometer. However, no differences were observed between the ECVE and culture medium (control) readings. Because ECVE does not alter the optical density value (Taylor et al., 2016), the resulting ECVE was filtered through a 0.22 μm pore size filter and considered as 100% (Romagna et al., 2013, Taylor et al., 2016). The desired concentrations were prepared accordingly, and then added to the cells already cultured with fresh medium. For all experiments, fresh ECVE was made on the day of the experiment and used immediately after preparation.

2.4 Cell treatment

2.4.1 CSE treatment under normoxic and hypoxic conditions

2.4.1.1 Pulmonary artery smooth muscle cells

Human PASMCs from three healthy donors were seeded in either 6- or 24-well plates at a density of 10,000 cells per cm^2 and maintained in DMEM+ until approximately 90% confluence was achieved. The cells were treated with different concentrations of CSE for 48 h with daily fresh DMEM+ and CSE under normoxic (21%

O_2, 5% CO_2, and 74% N_2) or hypoxic (1% O_2, 5% CO_2, and 94% N_2) conditions. The cells were then cultured for 24 h with fresh DMEM- containing fresh CSE under the same culture conditions. Initially, a pilot study was conducted to determine the desired CSE concentrations. Four CSE concentrations were used: 1%, 2.5%, 5%, and 10%. It should be noted that the 10% CSE concentration was excluded due to cytotoxicity.

2.4.1.2 Pulmonary artery endothelial cells

Human PAECs were seeded in either 6- or 24-well plates at a density of 10,000 cells per cm^2 and maintained in LS-ECGM until 100% confluence was achieved. The cells were treated with different concentrations of CSE for 24 h under normoxic (21% O_2, 5% CO_2, and 74% N_2) or hypoxic (1% O_2, 5% CO_2, and 94% N_2) conditions. Serum starving was not necessary, because LS-ECGM is considered a low-serum cell culture medium (2% foetal calf serum) and especially optimised for endothelial cells from large blood vessels.

Similar to the experimental conditions used with human PASMCs, human PAECs were initially treated with various concentrations of CSE (1%, 2.5%, and 5%) for 72 h. Due to cytotoxicity observed in human PAECs with this condition, a pilot study of extended range of CSE concentrations was conducted to determine the desired concentrations and duration of the treatment. To achieve this, human PAECs were treated with various concentrations of CSE for up to 72 h. Subsequently, the optimal condition (1%, 2%, and 3% CSE for 24 h) was determined.

2.4.2 ECVE treatment

2.4.2.1 Pulmonary artery smooth muscle cells

Human PASMCs from three healthy donors were seeded in a 6-well plate at a density of 10,000 cells per cm^2 and maintained in DMEM+ until approximately 90% confluence was achieved. To maintain the same conditions used in the CSE experiments, cells were treated with different concentrations of $ECVE^{+n}$, one concentration of $ECVE^{-n}$, and one concentration of CSE (5%) as a positive control for 48 h with daily DMEM+. The cells were then cultured for 24 h with fresh DMEM- containing fresh $ECVE^{+/-n}$ and CSE under the same culture conditions. The ECVE concentrations used in this study were 0.1%, 0.25%, 0.5% $ECVE^{+n}$, and 0.5% $ECVE^{-n}$ (as 1% $ECVE^{+/-n}$ was toxic to the cells).

2.4.2.2 Pulmonary artery endothelial cells

Human PAECs were seeded in a 6-well plate at a density of 10,000 cells per cm^2 and maintained in LS-ECGM until 100% confluence was achieved. To maintain the same conditions used in the CSE experiments, the cells were treated with different concentrations of $ECVE^{+n}$, one concentration of $ECVE^{-n}$, and one concentration of CSE (3%) as a positive control for 24 h. ECVE concentrations used in this study were 0.1%, 0.25%, 0.5% $ECVE^{+n}$, and 0.5% $ECVE^{-n}$ (as 1% $ECVE^{+/-n}$ was toxic to the cells).

2.4.3 Effect of drugs

Human PASMCs and PAECs were seeded at a density of 10,000 cells per cm^2 in a 24-well plate. The drugs were dissolved in either cell culture medium or DMSO following the instructions of the manufacturer (final concentration of DMSO = 0.2%). Then, confluent cells were pre-treated with the drugs for 1 h prior to stimulation with

CSE under either normoxic or hypoxic conditions. For the same period of time as the experimental cells, the group of control cells were treated with the drug vehicles.

2.5 Drug preparation

2.5.1 Celecoxib

Celecoxib, a selective COX-2 inhibitor, is an NSAID and is considered 10-20 times more selective for COX-2, with half-maximal inhibitory concentration (IC50) of 40 nM over COX-1 with IC50 of 15 μM. Celecoxib was obtained from Sigma-Aldrich and prepared according to the instructions of the manufacturer (Appendix, section 8.8). The compound was dissolved in DMSO to make an original stock of 0.5 M, diluted in DMSO and then added to the cells already cultured in a manner that maintained the final concentration of DMSO = 0.2%. The groups of control cells were incubated with DMSO for the same period of time as the experimental cells treated with the drugs.

2.5.2 Beraprost sodium

Beraprost sodium is a stable PGI_2 analogue with vasodilatory, antiplatelet, and anti-proliferative effects. Beraprost sodium was purchased from Sigma-Aldrich and prepared following the instructions of the manufacturer (Appendix, section 8.8). The compound was dissolved in DMSO at 0.05 M (original stock), diluted in DMSO, and then used with a final DMSO concentration = 0.2% for both control and experimental groups.

2.5.3 Daltroban

Daltroban, a TXA_2 receptor antagonist, is known to inhibit platelet aggregation and reduce vascular smooth muscle constriction. Daltroban was obtained from Sigma-Aldrich and prepared following the instructions of the manufacturer (Appendix, section

8.8). The compound was dissolved in DMSO at 0.5 M (original stock), diluted in DMSO, and then added together with its vehicle DMSO (group of controls) to the cells already cultured in a manner that maintained the final concentration of DMSO = 0.2%.

2.5.4 PF-03549184

PF-03549184, a potent inhibitor of mPGES-1, is believed to inhibit PGE_2 production. PF-03549184 was purchased from Sigma-Aldrich and prepared according to the instructions of the manufacturer (Appendix, section 8.8). After the drug was dissolved in DMSO at 0.5 M (original stock), a serial dilution was made in DMSO, and then added (in addition to its vehicle DMSO (group of controls)) to the cells already cultured in a manner that maintained the final concentration of DMSO = 0.2%.

2.5.5 Sodium nitroprusside dihydrate

Sodium nitroprusside, a nitric oxide donor, is a rapid-acting vasodilator and platelet aggregation inhibitor. Sodium nitroprusside was purchased from Sigma-Aldrich and prepared following the instructions of the manufacturer (Appendix, section 8.8). As sodium nitroprusside is water-soluble, it was dissolved in the cell culture medium at 0.5 M (original stock), filtered, and added to the cells already cultured to obtain various concentrations.

2.5.6 Bosentan hydrate

Bosentan, a dual ET-A and ET-B receptors antagonist, is a potent vasodilator and effective in the treatment of PAH. Bosentan was obtained from Sigma-Aldrich and prepared according to the instructions of the manufacturer (Appendix, section 8.8). The compound was dissolved in DMSO at 0.5 M (original stock), diluted in DMSO, and then used with a final DMSO concentration = 0.2% for both control and experimental groups.

2.6 Cell lysate preparation

At the end of the experiment, the cell culture medium was collected and cells were washed with ice-cold sterile PBS. Next, 150 µl radioimmunoprecipitation assay (RIPA) buffer (lysis buffer) with other additives (Appendix, section 8.9) was added to each well on ice. The cell lysates were then collected using a cell scraper and centrifuged (11,000 rpm, at 4°C for 5 min) to discard any cellular debris. The proteins in the supernatant were transferred to a fresh tube and store at -80°C until required.

2.7 Bicinchoninic acid protein assay

The bicinchoninic acid (BCA) assay is a colorimetric assay used to measure protein concentration. Thus, the BCA protein assay kit (Thermo Fisher Scientific) was used in this study to assess the total protein concentrations in the experimental samples. The bovine serum albumin (BSA) standard dilutions (2000 µg/ml-0 µg/ml) and the BCA working reagents A:B (1:50) were prepared following the instructions of the manufacturer. Next, 5 µl of the standards and the samples were then added to standard- and sample-wells. This was followed by adding 95 µl of working reagents to each well. The plate was covered and incubated at room temperature for 30 min. Then, the absorbance was measured at 562 nm using a FLUOstar Omega microplate reader (BMG labBtech, UK). The standard curve was used to calculate protein concentrations using Omega analysis software.

2.8 Western blotting analysis

2.8.1 Principle

Western blotting is semi-quantitative technique, commonly used to identify specific proteins from extracted cells or homogenised tissue (Mahmood and Yang, 2012).

Proteins are first separated according to their molecular weight by sodium dodecyl sulphate polyacrylamide gel electrophoresis (SDS-PAGE). The separated proteins are then transferred to polyvinylidene fluoride (PVDF) (BioRad) membrane via an electric current. Next, the membrane is blocked and probed with a primary antibody specific to the protein of interest and horseradish peroxidase (HRP) conjugated secondary antibody. ECL substrate for detection of HRP enzyme activity is finally used to detect bands specific to the protein of interest.

After being collected and quantified for protein concentrations using a BCA assay kit, protein samples were diluted (1:3 ratio) in 4× Laemmli buffer (Appendix, section 8.9) and 60 µl/1 ml β-mercaptoethanol. Prior to sample loading, the samples were boiled at 95-100°C for 10 min to denature the protein.

2.8.2 SDS-PAGE

In this study, SDS-PAGE was used to separate proteins according to their molecular weight. The Mini-PROTEAN Tetra casting system was set up following the instructions of the manufacturer (BioRad, UK), and gels were made using 10% polyacrylamide gel, containing 30% bis-acrylamide gel. Resolving gel was prepared (Appendix, section 8.9) and added to the casting system until the gel was solidified (20 min). Next, stacking gel was prepared (Appendix, section 8.9) and poured on top of the resolving gel and a gel comb was applied for 20 min. Once the gel was solidified and the comb was removed, 10 µl of the rainbow molecular weight markers (Amersham Biosciences) and 20 µg of samples were loaded to the gel. The electrophorator was filled with running buffer (Appendix, section 8.9), closed (red to red and black to black),

connected to a power supply, and electrophoresis was run at 150 constant voltages for approximately 80 min.

2.8.3 Protein transfer

Once the SDS-PAGE step was completed, the gel was carefully removed from the electrophorator and placed in 1× transfer buffer (Appendix, section 8.9). Next, PVDF membrane was soaked in 100% methanol for 30 s and then a sandwich of sponges, filter papers, PVDF membrane, and gel was made in 1× transfer buffer and placed in a Mini Trans-Blot Cell system (BioRad) between the positive and negative electrodes. The electrophoretic transfer system was filled with 1× transfer buffer, placed in ice, and run at 110 constant voltages for 40 min.

2.8.4 Blocking and antibody incubation

Following the transfer step, the membrane was washed 2× 5 min with 1× tris buffered saline plus tween 20 (TBS-T) buffer (Appendix, section 8.9) and then blocked with blocking buffer (Appendix, section 8.9) for 1 h at room temperature to reduce non-specific binding. The membrane was then incubated with a primary antibody in blocking buffer at 4°C overnight. The specificities of antibodies were tested using total cell lysates from cell types known to express the target protein. The antibodies were considered specific for the selected target protein when a single band at the expected molecular weight was detected. The following titrated primary antibodies were used: mouse anti-human COX-2 monoclonal antibody (1:1000), mouse anti-human eNOS monoclonal antibody (1:250), mouse anti-human prostaglandin I_2 synthase antibody (1:1000), mouse anti-human thromboxane synthase antibody (1:1000), and mouse anti-human glyceraldehyde-3-phosphate dehydrogenase (GAPDH) monoclonal antibody (1:2000)

(Appendix, section 8.6). The next day, the membrane was washed 3× 5 min with 1× TBS-T buffer and incubated with secondary antibody in the blocking buffer at room temperature for 1 h. The titrated secondary antibody rabbit polyclonal anti-mouse immunoglobulins/HRP antibody (1:2000) was used (Appendix, section 8.6).

2.8.5 Protein detection

Once the secondary antibody incubation was complete, the membrane was washed 3× 5 min with 1× TBS-T. In a dark room, the membrane was incubated in a mixture of enhanced chemiluminescence (ECL) solutions (1:1 ratio) for 2 min, ensuring that the ECL covered the entire surface of the membrane, before placing the membrane on a plastic wrap facing upwards. The membrane was then exposed to hyperfilm ECL (Amersham Biosciences, UK) for between 3 s and 15 min. After, the film was manually developed first using developer agent (Thermo Fisher Scientific) (1:5 ratio); then, the film was rinsed with water for 10 s. To ensure the film was permanent and light resistant, the fixer agent (Thermo Fisher Scientific) (1:5 ratio) was used, and then the film was dried. Finally, the molecular weight of protein bands was marked by comparing them to the molecular weight marker.

Although BCA was conducted to determine protein concentrations (aiming to achieve equal loading of the protein samples), the membrane was re-probed for a loading control to ensure equal loading of samples. In order to identify the most stable housekeeping gene, a panel of housekeeping genes were evaluated. Since the protein expression of GAPDH remained relatively constant in response to CSE, hypoxia, and ECVE$^{+/-n}$, it was selected as a reference gene for most experiments analysed by Western blot, in the current study, with the exception of the apoptosis biomarkers (section 2.12.2).

ImageJ software (National Institutes of Health, Bethesda, Maryland, USA) was used to quantify protein band density from Western blot (Zhou and Spector, 2008). The values were first normalised to the corresponding GAPDH and then to the control sample. Data were presented as fold changes over control.

2.9 Real-time reverse transcription-quantitative polymerase chain reaction analysis

2.9.1 Principle

Real-time reverse transcription-quantitative polymerase chain reaction (RT-qPCR) analysis is commonly used to determine gene expression within a cell or tissue by assessing the level of messenger RNA (mRNA), a product of gene transcription, which is translated into protein. The first step of RT-qPCR is to isolate total RNA from the sample on ice (due to the natural instability of RNA) using the NucleoSpin RNA II kit (Appendix, 8.7). The next step is to convert the mRNA into complementary DNA (cDNA) via a reverse transcription (RT) step. The final step is the qPCR itself, which consists of three separate steps: denaturation, annealing, and extension. The cycle threshold (C_T) is defined as the number of cycles needed for the fluorescent signal to cross the threshold. The increase in fluorescent signal is proportional to the increase in the amount of cDNA in the sample. In other words, a large amount of template results in few amplification cycles for the fluorescent signal to rise above the background and early C_T.

2.9.2 Total RNA isolation

Confluent cells were treated as required in a 6-well plate. At the end of the experiment, cell culture medium was completely aspirated and cells were washed with PBS, before the total RNA was extracted using the NucleoSpin RNA II Kit (Macherey

Nagel, Germany) according to the protocols of the supplier. All columns and buffers used to isolate total RNA were included in the kit.

After being washed with PBS, the cells were lysed with 350 µl lysis buffer RA1 (with β-mercaptoethanol (10 µl/ml)). Next, the lysed sample was filtered through NucleoSpin filters (pink ring) in a 2 ml collection tube by centrifuging the lysate at 11,000 rpm for 1 min to reduce viscosity and clear the lysate. To adjust the RNA binding condition, the filter was discarded and 350 µl of 70% ethanol was added directly to the collection tube and mixed thoroughly. The lysate was then loaded to the NucleoSpin RNA Column (light blue ring) and centrifuged at 11,000 rpm for 1 min. The column was placed in a new collection tube (2 ml) after the RNA was bound to the silica membrane of the column. Next, 350 µl membrane desalting buffer (MDB) was loaded in the column and then centrifuged at 11,000 rpm for 1 min to remove contaminating salts. Next, 95 µl deoxyribonuclease (DNase) reaction mixture (10 µl reconstituted recombinant (rDNase + 90 µl reaction buffer for rDNase) per sample was added to each column to digest any contaminating DNA on the membrane. The column was then incubated at room temperature for 15 min, washed with 200 µl RAW2 buffer and then centrifuged at 11,000 rpm for 1 min. Then, the silica membrane was washed and centrifuged twice with 600 µl and 250 µl of RA3 buffer, respectively. Finally, the RNA was collected by adding 50 µl RNase-free H_2O, centrifuged at 11,000 rpm for 1 min. The isolated RNA was either used immediately or stored at -80°C until required, as RNA is very unstable.

2.9.3 RNA quantification

A NanoDrop spectrophotometer (Thermo Fisher Scientific) was used to measure the concentration and quality of the RNA. For this, 1.5 µl of each RNA sample was

loaded onto the lower measurement pedestal. The ratio of sample absorbance at 260 and 280 nm was used. A ratio of ~2.0 is accepted as "pure" for RNA. After RNA quantification, 1 µg total RNA of each sample was used for the RT step.

2.9.4 RT

A high-capacity cDNA reverse transcription kit (Applied Biosystems, USA) was used to convert RNA into cDNA. The volume of RT master mix components per reaction was prepared according to the instructions of the supplier as follows: 2 µl of 10× RT buffer, 0.8 µl of 25× deoxynucleotide triphosphate (dNTP) mix (10 mM), 2 µl of 10× RT random primers, 1 µl of MultiScribeTM reverse transcriptase, and 0.2 µl of nuclease-free H_2O. Next, 6 µl of this RT master mix was added into each well of a 96-well reaction plate, followed by 1 µg total RNA. The reaction mixture was made up to 20 µl with nuclease-free H_2O (Table 2.1). The plate was then sealed and centrifuged to eliminate any air bubbles. The RT reaction was placed in a thermal cycler (BioRad). The thermal cycler was programmed following the protocols of the supplier: 25°C for 10 min, 37°C for 120 min, and 85°C for 5 min. The cDNA was then stored at -20°C for further use (Table 2.2).

Table 2.1 A summary of the volume of components used to prepare RT master mix.

Component	Volume
10× RT Buffer	2.0 µl
25× dNTP Mix (100 mM)	0.8 µl
10× RT Random Primers	2.0 µl
MultiScribeTM Reverse Transcriptase	1.0 µl
1 µg total RNA	As required
Nuclease-free H_2O	Up to 20 µl
Total per reaction	20 µl

Table 2.2 A summary of thermal profile of RT reaction.

Step	Temperature	Duration
Step 1	25°C	10 min
Step 2	37°C	120 min
Step 3	85°C	5 min
Step 4	4°C	∞

2.9.5 Primer specificity

The specificities of all primers were tested using a serial dilution of cDNA from untreated cells (1:10, 1:100, 1:1000, and 1:10000). After RT-qPCR was carried out, dissociation curves were generated. Primers were considered specific when dissociation curves contain a single peak.

2.9.6 qPCR

Reversed transcribed cDNA was diluted (1:10 ratio) with nuclease free water. In a qPCR 96-well non-skirted plate, 5 µl of the cDNA sample, 5µl of SYBR green DNA polymerase (Kapa Biosystems, USA), and 1 µl of specific gene primer (0.5 µl of each forward (FW) and reverse (RV)) were transferred to each well (Table 2.3). The SYBR green qPCR primers for the gene targets were obtained from Sigma-Aldrich (Table 2.4). All samples and controls were loaded in duplicates in a qPCR 96-well non-skirted plate. Control (nuclease-free water only) was also included in every experiment to detect any contamination.

Table 2.3 A summary of the volume of components used to prepare qPCR reaction.

Component	Volume
cDNA	5.0 µl
SYBR green DNA polymerase	5.0 µl
10 µM Forward primer	0.5 µl
10 µM Reverse primer	0.5 µl
Total per reaction	11 µl

Table 2.4 FW and RV primer sequences for the target and housekeeping genes.

The gene	Primer Sequences
TXAS	(FW): 5'-CTACTGCAATTACACCACAG-3' (RV): 5'-AAGAGTAAAACCAGGATAGGTC-3'
PGIS	(FW): 5'-GAAAGACTTTTACAAGGATGGG-3' (RV): 5'-ATTGTTTGATGCTGTTGACC-3'
Endothelin-1	(FW): 5'-CAAGCAGGAAAAGAACTCAG-3' (RV): 5'-CTGGTTTGTCTTAGGTGTTC-3'
COX-2	(FW): 5'-AAGCAGGCTAATACTGATAGG-3' (RV): 5'-TGTTGAAAAGTAGTTCTGGG-3'
β2M	(FW): 5'-AAGGACTGGTCTTTCTATCTC-3' (RV): 5'-GATCCCACTTAACTATCTTGG-3'
eNOS	(FW): 5'- CAACCCCAAGACCTACG-3' (RV): 5'- CGCAGACAAACATGTGG-3'

The qPCR reaction consisted of three different cycling procedures (denaturation, annealing, and extension) at different temperatures. The denaturation step was programmed at 95°C for 3 min to separate double-stranded DNA (dsDNA) into single-stranded DNA for amplification, followed by lowering the temperature to 65°C for 15 s for the annealing step to allow primers to bind to the template. Finally, the extension step was programmed at 65°C for 30 s where the new strand of DNA was made by the DNA polymerase enzyme. These steps were repeated for 40 cycles, resulting in an exponential amplification of the selected target sequence using a Stratagene Mx3005P qPCR System (Agilent Technologies, USA) (Table 2.5).

Table 2.5 A summary of thermal profile of the qPCR reaction.

Step	Temperature	Duration	Cycle
Denaturation	95°C	3 min	40
Annealing	65°C	15 s	
Extension	65°C	30 s	

The qPCR results were analysed using MxPro qPCR software (Agilent Technologies) after the C_T values from both controls and samples were obtained. Several methods can be used to analyse the data. In this study, relative quantification normalised to a reference gene method was used. To select the most suitable and stable housekeeping

gene, a panel of housekeeping genes were evaluated initially in treated and untreated samples. Both βeta-2-microglobulin (β2M) and GAPDH remained constant and stably expressed across treated and untreated samples; therefore, β2M was used as a reference gene for all experiments, because it is stable between samples and most routinely used as a housekeeping gene in our lab.

After obtaining average C_T values for the tested and housekeeping genes, the differences (ΔC_T = C_T tested-C_T β2M) were calculated, and then double delta C_T values ($\Delta\Delta C_T$ (ΔC_T treated-ΔC_T control) were obtained. Finally, the values of $2^{-\Delta\Delta CT}$ were calculated to obtain fold changes of the gene expression over control. Data were expressed as relative expression (fold increase).

2.10 Mediator release analysis

2.10.1 PGE_2

2.10.1.1 Assay principle

PGE_2 is produced by COX-2 conversion of arachidonic acid and is known to have either vasodilatory effects via EP_2 and EP_4 receptors, or vasoconstrictive effects via EP_1 and EP_3 receptors. To measure the concentrations of PGE_2 in cell culture supernatants, a PGE_2 ELISA kit-Monoclonal (Cayman Chemical, USA) was used. This is a competitive assay used to measure the level of PGE_2 in tissue culture supernatants, urine, and plasma, with a range of 7.8-1000 pg/ml and a sensitivity of 15 pg/ml (defined as 80% Bound/Maximum Bound (B/B0)). Cross reactivity of the assay is presented in Table 2.6.

Table 2.6 Cross reactivity of PGE_2 ELISA kit-monoclonal.

Cross Reactivity	(%)
Prostaglandin E_2	100%
Prostaglandin E_2 Ethanolamide	100%
Prostaglandin E_2-1-glyceryl ester	100%
Prostaglandin E_3	43.0%
Prostaglandin E_1	18.7%
8-*iso* Prostaglandin E_2	2.5%
All others	<0.01%

This assay is based on a competitive binding between the PGE_2 in the sample and a PGE_2-acetylcholinesterase (AChE) conjugate (PGE_2 tracer). As the variable level of PGE_2 present in the sample competes with the constant amount of PGE_2 tracer to bind to a limited amount of PGE_2 monoclonal antibody, the amount of PGE_2 tracer bound to the antibody is inversely proportional to the amount of PGE_2 in the sample. This antibody-PGE_2 complex then binds to goat polyclonal anti-mouse IgG that has been pre-coated onto the wells. Ellman's reagent (the substrate to AChE) is then added to the well. The reaction of Ellman's reagent results in a distinct yellow colour. The intensity of this distinct yellow colour is proportional to the amount of PGE_2 tracer bound to the well, but is inversely proportional to the amount of free PGE_2 present in the sample.

2.10.1.2 Method

PGE_2 in cell culture supernatants was assessed using a PGE_2 ELISA kit (Cayman Chemical) following the instructions of the manufacturer. At the end of the experiment, the supernatants were collected, the cells were washed with PBS, and the total cell lysate was then collected to determine the protein concentrations in the sample. All samples were stored at -80°C until needed.

After the dilution of all materials and buffers (supplied), the contents of the PGE_2 ELISA standard were diluted in DMEM- or LS-ECGM using two-fold serial dilutions to obtain an eight point standard curve ranging from 1000 pg/ml to 7.8 pg/ml following the

instructions of the manufacturer. Each plate contained a minimum of two blanks, two non-specific binding wells, two maximum binding wells, and an eight point standard curve performed in duplicate. Then, 50 µl of standards, blanks, samples, PGE_2 AChE tracer, and PGE_2 monoclonal antibody were added to the plate. The plate was then covered with plastic film and incubated at 4°C for 18 h. No antibody pre-coating or blocking was required, as polyclonal antibody had been pre-coated onto 96-well plates and blocked.

After incubation, the wells were emptied and rinsed five times with wash buffer, followed by 200 µl of Ellman's reagent for each well. The plate was covered with plastic film to allow the plate to develop in the dark, and was incubated until the maximum binding wells reached a minimum of 0.3 absorbance units (but not exceeding 1.5 absorbance units (blank subtracted)). This assay typically develops in 60-90 min. The optical density was then measured at 420 nm using a FLUOstar Omega microplate reader (BMG labBtech).

PGE_2 concentrations in unknown samples were calculated by using the standard curve. For accuracy and reproducibility, total PGE_2 was calculated (PGE_2 (pg/ml) × total volume of medium (ml)) and normalised to the total amount of protein (protein concentration (mg/ml) × total volume of protein lysate (ml)). The data were then presented as PGE_2 (pg/mg protein).

2.10.2 PGI_2

2.10.2.1 Assay principle

PGI_2, a potent vasodilator and an inhibitor of smooth muscle cell proliferation, is unstable and quickly converted to the major metabolite, 6-keto $PGF_{1\alpha}$ (Wu and Liou, 2005).

Therefore, 6-keto $PGF_{1\alpha}$ is commonly measured as an estimate of PGI_2, as it is an inactive and non-enzymatic hydrolysis product of PGI_2. To measure the concentrations of 6-keto $PGF_{1\alpha}$ in cell culture supernatants, a 6-keto $PGF_{1\alpha}$ ELISA kit (Cayman Chemical) was used. This 6-keto $PGF_{1\alpha}$ ELISA kit is a competitive assay used to measure the level of 6-keto $PGF_{1\alpha}$ in tissue culture supernatants, urine, and plasma, with a range of 1.6-1000 pg/ml and a sensitivity of 6 pg/ml (defined as 80% B/B0). The cross reactivity of the assay is shown in Table 2.7.

Table 2.7 Cross reactivity of 6-keto $PGF_{1\alpha}$ ELISA kit.

Cross Reactivity	**(%)**
6-keto $PGF_{1\alpha}$	100%
6-keto PGE_1	33.9%
Prostaglandin $F_{1\alpha}$	28.0%
Prostaglandin $F_{2\alpha}$	11.0%
2,3-dinor-6-keto Prostaglandin $F_{1\alpha}$	4.9%
Prostaglandin E_2	1.5%
6,15-diketo-13,14-dihydro Prostaglandin $F_{1\alpha}$	0.33%
13,14-dihydro-15-keto Prostaglandin $F_{1\alpha}$	0.05%
Thromboxane B_2	0.05%
All others	<0.01%

The 6-keto $PGF_{1\alpha}$ ELISA rabbit antiserum complex binds to mouse monoclonal anti-rabbit IgG that has been pre-coated onto the wells. As this assay is based on competitive binding between the concentrations of 6-keto $PGF_{1\alpha}$ present in the sample and a 6-keto $PGF_{1\alpha}$-AChE conjugate (6-keto $PGF_{1\alpha}$ Tracer), the variable level of 6-keto $PGF_{1\alpha}$ present in the sample competes with the constant amount of 6-keto $PGF_{1\alpha}$ tracer to bind to a limited amount of 6-keto $PGF_{1\alpha}$ ELISA rabbit antiserum. Thus, the amount of 6-keto $PGF_{1\alpha}$ tracer bound to the 6-keto $PGF_{1\alpha}$ ELISA rabbit antiserum is inversely proportional to the amount of 6-keto $PGF_{1\alpha}$ in the sample.

Ellman's reagent (the substrate to AChE) is added to the well. The reaction of Ellman's reagent results in a distinct yellow colour. The intensity of this distinct yellow colour is

proportional to the amount of 6-keto $PGF_{1\alpha}$ tracer bound to the well, but is inversely proportional to the amount of free 6-keto $PGF_{1\alpha}$ present in the sample.

2.10.2.2 Method

We assessed the 6-keto $PGF_{1\alpha}$ in cell culture supernatants using a 6-keto $PGF_{1\alpha}$ ELISA kit (Cayman Chemical) following the instructions of the manufacturer. At the end of the experiment, the supernatants were collected, the cells were washed with PBS, and then total cell lysate was collected to determine the protein concentration in the sample. All samples were stored at -80°C until needed.

After the dilution of all materials and buffers (supplied), the contents of the 6-keto $PGF_{1\alpha}$ ELISA standard were diluted in DMEM- or LS-ECGM, using two fold serial dilutions to obtain an eight point standard curve ranging from 1000 pg/ml to 1.6 pg/ml following the instructions of the manufacturer. Each plate contained a minimum of two blanks, two non-specific binding wells, two maximum binding wells, and an eight point standard curve performed in duplicate. Then, 50 µl of standards, blanks and samples, 6-keto $PGF_{1\alpha}$ AChE tracer, and the 6-keto $PGF_{1\alpha}$ ELISA rabbit antiserum were added to the plate. The plate was then covered with plastic film and incubated at 4°C for 18 h. No antibody pre-coating or blocking was required, as the 96-well plates were pre-coated with a mouse monoclonal anti-rabbit IgG and blocked. The next day, the wells were emptied and rinsed five times with wash buffer. Then, 200 µl of Ellman's reagent was added to each well. The plate was covered with plastic film to allow the plate to develop in the dark and incubated until the maximum binding wells reached a minimum of 0.3 absorbance units (but not exceeding 1.5 absorbance units (blank subtracted)). This assay

typically develops in 60-90 min. The optical density was then measured at 420 nm using a FLUOstar Omega microplate reader (BMG labBtech).

Next, 6-keto $PGF_{1\alpha}$ concentrations in unknown samples were calculated by using the standard curve. To ensure accurate and reproducible results, the concentrations of 6-keto $PGF_{1\alpha}$ were normalised as described in 2.10.1.2 and then the data were presented as 6-keto $PGF_{1\alpha}$ (pg/mg protein).

2.10.3 TXA_2

2.10.3.1 Assay principle

TXA_2 is produced from arachidonic acid by many cells, and is shown to cause contraction of both vascular and bronchial smooth muscle. TXA_2 is unstable and rapidly converted to the major metabolite, TXB_2 (Ellis et al., 1976). Therefore, TXB_2, the stable metabolite of TXA_2, is used as an estimate of TXA_2 release. To measure the concentrations of TXB_2 in cell culture supernatants, a TXB_2 ELISA kit (Cayman Chemical) was used. This TXB_2 ELISA kit is a competitive assay used to measure the level of TXB_2 in cell culture supernatants, urine, and plasma, with a range of 1.6-1000 pg/ml and a sensitivity of 5 pg/ml (defined as 80% B/B0). The cross reactivity of the assay is shown in Table 2.8.

Table 2.8 Cross reactivity of TXB_2 ELISA kit.

Cross Reactivity	**(%)**
Thromboxane B_2	100%
Thromboxane B_3	33.8%
2,3-dinor Thromboxane B_2	18.5%
11-dehydro Thromboxane B_2	5.4%
11-dehydro Thromboxane B_3	1.6%
Prostaglandin D_2	0.8%
All others	0.1%

The assay is based on competitive binding between the concentrations of TXB_2 present in the sample and a TXB_2-AChE conjugate (TXB_2 tracer). The amount of TXB_2 present in the sample competes with the constant amount of TXB_2 tracer to bind to a limited amount of TXB_2-

specific rabbit antiserum. Thus, the amount of TXB_2 tracer bound to the TXB_2-specific rabbit antiserum is inversely proportional to the amount of TXB_2 in the sample. This TXB_2-specific rabbit antiserum complex then binds to the mouse monoclonal anti-rabbit IgG that has been pre-coated onto the wells.

After appropriate incubation, Ellman's reagent (the substrate to AChE) is added to the well. The reaction of Ellman's reagent results in distinct yellow colour. The intensity of this distinct yellow colour is proportional to the amount of TXB_2 tracer bound to the well but inversely proportional to the amount of free TXB_2 present in the sample.

2.10.3.2 Method

TXB_2 in cell culture supernatants was assessed using a TXB_2 ELISA kit (Cayman Chemical) following the instructions of the manufacturer. At the end of the experiment, the supernatants were collected, the cells were washed with PBS, and then total cell lysate was collected to determine the protein concentration in the sample. All samples were stored at -80°C until needed.

After the dilution of all materials and buffers (supplied), the contents of the TXB_2 ELISA standard were diluted in either DMEM- or LS-ECGM following the instructions of the manufacturer. The concentrations of these standards were 1,000, 400, 160, 64, 25.6, 10.2, 4.1, and 1.6 pg/ml. Each plate contained a minimum of two blanks, two non-specific binding wells, two maximum binding wells, and an eight point standard curve performed in duplicate. Next, 50 µl of standards, blanks and samples, TXB_2 AChE tracer, and a TXB_2-specific rabbit antiserum were added to the plate. The plate was then covered with plastic film and incubated at 4°C for 18 h. No antibody pre-coating or blocking was

required, as the 96-well plates were pre-coated with mouse monoclonal anti-rabbit IgG and blocked.

After incubation, the wells were emptied and rinsed five times with wash buffer. Next, 200 µl of Ellman's reagent was added to each well. The plate was covered with plastic film to allow the plate to develop in the dark and was incubated until the maximum binding wells reached a minimum of 0.3 absorbance units (but not exceeding 1.5 absorbance units (blank subtracted)). This assay typically develops in 90-120 min. The optical density was then measured at 420 nm using a FLUOstar Omega microplate reader (BMG labBtech).

TXB_2 concentrations in unknown samples were calculated by using the standard curve. To ensure accurate and reproducible results, the concentrations of TXB_2 were normalised as described in 2.10.1.2 and then the data were presented as TXB_2 (pg/mg protein).

2.10.4 Nitric oxide

2.10.4.1 Assay principle

Nitric oxide is produced by the enzyme NOS with a half-life of 4 s. As nitric oxide is rapidly converted to its end product (nitrite and nitrate), total nitrate/nitrite fluorometric assay is used as a quantitative measurement of nitric oxide levels in cell culture medium with a detectable range of 60 nM-3.85 µM in two simple steps. The first step is to convert nitrate to nitrite using nitrate reductase. The second step involves the addition of an acidic solution (2, 3-diaminonaphthalene (DAN)) to form fluorescent as a result of the nitrite reaction with DAN and the sodium hydroxide (NaOH) to enhance the fluorescent detection. The intensity of fluorescence is proportional to the amount of total nitrate/nitrite present in the sample.

2.10.4.2 Method

Total nitrate/nitrite in cell culture supernatants was assessed using a nitrate/nitrite fluorometric assay kit (Cayman Chemical) according to the instructions of the manufacturer. At the end of the experiment, the supernatants were collected, the cells were washed with PBS, and then total cell lysate was collected for determination of the protein concentration in the sample. All samples were stored at -80°C until needed.

After the dilution of all materials and buffers (supplied), the contents of the nitrate standard were diluted in LS-ECGM following the instructions of the manufacturer. Concentrations of these standards were 3.85, 1.92, 0.96, 0.48, 0.24, 0.12, and 0.06 μM. Each plate contained a minimum of two blanks and an eight point standard curve performed in duplicate. Next, 80 μl of nitrate standards, samples, and cell culture medium (blank) were added to the appropriate wells. This was followed by adding 10 μl of the nitrate reductase and the enzyme cofactor mixture to each well. The plate was covered with plastic film and incubated at room temperature for 1 h. After the required incubation time, 10 μl of DAN reagent was added to each well and incubated for 10 min. Finally, 20 μl of NaOH was added to each well. A fluorometer was used to measure fluorescence intensity (excitation wavelength of 360 nm and an emission wavelength of 430 nm) using a FLUOstar Omega microplate reader (BMG labBtech).

Total nitrate/nitrite concentrations in unknown samples were calculated by using the standard curve. For accuracy and reproducibility, total nitrate/nitrite was calculated (total nitrate/nitrite (nmol/ml) × total volume of medium (ml)) and normalised to total amount of protein (protein concentration (μg/ml) × total volume of protein lysate (ml)). The data were then presented as total nitrate/nitrite (nmol/μg protein).

2.10.5 Endothelin

2.10.5.1 Assay principle

To measure the concentrations of endothelin in cell culture supernatants, an endothelin ELISA kit (Cayman Chemical) was used. This endothelin ELISA kit is a double-antibody 'sandwich' technique used to measure the level of endothelin in tissue culture supernatants, urine, and plasma, with a range of 7.8-250 pg/ml, a sensitivity of 7.8 pg/ml, specificity of 100% for pro-endothelin-1, endothelin-1, endothelin-2, and endothelin-3 detection, and no cross-reactivity with other factors.

The plate has been pre-coated with a monoclonal antibody specific for endothelin. This endothelin capture antibody binds to any endothelin-1, endothelin-2, or endothelin-3 present in the sample. After the addition of the sample and standard, an acetylcholinesterase:Fab (AChE:Fab) conjugate is added to bind selectively to a different epitope on the endothelin molecule. These two antibodies (endothelin capture antibody and AChE:Fab conjugate) form a 'sandwich' by binding to the endothelin present in the sample. The enzymatic activity of the AChE is measured by the addition of Ellman's reagent (substrate for AChE) to each well. The reaction of Ellman's reagent results in distinct yellow colour. The intensity of this distinct yellow colour is directly proportional to the amount of free endothelin present in the sample.

2.10.5.2 Method

Endothelin ELISA kit (Cayman Chemical) was used to assess the concentrations of endothelin in cell culture supernatants following the instructions of the manufacturer. At the end of the experiment, supernatants were collected, the cells were washed with PBS, and then total cell lysate was collected for protein quantification and stored at -80°C

until needed. All materials and buffers (supplied) were prepared. The contents of the endothelin ELISA standard (7.8-250 pg/ml) were diluted in either DMEM- or LS-ECGM following the instructions of the manufacturer. The ready to use 96-well plate, included with this endothelin ELISA kit, contained a minimum of two blanks and an eight point standard curve performed in duplicate.

According to the instructions of the manufacturer, 100 µl of endothelin ELISA standards, samples, and endothelin AChE Fab conjugate were added to the wells. The plate was then covered with plastic film and incubated overnight at 4°C. The following day, wells were emptied and rinsed five times with wash buffer. The plate was dried and 200 µl of Ellman's reagent was added to each well. In darkness, the plate was covered with plastic film and allowed to develop using an orbital shaker. The absorbance was periodically checked and the concentrations of endothelin were determined at a wavelength of 412 nm, once the absorbance of the highest value of the standard reached 0.3 absorbance units (blank subtracted). This was achieved using a FLUOstar Omega microplate reader (BMG labBtech).

Endothelin concentrations in unknown samples were calculated using the standard curve. To ensure accurate and reproducible results, the concentrations of endothelin were normalised as described in 2.10.1.2, and then the data were presented as endothelin (pg/mg protein).

2.11 Cell proliferation analysis

Cell proliferation is defined as an increase in cell number and can be measured either directly or indirectly. Although measuring cell proliferation directly (by counting the number of cells) is considered a gold standard method, other indirect measurements

of cell proliferation are widely used. This is because the nonradioactive assays, such as cell proliferation reagent water-soluble tetrazolium-1 (WST-1) and the cell counting kit-8 (CCK-8) are less toxic, more convenient, accurate, sensitive, and fast. Therefore, WST-1 was used as a primary method to assess cell proliferation in this study, and CCK-8 was used as a secondary method.

2.11.1 Cell proliferation reagent WST-1

2.11.1.1 Assay principle

WST-1-based colorimetric assay is used for the nonradioactive quantification of induction and inhibition of cell proliferation *in vitro* studies. Cell proliferation reagent WST-1 (4-(3-(4-Iodophenyl)-2-(4-nitrophenyl) 2H-5-tetrazolio)-1,3-benzene disulfonate) (Sigma-Aldrich), containing an electron mediator, is a ready-to-use solution based on the enzymatic conversion of the stable tetrazolium salt WST-1 into a soluble formazan by mitochondrial dehydrogenase in the viable cells. This biological reduction of WST-1 reagent to formazan in the presence of electron mediator 1-methoxy-5-methyl-phenazinium methyl sulfate is dependent on the production of glycolytic nicotinamide adenine dinucleotide phosphate (NADPH). Consequently, this complex cellular mechanism, occurring primarily at the cell surface, results in a distinct yellow colour. The intensity of this distinct yellow colour (formazan dye) is directly proportional to the number of metabolically active cells in the culture.

2.11.1.2 Method

Cell proliferation was assessed using cell proliferation reagent WST-1 (Sigma-Aldrich) following the instructions of the manufacturer. Human PASMCs and PAECs (10,000 cells per cm^2) were seeded in a 24-well plate until cells reached approximately

90% confluence. At the end of the experiment, supernatants were aspirated and 250 µl of either DMEM- or LS-ECGM with 10% of cell proliferation reagent WST-1 was added to each well and incubated at 37°C for approximately 30 min to reduce the reagent into the dye form. After this incubation period, the plate was shaken thoroughly for 1 min on a shaker, and 100 µl of the solution in each well was transferred to a new 96-well plate. This was to measure absorbance at 480 nm using a FLUOstar Omega microplate reader (BMG labBtech). The absorbance of the samples was measured against a background control, and data were presented as % change over control (100%)

2.11.2 CCK-8

2.11.2.1 Assay principle

CCK-8 is a sensitive colorimetric assay used for nonradioactive quantification of the number of viable cells in the proliferation and cytotoxicity assays using water-soluble tetrazolium-8 (WST-8, 2-(2-methoxy-4-nitrophenyl)-3-(4-nitrophenyl)-5-(2,4-disulfophenyl)-2H-tetrazolium, monosodium salt)). To further confirm cell proliferation, CCK-8 (Sigma-Aldrich) was used as a secondary method. CCK-8 (Sigma-Aldrich) is a ready-to-use solution, and is based on the conversion of stable tetrazolium salt WST-8 in the presence of an electron mediator (1-methoxy PMS) into a soluble formazan by mitochondrial dehydrogenase in the sample. This complex cellular mechanism results in distinct formazan dye. The intensity of this distinct yellow colour (formazan dye) is directly proportional to the number of metabolically active cells in the culture.

2.11.2.2 Method

CCK-8 (Sigma-Aldrich) was used as a secondary method to confirm cell proliferation, which was performed following the instructions of the manufacturer.

Human PASMCs and PAECs (10,000 cells per cm^2) were seeded in a 24-well plate until cells reached approximately 90% confluence. Supernatants were aspirated following appropriate stimulation, and 250 µl fresh DMEM- or LS-ECGM, including 10% of cell proliferation reagent CCK-8, was added to each well and incubated at 37°C for approximately 30 min to reduce the reagent into the dye form. After this incubation period, the plate was shaken thoroughly for 1 min. Next, 100 µl of the solution in each well was transferred to a new 96-well plate to measure absorbance at 450 nm using a FLUOstar Omega microplate reader (BMG labBtech, UK). The absorbance of the samples was measured against a background control. Data were presented as % change over control (100%).

2.12 Apoptosis analysis

2.12.1 Annexin v human ELISA kit

2.12.1.1 Assay principle

Annexin A5, commercially known as annexin v, is a calcium-dependent phospholipid-binding protein. Annexin v binds to procoagulant phospholipids with high affinity, and its preferential binding partner is phosphatidylserine (PS), a marker of apoptosis located on the outer surface of the plasma membrane. Therefore, measuring the concentrations of annexin v in cell culture supernatants by ELISA is commonly used to detect PS that is exposed on the outside of apoptotic cells. To measure the concentrations of annexin v in cell culture supernatants, an annexin v human ELISA Kit (Thermo Fisher Scientific) was used. This kit is capable of measuring the amount of the target bound between a matched antibody pair in both cell culture supernatants and serum with a range of 0.78-50 ng/ml and a sensitivity of 0.33 ng/ml. Annexin v present in the sample or

standard binds to an anti-human annexin v coating antibody that has previously been attached to the wells, followed by the addition of biotin-conjugated anti-human annexin v (secondary antibody) to form a sandwich. To produce a measurable signal, streptavidin-HRP and substrate solution (supplied) are added to the wells. The reaction of substrate solution results in distinct colour. The intensity of this distinct colour is directly proportional to the concentrations of annexin v present in cell culture supernatants.

2.12.1.2 Method

An annexin v human ELISA kit (Thermo Fisher Scientific) was used to assess the concentrations of annexin v in cell culture supernatants following the instructions of the manufacturer. A pre-coated 96-well plate with anti-human annexin v coating antibody, reagents, and buffers used were supplied with the kit. At the end of the experiment, the supernatants were collected, the cells were washed with PBS, and then total cell lysate was collected. All samples were stored at -80°C until required. Following the preparation of all materials and buffers, the annexin v ELISA standards (0.78-50 ng/ml) were serially diluted in the culture medium. The pre-coated 96-well plate contained a minimum of two blanks and seven point standard curve performed in duplicate.

According to the instructions of the manufacturer, 100 µl annexin v ELISA standards and samples were added to the standard and sample wells, followed by 50 µl Biotin-Conjugate to each well. The plate was then covered with plastic film and incubated for 2 h at room temperature. After the appropriate incubation, wells were emptied and rinsed five times with wash buffer. Next, 100 µl streptavidin-HRP was added to each well. The plate was then covered and incubated for 1 h at room temperature. The wells were emptied and rinsed five times with wash buffer, 100 µl TMB

substrate solution was added to all wells, and then the plate was allowed to develop in the dark for approximately 10 min. To stop the reaction, 50 µl stop solution was added and the concentrations of annexin v were obtained at a wavelength of 450 nm using a FLUOstar Omega microplate reader (BMG labBtech). The annexin v concentrations in unknown samples were calculated using the standard curve.

2.12.2 Apoptosis western blot cocktail biomarkers

2.12.2.1 Assay principle

The apoptosis Western blot cocktail (Abcam, UK) is commonly used to assess the induction of apoptosis in response to various stimuli. Mainly, this cocktail detects two apoptosis biomarkers, which are caspase 3 and Poly [ADP-ribose] polymerase 1 (PARP1). Caspase 3, an important marker for regulating cell death, is activated by proteolytic cleavage during apoptosis. It is known that the induction of apoptosis decreases pro-caspase 3 (32 kDa), whereas the cleaved caspase 3 (17 kDa) is increased in response to apoptosis stimuli. Both pro-caspase 3 and cleaved caspase 3 can be detected using this cocktail antibody. During apoptosis, caspase 3 cleaves PARP1 (89 kDa), a critical enzyme involved in DNA repair. Although the full-length PARP1 can not be detected by this antibody, the combined detection of both cleaved PARP1 and cleaved- and pro-caspase 3 allows for a convenient estimation of apoptosis. In this study, GAPDH was used as a reference gene for most experiments analysed by Western blot. Given the similar molecular weights of the protein of interest pro-caspase 3 (32 kDa) and GAPDH (35 kDa), β-2 actin (42 kDa) was used as a loading control for sample normalisation due to its different molecular weight and constant expression in response to the different stimuli used in the current study.

2.12.2.2 Method

Following appropriate stimulation of confluent human PASMCs and PAECs and at the end of the experiment, the cells were washed with PBS and total cell lysate was collected to assess the levels of apoptosis markers using Western blotting (materials and methods, section 2.8). The samples were stored at -80°C until needed. Briefly, the separated proteins (according to their molecular weight by SDS-PAGE) were transferred to a PVDF membrane via an electric current to produce a band for each protein. The membrane was then blocked with blocking buffer at room temperature for 1 h. Next, the membrane was probed with primary antibodies (1:250) for 1 h, washed 3× 5 min with 1× TBS-T, and incubated with secondary antibody in blocking buffer for 2 h at room temperature. The membrane was washed 3× 5 min with 1× TBS-T, incubated in a mixture of ECL solutions (1:1 ratio) for 2 min, and then the proteins were detected by developing the film in the dark room.

2.13 Cell viability

The cytotoxicity of CSE, hypoxia, and $ECVE^{+/-n}$ treatments on both human PASMCs and PAECs was assessed using 3-(4,5-dimethylthiazol-2-yl)-2,5-diphenyltetrazolium bromide (MTT) assay (Sigma-Aldrich). Cells were seeded in a 24-well plate. Following the appropriate treatments and incubation, the cell culture medium was aspirated at the end of each experiment and replaced with 250 µl MTT solution (dissolved in low serum medium) at a concentration of 1 mg/ml. Then, the plate was incubated at 37°C for 30 min. The medium was aspirated and the plate was allowed to dry at room temperature for approximately 6 h. To dissolve the blue-coloured tetrazolium, 250 µl DMSO was added to each well, mixed thoroughly, and then 100 µl

was transferred in duplicate to a 96-well plate to measure absorbance at 550 nm using a FLUOstar Omega microplate reader (BMG labBtech). Cell viability data were expressed as fold change over control.

2.14 Statistical analysis

Data were expressed as mean ± standard error of the mean (SEM) from experiments conducted in the specified number of cell lines unless otherwise stated. GraphPad Prism 7 was used to perform the statistical analysis. An unpaired Student's t test was carried out to compare two data sets. A one-way analysis of variance (ANOVA) followed by a t-test was performed to determine whether the differences between the control and the treated cells were significant. P values less than 0.05 were considered statistically significant.

Chapter 3. Effect of CSE on vasoactive gene expression and mediator release in human PASMCs and PAECs

3.1 Introduction

Pulmonary hypertension in patients with COPD is associated with increased mortality and morbidity and is characterised by pulmonary vasoconstriction and vascular remodelling as a result of cell proliferation (Zakynthinos et al., 2011). The balance between vasodilator and vasoconstrictor mediators maintains the physiological endothelial function and prevents PASMC proliferation. In patients with PAH, an imbalance with reduced vasodilators (e.g. nitric oxide and PGI_2) and increased vasoconstrictors (e.g. TXA_2 and endothelin-1) plays an important role in the development of vascular remodelling (Christman et al., 1992, Chester and Yacoub, 2014, Stewart et al., 1991). Pulmonary vascular remodelling, including vascular smooth muscle cell proliferation in the thickened intimas, has also been reported in patients with moderate COPD, as well as in smokers with no obvious signs of lung disease (Santos et al., 2002). This suggests that CS may contribute to pulmonary vascular remodelling in COPD patients. An accumulating body of evidence suggests that endothelial dysfunction, associated with an imbalance of reduced vasodilators/anti-proliferative and increased vasoconstrictors/proliferative may play a role in the cause of CS-induced pulmonary vascular remodelling in COPD (Ferrer et al., 2011, Ferrer et al., 2009). Whether CS, the major risk factor for COPD, can induce the imbalance in vasoactive gene expression and in the release of the consequent mediators in human PAECs and PASMCs is unknown. In addition, the extent of the imbalance, the role of the imbalanced individual vasoactive mediator in the cell function (e.g. proliferation) leading to vascular remodelling, and the contribution of PAECs, particularly PASMCs, in this process have not been explored.

3.2 Aims

Within this Chapter, we sought to assess whether CSE can induce imbalanced vasoactive gene expression and mediator release in human PAECs and PASMCs, the two major cell types in the vasculature that play a crucial role in the pathobiology of pulmonary hypertension.

The specific aims of this Chapter are:

- To determine the effect of CSE on the mRNA and protein expression of key enzymes of prostanoid synthesis, and the release of vasoactive lipid mediators, including COX-2, mPGES-1/PGE_2, PGIS/PGI_2, and TXAS/TXA_2 in human PASMCs and PAECs.
- To examine whether CSE has an effect on the mRNA and protein expression of eNOS and the production of nitric oxide in human PASMCs and PAECs.
- To assess the effect of CSE on the expression of endothelin-1 and the production of endothelin in human PASMCs and PAECs.

3.3 Materials and methods

3.3.1 Cigarette smoke extract preparation

Aqueous CSE was prepared as previously described in the materials and methods, section 2.3.1. A pilot study of extended range of CSE concentrations and duration of the treatment as described in materials and methods, section 2.4 was conducted before the optimal condition for each cell type was chosen. For all experiments, the fresh aqueous CSE was made on the day of the experiment and used immediately after preparation.

3.3.2 Cell treatment

3.3.2.1 Pulmonary artery smooth muscle cells

Human PASMCs from three different healthy donors at passage 6 were seeded in a 6-well plate at a density of 10,000 cells per cm^2 and maintained in DMEM+ until approximately 90% confluence was achieved. The cells were treated with different concentrations of CSE (0%, 1%, 2.5%, and 5%) for 48 h with daily fresh DMEM+ and CSE. The cells were then cultured for 24 h with fresh DMEM- containing fresh CSE under the same culture conditions. At the end of the experiment, supernatants, total RNA, and total cell lysates were collected.

3.3.2.2 Pulmonary artery endothelial cells

Human PAECs, isolated from main pulmonary artery of a healthy donor, were used at passage 8. The cells were seeded in a 6-well plate at a density of 10,000 cells per cm^2 and maintained in the LS-ECGM in a humidified cell culture incubator until 100% confluence was achieved. The cells were then treated with CSE for 24 h. The resulting supernatants, total RNA, and total cell lysates were collected.

3.3.3 RT-qPCR

Following cellular experimentation and total RNA isolation, RT-qPCR analysis was used to measure the mRNA expression of COX-2, PGIS, TXAS, endothelin-1, and eNOS (materials and methods, section 2.9). It should be noted that β2M was used as a reference gene for all experiments. Data were expressed as relative expression (fold change).

3.3.4 Western blotting

Total cell lysates of human PASMCs and PAECs stimulated with different concentrations of CSE for 72 h and 24 h, respectively, were collected and analysed for COX-2, mPGES-1, PGIS, TXAS, and eNOS proteins using Western blotting (materials and methods, section 2.8). GAPDH was used as loading control to ensure an equal loading of samples.

3.3.5 ELISA

Supernatants were collected following human PASMC and PAEC stimulation with CSE for 72 h and 24 h, respectively, and assayed for PGE_2, 6-keto $PGF_{1\alpha}$, TXB_2, and endothelin using ELISA analysis (materials and methods, section 2.10). Data were normalised with total protein and expressed as pg/mg protein.

3.3.6 Nitrate/nitrite assay

Following cellular experimentations (as described in materials and methods, section 2.4) and supernatants collection, total nitrate/nitrite in cell culture supernatants was assessed using fluorometric assay (materials and methods, section 2.10). Data were normalised with total protein and presented as nmol/μg protein.

3.4 Results

3.4.1 Effect of CSE on the mRNA and protein expression of COX-2 and PGE_2 production in human PASMCs and PAECs

COX-2 is regarded as a vasoactive gene, and its induction is important in mediating the production of its downstream prostanoid products that have potent anti-proliferative (e.g PGE_2 and PGI_2) and proliferative (e.g TXA_2) properties in vascular diseases (e.g. pulmonary hypertension). However, the effect of CSE on the mRNA and protein expression of COX-2 in both human PASMCs and PAECs is largely unknown. Thus, we started this study by stimulating human PASMCs with different concentrations of CSE for 72 h. At the end of the experiment, total RNA was isolated and the samples were assayed for the mRNA expression of COX-2 using RT-qPCR. The results, as shown in Figure 3.1, revealed that human PASMCs expressed COX-2 mRNA at basal levels. CSE treatment at the lowest two concentrations tested (1% and 2.5%) had no significant effect on COX-2 mRNA expression. Following cell stimulation with 5% CSE, the mRNA expression of COX-2 was significantly upregulated compared with unstimulated PASMCs (fold change 5.6±1.3, $p<0.05$) (Figure 3.1). Next, human PAECs were incubated with different concentrations of CSE for 24 h. Following total RNA isolation, RT-qPCR analysis was used to assess the mRNA expression of COX-2. COX-2 mRNA was basally expressed in PAECs. A significant increase of COX-2 mRNA expression was noted at all CSE concentrations tested (1%, 2%, and 3%) (fold change 2.0±0.28, 2.0±0.17, 2.7±0.40, respectively, $p<0.05$ for all) compared with untreated PAECs (Figure 3.2). This upregulation of COX-2 mRNA expression by CSE in both PASMCs and

PAECs suggests that CSE can upregulate COX-2 gene expression via a transcriptional mechanism.

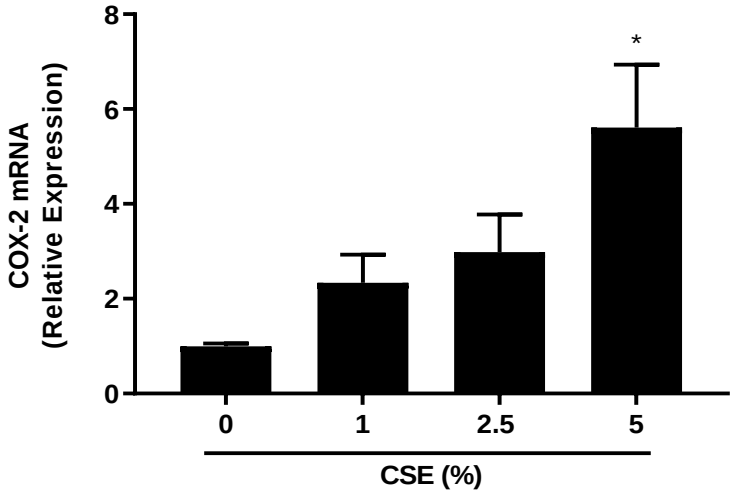


Figure 3.1 Effect of CSE on the mRNA expression of COX-2 in human PASMCs.
Confluent human PASMCs were stimulated with different concentrations of CSE (0%, 1%, 2.5%, and 5%) for 48 h with daily fresh DMEM+ and CSE and then with the same concentrations of CSE in DMEM- for 24 h. Total RNA was isolated and the samples were then assayed for the mRNA expression of COX-2 using RT-qPCR. Data were expressed as fold change over unstimulated cells (0% CSE). Each data point represents mean ± SEM from three independent experiments using cells from three different donors. *p<0.05 compared with unstimulated cells.

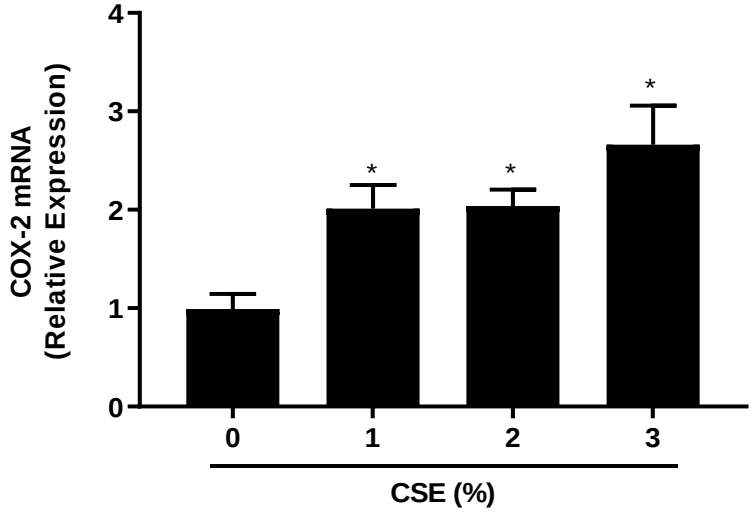


Figure 3.2 Effect of CSE on the mRNA expression of COX-2 in human PAECs.
Confluent human PAECs were treated with different concentrations of CSE (0%, 1%, 2%, and 3%) for 24 h prior to total RNA isolation. The samples were assayed for the mRNA expression of COX-2 using RT-qPCR. Data were expressed as fold change over untreated cells (0% CSE). Each data point represents mean ± SEM from three independent experiments using one cell line. *p<0.05 compared with untreated cells.

We next questioned whether the upregulation of COX-2 mRNA expression by CSE could lead to increased COX-2 protein expression. We found that the protein expression of COX-2 was undetectable in untreated PASMCs. Treatment with CSE induced COX-2 protein expression in a concentration-dependent manner (Figure 3.3A and B). Densitometry analysis showed that treatment with 1% and 2.5% CSE caused a modest but significant induction of COX-2 protein expression (fold change 5.1±1.4, 7.7±1.7, respectively, $p<0.05$ for all) over basal levels. This modest induction was followed by a further increase of COX-2 protein expression in response to 5% CSE (fold change 9.7±0.8, $p<0.001$) as shown in Figure 3.3B, compared with untreated PASMCs. The results also showed that the protein expression of COX-2 was undetectable at basal levels in human PAECs. Consistent with our findings from PASMCs, CSE treatment increased COX-2 protein expression in a concentration-dependent manner in human PAECs (Figure 3.4A and B). Although cell treatment with 1% CSE had no effect on the protein expression of COX-2, significant upregulation was observed in response to 2% and 3% CSE (fold change 18.8±6.1, $p<0.05$ and 62.9±13.1, $p<0.01$, respectively) compared with untreated PAECs as shown in the densitometry analysis (Figure 3.4B).

These observations suggest that the protein expression of COX-2 can also be regulated by CSE. Collectively, the mRNA and protein data suggest that CSE may regulate COX-2 expression via transcriptional regulation, and that upregulation of COX-2 in both human PASMCs and PAECs may play a role in CS-induced dysfunction of pulmonary artery cells and vascular remodelling by mediating the induction of imbalanced prostanoid production.

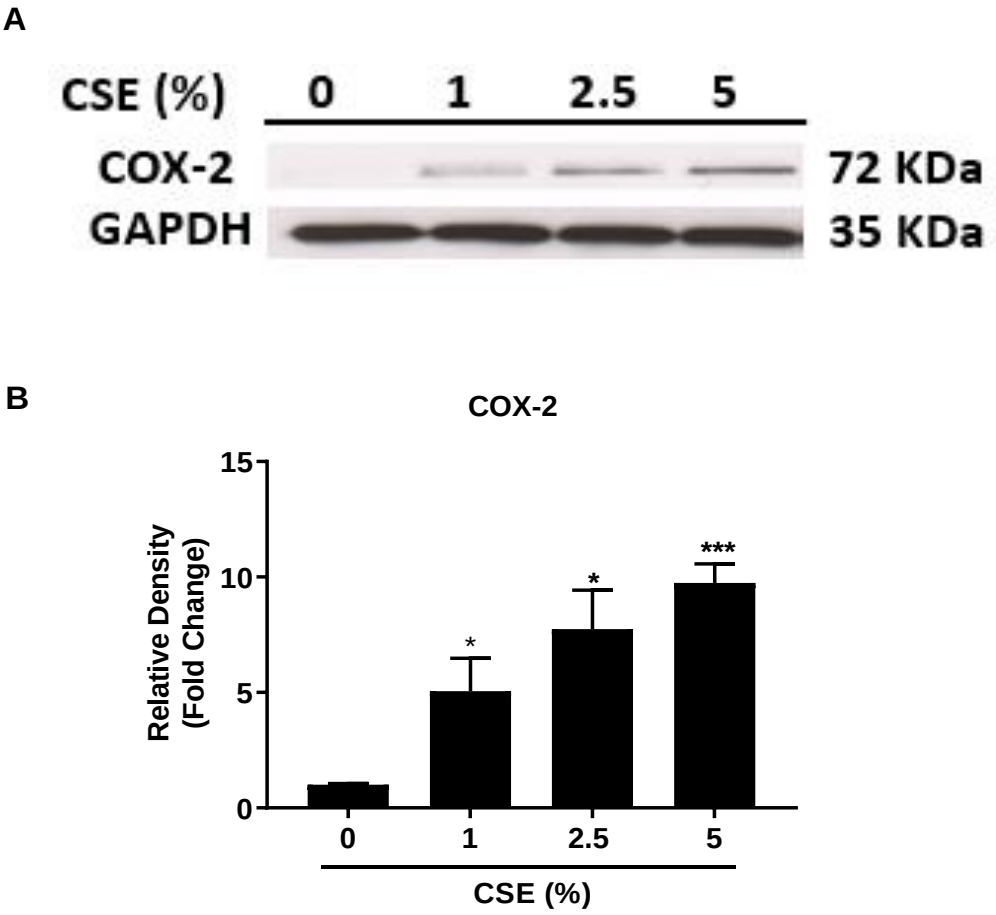


Figure 3.3 Effect of CSE on the protein expression of COX-2 in human PASMCs.
Confluent human PASMCs were treated with different concentrations of CSE (0%, 1%, 2.5%, and 5%) for 48 h with daily fresh DMEM+ and CSE and then with the same concentrations of CSE in DMEM- for 24 h. Total cell lysates were collected for Western blot analysis of COX-2 protein. A, a representative Western blot showing the effect of CSE on COX-2 protein expression. B, optical densitometry analysis of Western blotting bands. Data were normalised with the loading control GAPDH and were expressed as fold change over untreated cells (0% CSE). Each data point represents mean ± SEM from three independent experiments using cells from three different donors. *$p<0.05$, ***$p<0.001$ compared with untreated cells.

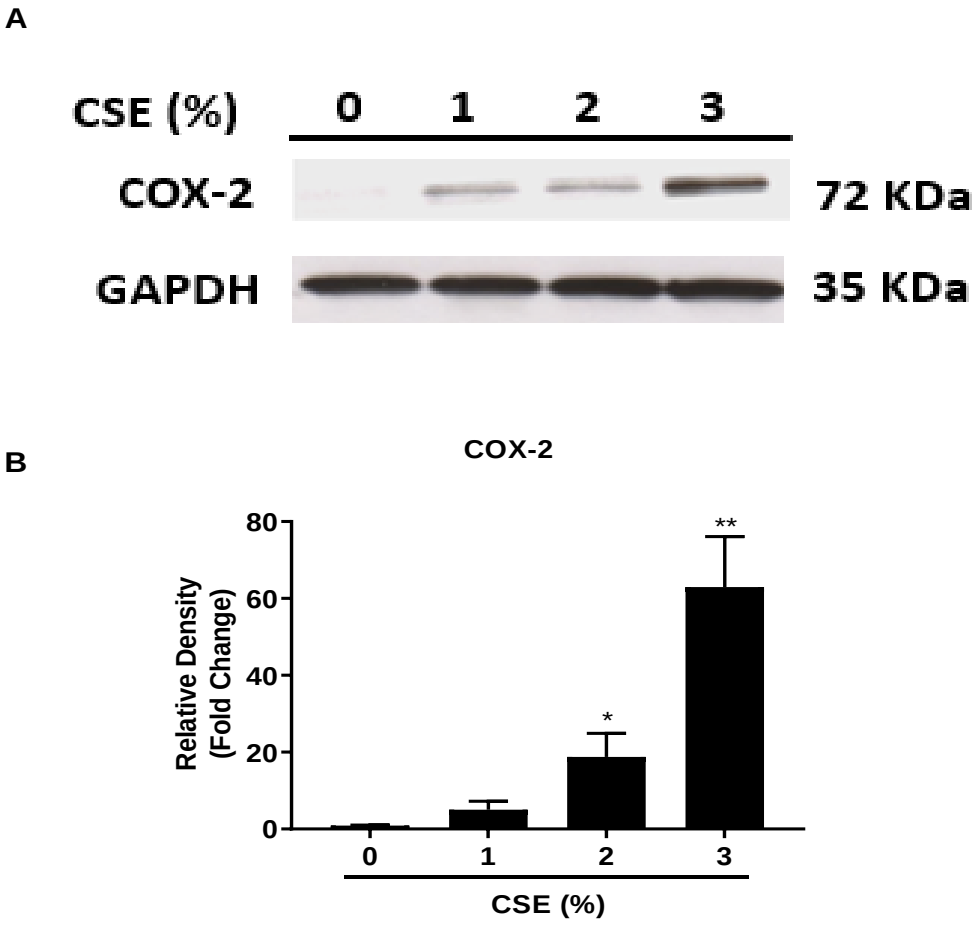


Figure 3.4 Effect of CSE on the protein expression of COX-2 in human PAECs.
Confluent human PAECs were treated with different concentrations of CSE (0%, 1%, 2%, and 3%) for 24 h. Total cell lysates were collected for Western blot analysis of COX-2 protein. A, a representative Western blot showing the effect of CSE on COX-2 protein expression. B, optical densitometry analysis of Western blotting bands. Data were normalised with the loading control GAPDH and were expressed as fold change over untreated cells (0% CSE). Each data point represents mean ± SEM from three independent experiments using one cell line. *$p<0.05$, **$p<0.01$ compared with untreated cells.

Since COX-2 is the rate-limiting enzyme in prostanoid synthesis, its upregulation should lead to the increase in the production of its downstream prostanoid products, such as PGE_2, PGI_2, and TXA_2. Thus, we next determined the effect of CSE on PGE_2 production in human PASMCs and PAECs, as PGE_2 is one of the main prostanoid products mediated by COX-2 activity. ELISA was used to measure the PGE_2 production in cultured human PASMCs and PAECs following CSE stimulation. The results demonstrated that human PASMCs constitutively produced PGE_2 (863.2±79.6 pg/mg protein) (Figure 3.5). Treatment with 1% CSE had no effect on PGE_2 production in PASMCs. Interestingly, compared with untreated cells, a significant concentration-dependent reduction in the production of PGE_2 was noted in response to 2.5% and 5% CSE-treated PASMCs (422.7±63.4 pg/mg protein, $p<0.05$ and 195.1±30.0 pg/mg protein, $p<0.01$, respectively). PGE_2 was also produced at basal levels in human PAECs (263.5±32.0 pg/mg protein). In contrast to the findings from PASMCs, CSE treatment induced PGE_2 production in a concentration-dependent manner (Figure 3.6). Significant increase of PGE_2 levels was observed following 1% CSE stimulation (458.3±15.3 pg/mg protein, $p<0.001$). PGE_2 increase was also noted in response to 2% and 3% CSE (846.4±125.5 and 1092.4±207.7 pg/mg protein, respectively, $p<0.01$) compared with untreated cells.

It is generally accepted that upregulation of COX-2 expression would lead to an increase in the production of its downstream products, including PGE_2 which regulates vascular tone. However, here it is shown that CSE reduced the production of PGE_2 in PASMCs, suggesting that the expression level of mPGES-1 may also play a role in this process.

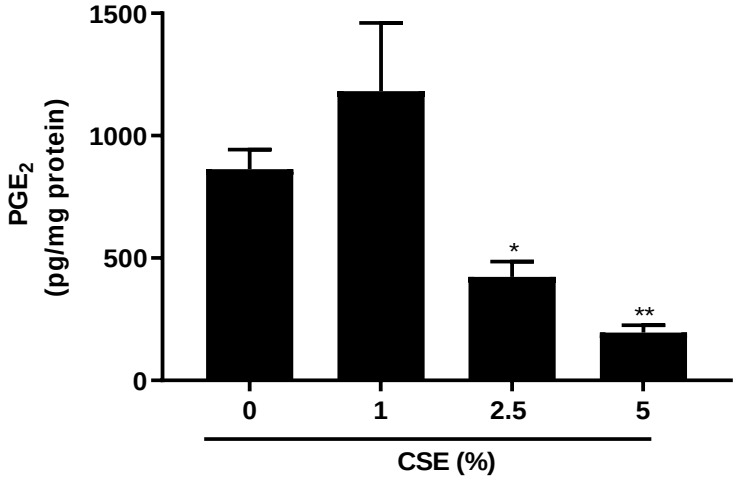


Figure 3.5 Effect of CSE on PGE_2 production in human PASMCs.
Confluent human PASMCs were treated with different concentrations of CSE (0%, 1%, 2.5%, and 5%) for 48 h with daily fresh DMEM+ and CSE and then with the same concentrations of CSE in DMEM- for 24 h. Supernatants were collected and assayed for PGE_2 using ELISA analysis. Data were normalised with total protein and expressed as pg/mg protein. Each data point represents mean ± SEM from three independent experiments using cells from three different donors. *p<0.05, **p<0.01 compared with untreated cells.

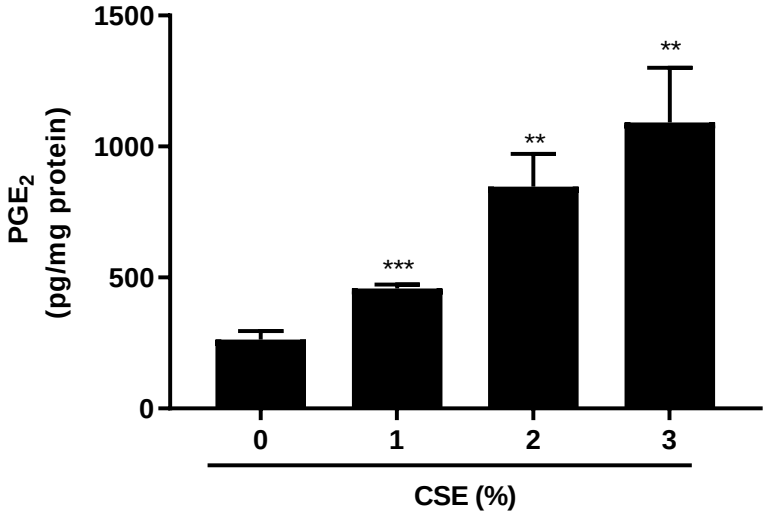


Figure 3.6 Effect of CSE on PGE_2 production in human PAECs.
Confluent human PAECs were treated with different concentrations of CSE (0%, 1%, 2%, and 3%) for 24 h. Supernatants were collected and assayed for PGE_2 using ELISA analysis. Data were normalised with total protein and expressed as pg/mg protein. Each data point represents mean ± SEM from five independent experiments using one cell line. **p<0.01, ***p<0.001 compared with untreated cells.

3.4.2 Effect of CSE on the protein expression of mPGES-1 in human PASMCs and PAECs

PGE_2 is one of the main products of COX-2, and its production is regulated by the enzyme mPGES-1. In the present study, we demonstrated that although CSE increased COX-2 expression, PGE_2 production was unexpectedly reduced in PASMCs. In contrast, the increase in COX-2 expression in PAECs as a result of CSE treatment led to increased PGE_2 production. This suggests that it is possible that CSE may regulate mPGES-1 expression differently in the two cell types. Therefore, the effect of CSE on mPGES-1 protein expression was assessed. We found that basal protein expression of mPGES-1 was readily detected in PASMCs (Figure 3.7A). Treatment with 5% CSE slightly but significantly reduced mPGES-1 protein expression (fold change 0.7±0.1, $p<0.05$) as shown in the densitometry analysis compared with untreated cells (Figure 3.7B). Human PAECs also expressed mPGES-1 protein basally at low levels (Figure 3.8A and B). CSE (3%) treatment seemed to increase the protein expression of mPGES-1 (Figure 3.8A and B). However, statistical analysis was not assessed, as this experiment was only conducted once. These observations may explain the difference observed between PASMCs and PAECs in the production of PGE_2, suggesting that CSE can regulate mPGES-1/PGE_2 differently in the two cell types.

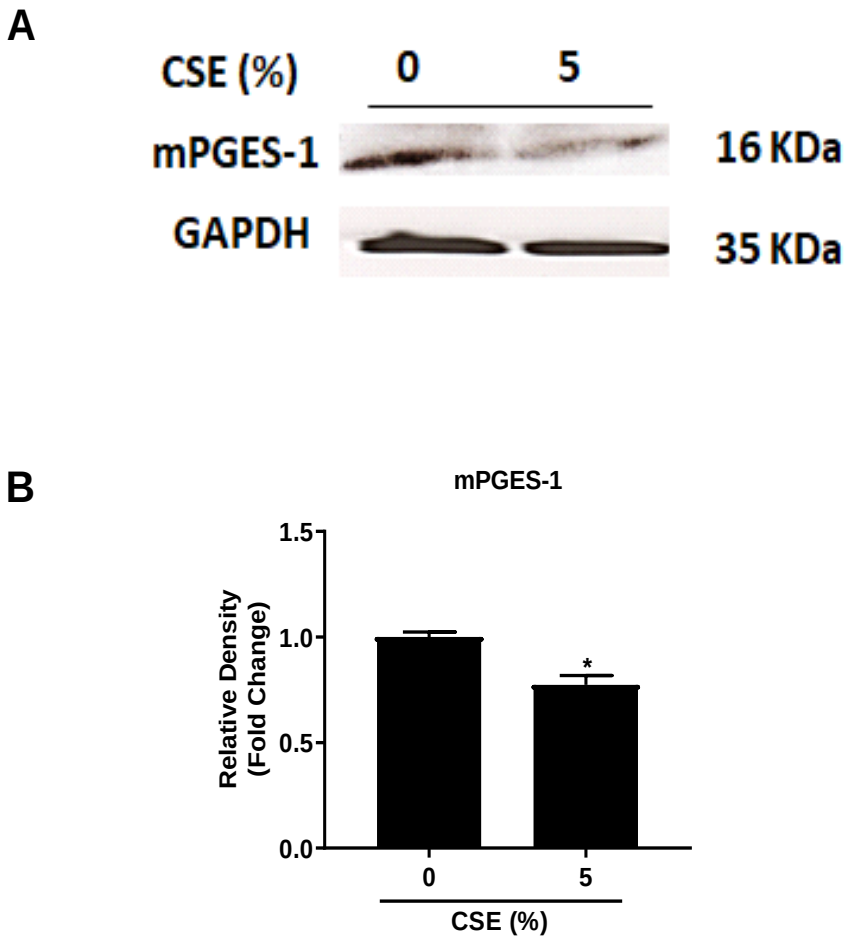


Figure 3.7 Effect of CSE on the protein expression of mPGES-1 in human PASMCs.
Confluent human PASMCs were treated with CSE (0% and 5%) for 48 h with daily fresh DMEM+ and CSE and then with the same concentration of CSE in DMEM- for 24 h. Total cell lysates were collected for Western blot analysis of mPGES-1 protein. A , a representative Western blot showing the effect of CSE on mPGES-1 protein expression. B, optical densitometry analysis of Western blotting bands. Data were normalised with the loading control GAPDH and were expressed as fold change over untreated cells (0% CSE). Each data point represents mean ± SEM from three independent experiments using cells from three different donors. *$p<0.05$ compared with untreated cells.

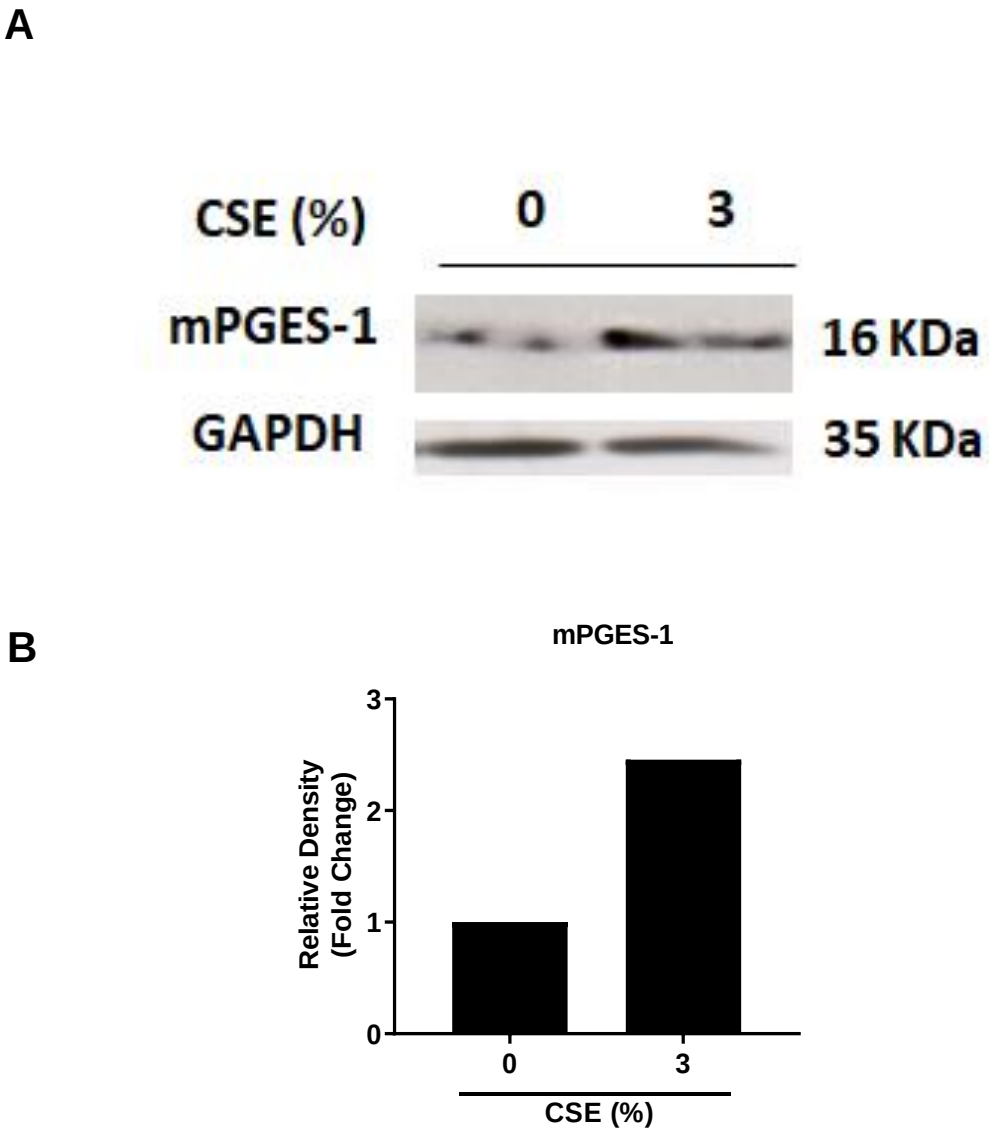


Figure 3.8 Effect of CSE on the protein expression of mPGES-1 in human PAECs.
Confluent human PAECs were treated with CSE (0% and 3%) for 24 h. Total cell lysates were collected for Western blot analysis of mPGES-1 protein. A, Western blot showing the effect of CSE on mPGES-1 protein expression. B, optical densitometry analysis of Western blotting bands. Data were normalised with the loading control GAPDH and were expressed as fold change over untreated cells (0% CSE). This figure shows data from one experiment.

3.4.3 Effect of CSE on the mRNA and protein expression of PGIS and PGI_2 production in human PASMCs and PAECs

PGI_2, one of the most abundant prostanoids, is a downstream product from COX-2 activity and its production is mediated by the enzyme PGIS. It is well established that reduced PGI_2 is involved in the manifestation of vascular dysfunction in group 1 pulmonary hypertension (Tuder et al., 1999). What is not yet clear is the role of PGIS/PGI_2 in COPD-associated pulmonary hypertension. We therefore assessed the effect of CSE on the vasoprotective PGIS and its product, PGI_2. The real-time RT-PCR analysis showed that PGIS mRNA was basally expressed, and CSE stimulation resulted in a significant reduction of PGIS expression in both PASMCs (Figure 3.9) and PAECs (Figure 3.10). In PASMCs, 1% CSE had no effect on PGIS mRNA expression, whereas treatment with 2.5% and 5% CSE significantly reduced the mRNA expression of PGIS (fold changed 0.7±0.05, $p<0.05$ and 0.5±0.03, $p<0.01$, respectively) as shown in Figure 3.9. Similarly, stimulation with 3% CSE caused a significant reduction of PGIS mRNA expression in PAECs (fold changed 0.7±0.05, $p<0.01$), whereas 1% and 2% CSE had no effect on PGIS mRNA expression as shown in Figure 3.10.

The mRNA data suggest that CSE is likely to regulate PGIS gene expression via transcriptional regulation.

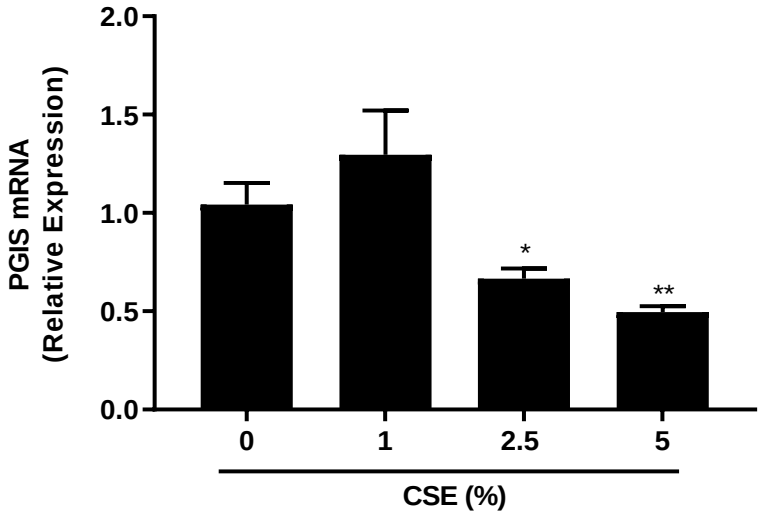


Figure 3.9 Effect of CSE on the mRNA expression of PGIS in human PASMCs.
Confluent human PASMCs were stimulated with different concentrations of CSE (0%, 1%, 2.5%, and 5%) for 48 h with daily fresh DMEM+ and CSE and then with the same concentrations of CSE in DMEM- for 24 h. Total RNA was isolated and then the samples were assayed for the mRNA expression of PGIS using RT-qPCR. Data were expressed as fold change over unstimulated cells (0% CSE). Each data point represents mean ± SEM from three independent experiments using cells from three different donors. *p<0.05, **p<0.01 compared with unstimulated cells.

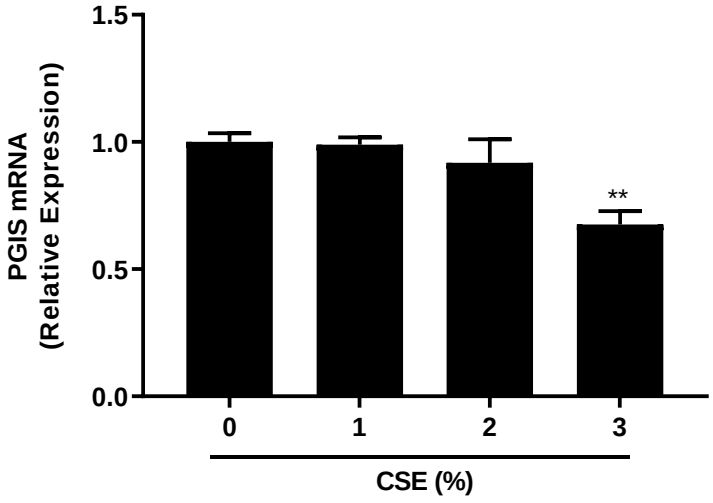


Figure 3.10 Effect of CSE on the mRNA expression of PGIS in human PAECs.
Confluent human PAECs were treated with different concentrations of CSE (0%, 1%, 2%, and 3%) for 24 h prior to total RNA isolation. The samples were assayed for the mRNA expression of PGIS using RT-qPCR. Data were expressed as fold change over untreated cells (0% CSE). Each data point represents mean ± SEM from three independent experiments using one cell line. **p<0.01 compared with untreated cells.

To find out whether the CSE-induced reduction of PGIS mRNA expression could lead to reduced PGIS protein expression, human PASMCs and PAECs were left either untreated or treated with various concentrations of CSE for 72 h and 24 h, respectively. Western blot analysis showed that the protein of PGIS was basally expressed in PASMCs. Treatment with CSE reduced PGIS protein expression in a concentration-dependent manner (Figure 3.11A). Although there was no apparent change in the protein expression of PGIS in response to 1% and 2.5% CSE as shown in the densitometry analysis, PGIS protein expression was reduced following stimulation with 5% CSE (fold change 0.2 ± 0.05, $p<0.01$) compared with untreated PASMCs (Figure 3.11B). Unexpectedly, unlike in human PASMCs, the protein expression of PGIS was undetectable under both basal and following CSE stimulation conditions in PAECs (Figure 3.12A and B).

The protein expression of PGIS is undetectable in PAECs, and the observation showing CSE-mediated downregulation of PGIS protein and mRNA expression in PASMCs suggests that it is likely that CSE downregulates PGIS gene expression via transcriptional mechanism.

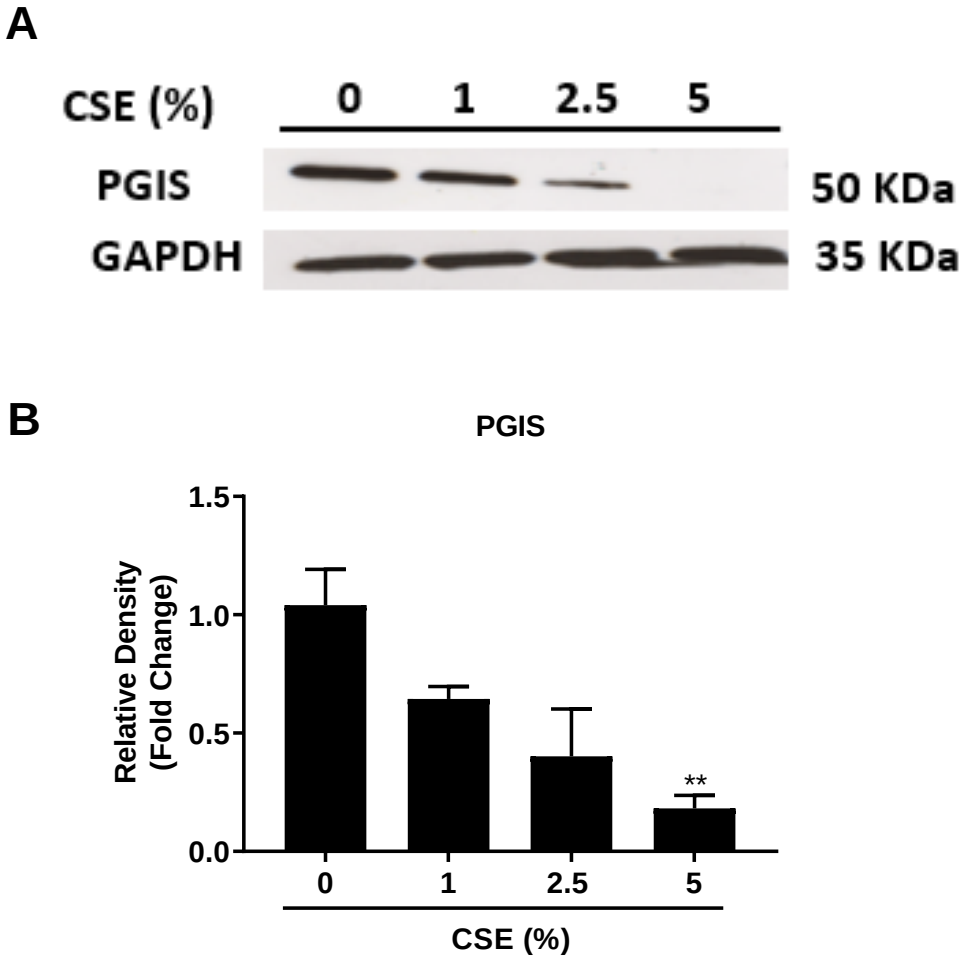


Figure 3.11 Effect of CSE on the protein expression of PGIS in human PASMCs.
Confluent human PASMCs were treated with different concentrations of CSE (0%, 1%, 2.5%, and 5%) for 48 h with daily fresh DMEM+ and CSE and then with the same concentrations of CSE in DMEM- for 24 h. Total cell lysates were collected for Western blot analysis of PGIS protein. A, a representative Western blot showing the effect of CSE on PGIS protein expression. B, optical densitometry analysis of Western blotting bands. Data were normalised with the loading control GAPDH and were expressed as fold change over untreated cells (0% CSE). Each data point represents mean ± SEM from three independent experiments using cells from three different donors. **$p<0.01$ compared with untreated cells.

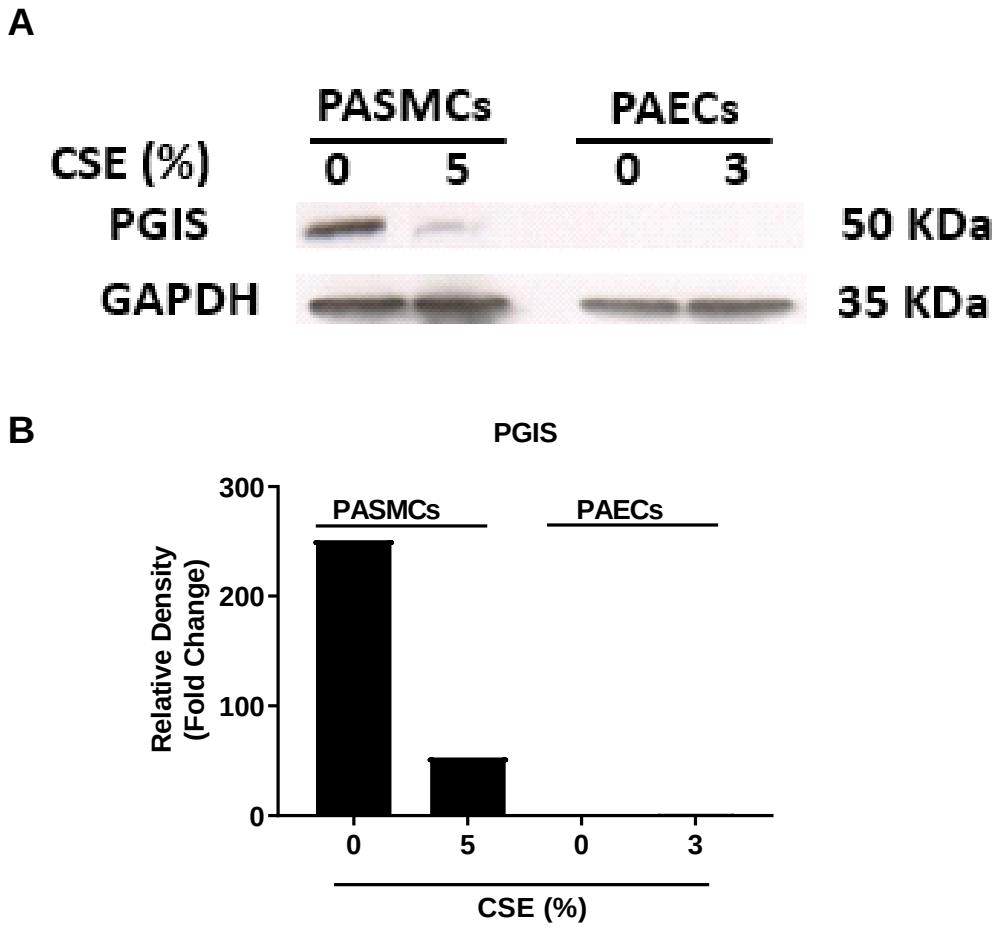


Figure 3.12 Effect of CSE on the protein expression of PGIS in human PAECs.
Confluent human PAECs were treated with CSE (0% and 3%) for 24 h. Total cell lysates were collected for Western blot analysis of PGIS protein. Total cell lysates from human PASMCs treated with and without CSE were used as a positive control. A, a representative Western blot showing the effect of CSE on PGIS protein expression. B, optical densitometry analysis of Western blotting bands. Data were normalised with the loading control GAPDH and were expressed as fold change over untreated human PAECs (0% CSE). A representative blot of three independent experiments using one cell line is shown.

Next, supernatants collected following CSE treatment were assayed for 6-keto $PGF_{1\alpha}$, (the stable metabolite of PGI_2) using ELISA analysis. The results showed that levels of 6-keto $PGF_{1\alpha}$ were basally observed in PASMCs (2987.2±403.5 pg/mg protein) as shown in Figure 3.13. Following CSE treatment, 6-keto $PGF_{1\alpha}$ levels were significantly and concentration-dependently decreased over basal levels in PASMCs. CSE (1%) slightly but insignificantly reduced 6-keto $PGF_{1\alpha}$; this was followed by a greater reduction in response to 2.5% and 5% CSE (1028.9±175.6 pg/mg protein, $p<0.05$ and 477.1±183.4 pg/mg protein, $p<0.01$, respectively) compared with untreated PASMCs. 6-keto $PGF_{1\alpha}$ was detectable at basal levels in PAECs (792.0±94.7 pg/mg protein) as shown in Figure 3.14. Interestingly, treatment with CSE (1%, 2%, and 3%) did not change 6-keto $PGF_{1\alpha}$ levels compared with untreated PAECs.

Taken together, our findings showing that CSE can reduce the mRNA and protein expression of PGIS and production of 6-keto $PGF_{1\alpha}$ in PASMCs, suggesting that reduced PGIS/PGI_2 by CSE is a key part of imbalanced vasoactive prostanoid production in PASMCs, but not in PAECs, and may ultimately lead to pulmonary vascular remodelling in COPD.

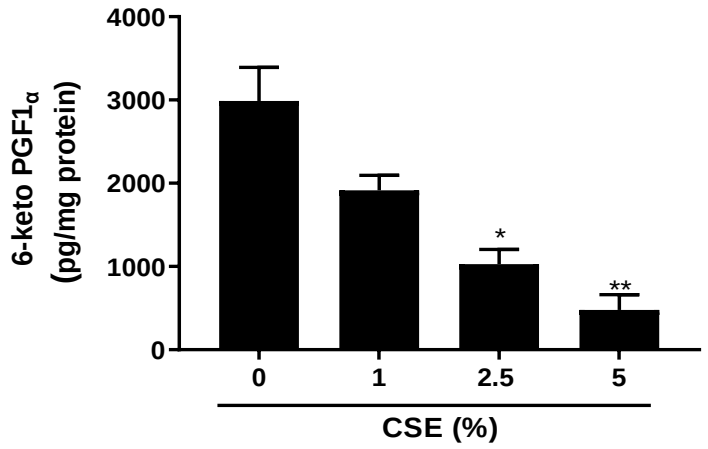


Figure 3.13 Effect of CSE on 6-keto $PGF_{1\alpha}$ production in human PASMCs.
Confluent human PASMCs were treated with different concentrations of CSE (0%, 1%, 2.5%, and 5%) for 48 h with daily fresh DMEM+ and CSE and then with the same concentrations of CSE in DMEM- for 24 h. Supernatants were collected and assayed for 6-keto $PGF_{1\alpha}$ using ELISA analysis. Data were normalised with total protein and expressed as pg/mg protein. Each data point represents mean ± SEM from three independent experiments using cells from three different donors. *$p<0.05$, **$p<0.01$ compared with untreated cells.

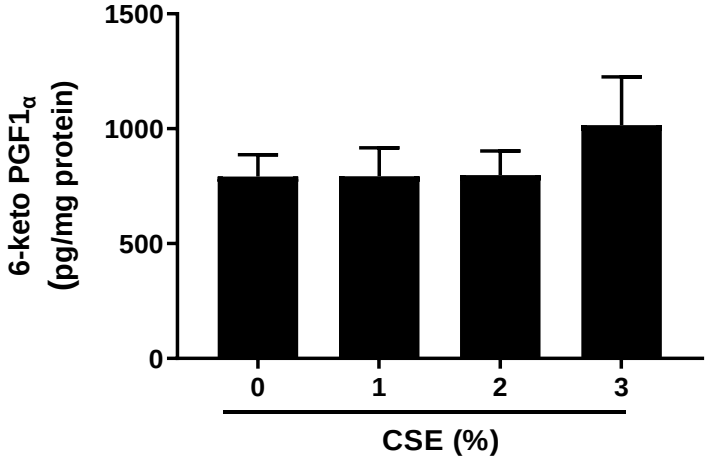


Figure 3.14 Effect of CSE on 6-keto $PGF_{1\alpha}$ production in human PAECs.
Confluent human PAECs were treated with different concentrations of CSE (0%, 1%, 2%, and 3%) for 24 h. Supernatants were collected and assayed for 6-keto $PGF_{1\alpha}$ using ELISA analysis. Data were normalised with total protein and expressed as pg/mg protein. Each data point represents mean ± SEM from six independent experiments using one cell line.

3.4.4 Effect of CSE on the mRNA and protein expression of TXAS and TXA_2 production in human PASMCs and PAECs

So far, it has clearly been demonstrated that CSE increased COX-2 expression but reduced PGI_2 and PGE_2 production, due to PGIS and mPGES-1 protein expression reduction in PASMCs, respectively. Although COX-2 expression was also increased in PAECs, CSE treatment caused unchanged PGI_2 but increased PGE_2 production as a result of undetected PGIS protein expression and upregulation of mPGES-1 protein expression in PAECs, respectively. This suggests that the marked reduction of PGIS/PGI_2 and mPGES-1/PGE_2 in CSE-treated human PASMCs is an important factor of cell dysfunction, and may play a key role in the proliferation of pulmonary artery cells.

The vasoconstrictive TXA_2 is also one of the downstream products from COX-2 activity, and its production is mediated by the enzyme TXAS. To study the effect of CSE on TXAS mRNA expression in both PASMCs and PAECs, total RNA was isolated following cell incubation with CSE. Then, the samples were assayed for TXAS mRNA using RT-qPCR. We first found that the mRNA expression of TXAS was basally detectable in PASMCs, and 1% CSE slightly induced TXAS mRNA expression (fold change 1.8±0.2, $p<0.05$) compared with untreated human PASMCs (Figure 3.15). Induction of TXAS mRNA expression was also noted in response to 2.5% and 5% CSE (fold change 2.5±0.05, $p<0.0001$ and 5.0±1.2, $p<0.05$, respectively) over basal levels in PASMCs. PAECs also expressed TXAS mRNA basally. Similar to our findings from PASMCs, significant upregulation of TXAS mRNA expression was observed following 1%, 2%, and 3% CSE treatment (fold change 1.5±0.07, $p<0.01$, 1.7±0.2, $p<0.05$ and 2.7±0.3, $p<0.01$, respectively) compared with untreated PAECs (Figure 3.16). This

upregulation of TXAS mRNA expression by CSE in both PASMCs and PAECs suggests that CSE may upregulate TXAS gene expression via transcriptional mechanism.

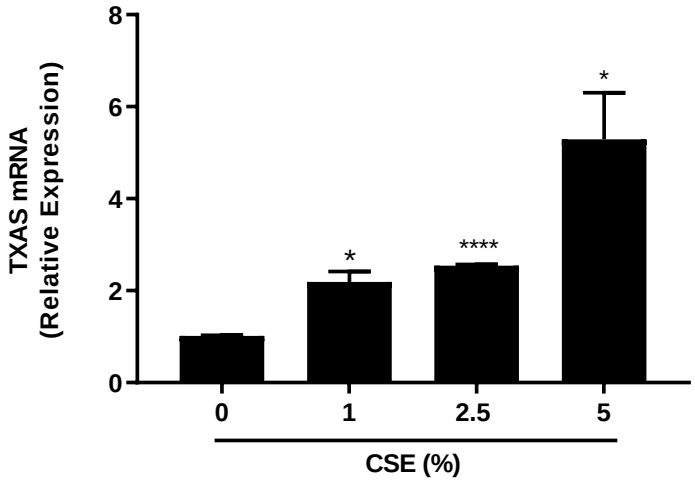


Figure 3.15 Effect of CSE on the mRNA expression of TXAS in human PASMCs.
Confluent human PASMCs were treated with different concentrations of CSE (0%, 1%, 2.5%, and 5%) for 48 h with daily fresh DMEM+ and CSE and then with the same concentrations of CSE in DMEM- for 24 h. Total RNA was isolated and then the samples were assayed for the mRNA expression of TXAS using RT-qPCR. Data were expressed as fold change over untreated cells (0% CSE). Each data point represents mean ± SEM from three independent experiments using cells from three different donors. *p<0.05, ****p<0.0001 compared with untreated cells.

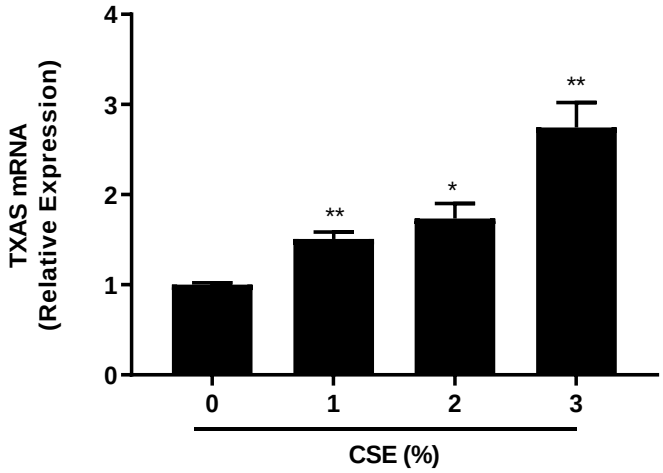


Figure 3.16 Effect of CSE on the mRNA expression of TXAS in human PAECs.
Confluent human PAECs were treated with different concentrations of CSE (0%, 1%, 2%, and 3%) for 24 h prior to total RNA isolation. The samples were assayed for the mRNA expression of TXAS using RT-qPCR. Data were expressed as fold change over untreated cells (0% CSE). Each data point represents mean ± SEM from three independent experiments using one cell line. *p<0.05, **p<0.01 compared with untreated cells.

Next, total cell lysates and supernatants were collected following human PASMC and PAEC treatment with and without CSE to assess TXAS protein expression and production of TXB_2 (the stable metabolite of TXA_2), using Western blotting and ELISA, respectively. In contrast to TXAS mRNA findings, we failed to detect the protein expression of TXAS under both basal and CSE-stimulated conditions in PASMCs and PAECs (Figure 3.17A and B). To ensure that the antibody recognised the target protein and that the Western blotting procedure was optimised and working, total cell lysates from immortalized human bronchial epithelial (BEAS-2B) cells treated with and without CSE were used as a positive control, and were found to express TXAS protein basally. TXAS protein expression was further induced by 5% CSE treatment in BEAS-2B (Figure 3.17A and B).

Further experiments to explore the effect of CSE on production of TXB_2 in PASMCs and PAECs were conducted. We found that the TXB_2 was produced under basal levels (267.4±39.2 pg/mg protein) and treatment with 1% CSE, but not 2.5% CSE, caused an increase in TXB_2 production in PASMCs (491.7±59.0 pg/mg protein, $p<0.05$) compared with 0% CSE (Figure 3.18). A greater increase of TXB_2 was seen following 5% CSE stimulation (842.3±52.5 pg/mg protein, $p<0.001$) compared with untreated PASMCs. Consistent with the finding that shows CSE induced TXB_2 in human PASMCs, it has also been shown that PAECs produced TXB_2 at basal levels (500.8±72.2 pg/mg protein), and CSE stimulation (1%, 2%, and 3%) induced the levels of TXB_2 significantly and concentration-dependently (1093.2±60.2 pg/mg protein, 1082.0±36.9 pg/mg protein and 1719.7±142.2 pg/mg protein, respectively, $p<0.01$ for all) compared with 0% CSE in PAECs (Figure 3.19).

These results demonstrate that the production of vasoconstrictive and proliferative prostanoid TXA_2 is increased in response to CSE in both cell types. These observations, together with the previous findings showing reduced and unchanged release of the vasodilator and anti-proliferative prostanoid PGI_2 by CSE in PASMCs and PAECs, respectively, suggest that the imbalance between PGI_2 and TXA_2 (reduced PGI_2/TXA_2 ratio) may play a key role in the dysfunction of both cell types, thereby contributing to vascular constriction and remodelling, and eventually pulmonary hypertension.

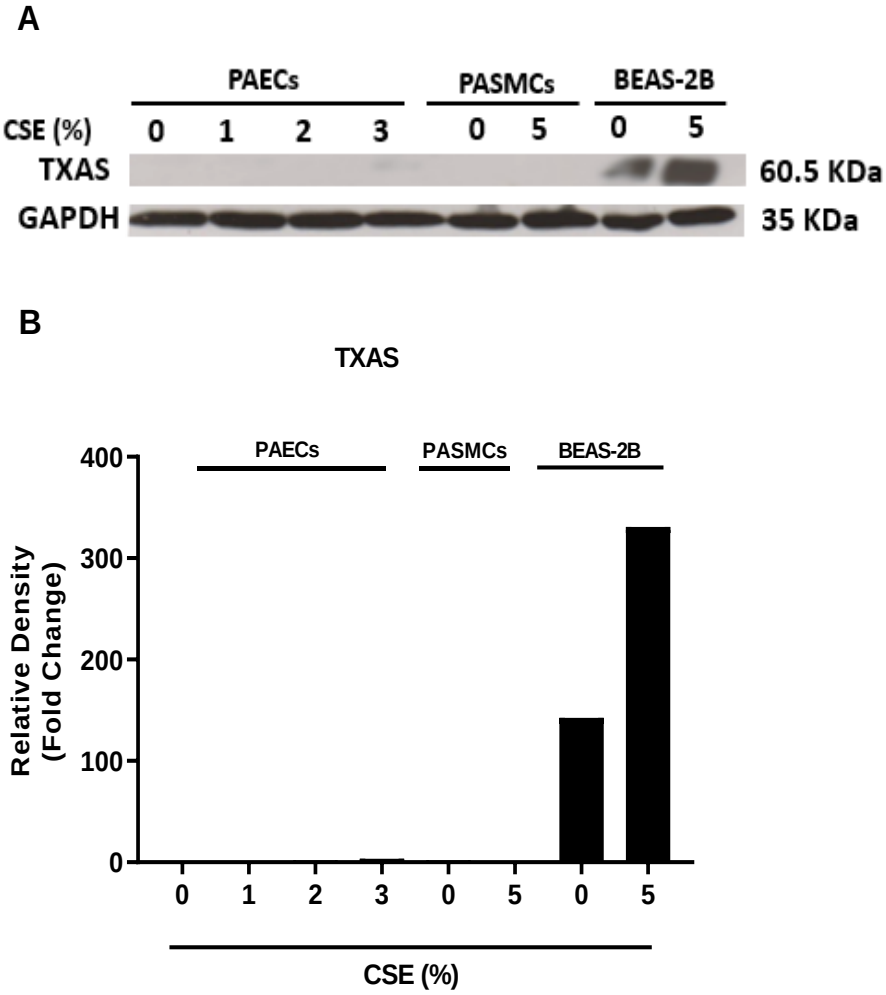


Figure 3.17 Effect of CSE on the protein expression of TXAS in human PASMCs and PAECs.
Confluent human PASMCs and PAECs were treated with or without CSE for either 72 h (PASMCs) or 24 h (PAECs). Total cell lysates were collected and Western blot analysis was carried out to assess TXAS protein expression. Total cell lysates from immortalized human bronchial epithelial (BEAS-2B) cells treated with or without CSE were used as a positive control. A, a representative Western blot showing the effect of CSE on TXAS protein expression in human PASMCs and PAECs. B optical densitometry analysis of Western blotting bands for PASMCs and PAECs. Data were normalised with the loading control GAPDH and were expressed as fold change over untreated cells (0% CSE). A representative blot of three independent experiments using cells from three different donors (PASMCs) and three independent experiments using one cell line (PAECs) is shown.

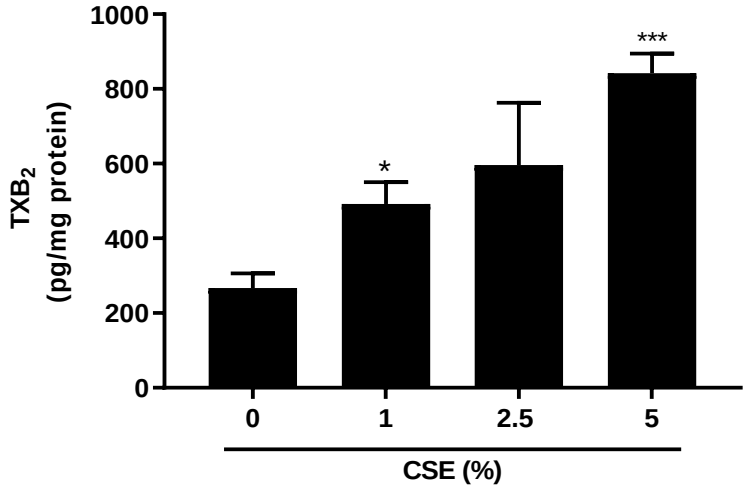


Figure 3.18 Effect of CSE on TXB_2 production in human PASMCs.
Confluent human PASMCs were treated with different concentrations of CSE (0%, 1%, 2.5%, and 5%) for 48 h with daily fresh DMEM+ and CSE and then with the same concentrations of CSE in DMEM- for 24 h. Supernatants were collected and assayed for TXB_2 using ELISA analysis. Data were normalised with total protein and expressed as pg/mg protein. Each data point represents mean ± SEM from three independent experiments using cells from three different donors. *p<0.05, ***p<0.001 compared with untreated cells.

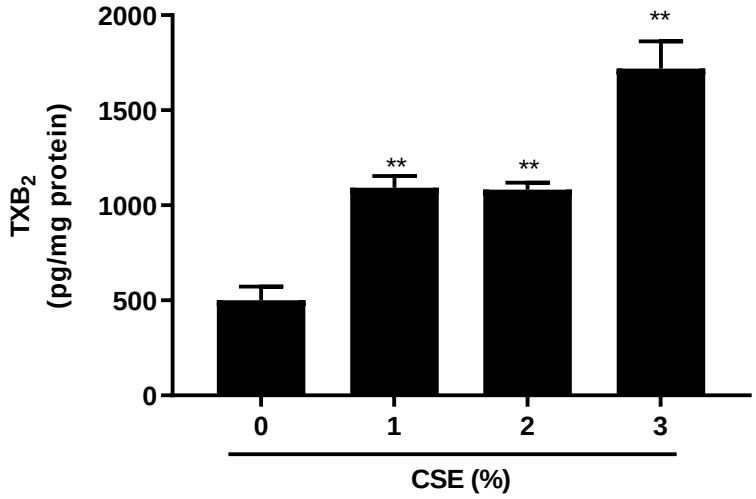


Figure 3.19 Effect of CSE on TXB_2 production in human PAECs.
Confluent human PAECs were treated with different concentrations of CSE (0%, 1%, 2%, and 3%) for 24 h. Supernatants were collected and assayed for TXB_2 using ELISA analysis. Data were normalised with total protein and expressed as pg/mg protein. Each data point represents mean ± SEM from three independent experiments using one cell line. **p<0.01 compared with untreated cells.

3.4.5 Effect of CSE on the PGI_2/TXA_2 ratio in human PASMCs and PAECs

It is known that endothelial cells maintain the balance between the vasodilatory and anti-proliferative mediator PGI_2 and vasoconstrictive and proliferative mediator TXA_2 and prevent PASMC proliferation. An imbalance with reduced vasodilators and increased vasoconstrictors plays an important role in the development of vascular remodelling in patients with PAH (Christman et al., 1992). However, it is unknown whether CSE can have an effect on the PGI_2/TXA_2 ratio in human PAECs and PASMCs. To explore the effect of CSE on the PGI_2/TXA_2 ratio, the production of 6-keto $PGF_{1\alpha}$ and TXB_2 (the stable metabolites of PGI_2 and TXA_2, respectively) were assessed by ELISA and the ratio of PGI_2 and TXA_2 was then calculated. We found that CSE reduced the PGI_2/TXA_2 ratio significantly and concentration-dependently in human PASMCs and PAECs, as shown in Figures 3.20 and 3.21. In PASMCs, 1% and 2.5% CSE reduced the PGI_2/TXA_2 ratio (4.0±0.5 and 2.3±1.2, $p<0.05$, respectively) compared with untreated cells (11.4±1.6). This was followed by a further reduction of PGI_2/TXA_2 ratio by 5% CSE (0.6±0.2, $p<0.01$). Similarly in PAECs, the PGI_2/TXA_2 ratio was significantly reduced by 1% CSE (0.8±0.2, $p<0.05$) compared with untreated cells (1.8±0.2). A further decrease in the PGI_2/TXA_2 ratio was noted following treatment with 2% and 3% CSE (0.6±0.1 and 0.6±0.1, $p<0.01$, respectively).

The reduced ratio of PGI_2/TXA_2 caused by CSE in both cell types suggests that CS may play a crucial role in the dysfunction of vascular cells by reducing the PGI_2/TXA_2 ratio, thereby contributing to pulmonary vascular remodelling in COPD.

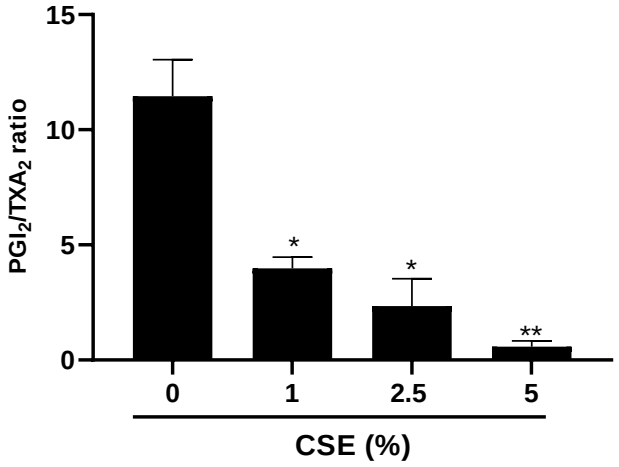


Figure 3.20 Effect of CSE on PGI_2/TXA_2 ratio in human PASMCs.
Confluent human PASMCs were treated with different concentrations of CSE (0%, 1%, 2.5%, and 5%) for 48 h with daily fresh DMEM+ and CSE and then with the same concentrations of CSE in DMEM- for 24 h. Supernatants were collected and assayed for 6-keto $PGF_{1\alpha}$ and TXB_2 using ELISA analysis. Data were normalised with total protein and presented as PGI_2/TXA_2 ratio. Each data point represents mean ± SEM from three independent experiments using cells from three different donors. *p<0.05, **p<0.01 compared with untreated cells.

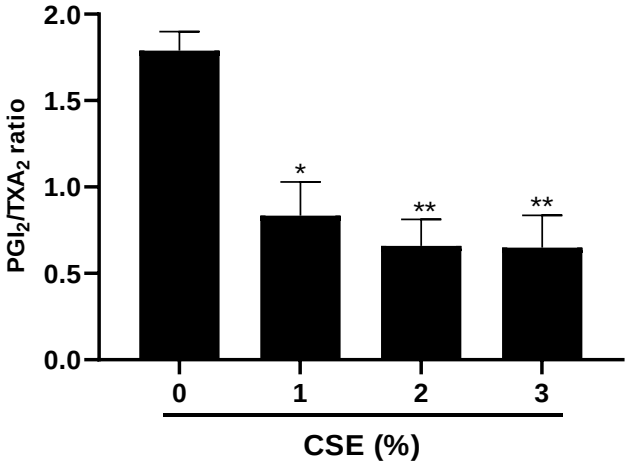


Figure 3.21 Effect of CSE on PGI_2/TXA_2 ratio in human PAECs.
Confluent human PAECs were treated with different concentrations of CSE (0%, 1%, 2%, and 3%) for 24 h. Supernatants were collected and assayed for TXB_2 using ELISA analysis. Data were normalised with total protein and presented as PGI_2/TXA_2 ratio. Each data point represents mean ± SEM from three independent experiments using one cell line. *p<0.05, **p<0.01 compared with untreated cells.

3.4.6 Effect of CSE on the mRNA and protein expression of eNOS and nitric oxide release in human PASMCs and PAECs

In addition to the imbalance between vasoactive PGs and TX, nitric oxide deficiency has also been reported to play a key role in the development of PAH (Giaid et al., 1993). However, the role of eNOS-derived nitric oxide in pulmonary hypertension in COPD is unknown. Thus, the effect of CSE treatment on the mRNA and protein expression of eNOS and total nitrate/nitrite production in PASMCs and PAECs was studied. It was first found that eNOS mRNA expression was undetectable in the absence and presence of CSE in human PASMCs (data not shown), whereas human PAECs expressed mRNA basally. Interestingly, CSE at all concentrations tested caused no significant change in the mRNA expression as shown in Figure 3.22.

Next, total cell lysates and cell culture supernatants were collected following PASMC and PAEC stimulation with CSE to determine the protein expression of eNOS and the total nitrate/nitrite using Western blotting and fluorometric assay analyses, respectively. It was shown that the protein expression of eNOS was undetectable with and without CSE stimulation in human PASMCs (Figure 3.23A and B). In contrast, the protein of eNOS was constitutively expressed in PAECs (Figure 3.24A) and remained unchanged in response to 1% CSE (Figure 3.24A and B). Treatment with 2% CSE caused a significant decrease in the protein expression of eNOS (fold change 0.3 ± 0.06, $p<0.01$), which was followed by a further reduction of eNOS protein expression when PAECs were stimulated with 3% CSE (fold change 0.1 ± 0.04, $p<0.001$) as shown in Figure 3.24A and B.

Nitric oxide is a major endothelial-derived mediator controlling vascular remodelling, is scavenged rapidly, and acts in a paracrine/autocrine fashion to induce vasoprotective and anti-proliferative effects. Since the final products of nitric oxide are nitrite and nitrate, which are known to be the best index of nitric oxide production, total nitrate/nitrite released to cell supernatants following CSE treatment was assessed using fluorometric assay. The results showed that human PAECs produced total nitrate/nitrite basally (0.07±0.009 nmol/µg protein). Although CSE (1% and 2%) had no effect on total nitrate/nitrite production, treatment with 3% CSE slightly but significantly reduced the total nitrate/nitrite levels in PAECs (0.04±0.007 nmol/µg protein, $p<0.05$) compared with basal levels (Figure 3.25). As eNOS expression at mRNA and protein levels in PASMCs are undetectable in PASMCs, no further experiments were conducted to assess total nitrate/nitrite in PASMCs.

Taken together, these results demonstrate that eNOS at both protein and mRNA levels was undetectable in PASMCs, whereas PAECs expressed eNOS and produced nitric oxide at basal levels. Stimulation of PAECs with CSE caused a concentration-dependent reduction in eNOS protein expression and total nitrate/nitrite, suggesting that eNOS/nitric oxide deficiency is a key part of CSE-induced PAEC dysfunction, which may then lead to pulmonary vascular remodelling in COPD.

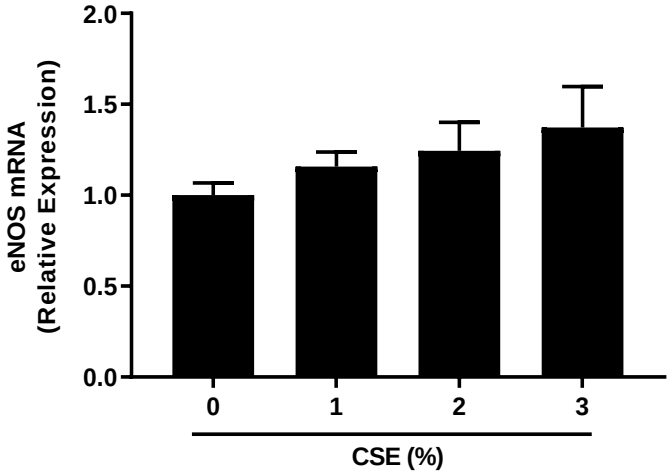


Figure 3.22 Effect of CSE on the mRNA expression of eNOS in human PAECs.
Confluent human PAECs were stimulated with different concentrations of CSE (0%, 1%, 2%, and 3%) for 24 h prior to total RNA isolation. The samples were assayed for the mRNA expression of eNOS using RT-qPCR. Data were expressed as fold change over unstimulated cells (0% CSE). Each data point represents mean ± SEM from three independent experiments using one cell line.

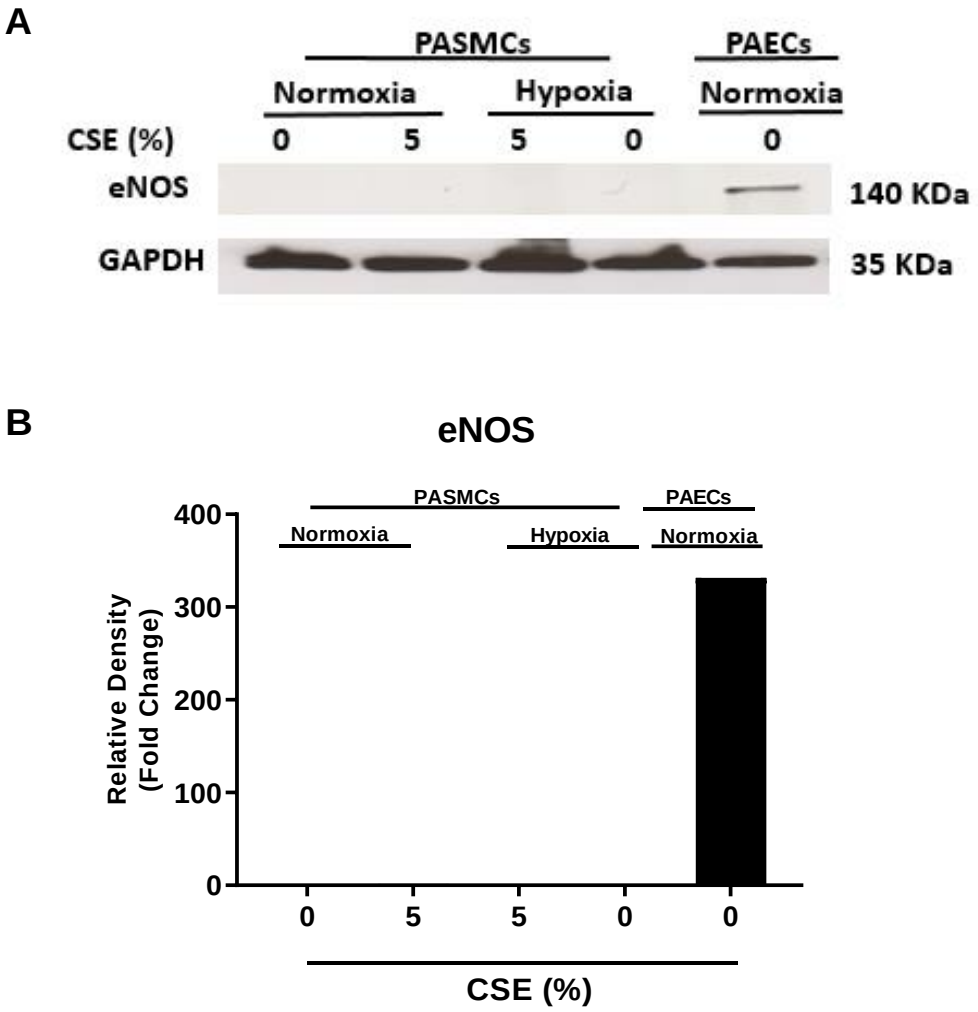


Figure 3.23 Effect of CSE on the protein expression of eNOS in human PASMCs.
Confluent human PASMCs were treated with CSE (0% and 5%) under normoxic (21% O_2) or hypoxic condition (1% O_2) for 48 h with daily fresh DMEM+ and CSE and then with the same concentrations of CSE in DMEM- for 24 h. Total cell lysates were collected for Western blot analysis of eNOS protein. Total cell lysates from untreated human PAECs were used as a positive control. A, a representative Western blot showing the effect of CSE under normoxic or hypoxic condition on eNOS protein expression. B, optical densitometry analysis of Western blotting bands. Data were normalised with the loading control GAPDH and were expressed as fold change over untreated human PASMCs (0% CSE). A representative blot of three independent experiments using cells from three different donors is shown.

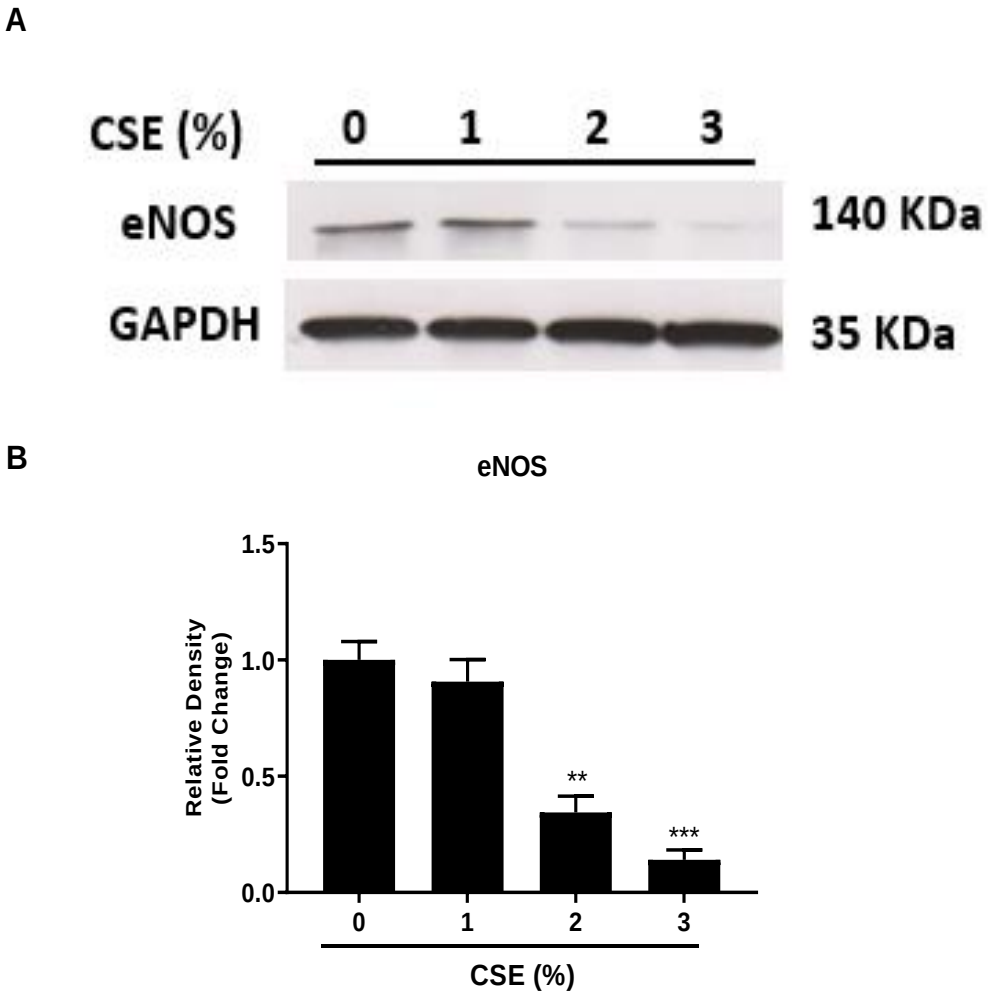


Figure 3.24 Effect of CSE on the protein expression of eNOS in human PAECs.
Confluent human PAECs were treated with different concentrations of CSE (0%, 1%, 2%, and 3%) for 24 h. Total cell lysates were collected for Western blot analysis of eNOS protein. A, a representative Western blot showing the effect of CSE on eNOS protein expression. B, optical densitometry analysis of Western blotting bands. Data were normalised with the loading control GAPDH and were expressed as fold change over untreated cells (0% CSE). Each data point represents mean ± SEM from three independent experiments using one cell line. **$p<0.01$, ***$p<0.001$ compared with untreated cells.

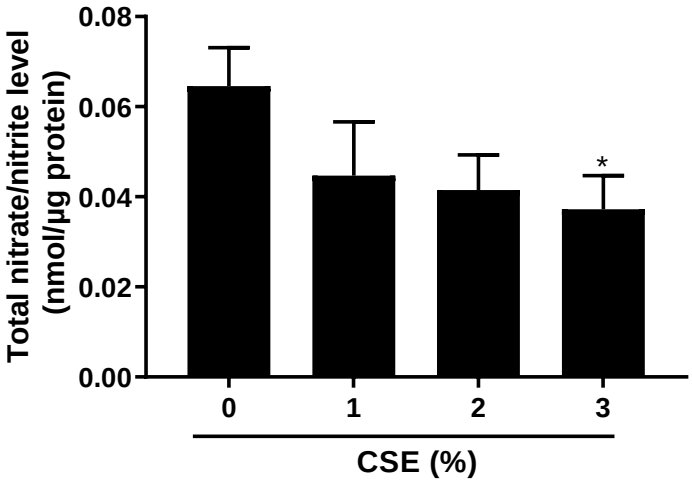


Figure 3.25 Effect of CSE on total nitrate/nitrite level in human PAECs.
Confluent human PAECs were treated with different concentrations of CSE (0%, 1%, 2%, and 3%) for 24 h. Supernatants were collected and assayed for total nitrate/nitrite using fluorometric assay. Data were normalised with total protein and expressed as nmol/µg protein. Each data point represents mean ± SEM from six independent experiments using one cell line. *$p<0.05$ compared with untreated cells.

3.4.7 Effect of CSE on the mRNA expression of endothelin-1 and production of endothelin in human PASMCs and PAECs

It is now widely recognised that increased endothelin-1 is a characteristic of endothelial dysfunction and can be an important indicator of pulmonary artery remodelling in PAH (Bourque et al., 2011). To determine whether CSE can induce endothelin-1 mRNA and endothelin-1 release in human PASMCs and PAECs, RT-qPCR analysis was first used to assess the mRNA expression in both cell types. Our results demonstrated that mRNA of endothelin-1 was basally expressed. Interestingly, CSE at all concentrations tested (1%, 2.5%, and 5%) had no effect on the mRNA expression of endothelin-1 compared with unstimulated PASMCs (Figure 3.26). We also found that human PAECs expressed mRNA of endothelin-1 at basal levels. Although treatment with 1% and 2% CSE had no effect on endothelin-1 mRNA expression, PAEC incubation with 3% CSE caused a slight but significant increase in the mRNA expression of endothelin-1 (fold change 1.5±0.1, $p<0.05$) compared with unstimulated PAECs (Figure 3.27).

Next, the effect of CSE on endothelin production was determined. Human PASMCs and PAECs were stimulated with various CSE concentrations for 72 h and 24 h, respectively. We found that endothelin production was detectable at basal levels in human PASMCs (372.7±46.3 pg/mg protein). Interestingly, CSE (1%, 2.5%, and 5%) had no effect on endothelin production in human PASMCs compared with basal levels (Figure 3.28). In addition, we showed that human PAECs produced more endothelin basally (6689.4±529.4 pg/mg protein) compared with PASMCs. Although treatment with CSE (1% and 2%) had no effect on endothelin release in PAECs, cell stimulation with 3% CSE significantly reduced endothelin production (2508.1±779.9 pg/mg protein,

$p<0.01$) compared with untreated cells (Figure 3.29). These findings suggest that PAECs are an important source of endothelin. Based on our observations, the functional consequence of CSE effect on endothelin in both cell types remains unclear.

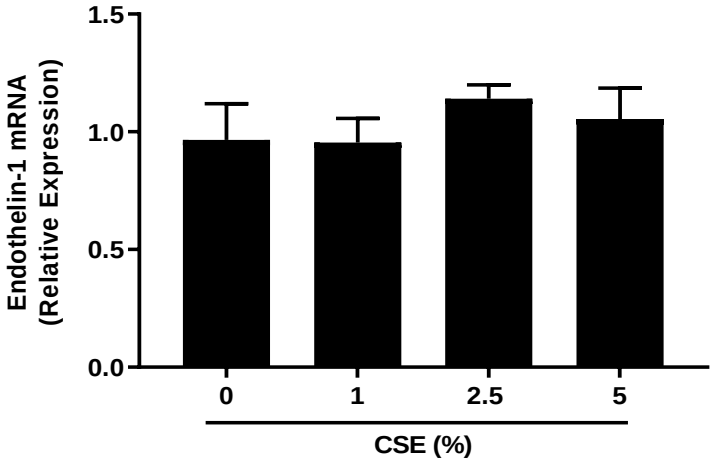


Figure 3.26 Effect of CSE on the mRNA expression of endothelin-1 in human PASMCs.
Confluent human PASMCs were stimulated with different concentrations of CSE (0%, 1%, 2.5%, and 5%) for 48 h with daily fresh DMEM+ and CSE and then with the same concentrations of CSE in DMEM- for 24 h. Total RNA was isolated and the samples were then assayed for the mRNA expression of endothelin-1 using RT-qPCR. Data were expressed as fold change over unstimulated cells (0% CSE). Each data point represents mean ± SEM from three independent experiments using cells from three different donors.

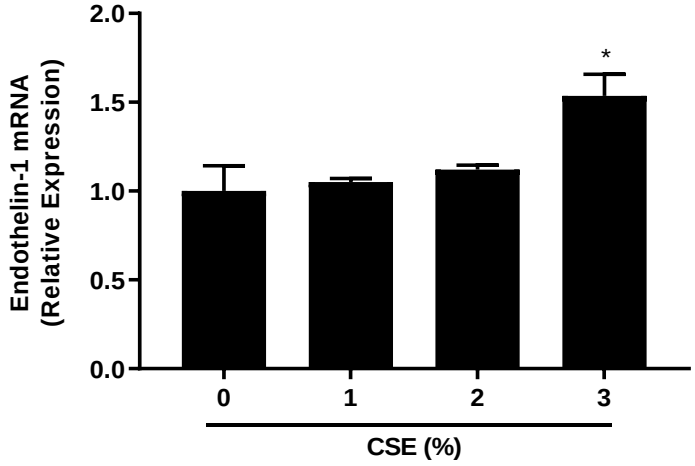


Figure 3.27 Effect of CSE on the mRNA expression of endothelin-1 in human PAECs.
Confluent human PAECs were stimulated with various concentrations of CSE (0%, 1%, 2%, and 3%) for 24 h prior to total RNA isolation. The samples were assayed for the mRNA expression of endothelin-1 using RT-qPCR. Data were expressed as fold change over unstimulated cells (0% CSE). Each data point represents mean ± SEM from three independent experiments using one cell line. *$p<0.05$ compared with unstimulated cells.

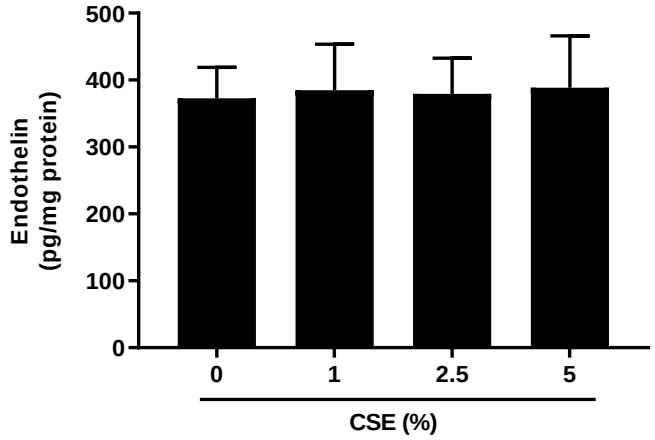


Figure 3.28 Effect of CSE on endothelin production in human PASMCs.
Confluent human PASMCs were treated with different concentrations of CSE (0%, 1%, 2.5%, and 5%) for 48 h with daily fresh DMEM+ and CSE and then with the same concentrations of CSE in DMEM- for 24 h. Supernatants were collected and assayed for endothelin using ELISA analysis. Data were normalised with total protein and expressed as pg/mg protein. Each data point represents mean ± SEM from three independent experiments using cells from three different donors.

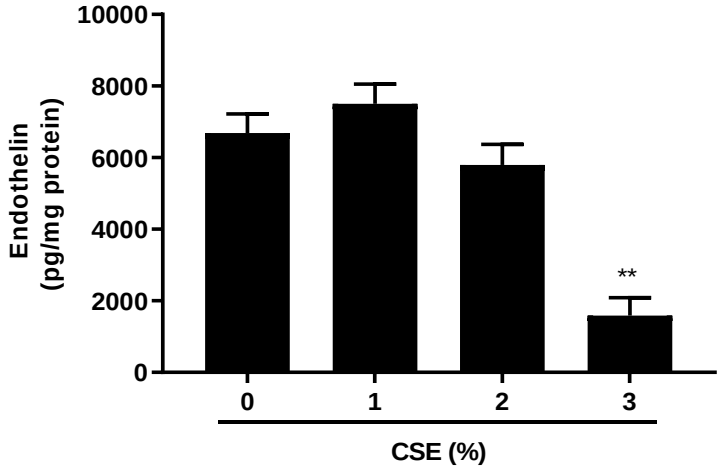


Figure 3.29 Effect of CSE on endothelin production in human PAECs.
Confluent human PAECs were treated with different concentrations of CSE (0%, 1%, 2%, and 3%) for 24 h. Supernatants were collected and assayed for endothelin using ELISA analysis. Data were normalised with total protein and expressed as pg/mg protein. Each data point represents mean ± SEM from three independent experiments using one cell line. **$p<0.01$ compared with untreated cells.

3.5 Discussion

The main aim of this Chapter was to investigate whether CSE can induce imbalanced vasoactive gene expression and mediator release in human PAECs and PASMCs. The key findings of this Chapter are that CSE reduced the production of the vasodilatory and anti-proliferative mediators PGE_2 and PGI_2, and increased the production of the vasoconstrictive and proliferative mediator TXA_2 in human PASMCs. Furthermore, it subsequently reduced the PGI_2/TXA_2 ratio. Although CSE induced vasodilatory and anti-proliferative PGE_2 production and did not have any effect on PGI_2 release in human PAECs, CSE induced TXA_2 production and consequently led to a reduced PGI_2/TXA_2 ratio in human PAECs as well. In addition, our results showed that CSE had no effects on the production of endothelin in human PASMCs, but reduced the production of nitric oxide and endothelin in human PAECs. A summary of the findings is presented in Table 3.1.

Taken together, our findings in this Chapter provide evidence for the first time that CSE can induce imbalanced vasoactive gene expression and mediator release, particularly by reducing PGE_2 production in PASMCs and the PGI_2/TXA_2 ratio in both PASMCs and PAECs. In addition, our data showing CSE-induced imbalanced vasoactive prostanoid mediator release is more prominent in PASMCs than in PAECs suggest that PASMC dysfunction may therefore be more important than the traditionally recognised PAEC dysfunction in contributing to pulmonary artery remodelling and pulmonary hypertension in COPD. This is a novel finding that has not been previously reported.

Table 3.1 A summary table of the findings of Chapter 3.

Gene/Mediator	Function	Effect of CSE	
COX-2	**Vasoactive gene**	**PASMCs**	**PAECs**
COX-2 mRNA		↑	↑
COX-2 protein		↑	↑
mPGES-1/PGE_2	**Vasodilator/ anti-proliferative gene via $EP_{2/4}$ receptors** **Vasoconstrictor/ proliferative gene via $EP_{1/3}$ receptors**	**PASMCs**	**PAECs**
mPGES-1 protein		↓	↑
PGE_2 release		↓	↑
PGIS/PGI_2	**Vasodilator/ anti-proliferative gene**	**PASMCs**	**PAECs**
PGIS mRNA		↓	↓
PGIS protein		↓	**UD**
PGI_2 release		↓	↔
TXAS/TXA_2	**Vasoconstrictor/ proliferative gene**	**PASMCs**	**PAECs**
TXAS mRNA		↑	↑
TXAS protein		**UD**	**UD**
TXA_2 release		↑	↑
eNOS/Nitric oxide	**Vasodilator/ anti-proliferative gene**	**PASMCs**	**PAECs**
eNOS mRNA		**UD**	↔
eNOS protein		**UD**	↓
Nitric oxide release		**UA**	↓
Endothelin	**Vasoconstrictor/ proliferative gene**	**PASMCs**	**PAECs**
Endothelin-1 mRNA		↔	↑
Endothelin release		↔	↓

CSE, Cigarette smoke extract; PASMCs, Pulmonary artery smooth muscle cells; PAECs, Pulmonary artery endothelial cells; COX-2, Cyclooxygenase-2; mPGES-1, Microsomal prostaglandin E synthase-1; PGE_2, Prostaglandin E_2; PGIS, Prostaglandin I synthase; PGI_2, Prostaglandin I_2; TXAS, Thromboxane A synthase; TXA_2, Thromboxane A_2; eNOS, Endothelial nitric oxide synthase; UA, Unassessed; UD, Undetected; ↔, Unchanged; ↑, Upregulated; ↓, Downregulated.

3.5.1 CSE and prostanoids

3.5.1.1 Human pulmonary artery smooth muscle cells

The results presented in this Chapter demonstrated that CSE upregulated the mRNA and protein expression of COX-2 in PASMCs, suggesting that CSE may regulate COX-2 expression via transcriptional regulation in PASMCs. Importantly, this novel finding also suggests that the aberrantly increased expression of COX-2 by CSE in PASMCs may play a role in CS-induced dysfunction of PASMCs, which then leads to vascular remodelling by mediating the induction of imbalanced prostanoid production, particularly PGE_2, PGI_2 and TXA_2, the most well known prostanoid products critically involved in pulmonary vascular remodelling. Although no similar studies have been previously reported regarding the effect of CSE on COX-2 expression in vascular smooth muscle cells (including PASMCs), the above finding is supported by studies conducted by Nana-Sinkam et al. (2007) and Shi et al. (2017). These authors examined the effect of CSE on COX-2 expression in human umbilical vein endothelial cells (Shi et al., 2017) and human pulmonary microvascular endothelial cells (Nana-Sinkam et al., 2007) and showed that CSE treatment can induce the expression of COX-2, suggesting an association of CSE and COX-2 induction in vascular endothelial cells. This is further supported by the fact that COX-2 expression is induced in the lung tissue of both patients with COPD and smokers without COPD compared with non-smokers without COPD (Shi et al., 2017).

It is widely recognised that increased COX-2 expression leads to the induction of PGE_2 production. Our previous findings demonstrating that inflammatory mediators such as IL-1β can induce the protein expression of COX-2 and its product PGE_2 production in

human PASMCs supports this concept (Bradbury et al., 2002). We found in the current study that there is a dissociation between increase of COX-2 expression and decrease of its downstream product PGE_2 in response to CSE. This strongly suggests that the expression of mPGES-1 (the enzyme that mediates PGE_2 conversion from the COX-2 product PGH_2) may play a role in this process. It was then interesting to assess the involvement of mPGES-1 expression in the reduction of PGE_2 production. We observed that mPGES-1 was reduced by CSE in PASMCs in line with PGE_2 findings, suggesting that the reduced PGE_2 production is due to mPEGS-1 expression downregulation, despite COX-2 expression upregulation. Our findings also suggest that the reduction of PGE_2 production by CSE may alter the function of PASMCs, thereby leading to abnormalities of vascular tone and structure. This is a novel finding that has not been previously reported in any cell type or tissue, especially considering that PGE_2 is poorly characterised as a key factor of cell dysfunction in pulmonary hypertension in COPD. As the role of CSE on mPGES-1-derived PGE_2 has not been previously investigated in any vascular cells, further studies are needed to understand how CSE-mediated reduced PGE_2 production can influence PASMC function (e.g. proliferation).

The study also showed for the first time that CSE reduced the mRNA and protein expression of PGIS in human PASMCs. Although several possible mechanisms may be responsible for the reduced expression of PGIS by CSE, it is likely that CSE regulates PGIS expression via transcriptional regulation. In addition, our results suggest that the reduced PGI_2 production is a key part of CSE-induced PASMC dysfunction and may have a potential role in CS-induced vascular remodelling via stimulation of PASMC proliferation. This altered PGIS-derived PGI_2 by CSE in PASMCs is supported by a

previous human study showing reduced PGIS expression and PGI_2 production in the lungs of smokers with COPD (Chen et al., 2012). This is further supported by the findings of the same group, demonstrating an association of decreased PGI_2 and induced apoptosis rate in the lungs of CSE-treated emphysematous rats (Chen et al., 2009). Furthermore, it has been previously reported that mice with lung-specific PGIS overexpression can reduce the endothelial apoptosis rate after chronic CS exposure (Nana-Sinkam et al., 2007), which also suggests that the presence of PGIS/PGI_2 may have anti-apoptotic effects, alongside its vasodilatory and anti-proliferative properties.

It is worth noting that this observation showing reduced PGI_2 production as a result of PGIS expression downregulation after CSE treatment in PASMCs is similar to our mPGES-1/PGE_2 findings discussed above. Although it is commonly accepted that an increase in COX-2 protein expression and COX-2 product PGH_2 usually leads to increased PGI_2 and PGE_2 production, our findings that CSE induced COX-2 expression but reduced both PGI_2 and PGE_2 production as a result of PGIS and mPGES-1 downregulation, respectively, strongly suggest that CSE can selectively reduce vasodilatory and anti-proliferative gene expression and mediator release in prostanoid biosynthesis pathway. These findings also suggest that the downregulated PGIS and mPGES-1 expression may divert the COX-2 product PGH_2 away from vasodilator mediators PGI_2 and PGE_2 towards the vasoconstrictor mediator TXA_2.

Furthermore, the current study demonstrated that although CSE induced the mRNA expression of TXAS, but to our surprise, Western blot analysis showed the protein expression of TXAS was undetectable in both absence and presence of CSE in PASMCs. To exclude the possibility that the antibody and Western blot techniques did

not work, total cell lysates from BEAS-2B normal human bronchial epithelial cells treated with or without CSE were used as a positive control. Our Western blot analysis showed that the TXAS protein was expressed at basal levels and was further induced by 5% CSE in BEAS-2B cells, suggesting that the used antibody and Western blot techniques in this study worked. This observation is further supported by our finding, which will be presented and discussed later in Chapter 4, showing that hypoxia (1% O_2) induced TXAS protein expression using the same human PASMCs and Western blot techniques. Although TXAS protein expression was undetectable under both basal and CSE-treated PASMCs, it is highly likely that PASMCs expressed TXAS protein below the detection levels of Western blotting. This is supported by the fact that the TXAS product TXA_2 was detected in unstimulated PASMCs by ELISA. Since we were able to show that CSE stimulated TXA_2 production, it is likely that the protein expression of TXAS was increased in response to CSE. However, we can not exclude the possibility that TXAS protein expression was decreased or unchanged. Despite this undetected TXAS protein expression, our finding demonstrating increased TXA_2 production after CSE treatment strongly suggests that it is likely this increase of TXA_2 comes as a result of the conversion by the existing TXAS of the increased PGH_2, due to the combined effect of CSE on COX-2 upregulation and PGIS and mPGES-1 downregulation. It is also possible that CSE may cause an increase in TXAS activity (through post-translational modifications) rather than its expression, although there is no direct evidence.

The increase of vasoconstrictive and proliferative TXA_2 in response to CSE treatment in our study suggests that TXA_2 may act as a key mediator of PASMC dysfunction, and may have a detrimental role in CS-induced vascular remodelling in

COPD-associated pulmonary hypertension. As far as we are aware, this is the first demonstration of CSE effect on TXAS-derived TXA_2 in any vascular smooth muscle cells, including PASMCs. Although there are no similar previous studies reporting CSE effect on TXAS-derived TXA_2, our observation is supported by human and animal studies showing elevated levels of TXA_2 in the urine of smokers and ex-smokers COPD patients, compared with healthy subjects (Davi et al., 1997). In addition, it has been demonstrated that TXA_2 is increased in both bronchoalveolar lavage fluid and the lung tissue of rat models exposed to CS (An et al., 2013). These observations alongside our finding provide strong evidence of an association between increased TXA_2 and CS.

Together with TXA_2, PGI_2 (the mediator that induces vasodilatory and anti-proliferative effects) plays an important role in maintaining homeostatic balance in pulmonary circulation. An imbalance with reduced PGI_2 and increased TXA_2 plays a key role in the pathogenesis of several cardiovascular diseases, including PAH (Christman et al., 1992). In the present study, we assessed the effect of CSE on the PGI_2/TXA_2 ratio and found that CSE reduced the vasodilator PGI_2 and increased the vasoconstrictor TXA_2, which then resulted in a reduced PGI_2/TXA_2 ratio in PASMCs. These observations suggest that CSE can cause PASMC dysfunction, particularly by inducing an imbalance between PGI_2 and TXA_2 and this reduced PGI_2/TXA_2 ratio is likely to play a role in CS-induced vascular remodelling in COPD.

To the best of our knowledge, this is the first report describing that PASMCs have important synthetic functions, and that CSE can cause PASMC dysfunction by reducing PGI_2 and PGE_2 releases as a result of PGIS and mPGES-1 protein expression downregulation and increasing TXA_2 release as a result of COX-2 expression

upregulation. This imbalance between reduced vasodilators PGI_2 and PGE_2 and increased vasoconstrictor mediator TXA_2 may play a key role in pulmonary vasoconstriction and proliferation of PASMCs, and eventually contribute to vascular remodelling and pulmonary hypertension in COPD. An illustrative figure of CSE effect on the expression of main enzymes of prostanoid biosynthesis and the release of vasoactive lipid mediators in human PASMCs is shown in Figure 3.30.

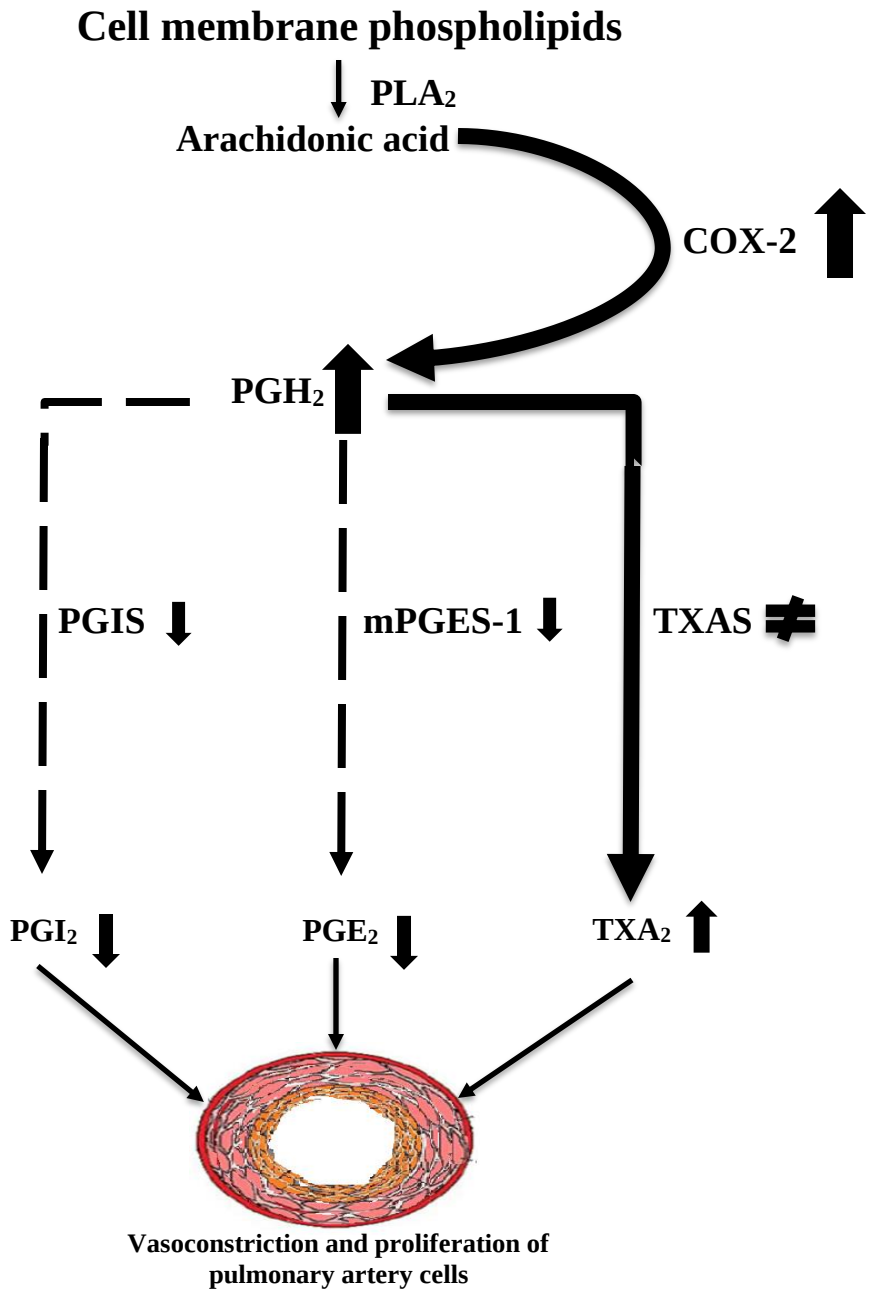


Figure 3.30 Schematic diagram of CSE effect on the expression of the main enzymes of prostanoid biosynthesis and the release of vasoactive lipid mediators in human PASMCs.
CSE reduces PGI_2 and PGE_2 releases in human PASMCs as a result of PGIS and mPGES-1 expression downregulation, respectively. Despite the undetected TXAS protein expression, CSE increases TXA_2 release in PASMCs as a result of an increase in COX-2 expression and its product PGH_2. This novel observation demonstrates shunting of the COX-2 product PGH_2 away from the vasodilatory and anti-proliferative mediators PGI_2 and PGE_2 due to the downregulation of the corresponding synthases PGIS and mPGES-1 towards the vasoconstrictive and proliferative mediator TXA_2. The imbalance may eventually contribute to vasoconstriction and proliferation of PASMCs. PLA_2, Phospholipase A_2; CSE, Cigarette smoke extract; PGH_2, Prostaglandin H_2; PGI_2, Prostaglandin I_2; PGE_2, Prostaglandin E_2; PGIS, Prostaglandin I synthase; mPGES-1, Microsomal prostaglandin E synthase-1; TXAS, Thromboxane A synthase; TXA_2, Thromboxane A_2; COX-2, Cyclooxygenase-2; PASMCs, Pulmonary artery smooth muscle cells; ≠, Undetected; ↑, Upregulated; ↓, Downregulated.

3.5.1.2 Human pulmonary artery endothelial cells

Similar to the findings from PASMCs, we also presented evidence that CSE induced the mRNA and protein expression of COX-2 in human PAECs, suggesting that COX-2 expression is likely to be regulated by CSE via transcriptional regulation. Although the effect of CSE on COX-2 expression has not been previously assessed in human PAECs, our observation is supported by previous studies conducted in other endothelial cell types. It has been shown that CSE can induce the mRNA expression of COX-2 in human pulmonary microvascular endothelial cells (Nana-Sinkam et al., 2007). This is further supported by a recent finding reporting an increase of mRNA and protein expression of COX-2 by CSE in human umbilical vein endothelial cells (Shi et al., 2017). Our findings from both cell types suggest that COX-2 upregulation may play a role in CS-induced PAEC and PASMC dysfunction and proliferation by mediating an imbalance of its downstream prostanoid products.

The finding that CSE induced PGE_2 production in PAECs is likely to occur as a result of the increase in the expression of COX-2, the rate-limiting enzyme in prostanoid production. Intriguingly, this observation is different from the findings discussed above showing that CSE increased COX-2 expression but reduced PGE_2 production due to mPGES-1 downregulation in PASMCs. To the best of our knowledge, this is the first report to show that CSE can cause different effects on PGE_2 in PASMCs and PAECs. It was then interesting to find out whether the expression level of mPGES-1 plays a role in CSE-induced PGE_2 production in PAECs. It was found that the basally expressed mPGES-1 seemed to be induced by CSE in PAECs, in line with PGE_2 findings (although this experiment was only conducted once). This interesting and novel finding suggests

that CSE can regulate mPGES-1 expression and PGE_2 production differently in the two cell types.

Since PGE_2 and its receptors have the capability to either induce or suppress vasodilatory/anti-proliferative and vasoconstrictive/proliferative effects, it is reasonable to speculate that the different effects of CSE on PGE_2 levels may lead to different functional consequences in the two cell types. This is supported by the fact that $EP_{2/4}$ receptors that mediate anti-proliferative effects are mainly expressed in PASMCs (Fan et al., 2018), while $EP_{1/3}$ receptors that mediate proliferative effects are predominantly expressed in vascular endothelial cells (Suzuki et al., 2013). For example, one study demonstrated that exogenous PGE_2 can stimulate proliferation of human umbilical vein endothelial cells, and this proliferation can be inhibited by combined $EP_{1/2}$ receptor antagonist AH6809 (Zhao et al., 2012). Considering the diverse roles of PGE_2 in vascular cells depending on its binding receptors (Yang and Chen, 2016), our findings suggest that CSE-induced PGE_2 is likely to play a role in CS-induced cell dysfunction, thereby leading to proliferative PAECs. However, since the functional consequence of CSE-induced PGE_2 in any human vascular cell types has not been studied, it would be of further interest to investigate how CSE effect on PGE_2 can influence the functions of PASMCs and PAECs.

Our results also showed that CSE reduced the mRNA expression of PGIS in PAECs. Surprisingly, the protein expression of PGIS in PAECs as assessed by Western blotting was undetectable under basal and CSE-treated PAECs conditions. As previously discussed, the observation that PGIS protein was expressed in untreated PASMCs suggests that the methods worked. Since PGI_2 production was presented at low basal

levels (792.0±94.7 pg/mg protein) compared with PASMCs (2987.2±403.5 pg/mg protein) and was unchanged following CSE treatment in PAECs, it is likely that PGIS protein was expressed below the detection levels of Western blotting. Although it is possible that CSE increased PGIS protein expression in PAECs, it is more likely that CSE had no effect or could reduce PGIS protein expression. This is supported by the observation that PGIS expression is reduced in vascular endothelial cells of human lung tissues of smokers with COPD, as assessed by immunohistochemical staining (Chen et al., 2012). Furthermore, the unchanged PGI_2 release in PAECs is in disagreement with the previous *in vitro* study showing reduced PGI_2 release in response to CSE (up to 10%) at 24 h in human umbilical vein endothelial cells (Chen et al., 2012). Differences between the two studies may be explained by the variations in cell types and cigarette brand (Marlboro) used to conduct their study. In addition, the present findings from PAECs differ from our findings, demonstrating reduced PGIS/PGI_2 by CSE in PASMCs. These differences may be explained by the fact that different cell types may behave differently, and there are variations in the duration of CSE treatment.

Although it is commonly considered that vascular endothelial cells are the main source of PGI_2, our combined findings provide evidence for the first time that PASMCs can be a more important source of PGI_2 than PAECs. This further suggests that the overall effect of CSE on PGIS/PGI_2 may have a detrimental role in CS-induced vascular remodelling in COPD-associated pulmonary hypertension, considering that PASMCs constitute a prominent feature in remodelled vasculature.

The finding that CSE induced TXAS mRNA expression (undetected TXAS protein expression) in PAECs is similar to our findings from PASMCs. It is likely that

PAECs expressed TXAS protein below the detection levels of Western blot analysis. Although we can not exclude the possibility that TXAS protein expression was decreased or unchanged, it is reasonable to speculate that the protein expression of TXAS was increased by CSE. This is because we were able to show that CSE stimulated TXA_2 production in PAECs. Despite this undetected TXAS protein expression, the increase of TXA_2 by CSE is consistent with our findings from PASMCs and is likely to occur as a result of the increased PGH_2 due to COX-2 upregulation by CSE. The possibility that CSE may cause an increase in TXAS activity via post-translational modifications, rather than its expression, may also explain the increase of TXA_2; however, currently there is no direct evidence to support this theory. CSE-induced TXA_2 production in PAECs and PASMCs together with the previous study showing TXA_2 increase by CSE (Milara et al., 2010) provides strong evidence that TXA_2 may act as a key mediator of PAEC and PASMC dysfunction.

Although CSE had no effect on PGI_2 production in PAECs, we provide the first evidence that CSE reduced the PGI_2/TXA_2 ratio in PAECs because the increase of TXA_2 is sufficient to override the unchanged PGI_2, suggesting CSE may cause PAEC dysfunction by reducing the PGI_2/TXA_2 ratio and increasing PGE_2. This imbalance of vasoactive prostanoid production in PAECs is likely to contribute to vascular remodelling in COPD. An illustration of CSE effect on the expression of main enzymes of prostanoid biosynthesis and the release of vasoactive lipid mediators in PAECs is presented in Figure 3.31.

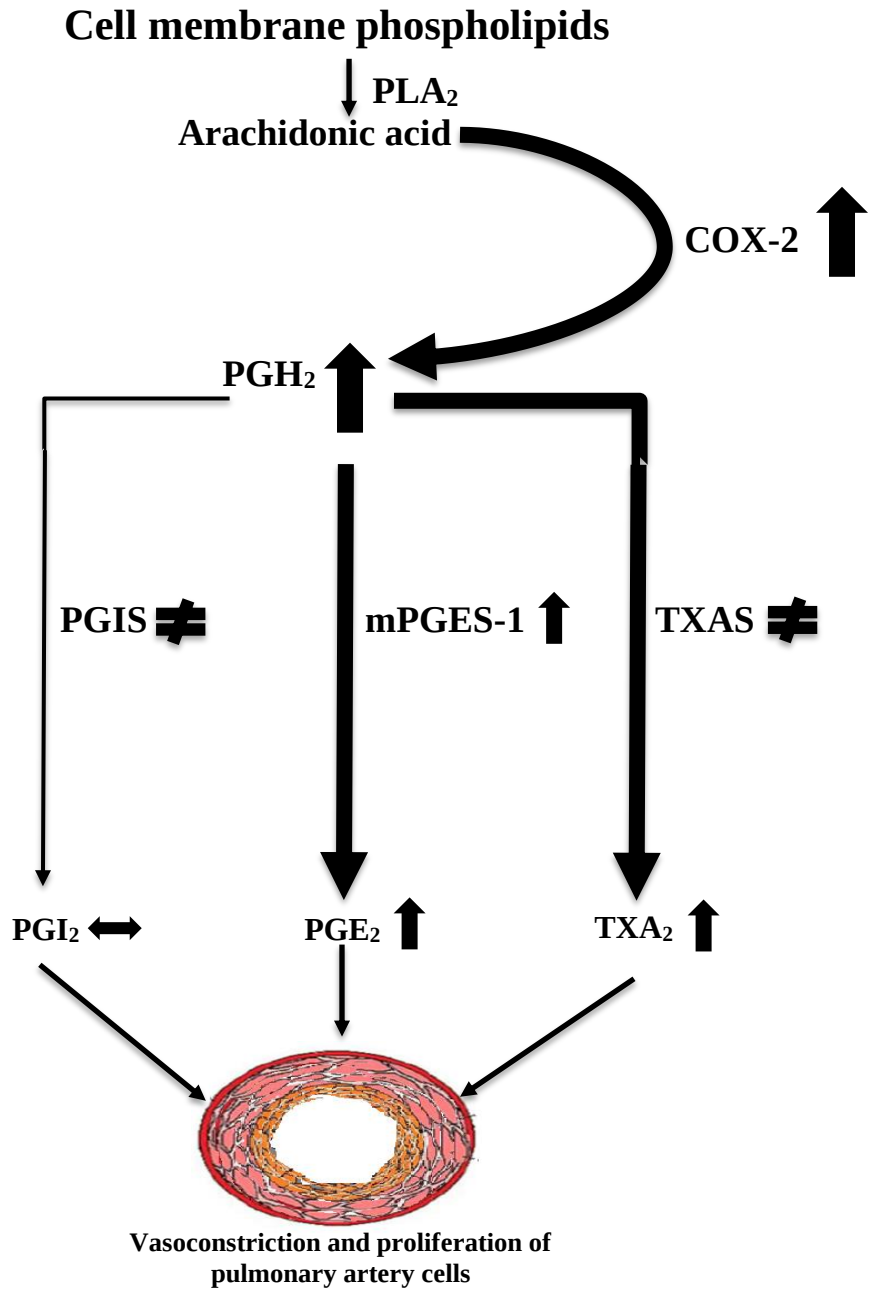


Figure 3.31 Schematic diagram of CSE effect on the expression of the main enzymes of prostanoid biosynthesis and the release of vasoactive lipid mediators in human PAECs.
CSE increases PGE_2 release in human PAECs due to COX-2 and mPGES-1 expression upregulation. Despite the undetected TXAS and PGIS expression, CSE increases TXA_2 as a result of an increase in COX-2 expression but has no effects on PGI_2 release and subsequently reduced the PGI_2/TXA_2 ratio in PAECs. This novel observation demonstrates a diversion of the COX-2 product PGH_2 towards PGE_2 and the vasoconstrictive and proliferative mediator TXA_2. The imbalance may eventually contribute to vasoconstriction and proliferation of pulmonary artery cells. PLA_2, Phospholipase A_2; CSE, Cigarette smoke extract; PGH_2, Prostaglandin H_2; PGI_2, Prostaglandin I_2; PGE_2, Prostaglandin E_2; PGIS, Prostaglandin I synthase; mPGES-1, Microsomal prostaglandin E synthase-1; TXAS, Thromboxane A synthase; TXA_2, Thromboxane A_2; COX-2, Cyclooxygenase-2; PAECs, Pulmonary artery endothelial cells; ↔, Unchanged; ≠, Undetected; ↑, Upregulated; ↓, Downregulated.

3.5.2 CSE and eNOS/nitric oxide

Since nitric oxide released from PAECs is known to have functional effects on PASMCs, we were interested to assess CSE effect on eNOS and nitric oxide levels in PASMCs. The observation that eNOS expression was undetectable in PASMCs suggests that it is likely that PASMCs are not a source of nitric oxide in pulmonary vasculature. Thus, no further experiments were carried out to assess the CSE effect on the production of nitric oxide. Although no previous studies have reported that human PASMCs can express eNOS (as far as can be determined), it has been recently demonstrated that the protein expression of eNOS is detected at low levels in rat PASMCs and is induced by suberanilohydroxamic acid (SAHA), a non-selective histone deacetylase (HDAC) class 1 and 2 inhibitor (Tan et al., 2017). The induced eNOS expression by SAHA (but not CSE) in PASMCs may be explained by the fact that SAHA can inhibit HDACs and then cause transcriptional upregulation of eNOS.

It is interesting that CSE reduced the basally expressed eNOS protein, but not the mRNA expression in PAECs. This dissociation could be because CSE is likely to regulate eNOS expression through post-transcriptional regulation or post-translational modifications. However, currently there is no direct evidence of this. Our finding is supported by previous studies reporting reduced eNOS protein expression in the lung tissues of smokers (Barbera et al., 2001) and in CSE-treated cultured PAECs isolated from pigs (Su et al., 1998). In the current study, it was also demonstrated that CSE reduced nitric oxide as a result of eNOS protein expression downregulation in human PAECs. This finding is consistent with a previous study showing reduced nitric oxide production in human PAECs in response to CSE (Milara et al., 2010); however, the

investigators did not assess CSE effect on the mRNA and protein expression of eNOS in their study.

Collectively, we found that CSE reduced nitric oxide production as a result of the reduced protein expression of eNOS in human PAECs. The results suggest that reduced nitric oxide bioavailability may be a key part of CS-induced PAEC dysfunction and may contribute to vascular remodelling in COPD.

3.5.3 CSE and endothelin

Although no previous studies have assessed CSE effect on endothelin-1 mRNA expression in human PASMCs, the finding that CSE increased endothelin-1 mRNA expression in human PAECs (but not in human PASMCs) is supported by studies demonstrating that CSE increased endothelin-1 mRNA expression in both human and bovine PAECs (Lee et al., 2001), as well as in the cardiovascular tissues of rats (Adachi et al., 2000). As with the mRNA, CSE had no effect on endothelin production in PASMCs. However, the reduction of endothelin production by CSE in PAECs is not consistent with increased mRNA endothelin-1 expression in PAECs. It is likely that this observation is due to post-translational modifications; however, there is no direct evidence of this. The ELISA results differ from previous studies that reported CSE (10%, 24 h treatment) increased endothelin release in human PAECs from three different donors (Milara et al., 2010), as well as in human PASMCs from one donor (Milara et al., 2012); however the mRNA expression was not assessed in that study. The different effects of CSE on endothelin are probably due to the difference in incubation time, particularly for PASMCs (72 h vs 24 h) with CSE and research cigarette used. Milara and colleagues (2010 and 2012) used a 2R4F research cigarette, which was replaced in 2006 by the

3R4F, the one used in the current study. In their studies, they also incubated PAECs with CSE in a different cell culture medium supplemented with 10% foetal calf serum and used the PASMCs at different cell passages (1 to 4) from those at passage 6 used in our study.

Although there are three different isoforms of endothelin (endothelin-1, endothelin-2, and endothelin-3), they have similar functions and their vasoconstrictive and vasodilatory effects are mediated by two types of receptors: ET-A and ET-B. It is worth noting that PAECs in our study released endothelin at high basal levels (6689.4±529.4 pg/mg protein) compared with PASMCs (372.7±46.3 pg/mg protein). This observation, together with the fact that ET-B receptor stimulation in healthy endothelial cells can cause vasodilation (Iglarz et al., 2015) suggests that endothelin may have vasodilatory properties by activating ET-B receptors in endothelial cells. However, the vasodilatory effects, mediated by the activation of the ET-B receptor, are lost in arteries of rats with pulmonary hypertension (Iglarz et al., 2015). Our findings suggest that PAECs are an important source of endothelin. Although CSE did not alter and reduced endothelin in PASMCs and PAECs, respectively, the functional consequence of this effect remains unclear. It would be of interest to conduct further experiments to explore the pathological consequences.

In summary, the findings in this Chapter support our hypothesis that CSE can induce imbalanced vasoactive gene expression and mediator release in human PAECs and PASMCs. Our data demonstrating that CSE can reduce the PGI_2/TXA_2 ratio in PASMCs and PAECs, and PGE_2 in PASMCs, provide evidence for the first time that the disrupted prostanoid pathway may be more critically involved in CS-induced dysfunction

of PASMCs and PAECs than the nitric oxide and endothelin pathways. Our findings also suggest that CSE-induced imbalanced vasoactive mediator release is more prominent in PASMCs than in PAECs, and that PASMC dysfunction may therefore be more important than the traditionally recognised PAEC dysfunction in contributing to vasoconstriction and proliferation of pulmonary artery cells in COPD. These novel observations provide new insights into the understanding of CS-induced PASMC and PAEC dysfunction and vascular remodelling and may eventually lead to therapeutic potentials for pulmonary hypertension in COPD by restoring the balance of vasoactive mediators. An illustrative diagram to summarise CSE effect is shown in Figure 3.32.

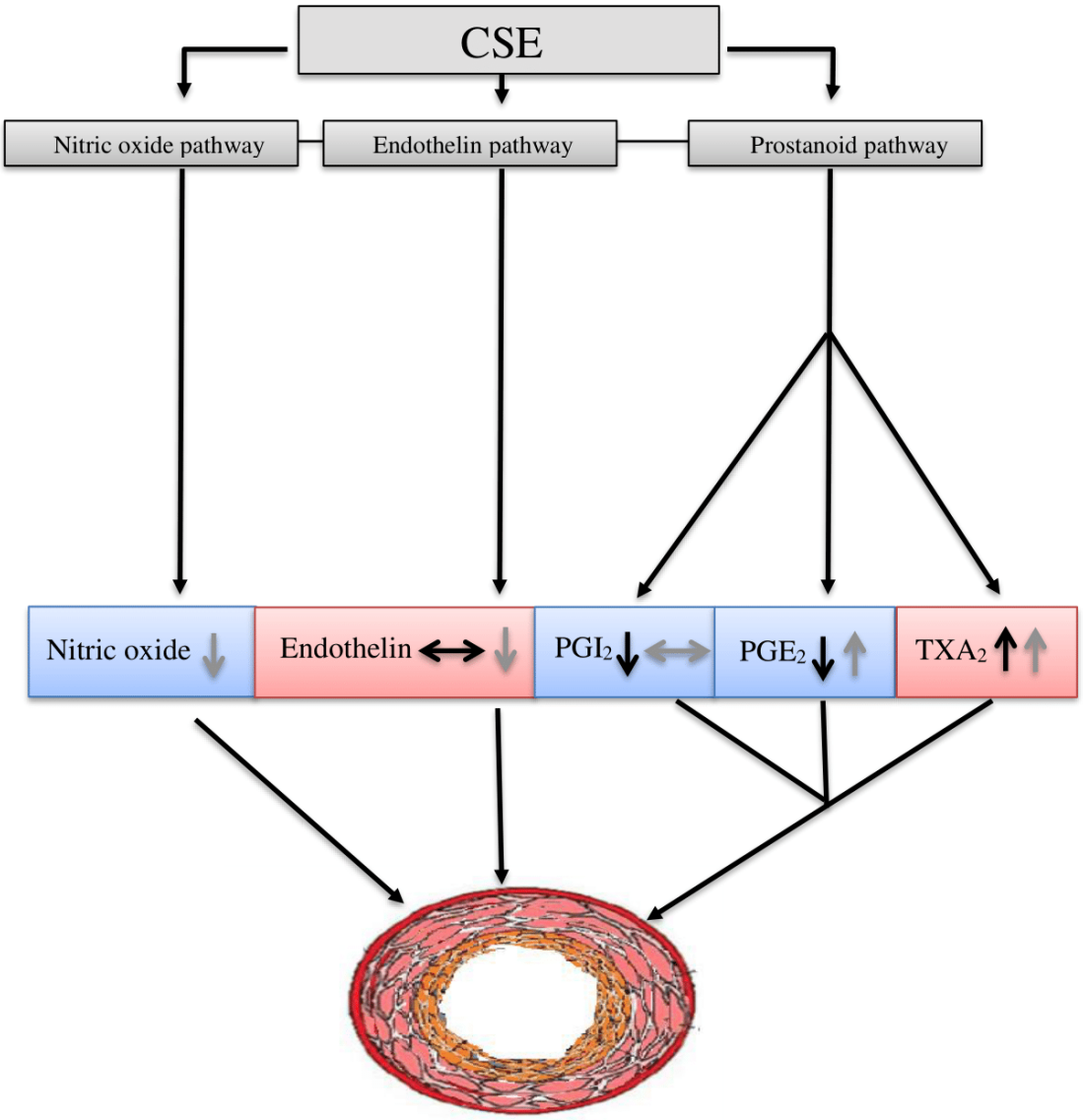


Figure 3.32 Schematic diagram of CSE effect on nitric oxide, endothelin and prostanoid production.

This is an illustrative diagram to summarise the deregulated vasoactive anti-proliferative and vasodilator mediators (blue rectangle) and proliferative and vasoconstrictor mediators (red rectangle) in human PASMCs (black arrow) and PAECs (grey arrow) that may contribute to CS-induced vascular remodelling in COPD. In PASMCs, CSE decreases PGI_2 and PGE_2 and increases TXA_2 production but has no effect on endothelin production. Nitric oxide was not assessed as endothelial nitric oxide synthase (eNOS) expression was undetectable in PASMCs. In PAECs, CSE reduces nitric oxide and endothelin production and induces PGE_2 and TXA_2 production but has no effect on PGI_2. CSE, Cigarette smoke extract; PGI_2, Prostaglandin I_2; PGE_2, Prostaglandin E_2; TXA_2, Thromboxane A_2; COX-2, Cyclooxygenase-2; ↔, Unchanged; ↑, Upregulated; ↓, Downregulated.

Chapter 4. Effect of hypoxia alone and in combination with CSE on vasoactive gene expression and mediator release in human PASMCs and PAECs

4.1 Introduction

In the previous Chapter, we showed that CSE caused an imbalance with reduced vasodilators PGI_2 and PGE_2 and increased vasoconstrictor TXA_2 in human PASMCs. In addition, although CSE resulted in increased and unchanged release of the PGE_2 and PGI_2 in PAECs, respectively, TXA_2 production was induced by CSE. This suggests that the imbalance mainly between PGI_2 and TXA_2 (reduced PGI_2/TXA_2 ratio) may play a key role in the dysfunction of both cell types, thereby contributing to vascular constriction and remodelling and eventually pulmonary hypertension in COPD. In addition to CS, it has long been thought that chronic hypoxia can cause pulmonary hypertension in COPD as a consequence of pulmonary vasoconstriction and vascular remodelling, including proliferation of pulmonary artery cells (Wang et al., 2018, Tuder et al., 1995). More prominent remodelling in the pulmonary arteries has been reported in animals exposed to hypoxia in combination with CS, compared with CS alone (Ferrer et al., 2011). These findings, showing hypoxia can further amplify CS-induced vascular remodelling, support the idea that CS can initiate vascular remodelling, which may be further amplified by chronic hypoxia in advanced COPD (Santos et al., 2002). However, the effect of hypoxia alone or in combination with CSE on vasoactive gene expression and mediator release, and the contribution of PASMCs and PAECs in this process remain unknown.

4.2 Aims

For the stated reasons, in this Chapter, the aim was to explore whether hypoxia can induce imbalanced vasoactive gene expression and mediator release in human PASMCs and PAECs, and to evaluate whether there is a synergetic or additive effect between CSE and hypoxia.

The specific aims of this Chapter were:

- To assess whether hypoxia has an effect on the mRNA and protein expression of key enzymes of prostanoid synthesis and the release of vasoactive lipid mediators, including COX-2/PGE_2, PGIS/PGI_2, and TXAS/TXA_2 in human PASMCs and PAECs.
- To evaluate the effect of hypoxia on the mRNA and protein expression of eNOS and the production of nitric oxide in human PASMCs and PAECs.
- To investigate the effect of hypoxia on the expression of endothelin-1 and the production of endothelin in human PASMCs and PAECs.
- To determine whether there is a synergetic or additive effect between CSE and hypoxia.

4.3 Materials and methods

4.3.1 Cigarette smoke extract preparation

Aqueous CSE was prepared as previously described in the materials and methods, section 2.3.1.

4.3.2 Cell treatment

4.3.2.1 Pulmonary artery smooth muscle cells

Human PASMCs from three different healthy donors at passage 6 were incubated with or without CSE for 48 h with daily fresh DMEM+ under normoxic (21% O_2, 5% CO_2, and 74% N_2) or hypoxic (1% O_2, 5% CO_2, and 94% N_2) conditions as described in section 2.4.1. The cells were then cultured with or without CSE in fresh DMEM- under the same culture conditions for another 24 h.

4.3.2.2 Pulmonary artery endothelial cells

Human PAECs from one healthy donor at passage 8 were treated with or without CSE under normoxic (21% O_2, 5% CO_2, and 74% N_2) or hypoxic (1% O_2, 5% CO_2, and 94% N_2) conditions for 24 h, as described in materials and methods, section 2.4.1.

4.3.3 RT-qPCR

At the end of the experiment, total RNA was isolated and RT-qPCR analysis was then carried out to assess the mRNA expression of COX-2, PGIS, TXAS, endothelin-1, and eNOS (materials and methods, section 2.9). It should be noted that β2M was used as a reference gene for all experiments. Data were expressed as relative expression (fold change).

4.3.4 Western blotting

Total cell lysates were collected and analysed for COX-2, mPGES-1, PGIS, TXAS, and eNOS proteins using Western blotting (materials and methods, section 2.8). GAPDH was used as loading control to ensure an equal loading of samples.

4.3.5 ELISA

Supernatants were collected and assayed for PGE_2, 6-keto $PGF_{1\alpha}$, TXB_2, and endothelin using ELISA analysis (materials and methods, section 2.10). Data were normalised with total protein and expressed as pg/mg protein.

4.3.6 Nitrate/nitrite assay

Following supernatants collection, total nitrate/nitrite in cell culture supernatants was assessed using fluorometric assay (materials and methods, section 2.10). Data were normalised with total protein and presented as nmol/μg protein.

4.4 Results

4.4.1 Effect of hypoxia alone and in combination with CSE on the mRNA and protein expression of COX-2 and PGE_2 production in human PASMCs and PAECs

In Chapter 3, we showed that CSE induced the mRNA and protein expression of COX-2 in PASMCs and PAECs. A previous study conducted by our group demonstrated that hypoxia can induce the protein expression of COX-2 in PASMCs (Bradbury et al., 2002). However, it is unknown whether the COX-2 expression upregulation by CSE can be further amplified by hypoxia. In addition, the effect of hypoxia alone and in combination with CSE on COX-2 expression in PAECs has not been explored. Thus, we started this Chapter by assessing the effect of hypoxia with or without CSE on COX-2 mRNA and protein expression in both human PASMCs and PAECs.

We found that COX-2 mRNA was detectable at basal levels in PASMCs. Consistent with our findings in Chapter 3, 5% CSE (but not 1% and 2.5% CSE) under normoxic conditions upregulated the mRNA expression of COX-2 compared with basal levels. Hypoxia alone also significantly increased the mRNA expression of COX-2 (fold change 2.5±0.1, $p<0.001$) compared with unstimulated cells. Although CSE at all concentrations significantly increased COX-2 mRNA expression under hypoxic conditions compared with unstimulated cells, no significant changes were observed, compared with corresponding CSE concentration under normoxic conditions in PASMCs (Figure 4.1). PAECs also expressed COX-2 mRNA basally. Similar to observations from the previous Chapter, CSE under normoxic conditions at all concentrations tested induced COX-2 mRNA expression compared with untreated cells. However, hypoxia alone did not alter the mRNA expression of COX-2 in PAECs and no further increase of COX-2

mRNA expression was observed following PAEC incubation with CSE concentrations under hypoxic conditions, compared with corresponding CSE concentrations under normoxic conditions (Figure 4.2).

Collectively, our results suggest that hypoxia alone can induce COX-2 mRNA expression in PASMCs, but not in PAECs, and that hypoxia does not further increase CSE-induced COX-2 mRNA expression in both cell types.

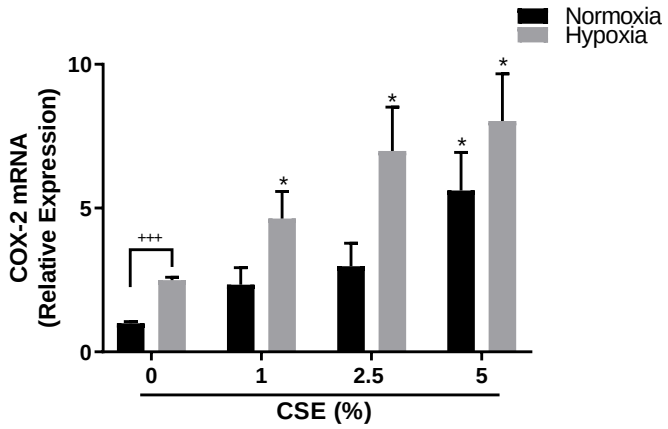


Figure 4.1 Effect of hypoxia and hypoxia+CSE on the mRNA expression of COX-2 in human PASMCs.
Confluent human PASMCs were stimulated with different concentrations of CSE (0%, 1%, 2.5%, and 5%) under normoxic (21% O_2) or hypoxic (1% O_2) conditions for 48 h with daily fresh DMEM+ and CSE and then with the same concentrations of CSE under normoxic or hypoxic conditions in DMEM- for 24 h. Total RNA was isolated and the samples were then assayed for the mRNA expression of COX-2 using RT-qPCR. Data were expressed as fold change over unstimulated cells (0% CSE). Each data point represents mean ± SEM from three independent experiments using cells from three different donors. *$p<0.05$ compared with unstimulated cells. $^{+++}p<0.001$ compared with corresponding CSE concentration under normoxic conditions.

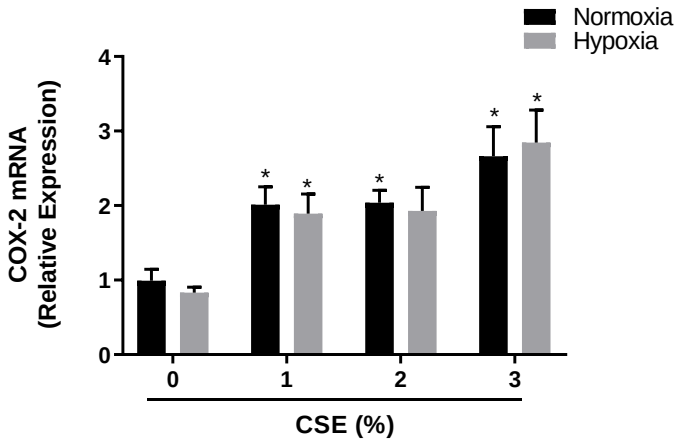


Figure 4.2 Effect of hypoxia and hypoxia+CSE on the mRNA expression of COX-2 in human PAECs.
Confluent human PAECs were treated with different concentrations of CSE (0%, 1%, 2%, and 3%) under normoxic (21% O_2) or hypoxic (1% O_2) conditions for 24 h prior to total RNA isolation. The samples were assayed for the mRNA expression of COX-2 using RT-qPCR. Data were expressed as fold change over untreated cells (0% CSE). Each data point represents mean ± SEM from three independent experiments using one cell line. *$p<0.05$ compared with untreated cells.

Further experiment was then carried out to investigate whether hypoxia-induced upregulation of the mRNA expression of COX-2 in PASMCs could lead to increased COX-2 protein expression. We also wanted to explore whether hypoxia could further amplify CSE-induced effects. The results, as presented in Figure 4.3A, revealed that COX-2 expression was undetectable under basal conditions in PASMCs. In agreement with the findings in Chapter 3, treatment with CSE induced COX-2 protein expression in a concentration-dependent manner. Hypoxia alone also induced COX-2 protein expression (fold change 2.9±0.3, $p<0.01$) compared with untreated PASMCs (Figure 4.3A and B). Interestingly, no further induction of COX-2 protein was noted when both hypoxia and CSE were combined, compared with CSE under normoxic conditions (Figure 4.3A and B). The results also showed that PAECs did not express COX-2 protein basally (Figure 4.4A). PAEC stimulation with CSE increased COX-2 expression significantly in a concentration-dependent manner. Consistent with COX-2 mRNA expression results, hypoxia alone had no effect on COX-2 protein expression and did not further increase CSE-induced COX-2 protein expression in PAECs (Figure 4.4A and B).

The protein data in conjunction with our mRNA data suggest that hypoxia alone can induce COX-2 expression at both mRNA and protein levels in PASMCs (but not in PAECs), and that hypoxia does not further enhance CSE-induced COX-2 mRNA and protein expression in PASMCs and PAECs. The observations also suggest that this COX-2 induction in PASMCs may play a role in regulating the induction of imbalanced prostanoid production, particularly PGE_2, PGI_2, and TXA_2, prostanoid products that are well known for their involvement in pulmonary vascular remodelling.

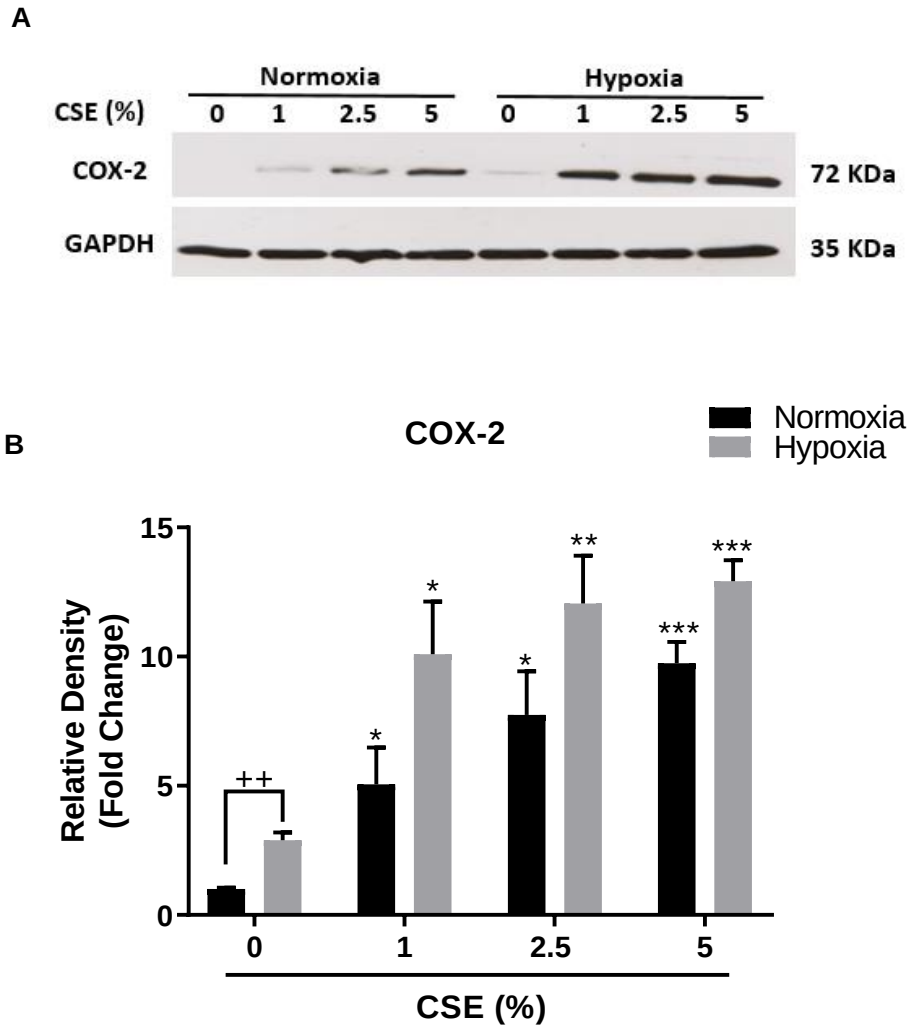


Figure 4.3 Effect of hypoxia and hypoxia+CSE on the protein expression of COX-2 in human PASMCs.

Confluent human PASMCs were treated with different concentrations of CSE (0%, 1%, 2.5%, and 5%) under normoxic (21% O_2) or hypoxic (1% O_2) conditions for 48 h with daily fresh DMEM+ and CSE and then with the same concentrations of CSE under normoxic or hypoxic conditions in DMEM- for 24 h. Total cell lysates were collected for Western blot analysis of COX-2 protein. A, a representative Western blot showing the effect of CSE under normoxic or hypoxic conditions on COX-2 protein expression. B, optical densitometry analysis of Western blotting bands. Data were normalised with the loading control GAPDH and were expressed as fold change over untreated cells (0% CSE). Each data point represents mean ± SEM from three independent experiments using cells from three different donors. *$p<0.05$, **$p<0.01$, ***$p<0.001$ compared with untreated cells. $^{++}p<0.01$ compared with corresponding CSE concentration under normoxic condition.

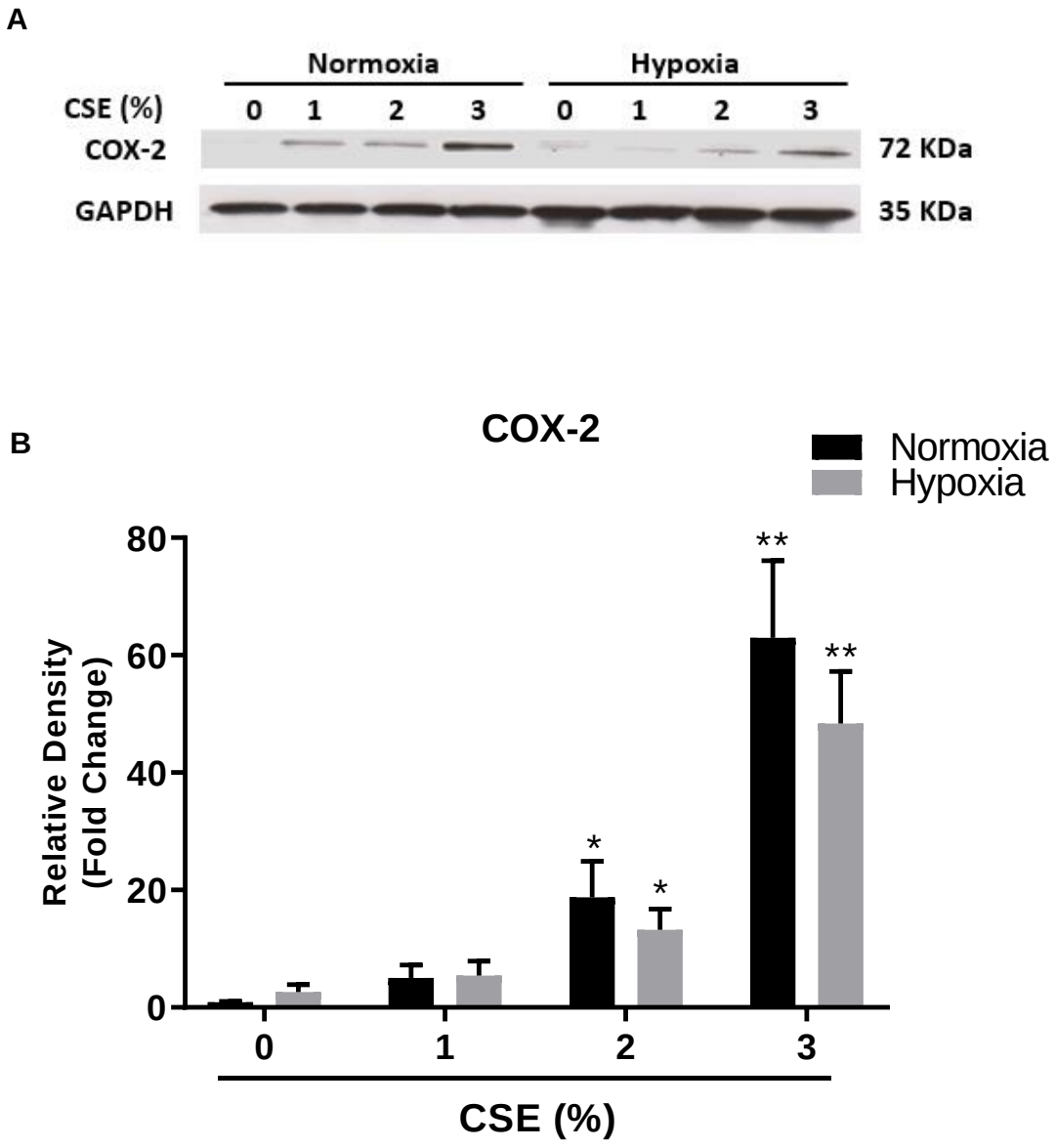


Figure 4.4 Effect of hypoxia and hypoxia+CSE on the protein expression of COX-2 in human PAECs.

Confluent human PAECs were treated with different concentrations of CSE (0%, 1%, 2%, and 3%) under normoxic (21% O_2) or hypoxic (1% O_2) conditions for 24 h. Total cell lysates were collected for Western blot analysis of COX-2 protein. A, a representative Western blot showing the effect of CSE under normoxic or hypoxic conditions on COX-2 protein expression. B, optical densitometry analysis of Western blotting bands. Data were normalised with the loading control GAPDH and were expressed as fold change over untreated cells (0% CSE). Each data point represents mean ± SEM from three independent experiments using one cell line. *$p<0.05$, **$p<0.01$ compared with untreated cells.

We then explored whether hypoxia alone has an effect on the production of PGE_2 and whether hypoxia can further enhance CSE-induced effects in both cell types. Since hypoxia did not further amplify CSE-induced COX-2 expression, it is less likely that CSE-induced effects on vasoactive mediator releases will be further enhanced by hypoxia. Thus, PASMCs and PAECs were treated with or without one concentration of CSE under normoxic or hypoxic conditions. Supernatants were then collected and assayed for PGE_2 using ELISA analysis. Our results showed that PASMCs were able to produce PGE_2 at basal levels (863.2±79.6 pg/mg protein). Consistent with our findings in Chapter 3, treatment with 5% CSE significantly reduced PGE_2 production (Figure 4.5). In contrast, hypoxia alone significantly induced PGE_2 production (5659.9±1115.9 pg/mg protein, $p<0.05$) compared with untreated cells; however, this induction of PGE_2 production by hypoxia was cancelled out when both stimuli were combined in PASMCs (Figure 4.5). PAECs produced lower levels of PGE_2 (241±29.5 pg/mg protein) (Figure 4.6) compared with PASMCs under basal conditions. Although stimulation with 3% CSE significantly induced the production of PGE_2, hypoxia caused no effect on the production of PGE_2 compared with untreated cells, and did not induce any additive effect on CSE-induced PGE_2 production in PAECs compared with CSE (Figure 4.6).

Together, these results suggest that hypoxia alone can increase PGE_2 production in PASMCs (but not in PAECs) as a result of COX-2 upregulation. In addition, hypoxia does not further enhance CSE-induced reduction and increase of PGE_2 production in PASMCs and PAECs, respectively.

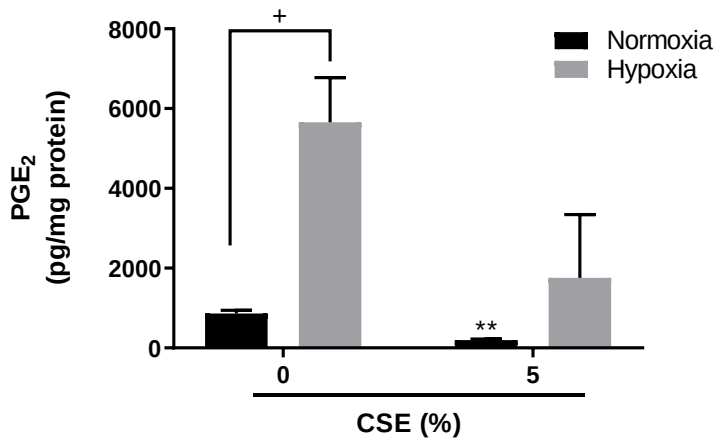


Figure 4.5 Effect of hypoxia and hypoxia+CSE on PGE_2 production in human PASMCs.
Confluent human PASMCs were treated with CSE (0% and 5%) under normoxic (21% O_2) or hypoxic (1% O_2) conditions for 48 h with daily fresh DMEM+ and CSE and then with the same concentrations of CSE under normoxic or hypoxic conditions in DMEM- for 24 h. Supernatants were collected and assayed for PGE_2 using ELISA analysis. Data were normalised with total protein and expressed as pg/mg protein. Each data point represents mean ± SEM from three independent experiments using cells from three different donors. **p<0.01 compared with untreated cells. $^{+}$p<0.05 compared with corresponding CSE concentration under normoxic condition.

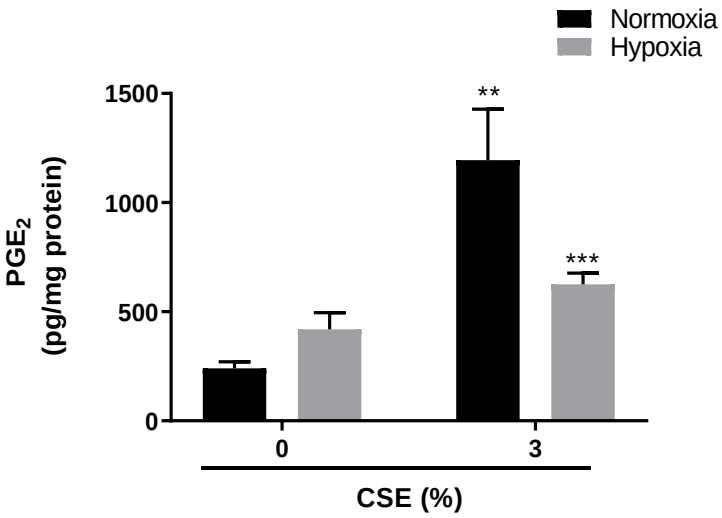


Figure 4.6 Effect of hypoxia and hypoxia+CSE on PGE_2 production in human PAECs.
Confluent human PAECs were treated with CSE (0% and 3%) under normoxic (21% O_2) or hypoxic (1% O_2) conditions for 24 h. Supernatants were collected and assayed for PGE_2 using ELISA analysis. Data were normalised with total protein and expressed as pg/mg protein. Each data point represents mean ± SEM from four independent experiments using one cell line. **p<0.01, ***p<0.001 compared with untreated cells.

4.4.2 Effect of hypoxia alone and in combination with CSE on the mRNA and protein expression of PGIS and PGI_2 production in human PASMCs and PAECs

Hypoxia is considered a strong stimulus of pulmonary vasoconstriction and vascular remodelling in COPD patients (Bogaard, 2017). However, it is unknown if PGIS-derived PGI_2 is involved in this process. Thus, we examined the effect of hypoxia on PGIS expression and PGI_2 production, and whether hypoxia could further amplify CSE-induced effects. We found that PGIS mRNA was constitutively expressed in PASMCs. In agreement with the findings reported in Chapter 3, 2.5% and 5% CSE (but not 1% CSE) under normoxic conditions reduced PGIS mRNA expression (Figure 4.7). Although hypoxia alone failed to have any effect on the mRNA expression of PGIS compared with unstimulated cells, these results demonstrated that hypoxia increased the effect of CSE (5%) on PGIS mRNA expression (fold change 0.87±0.03, $p<0.01$) compared with 5% CSE under normoxic conditions. PGIS mRNA was also expressed at basal levels in PAECs. As reported in Chapter 3, treatment with 3% CSE reduced the mRNA expression of PGIS (Figure 4.8). Consistent with PGIS mRNA expression results from PASMCs, hypoxia alone did not modify PGIS mRNA expression compared with untreated cells. Surprisingly, hypoxia cancelled out the effect of CSE on PGIS mRNA expression (Figure 4.8).

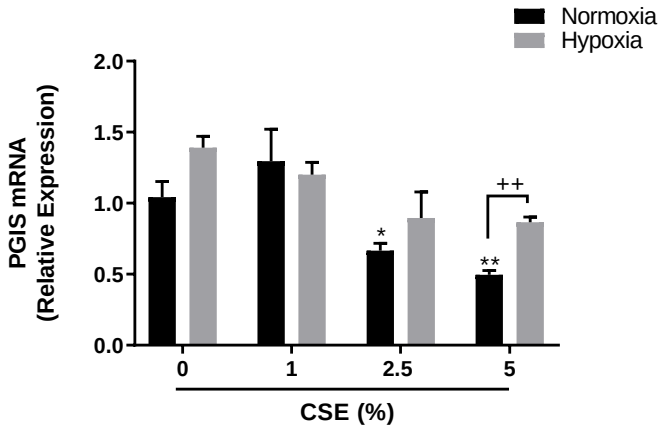


Figure 4.7 Effect of hypoxia and hypoxia+CSE on the mRNA expression of PGIS in human PASMCs.
Confluent human PASMCs were stimulated with different concentrations of CSE (0%, 1%, 2.5%, and 5%) under normoxic (21% O_2) or hypoxic (1% O_2) conditions for 48 h with daily fresh DMEM+ and CSE and then with the same concentrations of CSE under normoxic or hypoxic conditions in DMEM- for 24 h. Total RNA was isolated and then the samples were assayed for the mRNA expression of PGIS using RT-qPCR. Data were expressed as fold change over unstimulated cells (0% CSE). Each data point represents mean ± SEM from three independent experiments using cells from three different donors. *p<0.05, **p<0.01 compared with unstimulated cells. $^{++}$p<0.01 compared with corresponding CSE concentration under normoxic conditions.

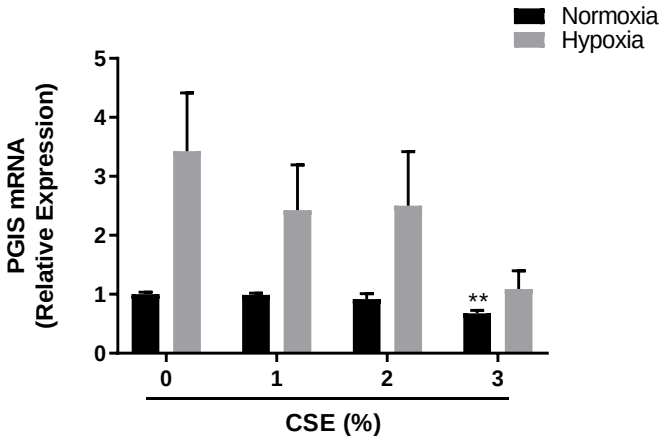


Figure 4.8 Effect of hypoxia and hypoxia+CSE on the mRNA expression of PGIS in human PAECs.
Confluent human PAECs were treated with different concentrations of CSE (0%, 1%, 2%, and 3%) under normoxic (21% O_2) or hypoxic (1% O_2) conditions for 24 h prior to total RNA isolation. The samples were assayed for the mRNA expression of PGIS using RT-qPCR. Data were expressed as fold change over untreated cells (0% CSE). Each data point represents mean ± SEM from three independent experiments using one cell line. **p<0.01 compared with untreated cells.

To determine whether the hypoxia effect on PGIS mRNA expression would lead to a similar effect at protein levels, Western blotting was carried out. The data in Figure 4.9A showed that human PASMCs expressed PGIS protein at basal levels, and stimulation of cells with CSE markedly reduced the PGIS protein expression (Figure 4.9A and B). Similar to PGIS mRNA expression results, hypoxia alone did not change PGIS protein levels; concomitantly, hypoxia did not further amplify CSE-induced downregulation of PGIS protein expression (Figure 4.9A and B). In agreement with our findings reported in Chapter 3, the protein expression of PGIS in human PAECs was undetectable under both basal and normoxic or hypoxic CSE treatment conditions (Figure 4.10A and B).

These observations suggest that hypoxia has no effect on the mRNA and protein expression of PGIS in PASMCs and PAECs. Although hypoxia results in a net increase in CSE-mediated downregulation of PGIS mRNA expression in PASMCs (but not in PAECs), it causes no further effect on CSE-induced decrease in PGIS protein expression in PASMCs.

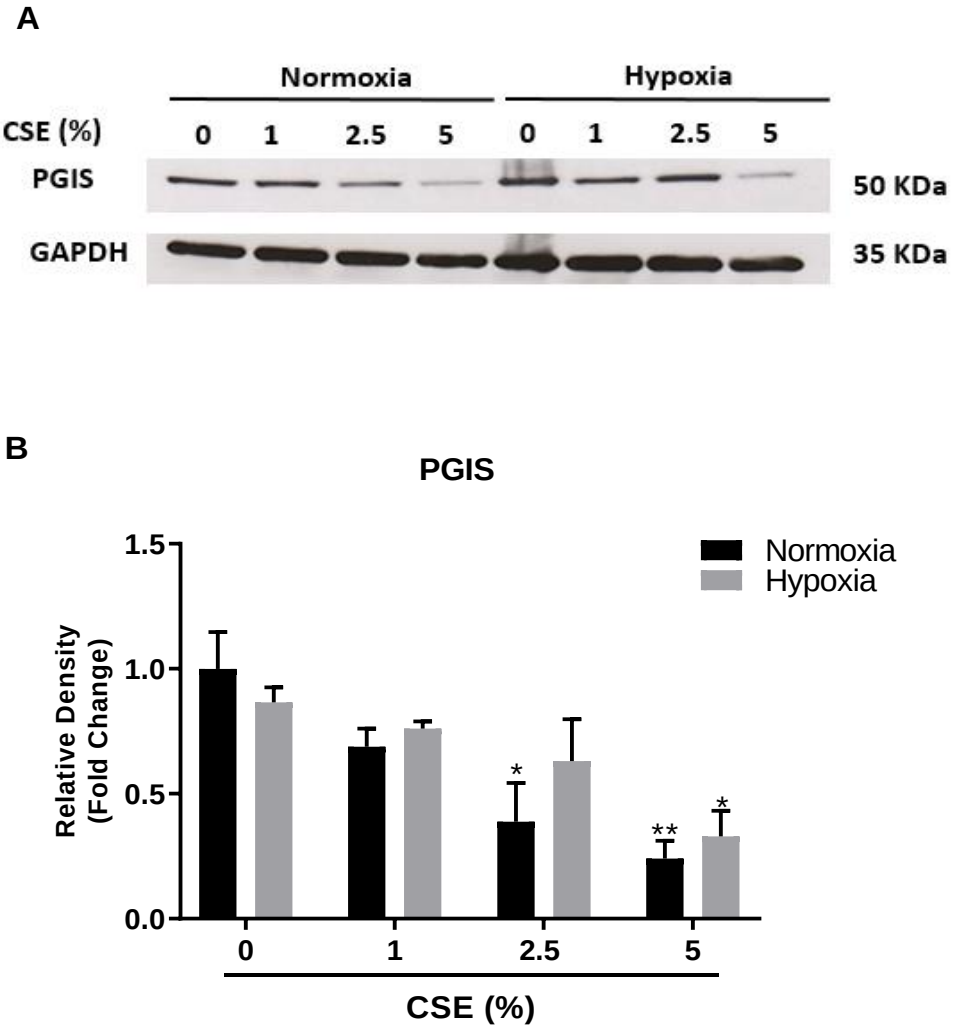


Figure 4.9 Effect of hypoxia and hypoxia+CSE on the protein expression of PGIS in human PASMCs.

Confluent human PASMCs were treated with different concentrations of CSE (0%, 1%, 2.5%, and 5%) under normoxic (21% O_2) or hypoxic (1% O_2) conditions for 48 h with daily fresh DMEM+ and CSE and then with the same concentrations of CSE under normoxic or hypoxic conditions in DMEM- for 24 h. Total cell lysates were collected for Western blot analysis of PGIS protein. A, a representative Western blot showing the effect of CSE under normoxic or hypoxic conditions on PGIS protein expression. B, optical densitometry analysis of Western blotting bands. Data were normalised with the loading control GAPDH and were expressed as fold change over untreated cells (0% CSE). Each data point represents mean ± SEM from three independent experiments using cells from three different donors. *$p<0.05$ and **$p<0.01$ compared with untreated cells.

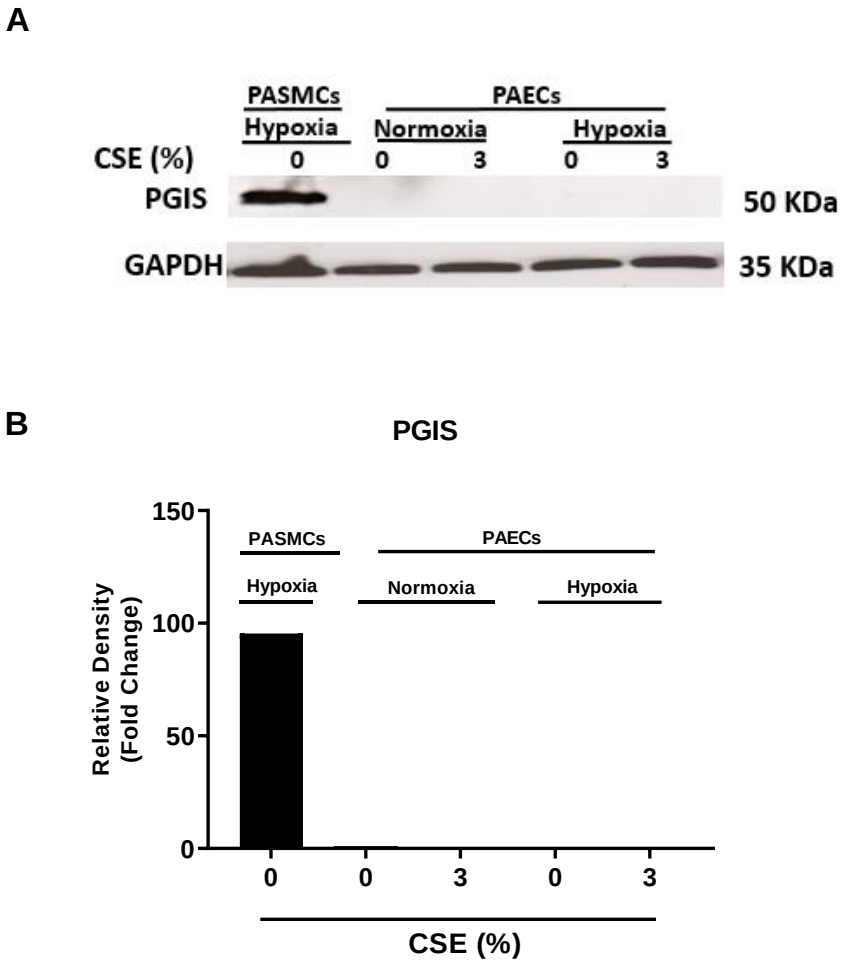


Figure 4.10 Effect of hypoxia and hypoxia+CSE on the protein expression of PGIS in human PAECs. Confluent human PAECs were treated with CSE (0% and 3%) under normoxic (21% O_2) or hypoxic (1% O_2) conditions for 24 h. Total cell lysates were collected for Western blot analysis of PGIS protein. Total cell lysates from human PASMCs exposed to hypoxia (1%) were used as a positive control. A, a representative Western blot showing the effect of CSE under normoxic or hypoxic conditions on PGIS protein expression. B, optical densitometry analysis of Western blotting bands. Data were normalised with the loading control GAPDH and were expressed as fold change over untreated human PAECs (0% CSE). A representative blot of three independent experiments using one cell line is shown.

We next explored whether hypoxia alone has an effect on PGI_2 production, and whether hypoxia can further enhance CSE-induced effects. We observed that the production of the PGI_2 inactive product, 6-keto $PGF_{1\alpha}$, was detectable at basal levels in PASMCs (3179.0±385.2 pg/mg protein). As reported in Chapter 3, 5% CSE reduced 6-keto $PGF_{1\alpha}$ production (Figure 4.11). In contrast, hypoxia exerted opposite effects to those of CSE on 6-keto $PGF_{1\alpha}$ production. Hypoxia alone enhanced 6-keto $PGF_{1\alpha}$ production (13248.2±3511.9 pg/mg protein, $p<0.05$) compared with untreated PASMCs. However, hypoxia caused no additive effect on CSE-induced reduction of 6-keto $PGF_{1\alpha}$ production, compared with corresponding CSE concentration under normoxic conditions (Figure 4.11). Furthermore, our studies performed in PAECs showed that although 6-keto $PGF_{1\alpha}$ was detectable under basal condition (792.0±94.7 pg/mg protein), CSE and hypoxia, either individually or in combination, did not change the levels of 6-keto $PGF_{1\alpha}$ compared with untreated PAECs (Figure 4.12).

Despite the unchanged PGIS expression, our results suggest that hypoxia alone can increase PGI_2 production in PASMCs (but not in PAECs) as a result of the increase in COX-2 expression; however, hypoxia does not further enhance CSE-induced effects on PGI_2 production.

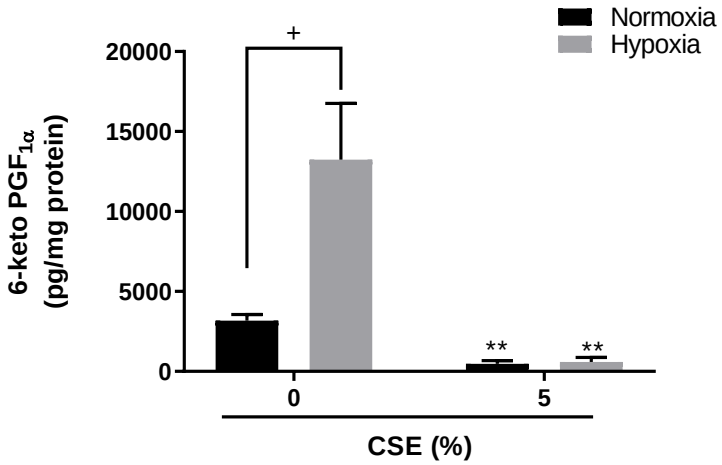


Figure 4.11 Effect of hypoxia and hypoxia+CSE on 6-keto $PGF_{1\alpha}$ production in human PASMCs. Confluent human PASMCs were treated with CSE (0% and 5%) under normoxic (21% O_2) or hypoxic (1% O_2) conditions for 48 h with daily fresh DMEM+ and CSE and then with the same concentrations of CSE under normoxic or hypoxic conditions in DMEM- for 24 h. Supernatants were collected and assayed for 6-keto $PGF_{1\alpha}$ using ELISA analysis. Data were normalised with total protein and expressed as pg/mg protein. Each data point represents mean ± SEM from three independent experiments using cells from three different donors. **$p<0.01$ compared with untreated cells. $^{+}p<0.05$ compared with corresponding CSE concentration under normoxic condition.

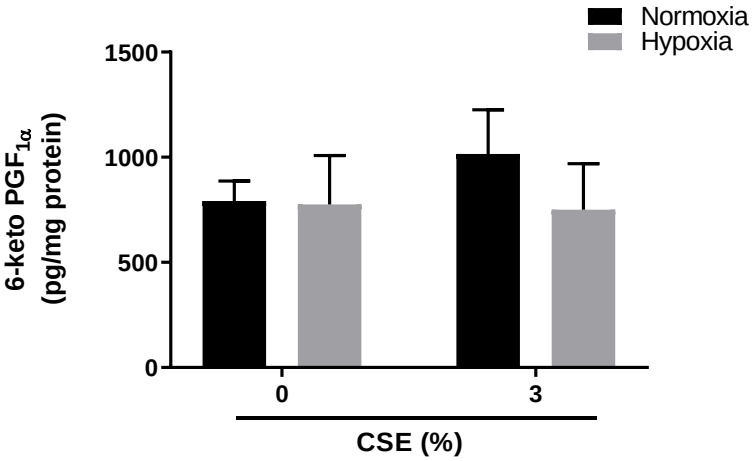


Figure 4.12 Effect of hypoxia and hypoxia+CSE on 6-keto $PGF_{1\alpha}$ production in human PAECs. Confluent human PAECs were treated with CSE (0% and 3%) under normoxic (21% O_2) or hypoxic (1% O_2) conditions for 24 h. Supernatants were collected and assayed for 6-keto $PGF_{1\alpha}$ using ELISA analysis. Data were normalised with total protein and expressed as pg/mg protein. Each data point represents mean ± SEM from six independent experiments using one cell line.

4.4.3 Effect of hypoxia alone and in combination with CSE on the mRNA and protein expression of TXAS and TXA_2 production in human PASMCs and PAECs

Thus far, we clearly demonstrated that hypoxia enhanced PGI_2 and PGE_2 production as a result of COX-2 expression upregulation in PASMCs, but not in PAECs. Here, we determined the effect of hypoxia on TXAS/TXA_2, and whether hypoxia can further enhance CSE-induced effects. As shown in Figure 4.13, TXAS was basally expressed. Consistent with the findings reported in Chapter 3, CSE treatment increased TXAS mRNA expression in PASMCs. However, hypoxia alone did not alter TXAS mRNA expression compared with unstimulated cells (Figure 4.13). Furthermore, hypoxia caused no additive effect on CSE-induced TXAS mRNA expression in PASMCs (Figure 4.13). In PAECs, it was also found that TXAS mRNA expression was detectable at basal levels and that CSE induced the mRNA expression of TXAS in PAECs (Figure 4.14) as previously shown in Chapter 3. Interestingly, hypoxia alone resulted in no significant changes in the mRNA expression of TXAS (Figure 4.14). In addition, hypoxia did not further enhance CSE-induced TXAS mRNA expression (Figure 4.14).

Our mRNA data suggest that hypoxia alone does not induce TXAS mRNA expression in PASMCs and PAECs, and that hypoxia causes no additive effect on CSE-induced TXAS mRNA expression in both cell types.

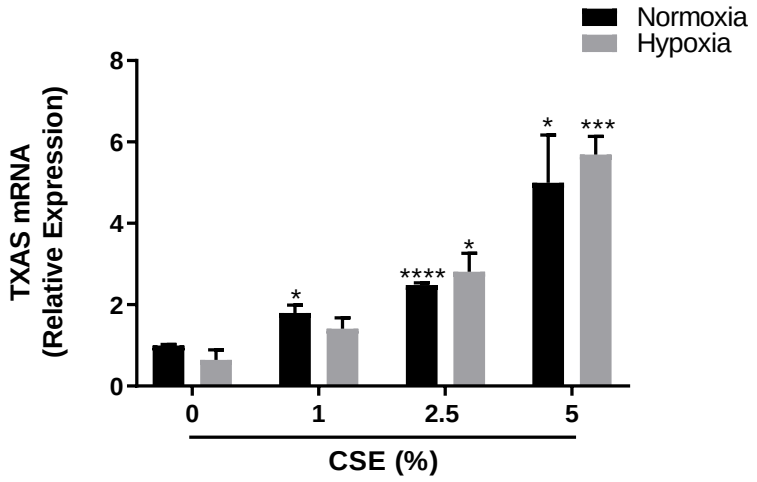


Figure 4.13 Effect of hypoxia and hypoxia+CSE on the mRNA expression of TXAS in human PASMCs.

Confluent human PASMCs were stimulated with different concentrations of CSE (0%, 1%, 2.5%, and 5%) under normoxic (21% O_2) or hypoxic (1% O_2) conditions for 48 h with daily fresh DMEM+ and CSE and then with the same concentrations of CSE under normoxic or hypoxic conditions in DMEM- for 24 h. Total RNA was isolated and then the samples were assayed for the mRNA expression of TXAS using RT-qPCR. Data were expressed as fold change over unstimulated cells (0% CSE). Each data point represents mean ± SEM from three independent experiments using cells from three different donors. *p<0.05, ***p<0.001, ****p<0.0001 compared with unstimulated cells.

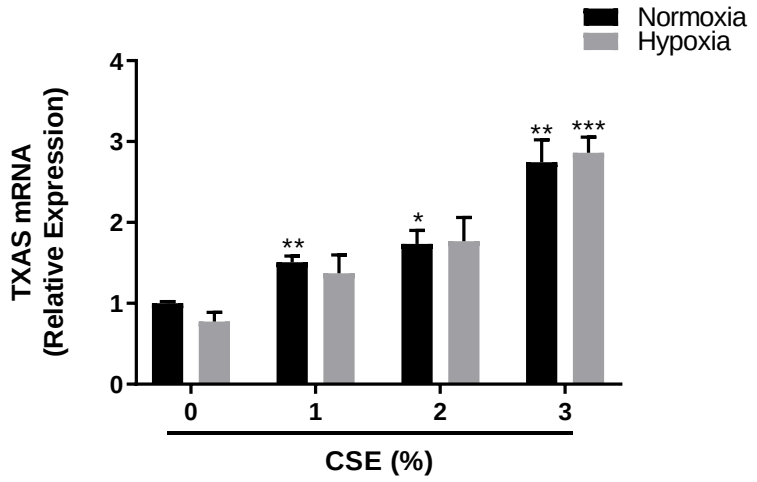


Figure 4.14 Effect of hypoxia and hypoxia+CSE on the mRNA expression of TXAS in human PAECs.

Confluent human PAECs were treated with different concentrations of CSE (0%, 1%, 2%, and 3%) under normoxic (21% O_2) or hypoxic (1% O_2) conditions for 24 h prior to total RNA isolation. The samples were assayed for the mRNA expression of TXAS using RT-qPCR. Data were expressed as fold change over untreated cells (0% CSE). Each data point represents mean ± SEM from three independent experiments using one cell line. *p<0.05, **p<0.01, ***p<0.001 compared with untreated cells.

Next, Western blot analysis was then carried out to assess the protein expression of TXAS in human PASMCs and PAECs. As shown in Figure 4.15A, and in agreement with findings reported in Chapter 3, the protein expression of TXAS under both basal and CSE treatment conditions was undetectable in PASMCs. In contrast to the effect of CSE, hypoxia alone upregulated the protein expression of TXAS (fold change 11.7±1.8, $p<0.05$) compared with untreated PASMCs (Figure 4.15A and B), and hypoxia-induced TXAS protein expression was unaltered by CSE treatment. Similar to the results in Chapter 3 demonstrating undetected TXAS protein expression under basal and CSE-treated PAECs conditions, we found that TXAS protein expression was undetectable in unstimulated PAECs and following cell exposure to hypoxia (Figure 4.15A and C).

Although no additive effect of hypoxia on CSE-treated cells is observed, the observation that hypoxia alone can induce the protein expression of TXAS in PASMCs (but not in PAECs) suggests a possible role of TXAS-derived TXA_2 in hypoxia-induced PASMC dysfunction and vascular remodelling.

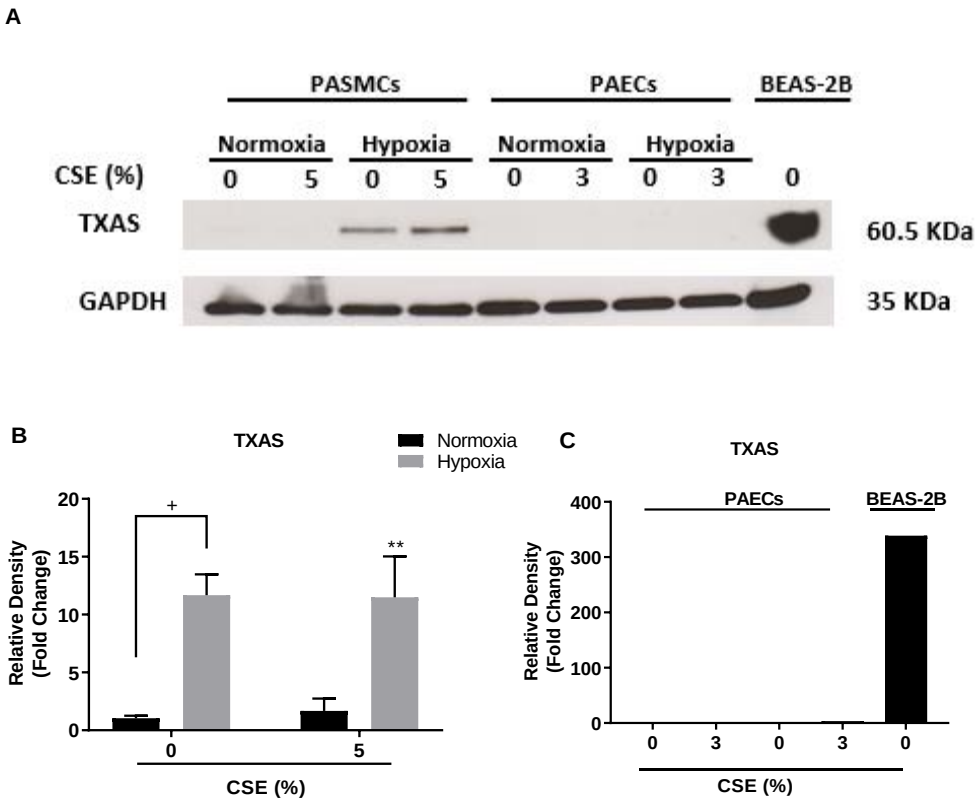


Figure 4.15 Effect of hypoxia and hypoxia+CSE on the protein expression of TXAS in human PASMCs and PAECs.

Confluent human PASMCs and PAECs were treated with or without CSE under normoxic (21% O_2) or hypoxic conditions (1% O_2) for either 72 h (PASMCs) or 24 h (PAECs). Total cell lysates were collected and Western blot analysis was carried out to assess TXAS protein expression. Total cell lysates from untreated immortalised human BEAS-2B were used as a positive control. A, a representative Western blot showing the effect of CSE under normoxic or hypoxic conditions on TXAS protein expression in human PASMCs and PAECs. B and C, optical densitometry analysis of Western blotting bands for PASMCs and PAECs, respectively. Data were normalised with the loading control GAPDH and were expressed as fold change over untreated cells (0% CSE). A representative blot of three independent experiments using cells from three different donors (PASMCs) and three independent experiments using one cell line (PAECs) is shown. **$p<0.01$ compared with untreated cells. $^{+}p<0.05$ compared with corresponding CSE concentration under normoxic condition.

It was then investigated whether hypoxia-induced TXAS protein expression could lead to an increase in TXA_2 production, and whether hypoxia could further amplify CSE-induced TXA_2 production in both cell types. Our results showed that the TXB_2 production was detectable at basal levels in PASMCs (224.7±24.6 pg/mg protein). Consistent with the findings in Chapter 3, cell stimulation with 5% CSE resulted in a significant increase in TXB_2 production (Figure 4.16). Similar to CSE effect, hypoxia alone induced TXB_2 production (687.5±102.6 pg/mg protein, $p<0.05$) compared with untreated PASMCs. Interestingly, hypoxia did not further increase CSE-induced TXB_2 production in PASMCs. Our results also demonstrated that PAECs produced TXB_2 at basal levels (500.8±72.2 pg/mg protein) as shown in Figure 4.17. In accordance with findings from PASMCs, treatment with 3% CSE induced TXB_2 levels in human PAECs. Although hypoxia alone caused an increase in TXB_2 levels (1470.8±269.6 pg/mg protein) compared with untreated PAECs, hypoxia did not further enhance CSE-induced TXB_2 production in PAECs (Figure 4.17).

Our data suggest that hypoxia alone can induce the production of the vasoconstrictive and proliferative mediator TXA_2 in both cell types, but that it does not further increase CSE-induced effects. These findings also suggest a role of increased TXA_2 in hypoxia-induced PASMC and PAEC dysfunction.

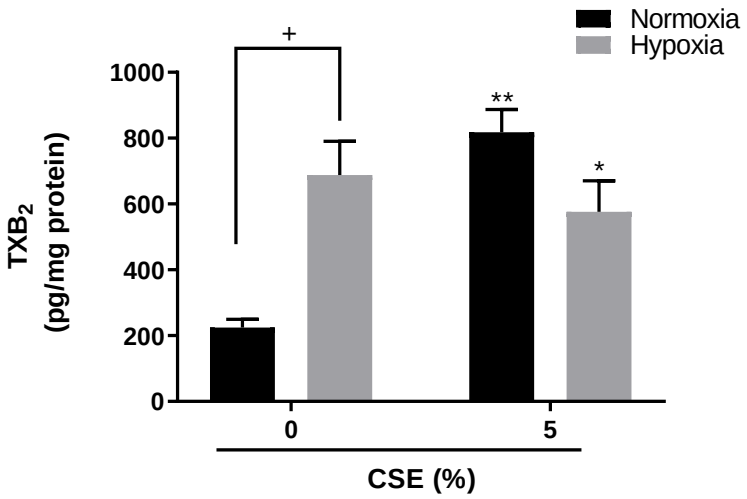


Figure 4.16 Effect of hypoxia and hypoxia+CSE on TXB_2 production in human PASMCs.
Confluent human PASMCs were treated with CSE (0% and 5%) under normoxic (21% O_2) or hypoxic (1% O_2) conditions for 48 h with daily fresh DMEM+ and CSE and then with the same concentrations of CSE under normoxic or hypoxic conditions in DMEM- for 24 h. Supernatants were collected and assayed for TXB_2 using ELISA analysis. Data were normalised with total protein and expressed as pg/mg protein. Each data point represents mean ± SEM from three independent experiments using cells from three different donors. *p<0.05, **p<0.01 compared with untreated cells. $^{+}$p<0.05 compared with corresponding CSE concentration under normoxic conditions.

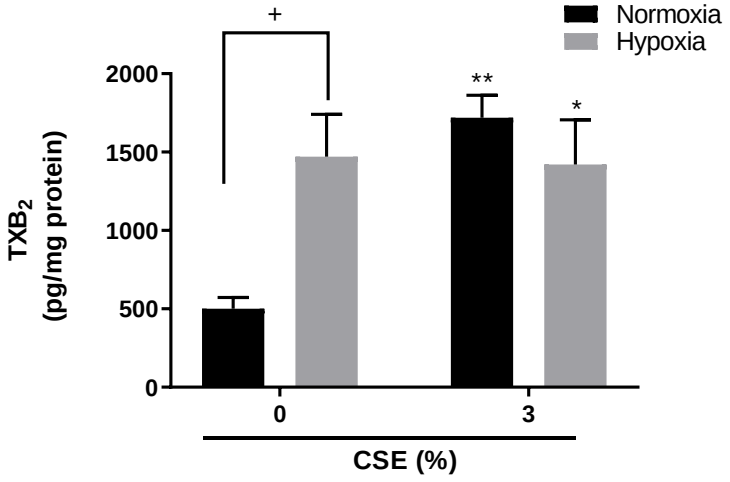


Figure 4.17 Effect of hypoxia and hypoxia+CSE on TXB_2 production in human PAECs.
Confluent human PAECs were treated with CSE (0% and 3%) under normoxic (21% O_2) or hypoxic (1% O_2) conditions for 24 h. Supernatants were collected and assayed for TXB_2 using ELISA analysis. Data were normalised with total protein and expressed as pg/mg protein. Each data point represents mean ± SEM from three independent experiments using one cell line. *p<0.05, **p<0.01 compared with untreated cells. $^{+}$p<0.05 compared with corresponding CSE concentration under normoxic conditions.

4.4.4 Effect of hypoxia alone and in combination with CSE on the PGI_2/TXA_2 ratio in human PASMCs and PAECs

It has been reported the balance between vasodilator PGI_2 and vasoconstrictor TXA_2 is disturbed in patients with PAH (Christman et al., 1992). However, the effect of hypoxia, a strong stimulus of pulmonary vasoconstriction and vascular remodelling in COPD patients (Bogaard, 2017), on the PGI_2/TXA_2 ratio has not been previously assessed. Thus, we were interested to determine whether hypoxia alone has an effect on the PGI_2/TXA_2 ratio, and whether hypoxia can cause an additive effect on CSE-induced reduction of the PGI_2/TXA_2 ratio. In agreement with our findings in Chapter 3, we demonstrated that CSE reduced the PGI_2/TXA_2 ratio in PASMCs and PAECs. Although hypoxia alone had no effect on the PGI_2/TXA_2 ratio in PASMCs (Figure 4.18), it decreased the PGI_2/TXA_2 ratio in PAECs (0.39±0.09 ratio, $p<0.001$) compared with untreated cells (1.79±0.11) as shown in Figure 4.19. Interestingly, hypoxia did not further enhance CSE-induced decrease in the PGI_2/TXA_2 ratio in both cell types (Figures 4.18 and 4.19).

Although hypoxia does not further amplify the effect of CSE, it reduced the ratio of PGI_2/TXA_2 in PAECs (but not PASMCs), suggesting a crucial role for the reduced PGI_2/TXA_2 ratio in hypoxia-induced vascular dysfunction and remodelling in COPD.

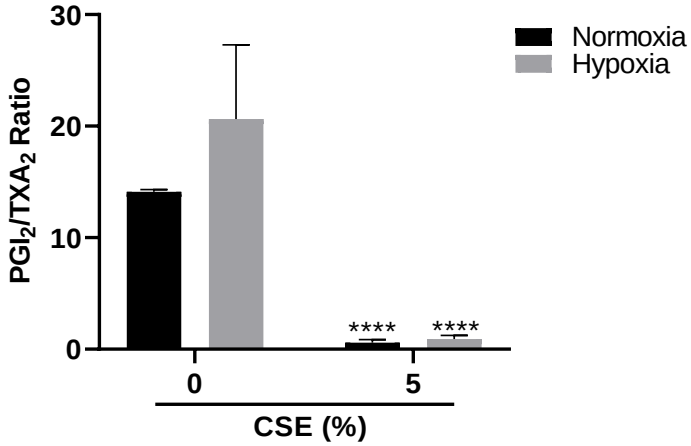


Figure 4.18 Effect of hypoxia and hypoxia+CSE on the PGI_2/TXA_2 ratio in human PASMCs.
Confluent human PASMCs were treated with CSE (0% and 5%) under normoxic (21% O_2) or hypoxic (1% O_2) conditions for 48 h with daily fresh DMEM+ and CSE and then with the same concentrations of CSE under normoxic or hypoxic conditions in DMEM- for 24 h. Supernatants were collected and assayed for 6-keto $PGF_{1\alpha}$ and TXB_2 using ELISA analysis. Data were normalised with total protein and presented as PGI_2/TXA_2 ratio. Each data point represents mean ± SEM from three independent experiments using cells from three different donors. ****$p<0.0001$ compared with untreated cells.

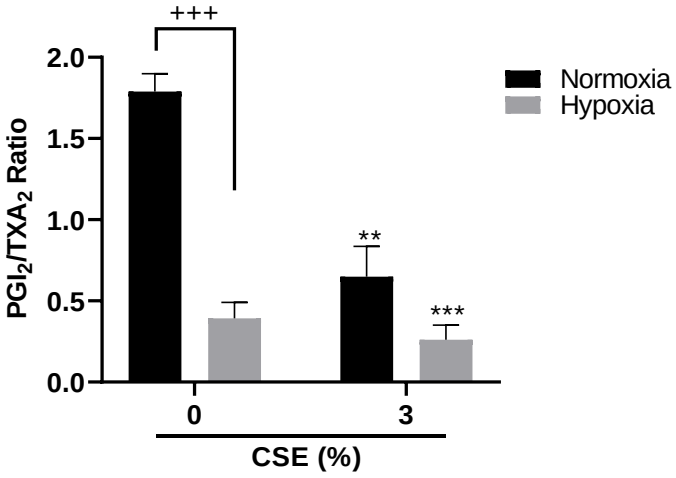


Figure 4.19 Effect of hypoxia and hypoxia+CSE on the PGI_2/TXA_2 ratio in human PAECs.
Confluent human PAECs were treated with CSE (0% and 3%) under normoxic (21% O_2) or hypoxic (1% O_2) conditions for 24 h. Supernatants were collected and assayed for 6-keto $PGF_{1\alpha}$ and TXB_2 using ELISA analysis. Data were normalised with total protein and presented as PGI_2/TXA_2 ratio. Each data point represents mean ± SEM from three independent experiments using one cell line. **$p<0.01$, ***$p<0.001$ compared with untreated cells. $^{+++}p<0.001$ compared with corresponding CSE concentration under normoxic conditions.

4.4.5 Effect of hypoxia alone and in combination with CSE on the mRNA and protein expression of eNOS and nitric oxide production in human PASMCs and PAECs

In the previous Chapter, we demonstrated that eNOS protein expression and nitric oxide production were diminished after PAEC treatment with CSE. However, the effect of hypoxia alone on the mRNA and protein expression of eNOS and nitric oxide production in PASMCs and PAECs and the effect of hypoxia on CSE-induced effects are unknown. As we have previously shown in Figure 3.25, the protein expression of eNOS under both basal and CSE- and hypoxia-exposed PASMCs conditions was undetectable.

Similar to the effect of CSE, the data in Figure 4.20 indicated that hypoxia alone had no effect on the mRNA expression of eNOS in human PAECs (Figure 4.20). No further effect was observed when cells were incubated with CSE under hypoxic conditions compared with CSE under normoxic conditions. Next, Western blotting analysis was performed to assess the protein expression of eNOS, which showed that eNOS was constitutively expressed in PAECs. CSE stimulation resulted in a downregulation of eNOS protein expression in a concentration-dependent manner (Figure 4.21A and B). Similarly, hypoxia alone reduced eNOS protein expression (fold change 0.5±0.03, $p<0.01$) compared with untreated cells (Figure 4.21A and B) and hypoxia-induced reduction of eNOS protein expression was not further amplified by CSE treatment (Figure 4.21A and B).

To determine whether the protein expression of eNOS downregulation by hypoxia in PAECs would lead to a reduction in the production of nitric oxide, we next assessed the total nitrate/nitrite released to cell supernatants following CSE treatment under

hypoxic and normoxic conditions. The results showed that human PAECs produced detectable amounts of total nitrate/nitrite basally (0.07±0.009 nmol/μg protein) as shown in Figure 4.22. It was found that 3% CSE and hypoxia markedly reduced the total nitrate/nitrite levels (0.037±0.007 nmol/μg protein, $p<0.05$ and 0.023±0.008 nmol/μg protein, $p<0.01$, respectively) compared with untreated PAECs (Figure 4.22). Surprisingly, hypoxia caused no further effect on CSE-induced reduction of total nitrate/nitrite levels compared with CSE alone.

Although no additive effect of hypoxia on CSE-induced reduction of eNOS protein expression and nitric oxide production is observed, our combined observation that hypoxia alone reduced nitric oxide production as a result of the downregulated eNOS protein expression suggests that eNOS/nitric oxide deficiency is a key feature of hypoxia-induced PAEC dysfunction, thereby contributing to pulmonary vascular alterations in COPD.

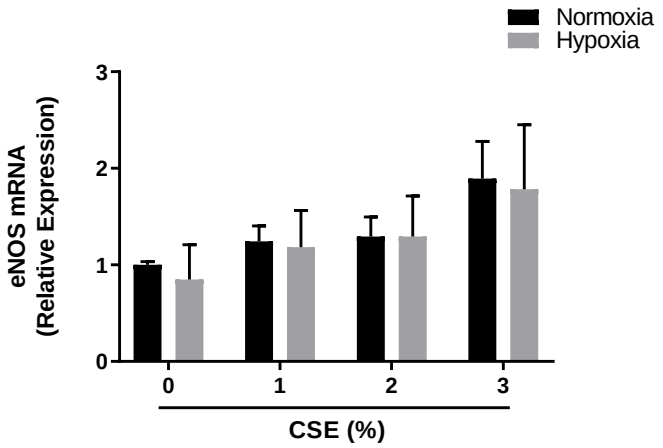


Figure 4.20 Effect of hypoxia and hypoxia+CSE on the mRNA expression of eNOS in human PAECs. Confluent human PAECs were stimulated with different concentrations of CSE (0%, 1%, 2%, and 3%) under normoxic (21% O_2) or hypoxic (1% O_2) conditions for 24 h prior to total RNA isolation. The samples were assayed for the mRNA expression of eNOS using RT-qPCR. Data were expressed as fold change over unstimulated cells (0% CSE). Each data point represents mean ± SEM from three independent experiments using one cell line.

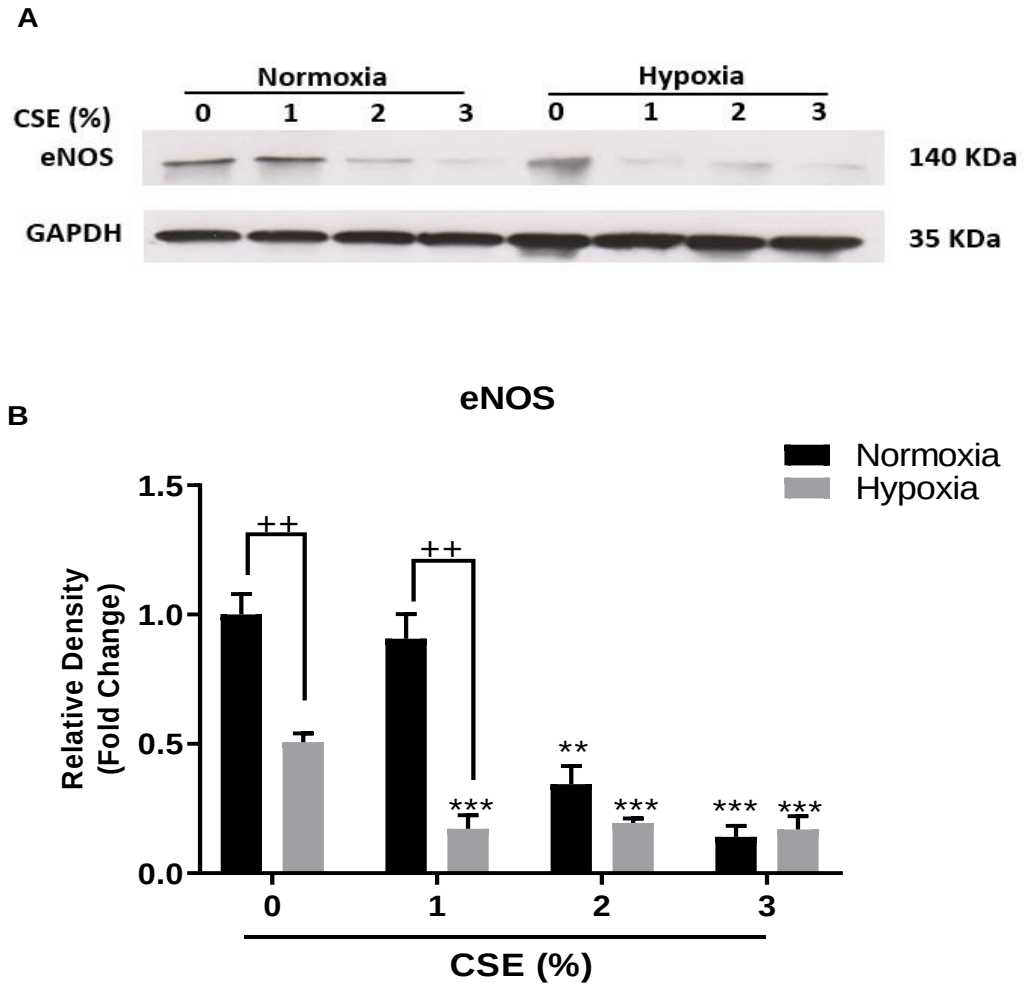


Figure 4.21 Effect of hypoxia and hypoxia+CSE on the protein expression of eNOS in human PAECs. Confluent human PAECs were treated with different concentrations of CSE (0%, 1%, 2%, and 3%) under normoxic (21% O_2) or hypoxic (1% O_2) conditions for 24 h. Total cell lysates were collected for Western blot analysis of eNOS protein. A, a representative Western blot showing the effect of CSE under normoxic or hypoxic conditions on eNOS protein expression. B, optical densitometry analysis of Western blotting bands. Data were normalised with the loading control GAPDH and were expressed as fold change over untreated cells (0% CSE). Each data point represents mean ± SEM from three independent experiments using one cell line. **p<0.01, ***p<0.001 compared with untreated cells. $^{++}$p<0.01 compared with corresponding CSE concentration under normoxic conditions.

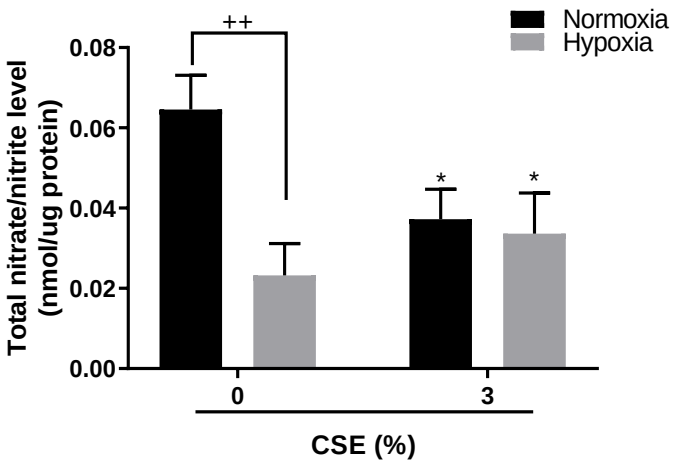


Figure 4.22 Effect of hypoxia and hypoxia+CSE on total nitrate/nitrite level in human PAECs.
Confluent human PAECs were treated with CSE (0% and 3%) under normoxic (21% O_2) or hypoxic (1% O_2) conditions for 24 h. Supernatants were collected and assayed for total nitrate/nitrite using fluorometric assay. Data were normalised with total protein and expressed as nmol/µg protein. Each data point represents mean ± SEM from six independent experiments using one cell line. *$p<0.05$ compared with untreated cells. $^{++}p<0.01$ compared with corresponding CSE concentration under normoxic conditions.

4.4.6 Effect of hypoxia alone and in combination with CSE on the mRNA expression of endothelin-1 and the production of endothelin in human PASMCs and PAECs

It is well known that hypoxia plays a key role in the development of pulmonary hypertension in COPD (Sakao et al., 2014). However, the contribution of endothelin pathway in this process remains unclear. It was therefore investigated whether hypoxia alone could induce the expression of endothelin-1 and the production of endothelin in human PASMCs and PAECs, and whether hypoxia could further amplify the effect of CSE. The results showed that endothelin-1 mRNA expression was detectable basally. CSE had no effect on the mRNA expression of endothelin-1 in PASMCs. Although hypoxia as single factor did not change the mRNA expression of endothelin-1, CSE (1%, 2.5%, and 5%) under hypoxic conditions significantly induced endothelin-1 mRNA expression in PASMCs (fold change 1.5±0.07, 2.4±0.4 and 1.9±0.3, respectively, $p<0.05$) compared with the corresponding CSE concentration under normoxic conditions (Figure 4.23). Human PAECs also expressed endothelin-1 mRNA basally. In agreement with findings in the previous Chapter, PAEC incubation with 3% CSE resulted in a slight but significant increase in the mRNA expression of endothelin-1 (fold change 1.5±0.1, $p<0.05$) as shown in Figure 4.24. Hypoxia alone caused no significant changes in endothelin-1 mRNA expression. In addition, hypoxia did not further enhance CSE-induced endothelin-1 mRNA expression (Figure 4.24).

Our ELISA results showed that the production of endothelin was detectable in the supernatants of PASMCs under basal conditions (372.8±46.3 pg/mg protein) as shown in Figure 4.25. Interestingly, CSE and hypoxia had no significant effect on endothelin production in PASMCs (Figure 4.25). We also found that PAECs produced endothelin at

basal levels (6689.4±529.4 pg/mg protein) (Figure 4.26). Although 3% CSE reduced endothelin production under normoxic conditions, hypoxia caused no remarkable changes in endothelin levels (Figure 4.26). Furthermore, no additive effect of hypoxia on CSE-induced reduction of endothelin levels was noted.

Collectively, our data suggest that hypoxia alone causes no effect on endothelin-1 mRNA expression and endothelin release in both cell types. Furthermore, the induction of endothelin-1 mRNA expression by CSE under hypoxic conditions does not lead to increased endothelin production in PASMCs. Our findings also suggest that hypoxia does not further amplify CSE-induced effects on endothelin-1 mRNA expression and endothelin release in PAECs.

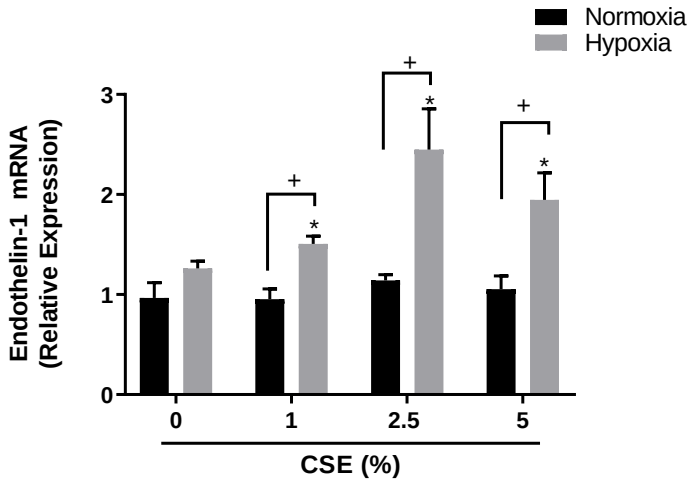


Figure 4.23 Effect of hypoxia and hypoxia+CSE on the mRNA expression of endothelin-1 in human PASMCs.

Confluent human PASMCs were stimulated with different concentrations of CSE (0%, 1%, 2.5%, and 5%) under normoxic (21% O_2) or hypoxic (1% O_2) conditions for 48 h with daily fresh DMEM+ and CSE and then with the same concentrations of CSE under normoxic or hypoxic conditions in DMEM- for 24 h. Total RNA was isolated and then the samples were assayed for the mRNA expression of endothelin-1 using RT-qPCR. Data were expressed as fold change over unstimulated cells (0% CSE). Each data point represents mean ± SEM from three independent experiments using cells from three different donors. *$p<0.05$ compared with unstimulated cells. $^{+}p<0.05$ compared with corresponding CSE concentration under normoxic conditions.

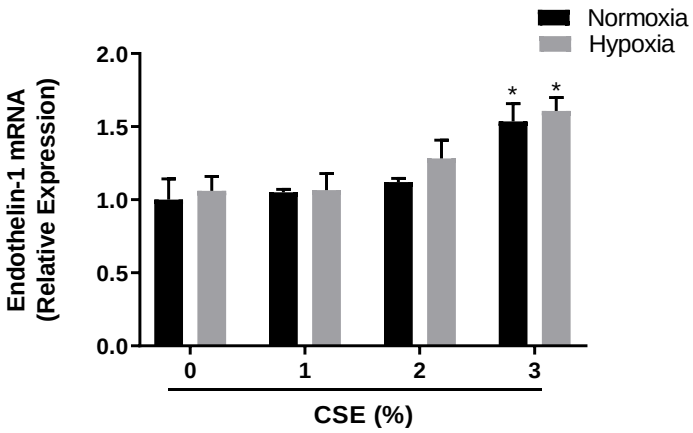


Figure 4.24 Effect of hypoxia and hypoxia+CSE on the mRNA expression of endothelin-1 in human PAECs.

Confluent human PAECs were treated with different concentrations of CSE (0%, 1%, 2%, and 3%) under normoxic (21% O_2) or hypoxic (1% O_2) conditions for 24 h prior to total RNA isolation. The samples were assayed for the mRNA expression of endothelin-1 using RT-qPCR. Data were expressed as fold change over untreated cells (0% CSE). Each data point represents mean ± SEM from three independent experiments using one cell line. *$p<0.05$ compared with untreated cells.

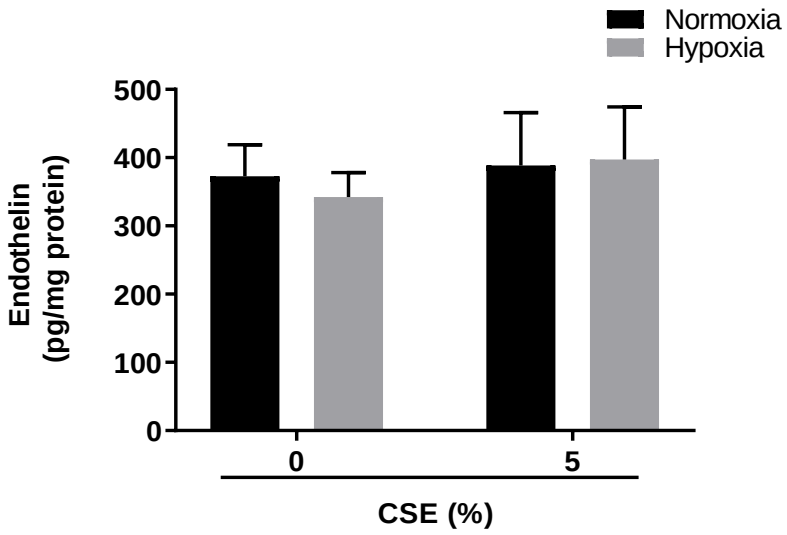


Figure 4.25 Effect of hypoxia and hypoxia+CSE on endothelin production in human PASMCs.
Confluent human PASMCs were treated with CSE (0% and 5%) under normoxic (21% O_2) or hypoxic (1% O_2) conditions for 48 h with daily fresh DMEM+ and CSE and then with the same concentrations of CSE under normoxic or hypoxic conditions in DMEM- for 24 h. Supernatants were collected and assayed for endothelin using ELISA analysis. Data were normalised with total protein and expressed as pg/mg protein. Each data point represents mean ± SEM from three independent experiments using cells from three different donors.

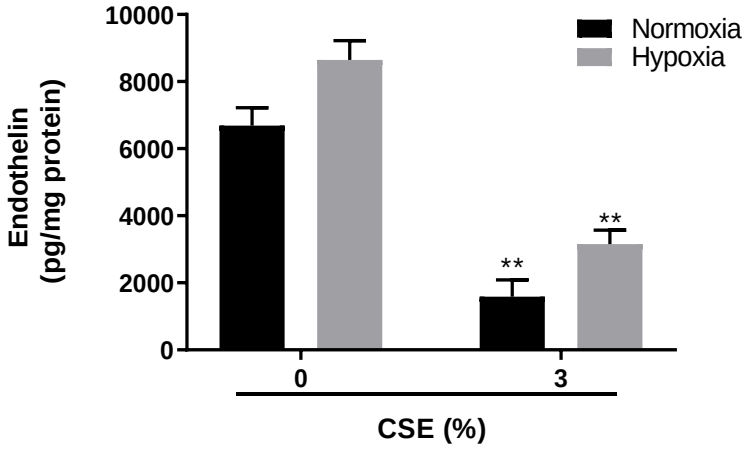


Figure 4.26 Effect of hypoxia and hypoxia+CSE on endothelin production in human PAECs.
Confluent human PAECs were treated with CSE (0% and 3%) under normoxic (21% O_2) or hypoxic (1% O_2) conditions for 24 h. Supernatants were collected and assayed for endothelin using ELISA analysis. Data were normalised with total protein and expressed as pg/mg protein. Each data point represents mean ± SEM from three independent experiments using one cell line. **$p<0.01$ compared with untreated cells.

4.5 Discussion

The main aim of this Chapter was to assess whether hypoxia could induce imbalanced vasoactive gene expression and mediator release in human PASMCs and PAECs, and whether hypoxia could further enhance CSE-induced effects. The key findings of the Chapter are that hypoxia alone induced the production of PGI_2, PGE_2, and TXA_2, resulting in an unchanged PGI_2/TXA_2 ratio in human PASMCs. Although hypoxia alone caused no effect on the production of PGI_2 and PGE_2, it increased the production of TXA_2 and subsequently decreased the PGI_2/TXA_2 ratio in human PAECs. To our surprise, hypoxia did not further amplify CSE-induced effects compared with CSE in both cell types. Our results also showed that hypoxia alone had no effect on endothelin production in both human PASMCs and PAECs, but reduced nitric oxide production in human PAECs with no additive effect of hypoxia on CSE-induced effects compared with CSE. A summary of the findings is presented in Table 4.1.

Here, we report for the first time that hypoxia alone can partially induce imbalanced vasoactive gene expression and mediator release. The imbalance of increased TXA_2 production in both human PASMCs and PAECs and reduced nitric oxide production in human PAECs may eventually contribute to vascular remodelling and pulmonary hypertension in COPD. Since hypoxia did not further amplify CSE-induced effects and it is mainly the effect of CSE when both stimuli were combined, our results suggest that CSE effect is more prominent than hypoxia on the induction of imbalanced vasoactive mediators in human PASMCs and PAECs.

Table 4.1 A summary table of the findings of Chapter 4.

Gene/Meditator	Function	CSE		Hypoxia		Hypoxia+CSE	
COX-2/PGE_2	**Vasoactive Gene**	**PASMCs**	**PAECs**	**PASMCs**	**PAECs**	**PASMCs**	**PAECs**
COX-2 mRNA		↑	↑	↑	↔	↑	↑
COX-2 protein		↑	↑	↑	↔	↑	↑
PGE_2 release		↓	↑	↑	↔	↔	↑
PGIS/PGI_2	**Vasodilator/ anti-proliferative gene**	**PASMCs**	**PAECs**	**PASMCs**	**PAECs**	**PASMCs**	**PAECs**
PGIS mRNA		↓	↓	↔	↔	↑↑	↔
PGIS protein		↓	**UD**	↔	**UD**	↓	**UD**
PGI_2 release		↓	↔	↑	↔	↓	↔
TXAS/TXA_2	**Vasoconstrictor/ proliferative gene**	**PASMCs**	**PAECs**	**PASMCs**	**PAECs**	**PASMCs**	**PAECs**
TXAS mRNA		↑	↑	↔	↔	↑	↑
TXAS protein		**UD**	**UD**	↑	**UD**	↑	**UD**
TXA_2 release		↑	↑	↑	↑	↑	↑
eNOS/nitric oxide	**Vasodilator/ anti-proliferative gene**	**PASMCs**	**PAECs**	**PASMCs**	**PAECs**	**PASMCs**	**PAECs**
eNOS mRNA		**UD**	↔	**UD**	↔	**UD**	↔
eNOS protein		**UD**	↓	**UD**	↓	**UD**	↓
Nitric oxide release		**UA**	↓	**UA**	↓	**UA**	↓
Endothelin	**Vasoconstrictor/ proliferative gene**	**PASMCs**	**PAECs**	**PASMCs**	**PAECs**	**PASMCs**	**PAECs**
Endothelin-1 mRNA		↔	↑	↔	↔	↑↑	↑
Endothelin release		↔	↓	↔	↔	↔	↓

CSE, Cigarette smoke extract; PASMCs, Pulmonary artery smooth muscle cells; PAECs, Pulmonary artery endothelial cells; COX-2, Cyclooxygenase-2; PGE_2, Prostaglandin E_2; PGIS, Prostaglandin I synthase; PGI_2, Prostaglandin I_2; TXAS, Thromboxane A synthase; TXA_2, Thromboxane A_2; eNOS, Endothelial nitric oxide synthase; UA, Unassessed; UD, Undetected; ↔, Unchanged; ↑, Upregulated; ↓, Downregulated; ↑↑, Further enhanced.

4.5.1 Hypoxia and prostanoids

4.5.1.1 Human pulmonary artery smooth muscle cells

Although no additive effect was observed when both stimuli were combined, the observation that hypoxia induced COX-2 mRNA and protein expression in PASMCs is similar to the CSE effect and suggests that hypoxia may regulate COX-2 expression via transcriptional regulation in PASMCs. This COX-2 expression upregulation was associated with increased PGE_2 production in response to hypoxia, suggesting that PGE_2 induction is likely to occur as a result of COX-2 expression upregulation. These findings are supported by previous studies (Bradbury et al., 2002, Yang et al., 2002) and the fact that the induction of COX-2 usually leads to the increase of COX-2 downstream prostanoid production. The interesting finding that hypoxia cancelled out the CSE-induced reduction of PGE_2 production could be due to the observation that CSE and hypoxia exerted opposite effects on PGE_2 production. It is likely that hypoxia-induced PGE_2 production may represent an adaptive response to hypoxic stress in PASMCs, considering the observation that the anti-proliferative and vasodilatory mediator PGE_2 was reduced by CSE. This is further supported by the fact that EP_4 receptor that mediates vasorelaxation is mainly expressed in PASMCs and the use of selective EP_2 receptor agonist inhibits proliferation of human PASMCs derived from patients with PAH (Fan et al., 2018).

It is interesting to observe that hypoxia was unable to demonstrate any effect on PGIS expression, but was able to cause a net increase in CSE-mediated downregulation of PGIS mRNA expression compared with CSE. Surprisingly, this increase did not lead to changes in the protein expression of PGIS. Although the hypoxia effect on PGIS

expression has not been assessed before in PASMCs, a previous study conducted in human aortic smooth muscle cells demonstrated that hypoxia increased PGIS mRNA and protein expression (Camacho et al., 2011). Those findings are different from these reported in the present study. Cell type difference is probably the main reason for the discrepancy observed between the two studies. In addition, some other factors may also play a role in the disparity between the results, such as the length of cell incubation time under hypoxic conditions. We incubated PASMCs under hypoxic conditions as previously described in Chapter 2 (for up to 72 h) in an attempt to mimic chronic hypoxic conditions, while Camacho and colleagues incubated the cells under hypoxic conditions for up to 48 h. Despite the unchanged PGIS, hypoxia-stimulated increase in the vasodilator and anti-proliferative PGI_2 production in PASMCs is likely to come as a result of the increase in COX-2 expression and its product PGH_2. This observation is supported by a previous study showing that COX-2 expression and the production of vasodilatory mediator PGI_2 are induced in response to hypoxia in human PASMCs (Yang et al., 2002). However, it must be noted that Yang and colleagues (2002) did not assess the hypoxia effect on PGIS protein and mRNA expression.

Both PGE_2 and PGI_2 are generally regarded as a vasodilator and an inhibitor of PASMC proliferation. The different effects of well known vascular remodelling inducers CS and hypoxia suggest that the reduced PGI_2 and PGE_2 are key part of CS-induced dysfunction PASMCs. However, hypoxia-induced endogenous PGI_2 and PGE_2 may have an adaptive response to hypoxic stress in PASMCs. These findings also suggest that hypoxia induced PGI_2 and PGE_2 as a result of COX-2 upregulation and the increase in the vasodilatory and anti-proliferative mediators may play a role in counteracting

hypoxia-induced vascular remodelling. The fact that hypoxia did not further enhance CSE-induced reduction of PGE_2 and PGI_2 production, and the net effect is mainly due to CSE, suggests that the CSE effect is stronger than hypoxia on prostaglandin production.

As far as we are aware, this study provides the first evidence that hypoxia induced TXAS protein expression in PASMCs, although the mRNA expression was unchanged. This suggests that it is likely that TXAS protein expression is regulated via post-transcriptional regulation. More importantly, the upregulated TXAS protein expression was associated with the increase of TXAS product TXA_2, suggesting that TXA_2 increase is probably because of the COX-2 and TXAS protein expression upregulation. It is also possible that TXAS post-translational modification to increase its activity may be important in this process, considering that CSE increased TXA_2 (despite the undetected TXAS protein expression). Based on these observations, it is likely that hypoxia may cause PASMC dysfunction by increasing the vasoconstrictive and proliferative mediator TXA_2 production due to TXAS upregulation, which may eventually lead to vasoconstriction and proliferation of PASMCs. It is interesting to note that this finding differs from those reported by Camacho and colleagues (2011), demonstrating that hypoxia had no effect on TXA_2 production in human aortic smooth muscle cells (Camacho et al., 2011). Surprisingly, the authors did not assess the expression of TXAS. As discussed above, several factors can explain the differences between the two studies, including cell type difference and the length of incubation time.

The balance between PGI_2 and TXA_2 plays an important role in the regulation of pulmonary vascular tone and structure. CSE reduced PGI_2 and increased TXA_2, suggesting that both mediators can contribute to the reduced PGI_2/TXA_2 ratio. Although

TXA_2 production was increased, the fact that hypoxia increased PGI_2 production may explain why hypoxia caused no effect on the PGI_2/TXA_2 ratio. The observation that the hypoxia effect was lost when combined with CSE and did not further amplify CSE-induced reduction of the PGI_2/TXA_2 ratio provides further evidence that CSE effect is more prominent than hypoxia on inducing an imbalance between PGI_2 and TXA_2 in PASMCs.

Collectively, although both exposures upregulated the expression of COX-2, the rate-limiting enzyme in the production of prostanoids (via transcriptional regulation), it is interesting to note that hypoxia exerted different or even opposite effects from CSE on prostaglandin production. CSE effect increased COX-2 expression and TXA_2 production, but reduced PGI_2 and PGE_2 production as a result of the downregulated PGIS and mPGES-1 expression, while hypoxia induced COX-2 expression and its downstream prostanoid production (PGI_2, PGE_2 and TXA_2). This suggests that PGI_2 and PGE_2 induction could be a feature of the adaptive response of PASMCs to hypoxic stress. The novel observation that hypoxia increased TXA_2 production due to TXAS protein expression upregulation is likely to cause PASMC dysfunction, thereby contributing to vasoconstriction and proliferation of PASMCs. Intriguingly, hypoxia caused no further effects on CSE-induced imbalanced vasoactive prostanoid mediators, suggesting that CSE may have stronger effect than hypoxia on the induction of imbalanced prostanoid mediators in human PASMCs. An illustration of the hypoxia effect on the expression of main enzymes of prostanoid biosynthesis and the release of vasoactive lipid mediators in human PASMCs is shown in Figure 4.27.

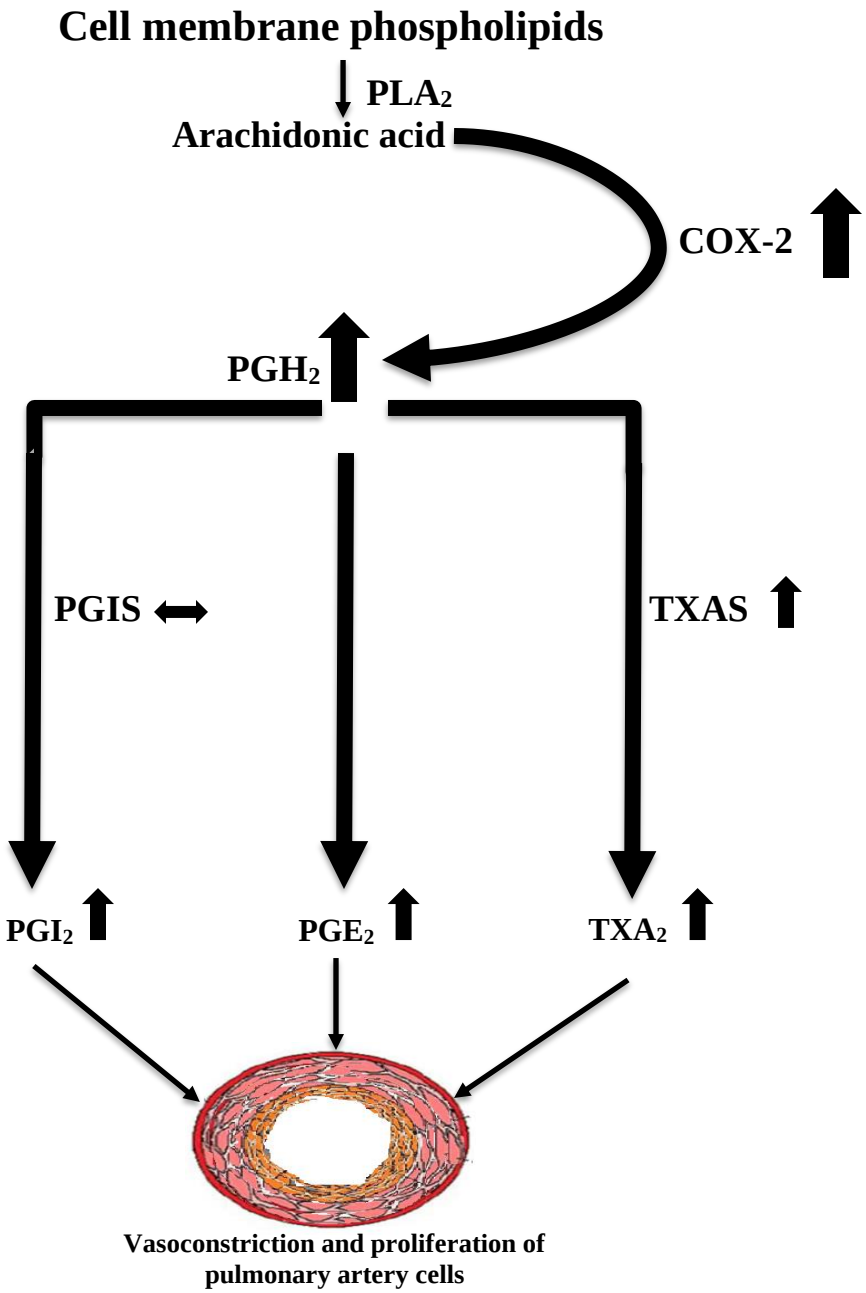


Figure 4.27: Schematic diagram of hypoxia effect on the expression of the main enzymes of prostanoid biosynthesis and the release of vasoactive lipid mediators in human PASMCs.
Hypoxia induces COX-2 expression and its downstream products PGI_2, PGE_2, and TXA_2 production in PASMCs. It is likely that hypoxia induces vasoadaptive responses in PASMCs by increasing the vasodilatory mediators PGI_2 and PGE_2, due to the increase in COX-2 product PGH_2. This observation demonstrates that hypoxia may cause PASMC dysfunction by increasing the vasoconstrictive and proliferative mediator TXA_2 production due to TXAS upregulation, which my eventually contribute to vasoconstriction and proliferation of PASMCs.

PLA_2, Phospholipase A_2; PGH_2, Prostaglandin H_2; PGI_2, Prostaglandin I_2; PGE_2, Prostaglandin E_2; PGIS, Prostaglandin I synthase; TXAS, Thromboxane A synthase; TXA_2, Thromboxane A_2; COX-2, Cyclooxygenase-2; PASMCs, Pulmonary artery smooth muscle cells; ↔, Unchanged; ↑, Upregulated; ↓, Downregulated.

4.5.1.2 Human pulmonary artery endothelial cells

Since previous studies only looked at the effect of hypoxia on COX-2 expression in other endothelial cell types rather than PAECs, we assessed the effect of hypoxia on COX-2 and its downstream products in human PAECs. Surprisingly, and unlike our findings from human PASMCs, hypoxia alone failed to have any effect on the COX-2 mRNA and protein expression and PGE_2 production, and did not further enhance CSE-induced effects in human PAECs. It is possible that COX-2/PGE_2 in vascular endothelial cells under hypoxic conditions has a biphasic effect depending on incubation time. This is supported by a previous study that reported a significant increase in COX-2/PGE_2 in response to hypoxia at 3 h, followed by a significant time-dependent reduction of COX-2/PGE_2 in human umbilical vein endothelial cells (Zhao et al., 2012).

As previously mentioned, the protein expression of PGIS in PAECs was undetectable. The observation that the positive control was detected confirms that the methods worked. Since PGI_2 production was detected basally and hypoxia did not change PGI_2 production, it is likely that PGIS was expressed in PAECs below the detection levels of Western blot analysis and was unaffected by hypoxia. This is similar to the effect of CSE, and suggests PGI_2 may not play a key role in hypoxia-induced PAEC dysfunction. Although the effect of hypoxia on PGIS/PGI_2 has not been previously studied in human PAECs, Camacho and colleagues (2011) found that cell exposure to hypoxia for 24 h increases the mRNA and protein expression of PGIS. The difference between the two studies may be explained by the fact that different cell types may

responed differently to hypoxia. More studies with additional cell lines are needed as we used PAECs from one donor, although the experiment was repeated at least three times.

TXA_2 is one of the downstream products from COX-2 activity, and its production is mediated by the enzyme TXAS. Although TXAS mRNA expression was not affected, and TXAS protein expression was undetectable, the observation that hypoxia increased TXA_2 production is supported by previous animal studies reporting increased TXA_2 levels in the arterial and venous plasma of hypoxic rats (Su and Jin, 1989) and in piglet models of hypoxia-induced pulmonary hypertension (Fike et al., 2005). Despite the undetected TXAS protein expression, our finding that hypoxia induced TXA_2 production goes hand in hand with those reported above in human PASMCs and suggests the increase of TXA_2 is a key part of PASMC and PAEC dysfunction and may critically be involved in the development of pulmonary hypertension in COPD. More importantly, the increase of TXA_2 is sufficient to override the unchanged PGI_2, thereby reducing the PGI_2/TXA_2 ratio in PAECs. Interestingly, hypoxia did not further amplify CSE-induced effects, even though CSE alone reduced the PGI_2/TXA_2 ratio.

It is also worth noting that increased TXA_2 (despite the undetected TXAS protein expression) is also similar to what was observed in Chapter 3 that CSE increased TXA_2 production in both PASMCs and PAECs. This implies that TXAS post-translational modification to increase its activity may be more important than its expression. Although there is no direct evidence of TXAS post-translational modification, there is preliminary evidence to suggest that COX-2 activity can be post-translationally modified (Jaen et al., 2018).

To the best of our knowledge, this is the first description of hypoxia effect on prostanoid biosynthesis and the release of vasoactive lipid mediators in human PAECs. Notably, our results support the observation above in PASMCs that CSE effect is stronger than hypoxia, as hypoxia does not further enhance CSE-induced effects in PAECs. This suggests that TXA_2 can be more critically involved in hypoxia-induced PAEC dysfunction than prostaglandin mediators PGI_2 and PGE_2. The reduced PGI_2/TXA_2 ratio (as a result of unchanged PGI_2 and increased TXA_2) may eventually contribute to dysfunction and proliferation of pulmonary artery cells in COPD-associated pulmonary hypertension. An illustration of the hypoxia effect on the expression of main enzymes of prostanoid biosynthesis and the release of vasoactive lipid mediators in human PAECs is shown in Figure 4.28.

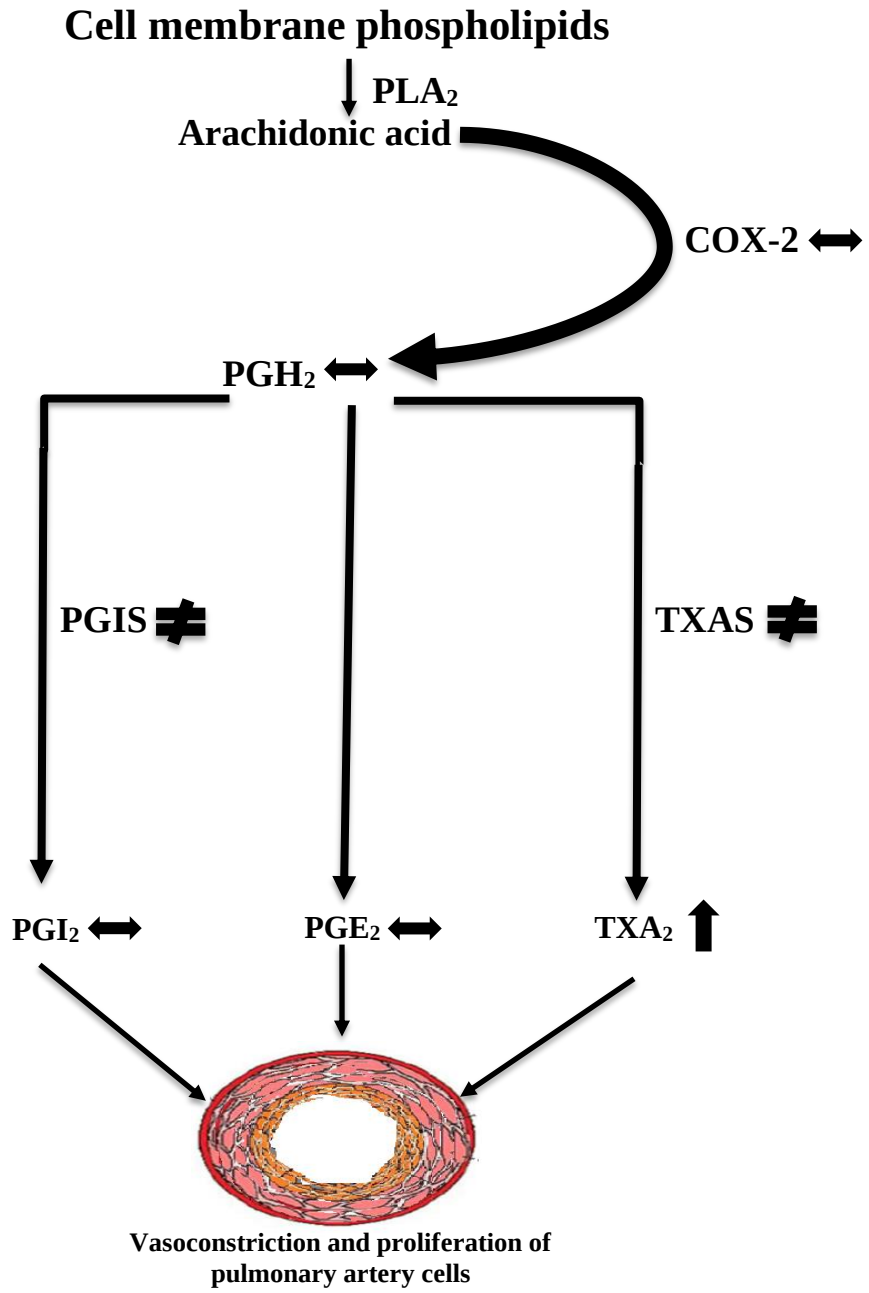


Figure 4.28 Schematic diagram of hypoxia effect on the expression of the main enzymes of prostanoid biosynthesis and the release of vasoactive lipid mediators in human PAECs.
Hypoxia has no effect on COX-2 expression and its downstream products PGI_2 and PGE_2 in PAECs. The protein expression of PGIS and TXAS was undetectable. Despite the undetected TXAS expression, hypoxia increases the vasoconstrictive and proliferative mediator TXA_2 (likely via posttranslational modifications). The increase in TXA_2 may eventually contribute to vasoconstriction and proliferation of pulmonary artery cells.

PLA_2, Phospholipase A_2; PGH_2, Prostaglandin H_2; PGI_2, Prostaglandin I_2; PGE_2, Prostaglandin E_2; PGIS, Prostaglandin I synthase; TXAS, Thromboxane A synthase; TXA_2, Thromboxane A_2; COX-2, Cyclooxygenase-2; PAECs, Pulmonary artery endothelial cells; ↔, Unchanged; ≠, Undetected; ↑, Upregulated; ↓, Downregulated.

4.5.2 Hypoxia and eNOS/nitric oxide

Nitric oxide has long been regarded as a fundamental vasodilator. Considering the fact that nitric oxide produced by vascular endothelial cells can diffuse into PASMCs where it inhibits cell proliferation, we sought to determine whether hypoxia alone has an effect on eNOS expression (and its product, nitric oxide) in PASMCs and PAECs, and whether it could further modify CSE-induced effects. Although eNOS expression was undetectable in PASMCs (as previously discussed in Chapter 3), eNOS expression was detectable in PAECs and was reduced (at protein but not mRNA levels) in response to hypoxia, suggesting it is likely that the hypoxia effect on eNOS expression is mediated via post-transcriptional regulation or post-translational modifications.

It is interesting to note that hypoxia caused a net reduction of eNOS protein expression in 1% (but not 2% and 3%) CSE-treated PAECs compared with CSE alone. The fact that CSE (1%) under normoxic conditions was not sufficient to reduce eNOS levels suggests the observed net reduction caused by CSE under hypoxic conditions is mainly due to the hypoxia effect. Once CSE at the highest two concentrations under normoxic conditions reduced eNOS protein expression, no additive effect of hypoxia was noted. This finding is further strengthened by the demonstration that hypoxia did not further enhance 3% CSE-induced decrease in nitric oxide production, although hypoxia alone reduced nitric oxide production, which also suggests that this reduction occurs as a result of eNOS protein expression downregulation. These findings are supported by the results of previous studies reporting reduced nitric oxide production and eNOS expression in homogenates of the lungs of piglets exposed to chronic hypoxia (Fike et al., 1998), as well as in human saphenous vein endothelial cells (Takemoto et al., 2002). Our

new findings presented here provide important evidence that this reduced nitric oxide (as a result of the downregulated eNOS expression in human PAECs) strongly indicates a key role for reduced eNOS and nitric oxide in hypoxia-induced vascular dysfunction and remodelling.

4.5.3 Hypoxia and endothelin

We were somewhat surprised by the observation that hypoxia had no effect on the mRNA endothelin-1 expression in PASMCs and PAECs. This suggests that hypoxia does not regulate endothelin-1 gene expression in both cell types. Previous studies reported that exposure of human PAECs to hypoxia induced endothelin-1 mRNA expression in human PAECs (Zhang et al., 2009), in human microvascular endothelial cells (Minchenko and Caro, 2000), and in human coronary artery smooth muscle cells (Hisada et al., 2012). There may be a number of possible reasons for this difference: cell type difference, the variations in experimental conditions, and the length of cell incubation time under hypoxic conditions. The fact that a net increase of endothelin-1 mRNA expression was observed in response to CSE under hypoxic conditions in PASMCs, but not in PAECs compared with CSE alone, suggests it is likely that CSE under hypoxic conditions may regulate endothelin-1 expression via transcriptional regulation. However, this increase did not lead to increased endothelin release in PASMCs. Perhaps also surprisingly, hypoxia did not change endothelin production in PASMCs. This is consistent with our findings from PAECs, but is in contrast to a previously reported study demonstrating an increase in the endothelin-1 production in human coronary artery smooth muscle cells exposed to hypoxia (1% O_2) for up to 24 h (Hisada et al., 2012). Cell type difference is probably the main reason for the disparity between our findings and

those reported by Hisada and colleagues (2012). In addition, the variations in the number of biological replications could be an alternative explanation for the difference. In the present study, we used PASMCs from three different donors, whereas Hisada and colleagues (2012) used coronary artery smooth muscle cells from one donor. The fact that the length of incubation time under hypoxic conditions (24 h) used in their study is different from the incubation time (72 h) used in our study for PASMCs may also explain why the findings reported in the two studies are different. Based on our observation, it is likely that PASMC and PAEC dysfunction and remodelling caused by the effect of hypoxia may not be mediated by dysregulation of the endothelin pathway.

To sum up, although it is unlikely that hypoxia can further amplify CSE-induced effects in our experimental setting, the findings in this Chapter partially support our hypothesis that hypoxia can induce imbalanced vasoactive gene expression and mediator release in human PAECs and PASMCs. The reduced nitric oxide and PGI_2/TXA_2 ratio in PAECs and increased TXA_2 in both cell types by hypoxia provide a new concept: that nitric oxide and prostanoid pathways, rather than the endothelin pathway, may be associated with hypoxia-induced PASMC and PAEC dysfunction. These findings are also important in understanding the role of vasoactive pathways in the regulation of hypoxia-induced PASMC and PAEC dysfunction, and may be of therapeutic benefit by targeting the dysregulated vasoactive mediators involved in hypoxia-induced vascular dysfunction and remodelling in COPD-associated pulmonary hypertension. Our novel observations presented in this Chapter also suggest that CSE is more prominent than hypoxia in terms of the induction of imbalanced vasoactive mediators in human PASMCs and PAECs. An illustration to summarise hypoxia effect is presented in Figure 4.29.

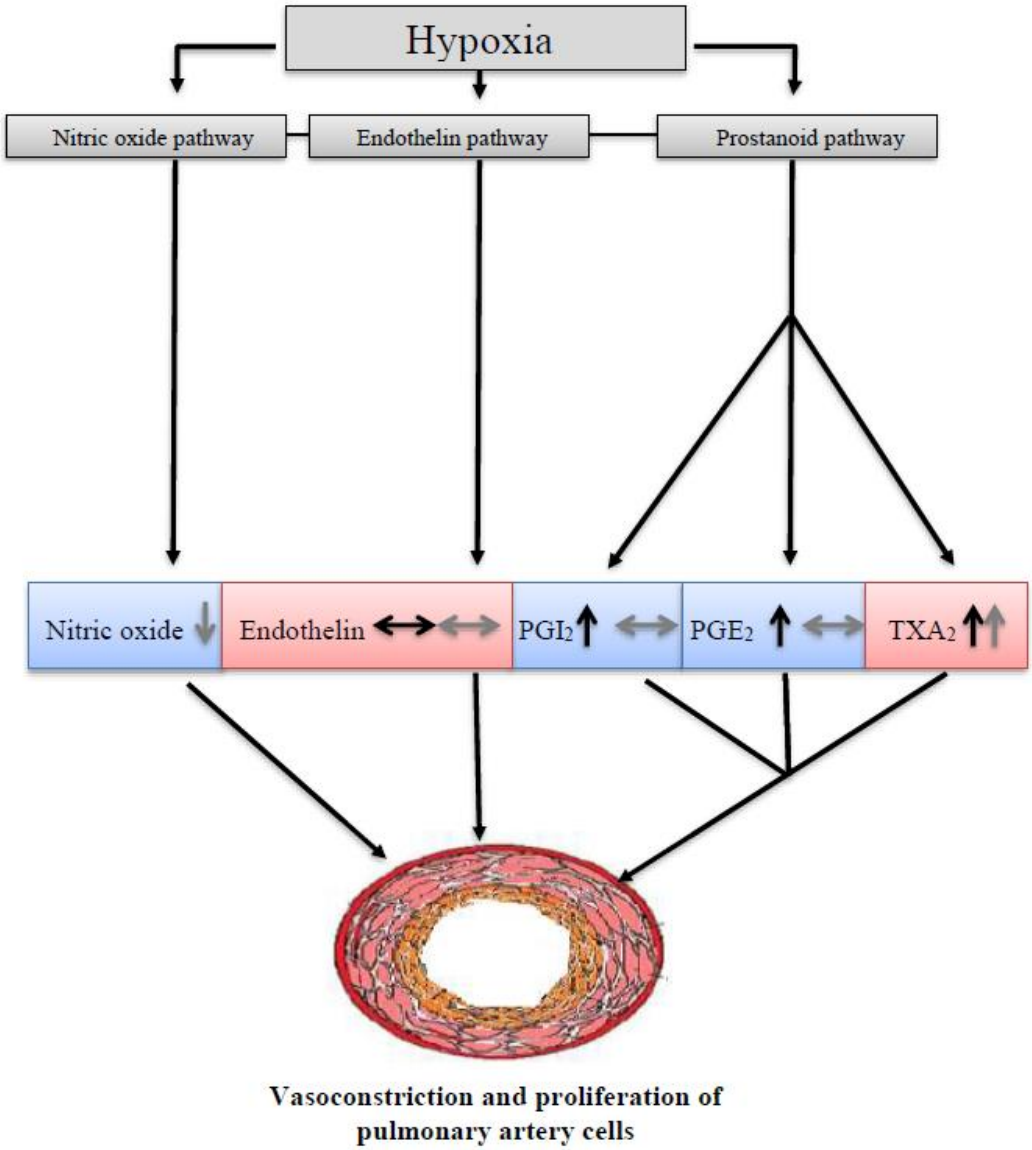


Figure 4.29 Schematic diagram of hypoxia effect on nitric oxide, endothelin and prostanoid production.

This is an illustrative diagram to summarise the deregulated vasoactive anti-proliferative and vasodilator mediators (blue rectangle) and proliferative and vasoconstrictor mediators (red rectangle) in human PASMCs (black arrow) and PAECs (grey arrow) that may contribute to hypoxia-induced vascular remodelling in COPD. In PASMCs, hypoxia increases PGI_2, PGE_2, and TXA_2 production but has no effect on endothelin production. In PAECs, hypoxia reduces nitric oxide and increases TXA_2 production but has no effect on endothelin PGE_2 and PGI_2 production.

PGI_2, Prostaglandin I_2; PGE_2, Prostaglandin E_2; TXA_2, Thromboxane A_2; PASMCs, Pulmonary artery smooth muscle cells; PAECs, Pulmonary artery endothelial cells; ↔, Unchanged; ↑, Upregulated; ↓, Downregulated.

Chapter 5. Effect of ECVE with and without nicotine on vasoactive gene expression and mediator release in human PASMCs and PAECs

5.1 Introduction

We demonstrated in Chapter 3 that CSE can induce an imbalance between proliferative/vasoconstrictor mediators and anti-proliferative/vasodilator mediators, in human PAECs and PASMCs, thereby contributing to vascular remodelling in COPD. It is suggested that the use of e-cig may aid smokers with COPD to reduce their cigarette smoking consumption, which consequently improves the annual rate of COPD exacerbations (Polosa et al., 2016). However, recent reports showed that e-cig use may play a role in inducing pro-inflammatory mediators in some cell types within the airway (Higham et al., 2018, Higham et al., 2016, Bozier et al., 2019). In addition, preliminary clinical studies have identified a role for e-cig in alteration of vascular endothelial function markers (Carnevale et al., 2016, Antoniewicz et al., 2016, Vlachopoulos et al., 2016, Caporale et al., 2019, Kuntic et al., 2019). These observations suggest that although e-cig may reduce the annual rate of COPD exacerbations, the use of e-cig may lead to vascular diseases and other acute lung injury disorders. In support of this notion, more than 37 deaths have recently been confirmed and 1,888 cases of EVALI have been reported to CDC. However, the underlying cause of this acute lung injury disorder and subsequent effect on cardiovascular disease has not been identified due to limited data. In addition, no data are available on what effect e-cig, with and without the presence of nicotine, may have on human PASMC and PAEC dysfunction.

5.2 Aims

The aim of this Chapter was to evaluate if ECVE$^{+/-n}$ has similar effects as CSE on the induction of imbalanced vasoactive gene expression and mediator release in human PASMCs and PAECs.

The specific aims of this Chapter were:

- To assess the effect of ECVE$^{+/-n}$ on the expression of key enzymes of prostanoid synthesis and the release of vasoactive lipid mediators in human PASMCs and PAECs.
- To determine whether ECVE$^{+/-n}$ has an effect on the expression of eNOS and endothelin-1 and the production of nitric oxide and endothelin in human PASMCs and PAECs.

5.3 Materials and methods

5.3.1 ECVE preparation

ECVE$^{+/-n}$ was prepared as previously described in the materials and methods, section 2.3.2. Briefly, ECVE$^{+/-n}$ was prepared the same way as CSE under standardised conditions by bubbling the vapour into 20 ml DMEM- or 20 ml LS-ECGM at 3 seconds per puff. The resulting ECVE$^{+/-n}$ was filtered and considered as 100% (Romagna et al., 2013, Taylor et al., 2016). For all experiments, fresh ECVE$^{+/-n}$ was used immediately after preparation.

5.3.2 Cell treatment

5.3.2.1 Pulmonary artery smooth muscle cells

Human PASMCs from three different healthy donors at passage 6 were treated with different concentrations of ECVE^{+n} (0.1%-0.5%), one concentration ECVE^{-n} (0.5%), and one concentration CSE (5%) for 48 hours with daily fresh DMEM+ and ECVE$^{+/-n}$ or CSE. The cells were then cultured for 24 hours with fresh DMEM- containing fresh ECVE$^{+/-n}$ or CSE under the same culture conditions.

5.3.2.2 Pulmonary artery endothelial cells

Human PAECs, isolated from of a healthy donor, were incubated with ECVE^{+n} (0.1%-0.5%), one concentration ECVE^{-n} (0.5%), and one concentration CSE (3%) for 24 hours.

5.3.3 RT-qPCR

Total RNA was isolated and RT-qPCR analysis was then conducted to measure the mRNA expression of COX-2, PGIS, TXAS, endothelin-1 and eNOS (materials and

methods section 2.9). β2M was used as a reference gene for all experiments. Data were expressed as relative expression (fold change).

5.3.4 Western blotting

At the end of the experiment, total cell lysates were collected and analysed for COX-2, PGIS and eNOS proteins using Western blotting (materials and methods, section 2.8). GAPDH was used as loading control to ensure an equal loading of samples.

5.3.5 ELISA

Supernatants were collected and assayed for PGE_2, 6-keto $PGF_{1\alpha}$, TXB_2 and endothelin using ELISA analysis (materials and methods, section 2.10). Data were normalised with total protein and expressed as pg/mg protein.

5.3.6 Nitrate/nitrite assay

Total nitrate/nitrite in cell culture supernatants was assessed using fluorometric assay (materials and methods, section 2.10). Data were normalised with total protein and presented as nmol/μg protein.

5.4 Results

5.4.1 Effect of ECVE$^{+/-n}$ on the mRNA and protein expression of COX-2 and PGE_2 production in human PASMCs and PAECs

To investigate whether ECVE$^{+/-n}$ has similar effects as CSE on the induction of COX-2 expression, human PASMCs and PAECs were treated with ECVE$^{+/-n}$ or CSE (positive control) for 72 and 24 hours, respectively. At the end of the experiment, total RNA and cell lysates were collected and Western blotting and RT-qPCR were used to assess protein and mRNA expression of COX-2, respectively. The mRNA results showed that PASMCs and PAECs expressed COX-2 basally. Interestingly, ECVE$^{+/-n}$ at all concentrations tested did not have any effect on the mRNA expression of COX-2 in PASMCs (Figure 5.1) and PAECs (Figure 5.2) compared with control, whereas cell treatment with CSE increased the mRNA expression of COX-2 in both cell types. We next found that the protein of COX-2 was not basally expressed and was upregulated in response to CSE in both PASMCs and PAECs. Consistent with the mRNA data, cell stimulation with ECVE$^{+/-n}$ caused no effect on the protein expression of COX-2 in PASMCs (Figure 5.3) and PAECs (Figure 5.4) compared with control.

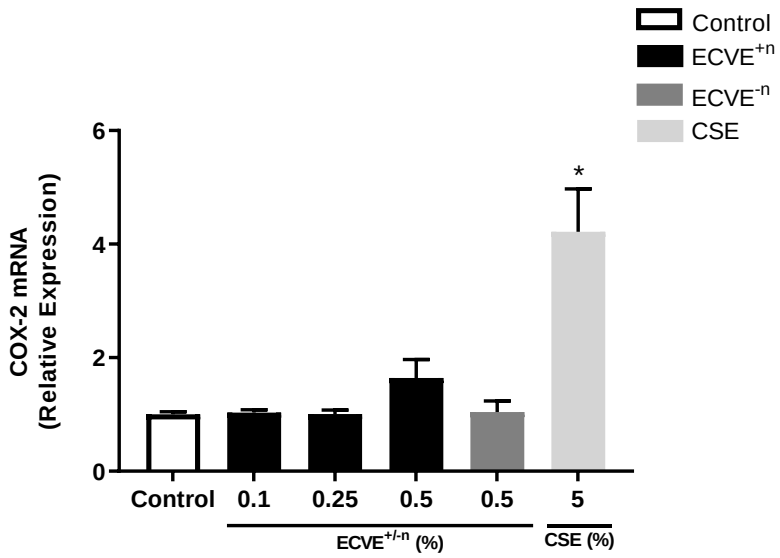


Figure 5.1 Effect of ECVE$^{+/-n}$ on the mRNA expression of COX-2 in human PASMCs.
Confluent human PASMCs were stimulated with or without ECVE^{+n} (0.1%, 0.25% and 0.5%), ECVE^{-n} (0.5%) and CSE (5%) for 48 hours with daily fresh DMEM+ and ECVE$^{+/-n}$ or CSE and then with the same concentrations of ECVE$^{+/-n}$ or CSE in DMEM- for 24 hours. Total RNA was isolated and the samples were then assayed for the mRNA expression of COX-2 using RT-qPCR. Data were expressed as fold change over control. Each data point represents mean ± SEM from three independent experiments using cells from three different donors. *P<0.05 compared with control.

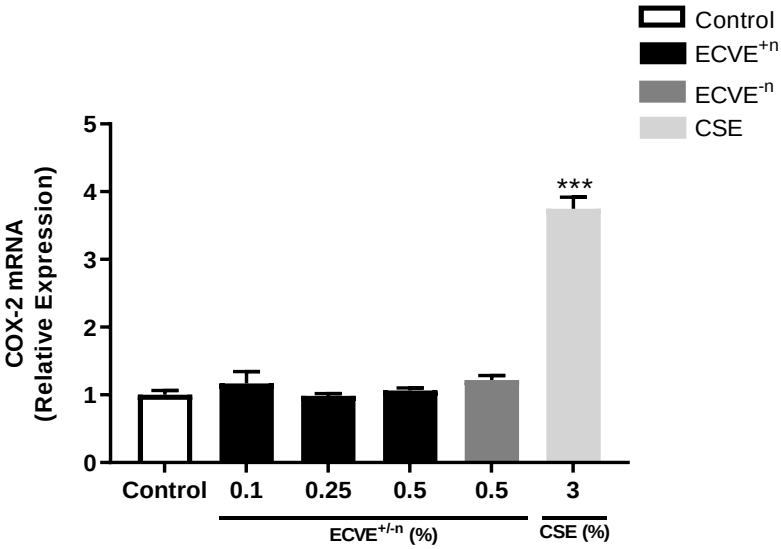


Figure 5.2 Effect of ECVE$^{+/-n}$ on the mRNA expression of COX-2 in human PAECs.
Confluent human PAECs were treated with or without ECVE^{+n} (0.1%, 0.25% and 0.5%), ECVE^{-n} (0.5%) and CSE (3%) for 24 hours prior to total RNA isolation. The samples were assayed for the mRNA expression of COX-2 using RT-qPCR. Data were expressed as fold change over control. Each data point represents mean ± SEM from three independent experiments using one cell line. ***P<0.001 compared with control.

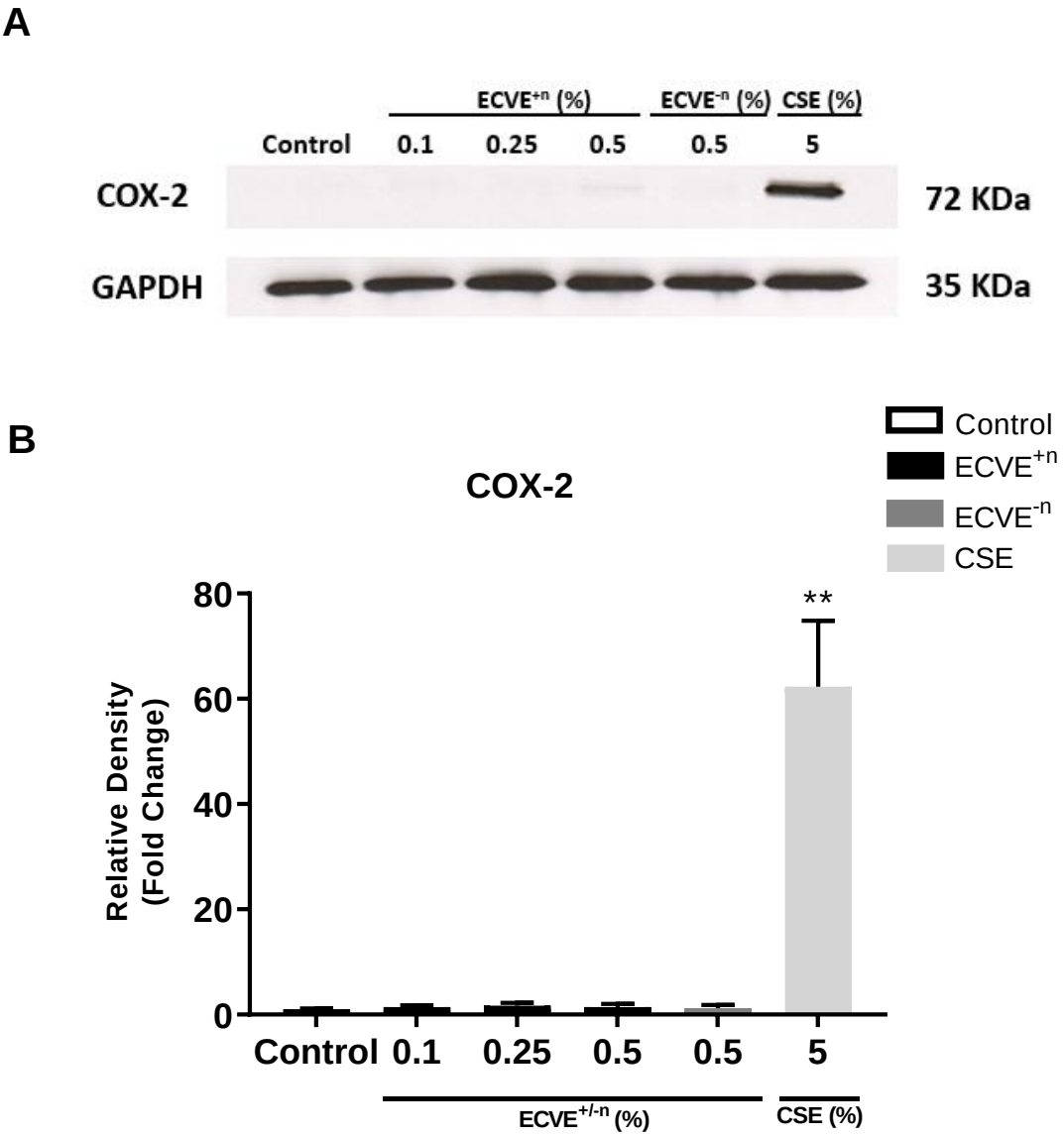


Figure 5.3 Effect of ECVE$^{+/-n}$ on the protein expression of COX-2 in human PASMCs.
Confluent human PASMCs were treated with or without ECVE^{+n} (0.1%, 0.25% and 0.5%), ECVE^{-n} (0.5%) and CSE (5%) for 48 hours with daily fresh DMEM+ and ECVE$^{+/-n}$ or CSE and then with the same concentrations of ECVE$^{+/-n}$ or CSE in DMEM- for 24 hours. Total cell lysates were collected for Western blot analysis of COX-2 protein. A, a representative Western blot showing the effect of ECVE$^{+/-n}$ and CSE on COX-2 protein expression. B, optical densitometry analysis of Western blotting bands. Data were normalised with the loading control GAPDH and were expressed as fold change over control. Each data point represents mean ± SEM from three independent experiments using cells from three different donors. **p<0.01 compared with control.

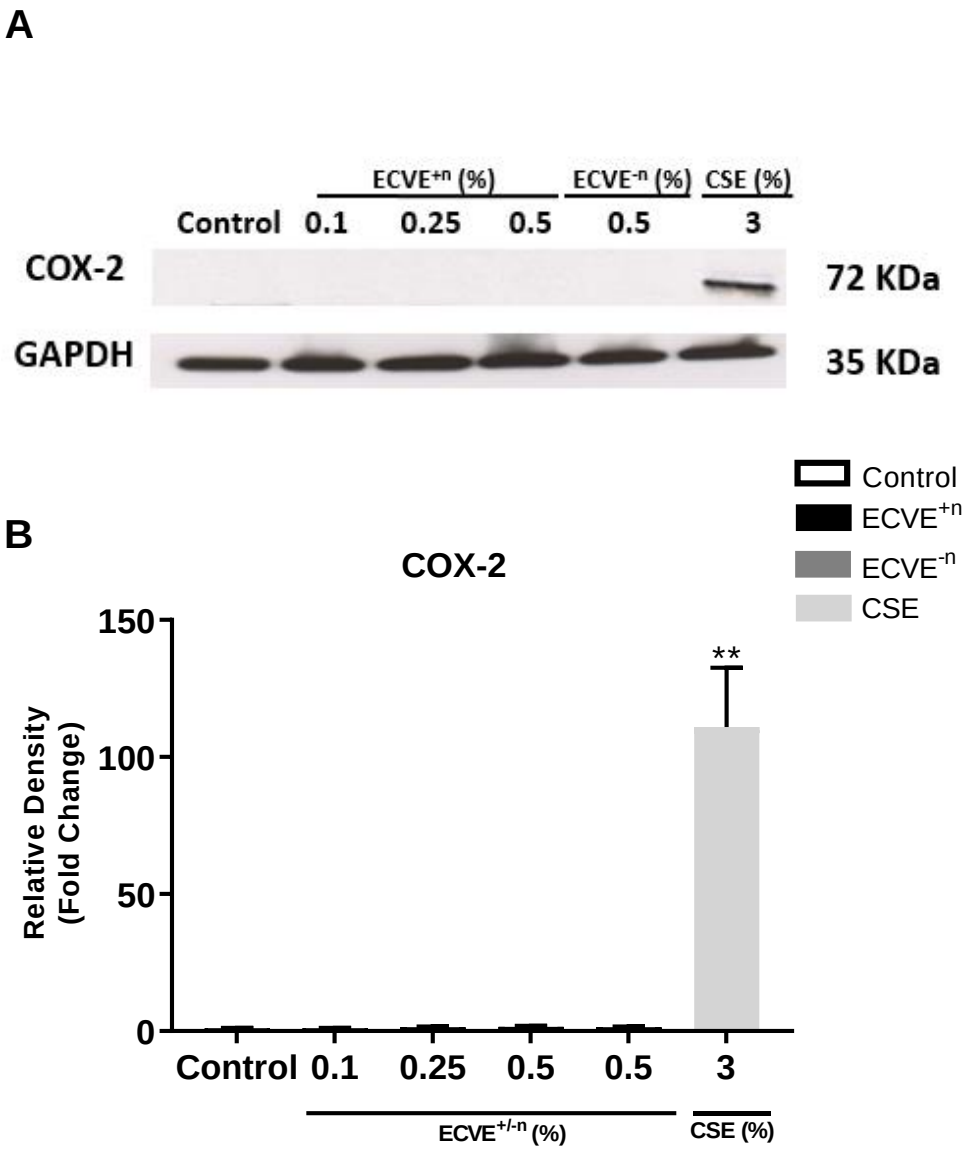


Figure 5.4 Effect of ECVE$^{+/-n}$ on the protein expression of COX-2 in human PAECs
Confluent human PAECs were treated with or without ECVE^{+n} (0.1%, 0.25% and 0.5%), ECVE^{-n} (0.5%) and CSE (3%) for 24 hours. Total cell lysates were collected for Western blot analysis of COX-2 protein. A, a representative Western blot showing the effect of ECVE$^{+/-n}$ and CSE on COX-2 protein expression. B, optical densitometry analysis of Western blotting bands. Data were normalised with the loading control GAPDH and were expressed as fold change over control. Each data point represents mean ± SEM from three independent experiments using one cell line. **p<0.01 compared with control.

In Chapter 3, we demonstrated that CSE reduced and increased the production of PGE_2 in PASMCs and PAECs, respectively. To examine whether $ECVE^{+/-n}$ would have similar effects as CSE, ELISA analysis was used to assess $ECVE^{+/-n}$ treatment effect on the production of PGE_2, one of the main prostanoid product downstream of COX-2, in cultured PASMCs and PAECs. Our results showed that PGE_2 was constitutively produced in PASMCs (933.0±142.3 pg/mg protein) (Figure 5.5). CSE reduced the production of PGE_2, while treatment with $ECVE^{+/-n}$ caused no significant effect on PGE_2 production in PASMCs. PGE_2 was also produced at basal levels in PAECs (398.1±19.6 pg/mg protein) (Figure 5.6). Consistent with findings from PASMCs, no significant changes in PGE_2 production were noted in response to treatment with $ECVE^{+/-n}$ at all concentrations tested.

Our data suggest that it is unlikely that $ECVE^{+/-n}$ has similar effects as CSE on COX-2 mRNA and protein expression and PGE_2 release in both human PASMCs and PAECs.

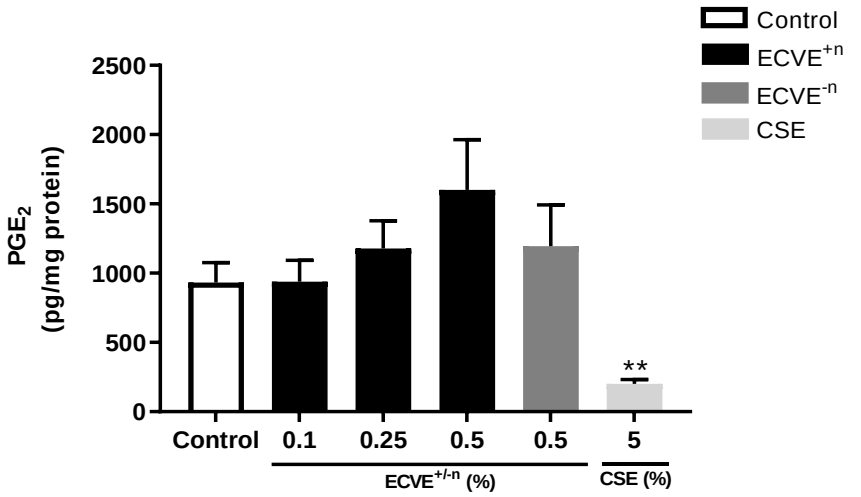


Figure 5.5 Effect of ECVE$^{+/-n}$ on PGE_2 production in human PASMCs.
Confluent human PASMCs were stimulated with or without ECVE^{+n} (0.1%, 0.25% and 0.5%), ECVE^{-n} (0.5%) and CSE (5%) for 48 hours with daily fresh DMEM+ and ECVE$^{+/-n}$ or CSE and then with the same concentrations of ECVE$^{+/-n}$ or CSE in DMEM- for 24 hours. Supernatants were collected and assayed for PGE_2 using ELISA analysis. Data were normalised with total protein and expressed as pg/mg protein. Each data point represents mean ± SEM from three independent experiments using cells from three different donors. **p<0.01 compared with control.

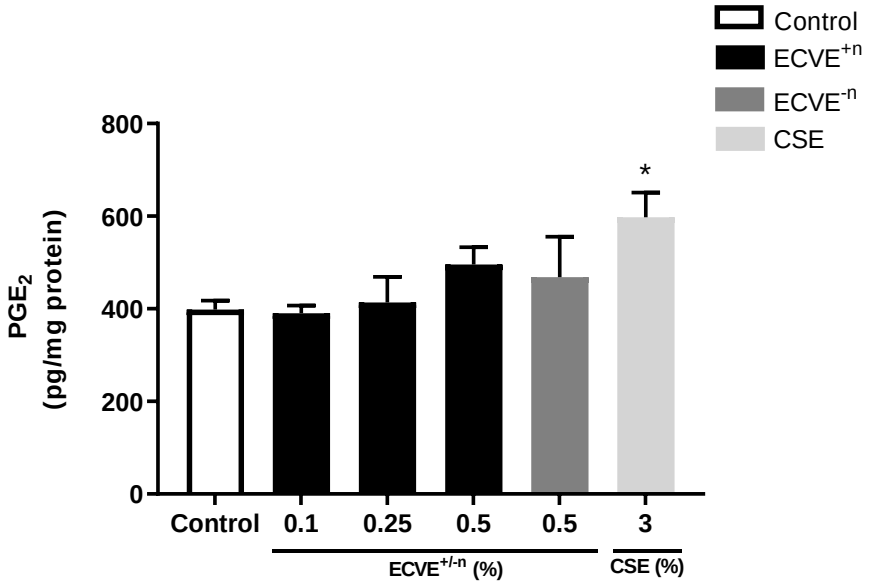


Figure 5.6 Effect of ECVE$^{+/-n}$ on PGE_2 production in human PAECs.
Confluent human PAECs were treated with or without ECVE^{+n} (0.1%, 0.25% and 0.5%), ECVE^{-n} (0.5%) and CSE (3%) for 24 hours. Supernatants were collected and assayed for PGE_2 using ELISA analysis. Data were normalised with total protein and expressed as pg/mg protein. Each data point represents mean ± SEM from three independent experiments using one cell line. *p<0.05 compared with control.

5.4.2 Effect of ECVE$^{+/-n}$ on the mRNA and protein expression of PGIS and PGI_2 production in human PASMCs and PAECs

PGIS is one of the main enzymes downstream of COX-2 activity, which converts PGH_2 to PGI_2. Here, we wanted to find out whether ECVE$^{+/-n}$ has an effect on the vasoprotective PGIS and its product, PGI_2. The data in Figure 5.7 and Figure 5.8 showed that PGIS mRNA was basally expressed in PASMCs and PAECs and CSE reduced the mRNA expression of PGIS in both cell types. Interestingly, ECVE$^{+/-n}$ stimulation failed to cause significant changes in PGIS expression in PASMCs (Figure 5.7) and PAECs (Figure 5.8) compared with control. To evaluate the protein expression of PGIS, Western blotting analysis was carried out. We found that PASMCs expressed PGIS protein basally (Figure 5.9A). Although 0.1% ECVE$^{+/-n}$ did not have any effect on PGIS protein expression, treatment with 0.25% ECVE^{+n} and 0.5% ECVE$^{+/-n}$ significantly reduced the protein expression of PGIS (fold changed 0.40±0.05, $p<0.01$, 0.27±0.04, $p<0.001$ and 0.22±0.07, $p<0.001$, respectively) compared with the control (Figure 5.9A and B). As previously reported in Chapter 3 and 4 (Figure 3.12A and B and Figure 4.10A and B), the protein expression of PGIS was undetectable under normoxic or hypoxic condition without or with CSE in PAECs. Thus, the effect of ECVE$^{+/-n}$ on PGIS protein expression in PAECs was not assessed in the current study.

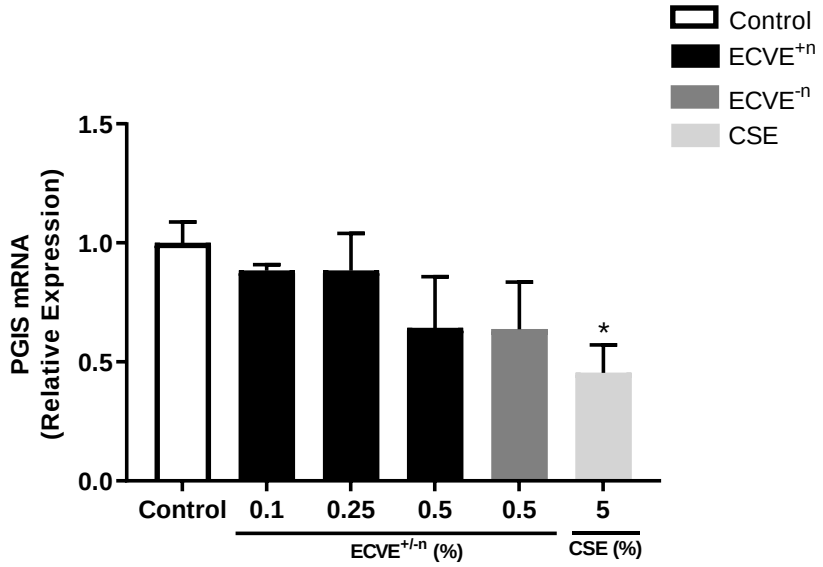


Figure 5.7 Effect of ECVE$^{+/-n}$ on the mRNA expression of PGIS in human PASMCs.
Confluent human PASMCs were stimulated with or without ECVE^{+n} (0.1%, 0.25% and 0.5%), ECVE^{-n} (0.5%) and CSE (5%) for 48 hours with daily fresh DMEM+ and ECVE$^{+/-n}$ or CSE and then with the same concentrations of ECVE$^{+/-n}$ or CSE in DMEM- for 24 hours. Total RNA was isolated and the samples were then assayed for the mRNA expression of PGIS using RT-qPCR. Data were expressed as fold change over control. Each data point represents mean ± SEM from three independent experiments using cells from three different donors. *P<0.05 compared with control.

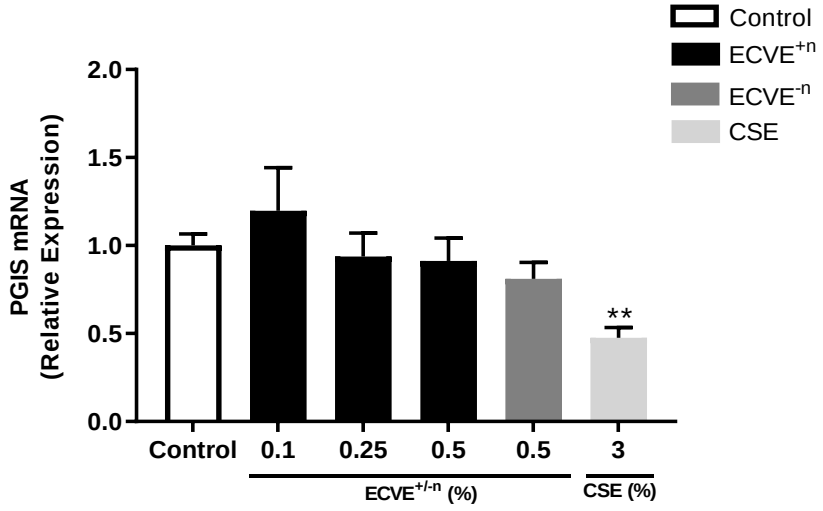


Figure 5.8 Effect of ECVE$^{+/-n}$ on the mRNA expression of PGIS in human PAECs.
Confluent human PAECs were treated with or without ECVE^{+n} (0.1%, 0.25% and 0.5%), ECVE^{-n} (0.5%) and CSE (3%) for 24 hours prior to total RNA isolation. The samples were assayed for the mRNA expression of PGIS using RT-qPCR. Data were expressed as fold change over control. Each data point represents mean ± SEM from three independent experiments using one cell line. **P<0.01 compared with control.

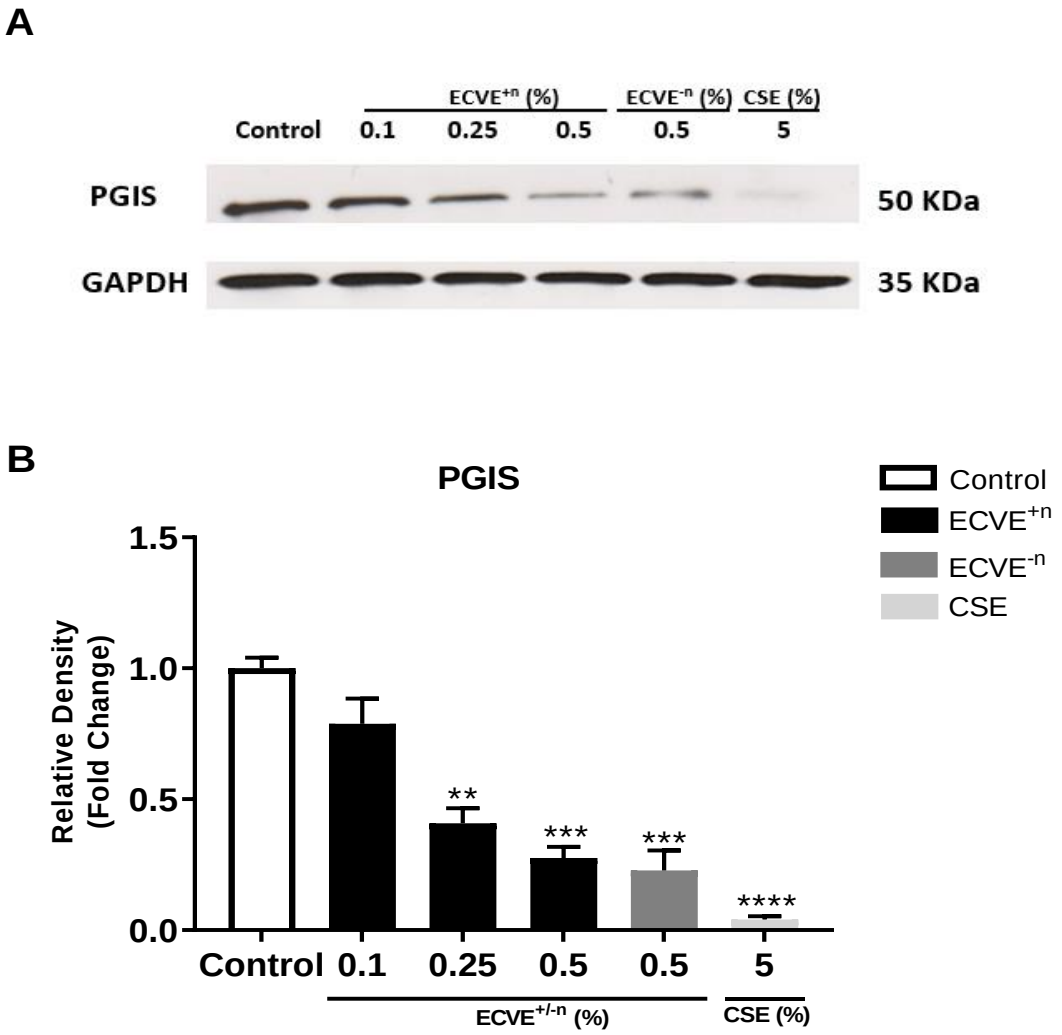


Figure 5.9 Effect of ECVE$^{+/-n}$ on the protein expression of PGIS in human PASMCs.
Confluent human PASMCs were treated with or without ECVE^{+n} (0.1%, 0.25% and 0.5%), ECVE^{-n} (0.5%) and CSE (5%) for 48 hours with daily fresh DMEM+ and ECVE$^{+/-n}$ or CSE and then with the same concentrations of ECVE$^{+/-n}$ or CSE in DMEM- for 24 hours. Total cell lysates were collected for Western blot analysis of PGIS protein. A, a representative Western blot showing the effect of ECVE$^{+/-n}$ and CSE on PGIS protein expression. B, optical densitometry analysis of Western blotting bands. Data were normalised with the loading control GAPDH and were expressed as fold change over control. Each data point represents mean ± SEM from three independent experiments using cells from three different donors. **p<0.01, ***p<0.001 and ****p<0.0001 compared with control.

To assess if $ECVE^{+/-n}$-induced downregulation of PGIS protein expression would lead to a reduction of PGIS product PGI_2, cells were incubated with $ECVE^{+/-n}$ and supernatants were then collected and PGI_2 production was estimated by measuring the production of 6-keto $PGF_{1\alpha}$ using ELISA analysis. Our results showed that levels of 6-keto $PGF_{1\alpha}$ were basally observed in PASMCs (2944.5±461.2 pg/mg protein) (Figure 5.10). Similarly, 6-keto $PGF_{1\alpha}$ was also detectable at basal levels in PAECs (471.3±143.0 pg/mg protein) (Figure 5.11). Although CSE treatment reduced 6-keto $PGF_{1\alpha}$ production over basal level in PASMCs, cell stimulation with $ECVE^{+/-n}$ did not change 6-keto $PGF_{1\alpha}$ levels in both PASMCs and PAECs compared with control.

Collectively, although $ECVE^{+/-n}$ reduces PGIS expression at protein levels in PASMCs, $ECVE^{+/-n}$ does not alter the production of PGI_2 in both cell types. This together with the unchanged PGE_2 suggests that it is most likely that $ECVE^{+/-n}$ has no effect on the production of the vasoactive prostaglandins or PGs.

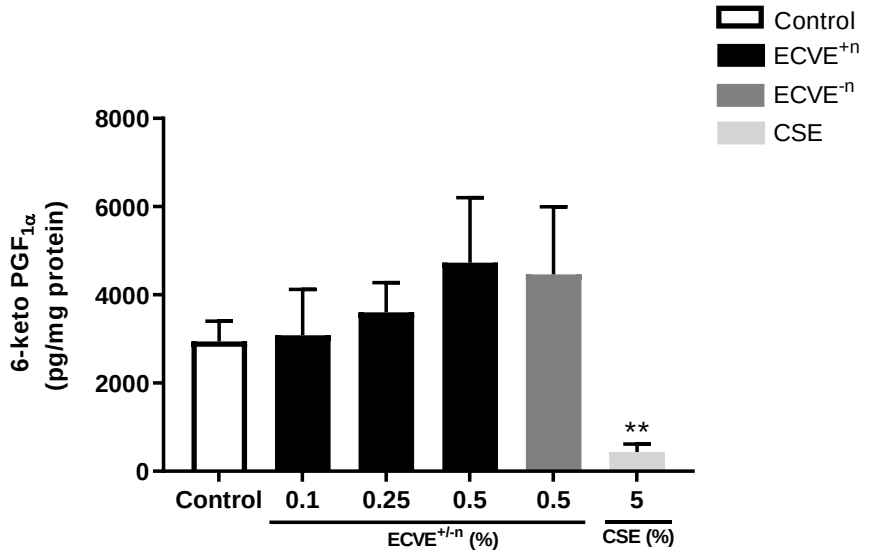


Figure 5.10 Effect of ECVE$^{+/-n}$ on 6-keto PGF$_{1\alpha}$ production in human PASMCs.
Confluent human PASMCs were stimulated with or without ECVE^{+n} (0.1%, 0.25% and 0.5%), ECVE^{-n} (0.5%) and CSE (5%) for 48 hours with daily fresh DMEM+ and ECVE$^{+/-n}$ or CSE and then with the same concentrations of ECVE$^{+/-n}$ or CSE in DMEM- for 24 hours. Supernatants were collected and assayed for 6-keto PGF$_{1\alpha}$ using ELISA analysis. Data were normalised with total protein and expressed as pg/mg protein. Each data point represents mean ± SEM from three independent experiments using cells from three different donors. **p<0.01 compared with control.

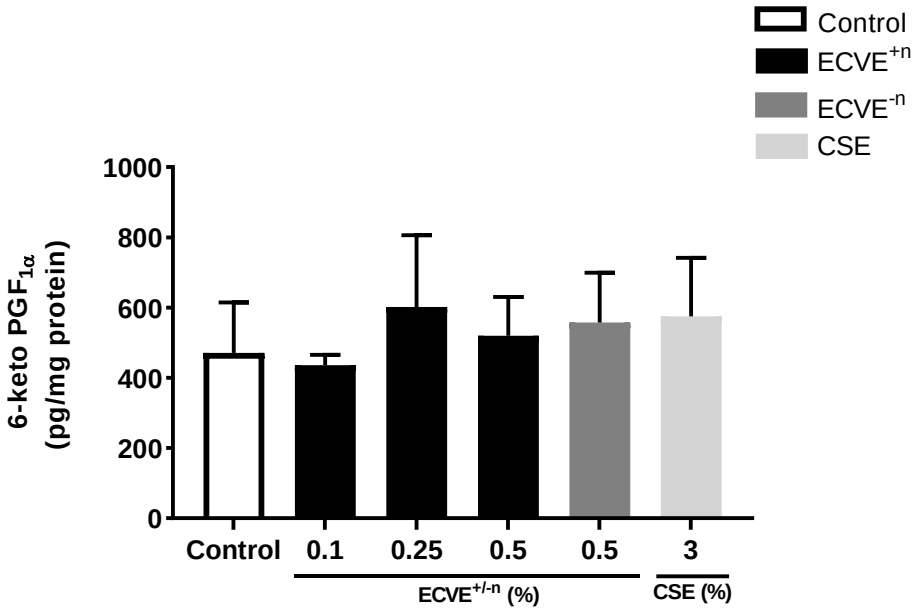


Figure 5.11 Effect of ECVE$^{+/-n}$ on 6-keto PGF$_{1\alpha}$ production in human PAECs.
Confluent human PAECs were treated with or without ECVE^{+n} (0.1%, 0.25% and 0.5%), ECVE^{-n} (0.5%) and CSE (3%) for 24 hours. Supernatants were collected and assayed for 6-keto PGF$_{1\alpha}$ using ELISA analysis. Data were normalised with total protein and expressed as pg/mg protein. Each data point represents mean ± SEM from three independent experiments using one cell line.

5.4.3 Effect of ECVE$^{+/-n}$ on the expression of TXAS and TXA_2 production in human PASMCs and PAECs

Our data presented in the previous Chapters suggest an important role of increased TXA_2 in CS-induced PASMC and PAEC dysfunction, which may eventually contribute to vascular remodelling and pulmonary hypertension. However, it is unknown whether ECVE$^{+/-n}$ has similar effects as CSE on TXAS/TXA_2. Our mRNA data showed that TXAS was basally detectable in PASMCs (Figure 5.12) and PAECs (Figure 5.13). In contrast to CSE effect, treatment with ECVE$^{+/-n}$ failed to have any effect on TXAS mRNA expression in both cell types. Since TXAS protein expression was undetectable under both basal and CSE-treated cells conditions, the protein expression of TXAS was not assessed. Further experiments were then carried out to explore the effect of ECVE$^{+/-n}$ on the production of TXB_2 in PASMCs (Figure 5.14) and PAECs (Figure 5.15). We found that the TXB_2 was produced under basal levels in PASMCs (140.4±35.1 pg/mg protein) and in PAECs (321.8±23.4 pg/mg protein). Surprisingly, ECVE$^{+/-n}$ did not modify TXB_2 production in both PASMCs and PAECs compared with control.

The unchanged vasoconstrictive TXAS expression and TXA_2 production in response to ECVE$^{+/-n}$ in both cell types further suggest that it is unlikely that ECVE$^{+/-n}$ has similar effects as CSE on the induction of imbalanced release of vasoactive prostanoids.

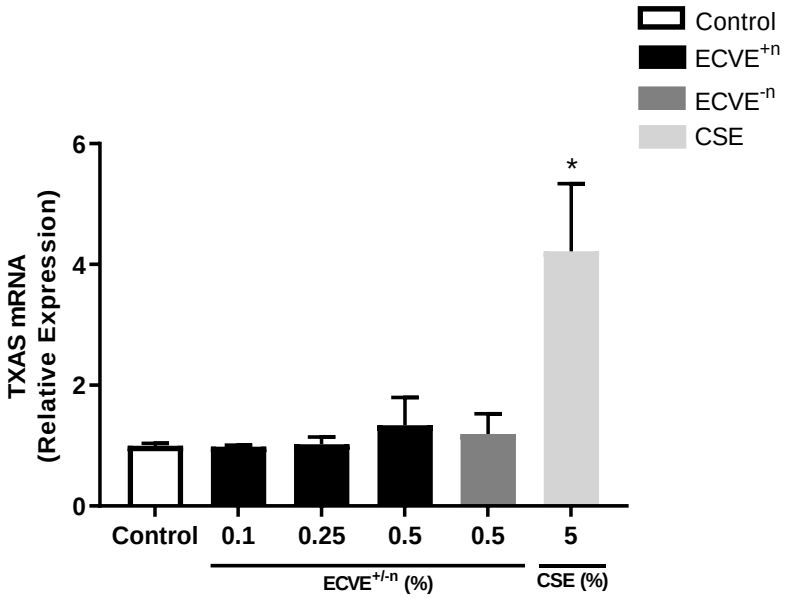


Figure 5.12 Effect of ECVE$^{+/-n}$ on the mRNA expression of TXAS in human PASMCs.
Confluent human PASMCs were stimulated with or without ECVE^{+n} (0.1%, 0.25% and 0.5%), ECVE^{-n} (0.5%) and CSE (5%) for 48 hours with daily fresh DMEM+ and ECVE$^{+/-n}$ or CSE and then with the same concentrations of ECVE$^{+/-n}$ or CSE in DMEM- for 24 hours. Total RNA was isolated and the samples were then assayed for the mRNA expression of TXAS using RT-qPCR. Data were expressed as fold change over control. Each data point represents mean ± SEM from three independent experiments using cells from three different donors. *p<0.05 compared with control.

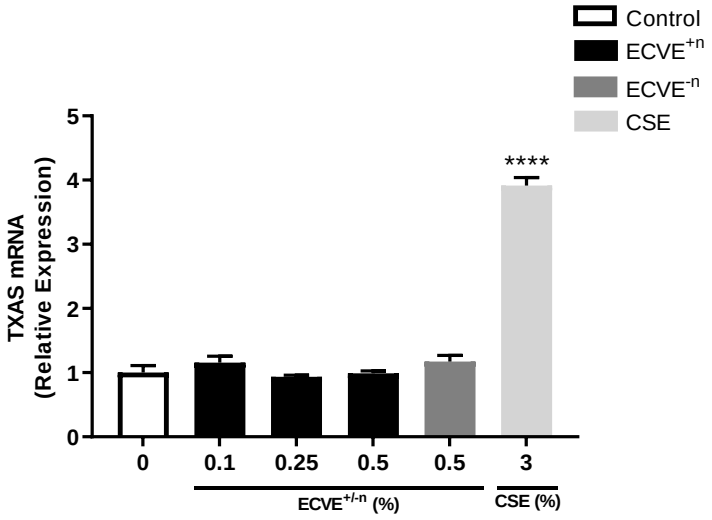


Figure 5.13 Effect of ECVE$^{+/-n}$ on the mRNA expression of TXAS in human PAECs.
Confluent human PAECs were treated with or without ECVE^{+n} (0.1%, 0.25% and 0.5%), ECVE^{-n} (0.5%) and CSE (3%) for 24 hours prior to total RNA isolation. The samples were assayed for the mRNA expression of TXAS using RT-qPCR. Data were expressed as fold change over control. Each data point represents mean ± SEM from three independent experiments using one cell line. ****p<0.0001 compared with control.

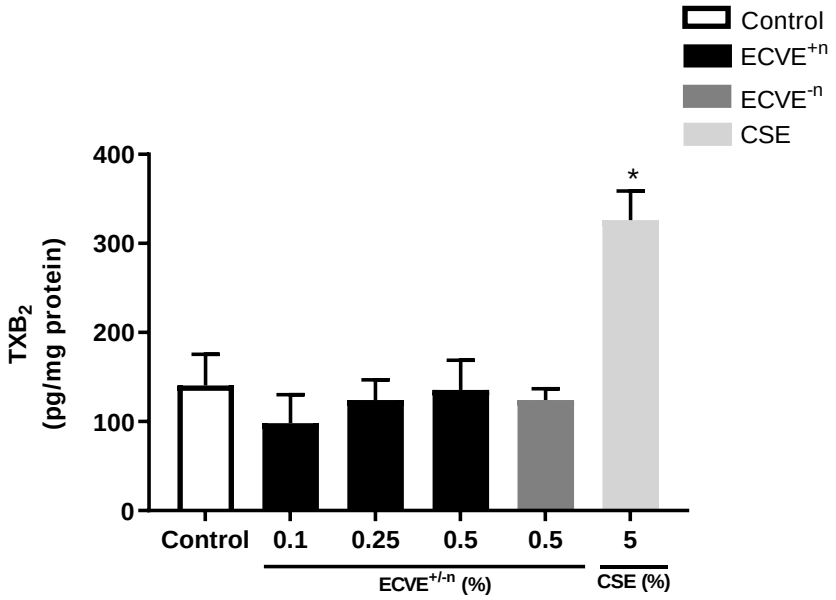


Figure 5.14 Effect of ECVE$^{+/-n}$ on TXB_2 production in human PASMCs.
Confluent human PASMCs were stimulated with or without ECVE^{+n} (0.1%, 0.25% and 0.5%), ECVE^{-n} (0.5%) and CSE (5%) for 48 hours with daily fresh DMEM+ and ECVE$^{+/-n}$ or CSE and then with the same concentrations of ECVE$^{+/-n}$ or CSE in DMEM- for 24 hours. Supernatants were collected and assayed for TXB_2 using ELISA analysis. Data were normalised with total protein and expressed as pg/mg protein. Each data point represents mean ± SEM from three independent experiments using cells from three different donors. *$p<0.05$ compared with control.

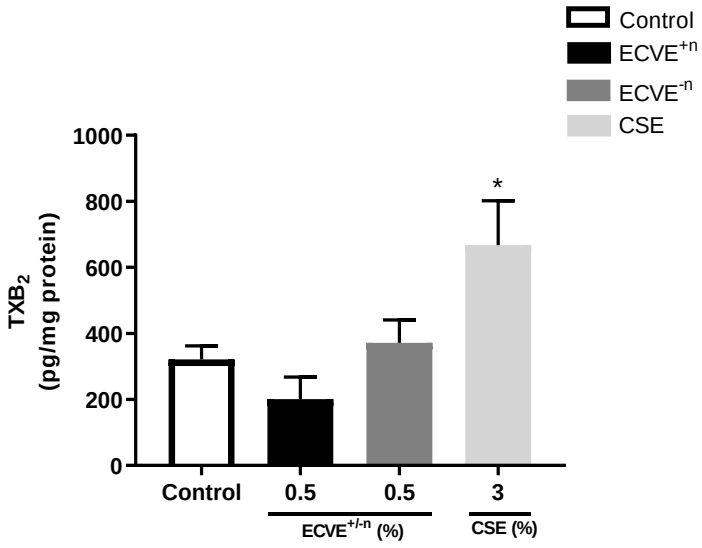


Figure 5.15 Effect of ECVE$^{+/-n}$ on TXB_2 production in human PAECs.
Confluent human PAECs were treated with or without ECVE$^{+/-n}$ (0.5%) and CSE (3%) for 24 hours. Supernatants were collected and assayed for TXB_2 using ELISA analysis. Data were normalised with total protein and expressed as pg/mg protein. Each data point represents mean ± SEM from three independent experiments using one cell line. *$p<0.05$ compared with control.

5.4.4 Effect of ECVE$^{+/-n}$ on the mRNA and protein expression of eNOS and nitric oxide production in human PAECs

Nitric oxide deficiency has been associated with endothelial dysfunction and identified in several pulmonary vascular diseases, including pulmonary hypertension (Klinger et al., 2013). Recently, deficient nitric oxide has been reported in serum collected from non-tobacco smoker pre and post the use of e-cig (Chatterjee et al., 2019). However, the direct effect of ECVE$^{+/-n}$ treatment on the mRNA and protein expression of eNOS and nitric oxide production in human PAECs remain to be identified. We first found that eNOS mRNA expression was detectable at basal levels in PAECs (Figure 5.16). However, cell exposure to ECVE$^{+/-n}$ had no effect on the eNOS expression. We also found that protein of eNOS was basally expressed (Figure 5.17A). Consistent with the mRNA data, ECVE$^{+/-n}$ at all concentrations tested caused no significant changes in the protein expression of eNOS as shown in densitometry analysis of Western blotting bands in Figure 5.17B.

Next, cell culture supernatants were collected following PAEC stimulation with ECVE$^{+/-n}$ to assess changes in the production of nitric oxide using total nitrate/nitrite assay. The results showed that the total nitrate/nitrite was constitutively produced in PAECs (0.04±0.009 nmol/µg protein) (Figure 5.18) and remained unchanged in response to ECVE$^{+/-n}$. Since we were not able to detect eNOS expression at mRNA and protein levels in PASMCs under basal and CSE-treated cells conditions as shown earlier in Figure 23A and B, no further experiments were conducted to assess the effect of ECVE$^{+/-n}$ on eNOS expression and total nitrate/nitrite production in PASMCs.

Collectively, although CSE reduces nitric oxide as a result of the downregulated eNOS expression in PAECs, our results indicate that stimulation of PAECs with $ECVE^{+/-n}$ does not affect eNOS expression and nitric oxide production. This suggests that it is likely that $ECVE^{+/-n}$ does not cause similar effects on eNOS protein expression and nitric oxide production as CSE does.

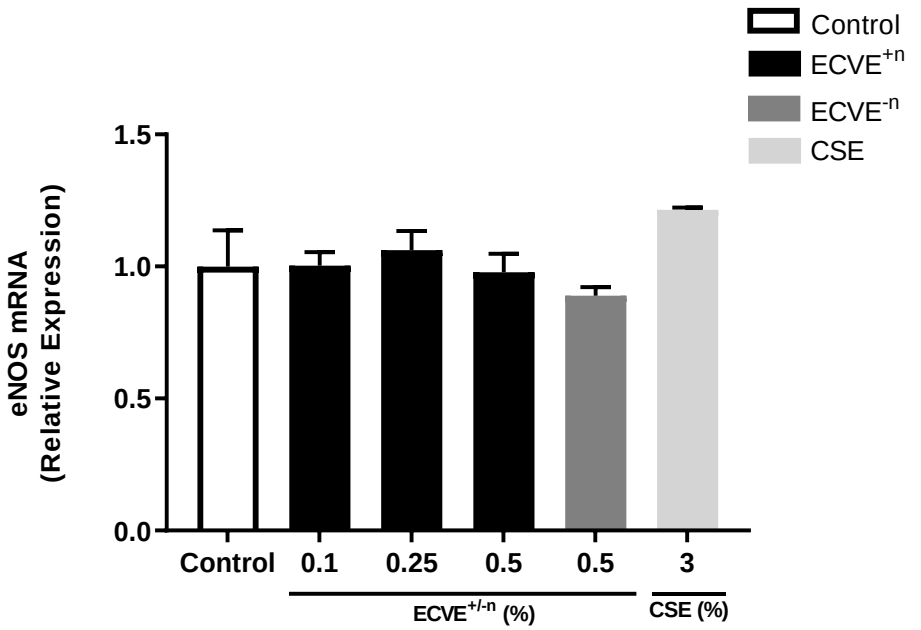


Figure 5.16 Effect of ECVE$^{+/-n}$ on the mRNA expression of eNOS in human PAECs.
Confluent human PAECs were treated with or without ECVE^{+n} (0.1%, 0.25% and 0.5%), ECVE^{-n} (0.5%) and CSE (3%) for 24 hours prior to total RNA isolation. The samples were assayed for the mRNA expression of eNOS using RT-qPCR. Data were expressed as fold change over control. Each data point represents mean ± SEM from three independent experiments using one cell line.

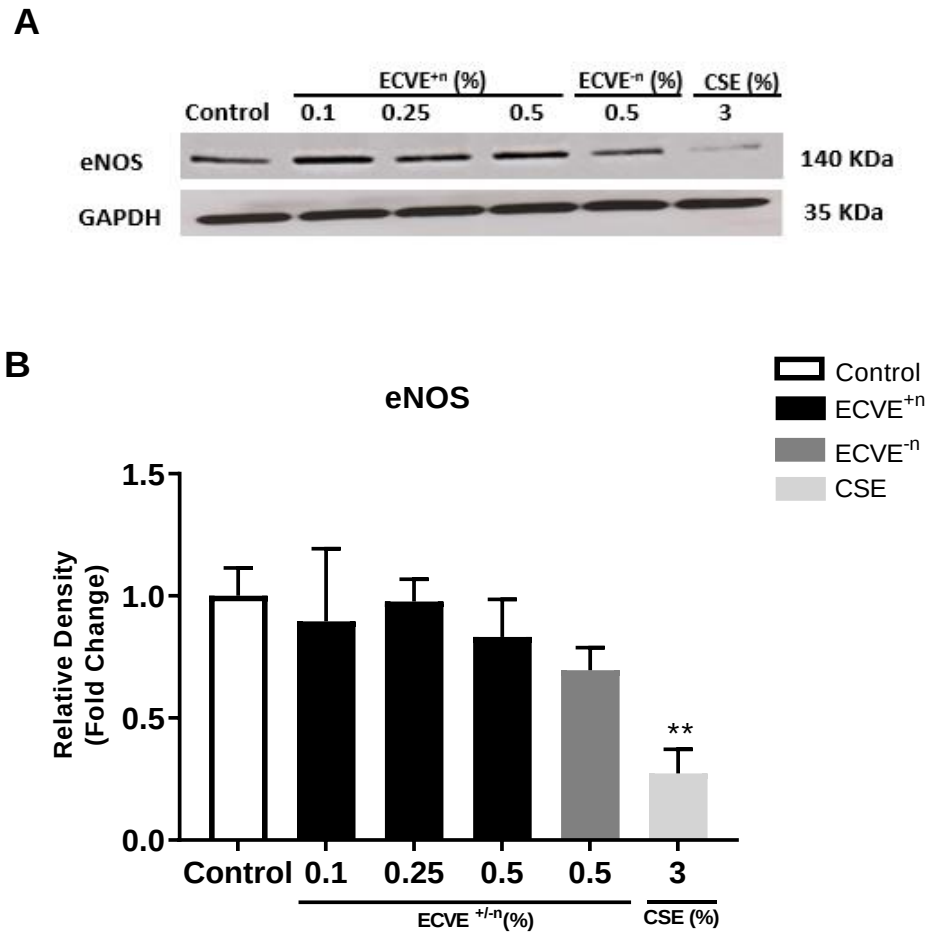


Figure 5.17 Effect of ECVE$^{+/-n}$ on the protein expression of eNOS in human PAECs.
Confluent human PAECs were treated with or without ECVE^{+n} (0.1%, 0.25% and 0.5%), ECVE^{-n} (0.5%) and CSE (3%) for 24 hours. Total cell lysates were collected for Western blot analysis of eNOS protein. A, a representative Western blot showing the effect of ECVE$^{+/-n}$ and CSE on eNOS protein expression. B, optical densitometry analysis of Western blotting bands. Data were normalised with the loading control GAPDH and were expressed as fold change over control. Each data point represents mean ± SEM from three independent experiments using one cell line. **p<0.01 compared with control.

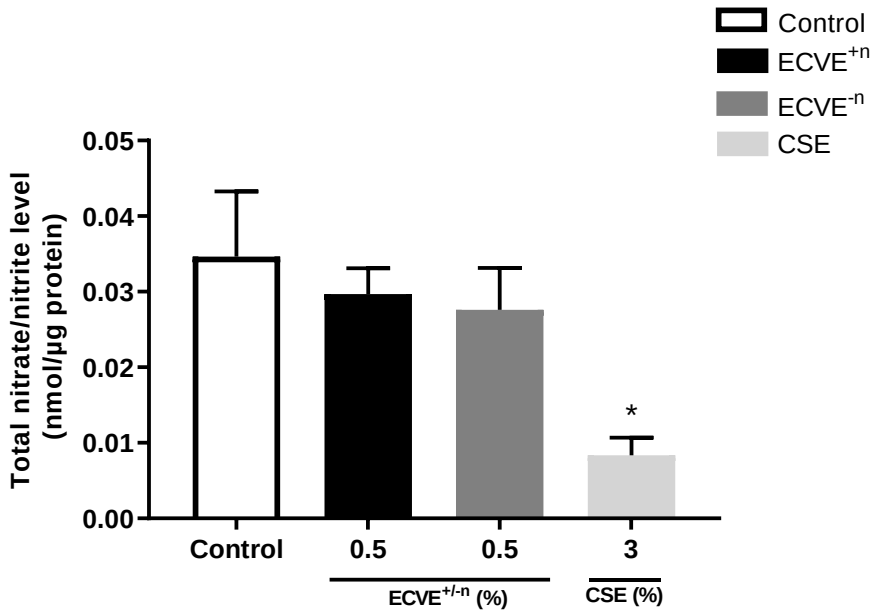


Figure 5.18 Effect of ECVE$^{+/-n}$ on total nitrate/nitrite level in human PAECs.
Confluent human PAECs were treated with or without ECVE$^{+/-n}$ (0.5%) and CSE (3%) for 24 hours. Supernatants were collected and assayed for total nitrate/nitrite using fluorometric assay. Data were normalised with total protein and expressed as nmol/µg protein. Each data point represents mean ± SEM from three independent experiments using one cell line. *$p<0.05$ compared with control.

5.4.5 Effect of ECVE$^{+/-n}$ on the mRNA expression of endothelin-1 and endothelin production in human PASMCs and PAECs

Because the effect of ECVE$^{+/-n}$ on endothelin pathway is unknown in PASMCs and PAECs, we here investigated ECVE$^{+/-n}$ effect on endothelin-1 mRNA and endothelin production in human PASMCs and PAECs. Our RT-qPCR analysis showed that the mRNA of endothelin-1 was basally expressed in PASMCs. Although 0.1%, 0.25% ECVE^{+n} and 0.5% ECVE^{-n} caused no significant effect on the mRNA expression of endothelin-1, 0.5% ECVE^{+n} significantly increased endothelin-1 mRNA expression in PASMCs (fold change 1.8±0.07, $p<0.01$) (Figure 5.19) compared with control. We also found that human PAECs expressed mRNA of endothelin-1 at basal levels. Interestingly, treatment with ECVE$^{+/-n}$ at all concentrations tested did not have any effect on the mRNA expression of endothelin-1 (Figure 5.20). We then went on to determine the effect of ECVE$^{+/-n}$ on the production of endothelin. We found that endothelin production was detectable at basal levels in PASMCs (169.0±31.8 pg/mg protein) (Figure 5.21) and PAECs (3917.5±479.9 pg/mg protein) (Figure 5.22). To our surprise, treatment with ECVE$^{+/-n}$ resulted in no effect on the production of endothelin in both PASMCs and PAECs.

Taken together, ECVE^{+n} increases the mRNA expression of endothelin-1 in PASMCs, but this does not lead to increased endothelin production. Our data also suggest ECVE$^{+/-n}$ does not have any effect on the mRNA expression of endothelin-1 and the production of endothelin in PAECs. The unchanged endothelin production further supports our findings presented in this Chapter and suggests that ECVE$^{+/-n}$ does not directly alter the release of vasoactive mediators in human PASMCs and PAECs.

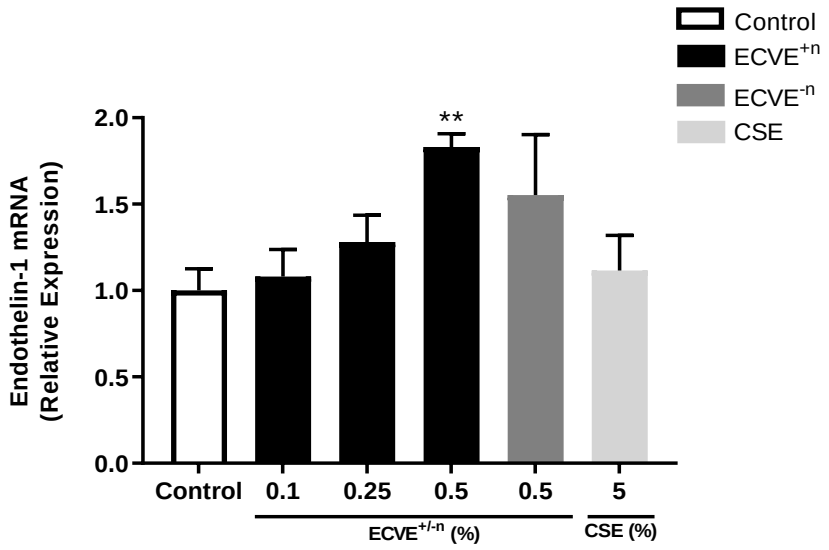


Figure 5.19 Effect of ECVE$^{+/-n}$ on the mRNA expression of endothelin-1 in human PASMCs.
Confluent human PASMCs were stimulated with or without ECVE^{+n} (0.1%, 0.25% and 0.5%), ECVE^{-n} (0.5%) and CSE (5%) for 48 hours with daily fresh DMEM+ and ECVE$^{+/-n}$ or CSE and then with the same concentrations of ECVE$^{+/-n}$ or CSE in DMEM- for 24 hours. Total RNA was isolated and the samples were then assayed for the mRNA expression of endothelin-1 using RT-qPCR. Data were expressed as fold change over control. Each data point represents mean ± SEM from three independent experiments using cells from three different donors. **p<0.01 compared with control.

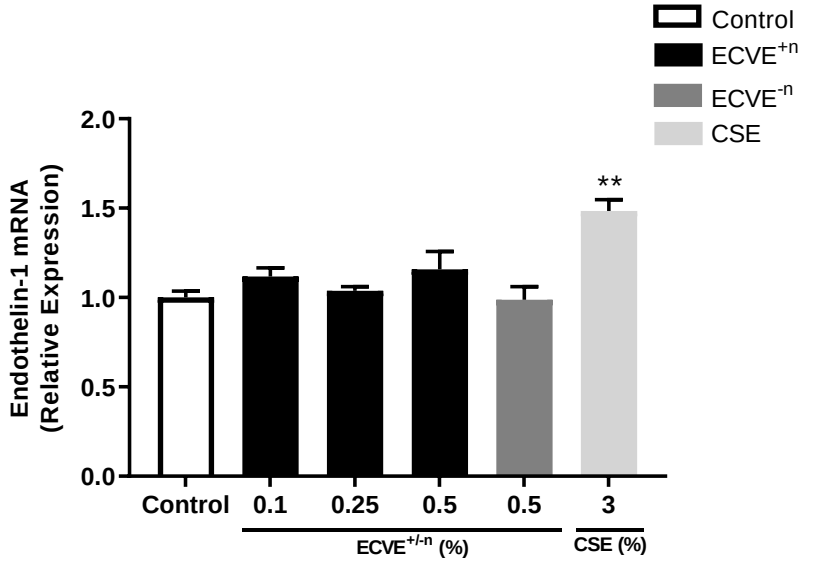


Figure 5.20 Effect of ECVE$^{+/-n}$ on the mRNA expression of endothelin-1 in human PAECs.
Confluent human PAECs were treated with or without ECVE^{+n} (0.1%, 0.25% and 0.5%), ECVE^{-n} (0.5%) and CSE (3%) for 24 hours prior to total RNA isolation. The samples were assayed for the mRNA expression of endothelin-1 using RT-qPCR. Data were expressed as fold change over control. Each data point represents mean ± SEM from three independent experiments using one cell line. **p<0.01 compared with control.

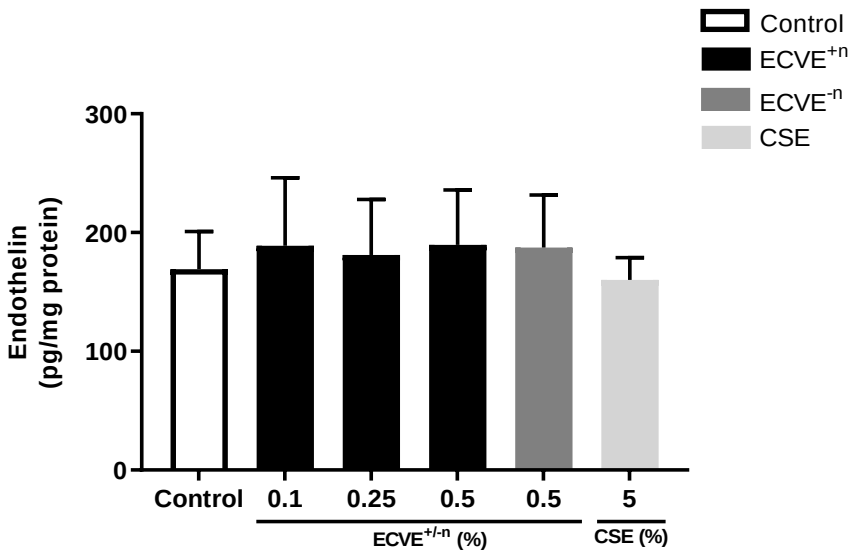


Figure 5.21 Effect of ECVE$^{+/-n}$ on endothelin production in human PASMCs.
Confluent human PASMCs were stimulated with or without ECVE^{+n} (0.1%, 0.25% and 0.5%), ECVE^{-n} (0.5%) and CSE (5%) for 48 hours with daily fresh DMEM+ and ECVE$^{+/-n}$ or CSE and then with the same concentrations of ECVE$^{+/-n}$ or CSE in DMEM- for 24 hours. Supernatants were collected and assayed for endothelin using ELISA analysis. Data were normalised with total protein and expressed as pg/mg protein. Each data point represents mean ± SEM from three independent experiments using cells from three different donors.

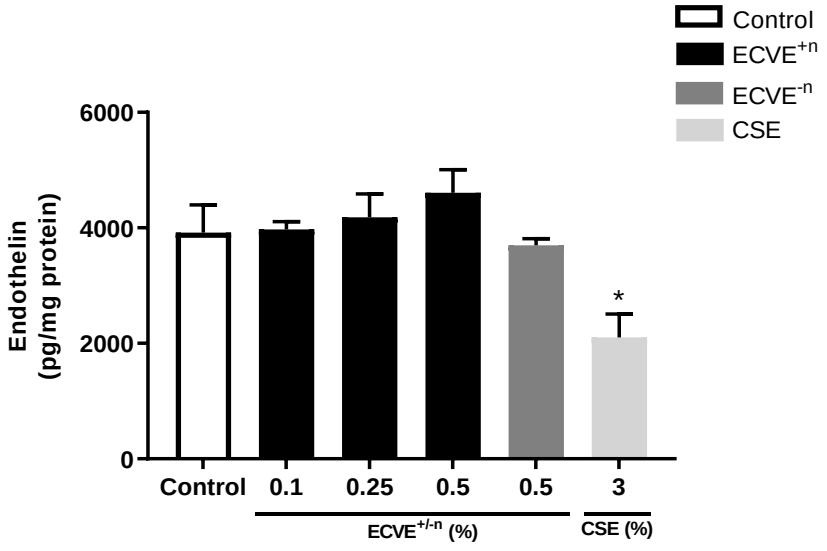


Figure 5.22 Effect of ECVE$^{+/-n}$ on endothelin production in human PAECs.
Confluent human PAECs were treated with or without ECVE^{+n} (0.1%, 0.25% and 0.5%), ECVE^{-n} (0.5%) and CSE (3%) for 24 hours. Supernatants were collected and assayed for endothelin using ELISA analysis. Data were normalised with total protein and expressed as pg/mg protein. Each data point represents mean ± SEM from three independent experiments using one cell line. *$p<0.05$ compared with control.

5.5 Discussion

The main aim of this Chapter was to determine whether ECVE$^{+/-n}$ has similar effects as CSE on the induction of imbalanced vasoactive gene expression and mediator release in human PASMCs and PAECs. The key findings of this Chapter are that ECVE$^{+/-n}$ did not have any effect on the production of PGE_2, PGI_2, TXA_2, nitric oxide and endothelin. A summary of the findings is shown in Table 5.1.

As far as we are aware, this is the first description of ECVE$^{+/-n}$ effect on vasoactive gene expression and mediator release in human pulmonary artery cells. Our results suggest that ECVE$^{+/-n}$ is unlikely to have similar effects as CSE on the induction of an imbalance between excessive vasoconstrictors and deficient vasodilators in human PASMCs and PAECs and may not contribute to pulmonary artery remodelling in pulmonary hypertension.

Table 5.1 A summary table of the findings of Chapter 5.

Gene/Mediator	Function	Effect of ECVE$^{+/-n}$	
COX-2/PGE_2	**Vasoactive gene**	**PASMCs**	**PAECs**
COX-2 mRNA		↔	↔
COX-2 protein		↔	↔
PGE_2 release		↔	↔
PGIS/PGI_2	**Vasodilator/ anti-proliferative gene**	**PASMCs**	**PAECs**
PGIS mRNA		↔	↔
PGIS protein		↓	**UA**
PGI_2 release		↔	↔
TXAS/TXA_2	**Vasoconstrictor/ proliferative gene**	**PASMCs**	**PAECs**
TXAS mRNA		↔	↔
TXAS protein		**UA**	**UA**
TXA_2 release		↔	↔
eNOS/Nitric oxide	**Vasodilator/ anti-proliferative gene**	**PASMCs**	**PAECs**
eNOS mRNA		**UA**	↔
eNOS protein		**UA**	↔
Nitric oxide release		**UA**	↔
Endothelin	**Vasoconstrictor/ proliferative gene**	**PASMCs**	**PAECs**
Endothelin-1 mRNA		↔	* ↑
Endothelin release		↔	↔

ECVE$^{+/-n}$, e-cig vapour extract with and without nicotine; PASMCs, Pulmonary artery smooth muscle cells; PAECs, Pulmonary artery endothelial cells; COX-2, Cyclooxygenase-2; PGE_2, Prostaglandin E_2; PGIS, Prostaglandin I synthase; PGI_2, Prostaglandin I_2; TXAS, Thromboxane A synthase; TXA_2, Thromboxane A_2; eNOS, Endothelial nitric oxide synthase; UA, Unassessed; ↔, Unchanged; ↑, Upregulated; ↓, Downregulated; *The effect of ECVE^{+n} only.

In this study, we developed a new method to extract e-cig vapour for *in vitro* work using fully licensed and FDA compliant e-cig delivery system (SmokTech) and e-cig liquid (Vapor Vapes). Commercially provided brands were used, as no standardised research e-cig delivery system and e-cig liquid are currently available. Although several cellular studies looked into the direct effect of e-cig liquid (fluid), we used the extract of vapourised e-cig liquid rather than e-cig liquid. This is because it is suggested that many harmful chemicals are produced by the heating process of the vapour (Scott et al., 2018). To avoid confounders, only unflavoured e-cig liquid was used in the present study.

It is widely recognised that e-cig may contain fewer toxicants than the conventional cigarette. In the current study, it was demonstrated that 1% $ECVE^{+/-n}$ reduced the cell viability in both human PASMCs and PAECs (Appendix, Figure 8.5 and Figure 8.6), suggesting that PASMCs and PAECs can respond to $ECVE^{+/-n}$. More importantly, this observed cytotoxicity of $ECVE^{+/-n}$ also suggests that even in the absence of nicotine, cell exposure to $ECVE^{+/-n}$ can still induce cytotoxicity. Our observation is supported by a recent study conducted by Kuntic and colleagues (2019) that reported that e-cig can induce cytotoxicity of EA.hy 926 (a permanent cell line derived by fusing human umbilical vein endothelial cells with cell line A549) (Kuntic et al., 2019). The findings of the same group also identified acrolein as a key mediator of e-cig-induced cytotoxicity of EA.hy 926. This suggests the observed cytotoxicity of PASMCs and PAECs, in the present study, may also come as a result of the toxic substance acrolein, which is produced by the heating process of the main constituent of e-cig liquid (glycerol).

Although there is evidence to suggest that the use of e-cig may have the potential to aid adult cigarette smokers to quit (Polosa et al., 2016), the fact that ECVE$^{+/-n}$ induced cytotoxicity of PASMCs and PAECs (the two main cell types that play a role in the development of pulmonary hypertension) raises the concerns over the safety of e-cig. This finding, together with our previous observation demonstrating that ECVE$^{+/-n}$ induced human airway smooth muscle cell cytotoxicity (unpublished observation), also suggests that the use of e-cig may cause pulmonary vascular and airway injuries and therefore has deleterious effects on the pulmonary system. However, further research is needed to explore the possible pathways responsible for these observations and clarify the implication of the cytotoxic effect of e-cig on e-cig users.

The effect of e-cig on pro-inflammatory mediators in some cell types within the airway has been extensively studied. Work by our group and other researchers suggested that e-cig use is harmful to the airway and can also cause airway inflammation. This supports the ongoing outbreak of lung injury associated with the use of e-cig. However, it is still unknown whether this effect is only limited to the first line of defence (airway cells) against inhaled particles of e-cig exposures. It is therefore important to assess effect of e-cig on vasoactive mediators produced by PASMCs and PAECs.

In Chapter 3, we provide evidence that CSE can induce PASMC and PAEC dysfunction. This cell dysfunction may eventually contribute to vascular remodelling and pulmonary hypertension in COPD. Although preliminary evidence suggests e-cig may also lead to impaired endothelial function (Carnevale et al., 2016, Kuntic et al., 2019), this is the first study to report ECVE$^{+/-n}$ effect on the expression of COX-2 and its downstream vasoactive prostanoid synthases and on the release of vasoactive prostanoid

in cultured human pulmonary artery cells, including PASMCs and PAECs. Our observation demonstrating $ECVE^{+/-n}$ reduced PGIS protein expression suggests that the e-cig vapour itself (but not the nicotine in e-cig liquid) is responsible for this detrimental effect. Although it is therefore expected that changes in the protein expression of PGIS would lead to PGI_2 reduction, it is of interest to note that PGI_2 production was not affected. There is evidence, which suggests that the dissociation of increased PGIS expression and unchanged and reduced PGI_2 production in response to curcumin-treated human coronary artery endothelial cells (Tan et al., 2011) and high glucose-treated human aortic endothelial cells, respectively (Cosentino et al., 2003) could be due to the fact that PGIS activity can be post-translationally modified. This could explain our results, but further studies will be required. Together, the overall observations indicate that $ECVE^{+/-n}$ does not alter the balance between the production of prostanoid (PGI_2, TXA_2, and PGE_2) in PASMCs and PAECs as CSE does.

Nitric oxide signalling plays a crucial role in the regulation of vascular tone and structure. We demonstrated that $ECVE^{+/-n}$ caused no effect on eNOS expression and its product nitric oxide. This observation does not support the available preliminary results from clinical studies suggesting an association of e-cig use with impairment in endothelial function biomarkers, including nitric oxide. A recent study conducted by Chatterjee and colleagues (2019) reported reduced serum levels of nitric oxide in healthy subjects following the use of non-nicotinised e-cig (Chatterjee et al., 2019). The disparity is most likely to be attributed to the fact that the reduced levels of nitric oxide do not necessarily mean that PAECs are the source of the impairment as some other cell types can also produce and mediate nitric oxide. In addition, the variability in e-cig products

may also explain the difference between the findings of this study and those reported by Chatterjee and colleagues (2019). During the course of this project, a study was conducted by Kuntic and colleagues (2019) who reported an increase in the expression of endothelin-1 in aortic tissue of mice after exposure to acute e-cig vapour (the authors did not assess endothelin release) (Kuntic et al., 2019). This observation is in agreement with our finding that $ECVE^{+n}$ (but not $ECVE^{-n}$) increased endothelin-1 expression in PASMCs and suggests that the nicotine in e-cig liquid (but not e-cig vapour itself) plays important role in endothelin-1 mRNA expression increase in PASMCs. It is interesting to note, this increase did not lead to changes in endothelin production in PASMCs. Perhaps also surprisingly, this effect of $ECVE^{+n}$ on endothelin-1 expression in PASMCs was not observed in PAECs. In addition to the difference in cell type, the fact that the length of cell incubation time with $ECVE^{+/-n}$ is different as previously mentioned in the methods (72 hours for PASMCs and 24 hours for PAECs) may also explain this disparity. Although there is much remains to be done to assess the potential role of e-cig on vascular endothelial cell dysfunction, the unaffected nitric oxide and endothelin production, in addition to the unaltered prostanoid production, in both PASMCs and PAECs, suggest that it is likely that $ECVE^{+/-n}$ does not cause a similar dysfunction of pulmonary artery cells as CSE does.

In summary, the present study provides evidence that $ECVE^{+/-n}$ does not alter the release of vasoactive mediators. This suggests that the e-cig vapour extract, regardless of the presence or absence of nicotine, is unlikely to have similar effects as CSE on the induction of imbalanced vasoactive gene expression and mediator release in human PASMCs and PAECs and may not contribute to pulmonary artery remodelling in

pulmonary hypertension. Based on these observations, no further investigations were conducted to assess the functional consequences. In the next Chapter, we explored the role of the altered release of individual vasoactive mediator in CSE- and hypoxia-induced proliferation and apoptosis of human PASMCs and PAECs.

Chapter 6. The role of the altered release of individual vasoactive mediator in CSE- and hypoxia-induced proliferation and apoptosis of human PASMCs and PAECs

6.1 Introduction

Pulmonary hypertension is a common and serious complication of COPD, characterised by pulmonary vasoconstriction and pulmonary vascular remodelling, including proliferation of pulmonary artery cells and is considered to come as a result of mainly hypoxia and CS effects. Although there are a limited amount of experimental data on the effect of hypoxia on human PASMC and PAEC apoptosis, previous studies showed that hypoxia can increase proliferation of human PASMCs (Wang et al., 2018, Yu and Hales, 2011) and human PAECs (Porter et al., 2014, Dabral et al., 2016). Furthermore, it has also been suggested that hypoxia is an important contributor to the vascular remodelling in COPD at a late stage of the disease and that the degree of pulmonary hypertension is directly related to the severity of hypoxemia (Sakao et al., 2014). In addition, CS is believed to play an important role in the vascular remodelling in COPD. This is supported by clinical evidence demonstrating that vascular remodelling is noted in patients with COPD and smokers with no sign of airway obstruction (Santos et al., 2002), suggesting that CS can initiate vascular remodelling, which may be further amplified by hypoxia at advanced COPD, leading to pulmonary hypertension. Although the effect of CSE (alone or in combination with hypoxia) on human PAEC apoptosis and proliferation and human PASMC apoptosis has not been explored, CSE has been shown to induce proliferation of human PASMCs (Xiang et al., 2010), which ultimately may contribute to pulmonary vascular remodelling. These observations suggest that CS and hypoxia may contribute to vascular remodelling as a result of excessive proliferation of PASMCs. However, the underlying cause is unclear.

We have shown earlier in Chapters 3 and 4, CSE and to lesser extent hypoxia can induce an imbalance between proliferative/vasoconstrictor mediators and anti-proliferative/vasodilator mediators, in human PAECs and PASMCs. However, the extent of the imbalance, the role of the altered release of individual vasoactive mediator in vascular remodelling and the contribution of PAEC and PASMC function (e.g. proliferation and apoptosis) in this process remain unknown.

6.2 Aims

This Chapter aims to determine the role of the altered release of individual vasoactive mediator in CSE- and hypoxia-induced proliferation and apoptosis of human PASMCs and PAECs.

The specific aims of this Chapter were:

- To investigate whether CSE and hypoxia either alone or in combination can stimulate proliferation and apoptosis of human PASMCs and PAECs.
- To assess whether celecoxib, a selective COX-2 inhibitor and beraprost sodium, stable PGI_2 analogue, PF-03549184, mPGES-1 inhibitor, and daltroban, receptor antagonist of vasoconstrictor TXA_2, are able to inhibit CSE- and hypoxia-induced proliferation and apoptosis of human PASMCs and PAECs.
- To determine whether sodium nitroprusside, nitric oxide donor, and bosentan, ET-A and ET-B receptor antagonist, can prevent CSE- and hypoxia-induced proliferation and apoptosis of human PASMCs and PAECs.

6.3 Materials and methods

6.3.1 CSE treatment under normoxic and hypoxic conditions

Human PASMCs and PAECs were seeded at a density of 10,000 cells per cm^2 in 24-well plate. Cell treatment condition was described in the materials and methods, section 2.2.2. Briefly, PASMCs were left untreated or treated with CSE (5%) under normoxic or hypoxic conditions for 48 h with daily fresh DMEM+ and CSE and then with the same concentration of CSE in DMEM- for 24 h, similar to the cell culture condition used to assess CSE and hypoxia effect on vasoactive gene expression and mediator release. PAECs were also treated with or without CSE (3%) under normoxic or hypoxic conditions for up to 24 h.

6.3.2 Effect of drugs

The drugs were dissolved in either cell culture medium or DMSO following the instructions of the manufacturer (final concentration of DMSO = 0.2%). Then, cells were pre-treated in DMEM+ or LS-ECGM with the drugs for 1 hour prior to cell stimulation with or without CSE under normoxic or hypoxic conditions. For the same period of time as the experimental cells, the group of control cells were treated with the drug vehicles.

6.3.3 Cell proliferation analysis

WST-1 assay was used as a primary method to assess cell proliferation in this study, and CCK-8 assay was used as a secondary method following the instructions of the manufacturers (materials and methods, section 2.11). Data were presented as % change over control (100%).

6.3.4 Apoptosis analysis

Western blotting was conducted to measure the levels of apoptosis markers, including pro/cleaved caspase 3 and cleaved PARP1 and ELISA was then carried out to assess the levels of annexin v, a marker of apoptosis (materials and methods, section 2.12).

6.4 Results

6.4.1 Effect of CSE on proliferation of human PASMCs and PAECs

We found that CSE significantly stimulated proliferation of PASMCs at all time points tested (% change 251.2±13.9, 381.9±14, and 355.7±16.5, respectively, $p<0.0001$ for all) compared with control at the corresponding time point (Figure 6.1A). As cell proliferation was observed at the shortest time point (24 h), cell proliferation reagent CCK-8 was used to further confirm this observation. Consistent with WST-1 data, our CCK-8 results showed that CSE caused a significant increase in PASMC proliferation (% change 131.9±3.7, $p<0.0001$) compared with control (Figure 6.1B).

Although CSE caused no significant increase in proliferation of PAECs at 3 h, we showed that PAEC stimulation with CSE significantly increased cell proliferation at 16 and 24 h (% change 427.8±59.8 and 799.1±133.1, respectively, $p<0.05$ for both) compared with control at the corresponding time point (Figure 6.2A). This increase of cell proliferation following CSE treatment was further confirmed at 24 h (% change 255.5±10.5, $p<0.0001$) compared with control as assessed by cell proliferation reagent CCK-8 (Figure 6.2B).

Our findings showing that CSE causes proliferation of PASMCs and PAECs suggests that CSE effect may eventually lead to pulmonary vascular remodelling.

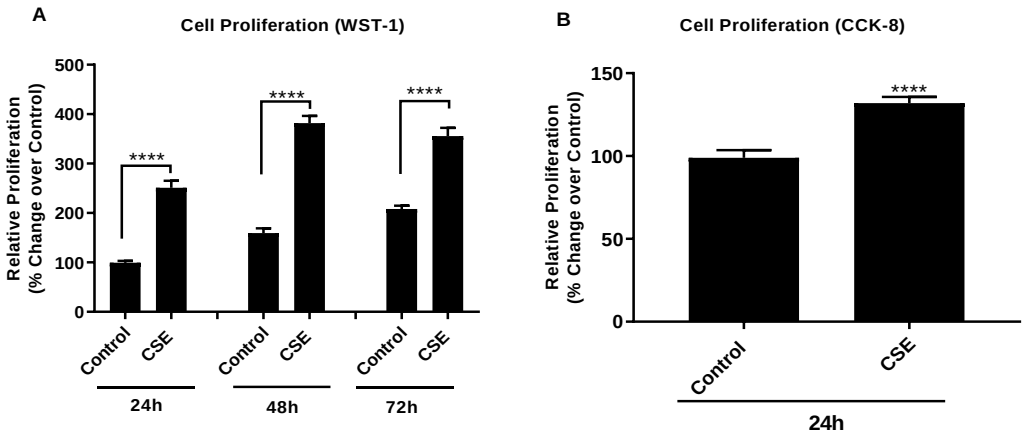


Figure 6.1 Effect of CSE on proliferation of human PASMCs.
Confluent human PASMCs were treated with or without CSE (5%) for 48 h with daily fresh DMEM+ and CSE and then with the same concentrations of CSE in DMEM- for 24 h. Cell proliferation was assessed at various time points (24, 48, and 72 h) using WST-1 (A) and at 24 h using CCK-8 (B). Data were expressed as relative proliferation (% change over control). Each data point represents mean ± SEM from one experiment performed in eight different wells. ****p<0.0001 compared with control at the corresponding time point.

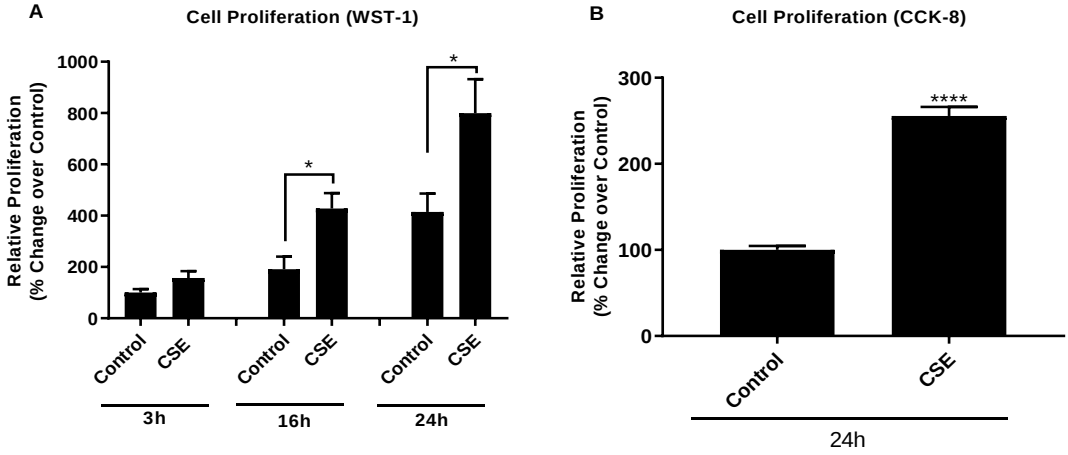


Figure 6.2 Effect of CSE on proliferation of human PAECs.
Confluent human PAECs were treated with or without CSE (3%) for 24 h. Cell proliferation was assessed at various time points (3, 16, and 24 h) using WST-1 and at 24 h using CCK-8 (B). Data were expressed as relative proliferation (% change over control). Each data point represents mean ± SEM from one experiment performed in six different wells. *p<0.05, ****p<0.0001 compared with control at the corresponding time point.

6.4.2 Effect of hypoxia on proliferation of human PASMCs and PAECs

Here, it was of interest to find out whether hypoxia (1% O_2) can stimulate human PASMC growth. Our results showed that hypoxia significantly induced proliferation of PASMCs at all time points tested (24, 48, and 72 h) (% change 186.8±8.9, $p<0.0001$, 250.5±16.2, $p<0.001$, and 261.8±14.2, $p<0.01$, respectively) compared with control at the corresponding time point as assessed by cell proliferation reagent WST-1 (Figure 6.3A). CCK-8 assay was then conducted at 24 h to confirm this finding. As shown in Figure 6.3B, hypoxia caused a significant increase in PASMC proliferation (% change 126.9±6.0, $p<0.01$) compared with control.

Next, we determined the hypoxia effect on PAEC proliferation. PAECs were exposed to hypoxia and cell proliferation was assessed at different time points using WST-1 assay (3, 16, and 24 h). Although no obvious effect in cell proliferation was observed in response to hypoxia exposure at 3 h, PAEC exposure to hypoxia significantly increased cell proliferation at 16 and 24 h (% change 470.6±84.6 and 680.1±66.3, respectively, $p<0.05$ for both) compared with control at the corresponding time point (Figure 6.4A). To further confirm this, PAECs were exposed to hypoxia and CCK-8 assay was used to assess cell proliferation at 24 h. Consistent with the result obtained from WST-1 assay, hypoxia caused a significant increase in PAEC proliferation (% change 206.6±9.8, $p<0.0001$) compared with control (Figure 6.4B).

These observations suggest hypoxia may contribute to pulmonary vascular remodelling as a result of the induction of PASMC and PAEC proliferation.

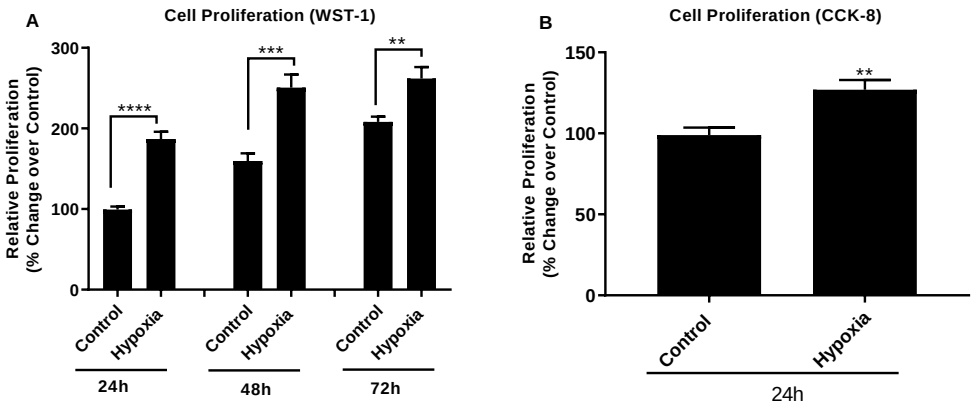


Figure 6.3 Effect of hypoxia on proliferation of human PASMCs.
Confluent human PASMCs were exposed to normoxic (21% O_2) or hypoxic (1% O_2) conditions for 48 h with daily fresh DMEM+. The cells were then cultured for 24 h with DMEM- under the same culture conditions. Cell proliferation was assessed at various time points (24, 48, and 72 h) using WST-1 and at 24 h using CCK-8 (B). Data were expressed as relative proliferation (% change over control). Each data point represents mean ± SEM from one experiment performed in eight different wells. **p<0.01, ***p<0.001, ****p<0.0001 compared with control at the corresponding time point.

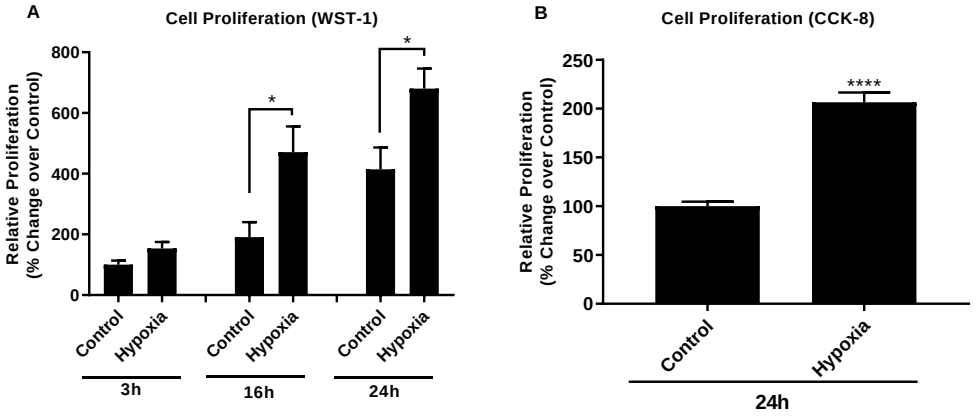


Figure 6.4 Effect of hypoxia on proliferation of human PAECs.
Confluent human PAECs were exposed to normoxic (21% O_2) or hypoxic (1% O_2) conditions for 24 h. Cell proliferation was assessed at various time points (3, 16, and 24 h) using WST-1 and at 24 h using CCK-8 (B). Data were expressed as relative proliferation (% change over control). Each data point represents mean ± SEM from one experiment performed in six different wells. *p<0.05, ****p<0.0001 compared with control at the corresponding time point.

6.4.3 Effect of hypoxia and CSE in combination on proliferation of human PASMCs and PAECs

As we have previously mentioned, the effect of hypoxia and CSE as single factors significantly stimulated proliferation of both PASMCs and PAECs. Here, we wanted to evaluate whether hypoxia can further enhance CSE-induced cell proliferation. The results showed that hypoxia+CSE significantly induced PASMC proliferation at all time points tested (24, 48, and 72 h) compared with control at the corresponding time point (319.6±13.72, 357.9±18.3 and 350.8±23.4, $p<0.0001$) (Figure 6.5A). Compared with hypoxia alone, hypoxia+CSE caused a significant increase in cell growth at 24 h ($p<0.0001$), at 48 h ($p<0.001$), and at 72 h ($p<0.01$). Although a significant induction in cell proliferation was observed at 24 h in response to hypoxia+CSE compared with CSE alone ($p<0.01$), no significant difference was noted between hypoxia+CSE compared with CSE alone at 48 and 72 h (Figure 6.5A). Next, CCK-8 assay was conducted to evaluate the effect of hypoxia+CSE on proliferation of PASMCs at 24 h. Similar to WST-1 assay data, we observed that hypoxia+CSE significantly induced cell proliferation compared with control (135.2±6.8, $p<0.001$) (Figure 6.5B). However, compared with hypoxia or CSE alone, hypoxia+CSE had no additive effect on cell proliferation (Figure 6.5B).

We then moved on to assess the effect of hypoxia+CSE on proliferation of PAECs. Following exposure of PAECs to hypoxia and CSE in combination for up to 24 h, WST-1 assay was then conducted to measure cell proliferation at three different time points. As shown in Figure 6.6A, we found that hypoxia+CSE significantly stimulated proliferation of PAECs in time-dependent manner compared with control at the

corresponding time point (229.8±37.5, 841.3±139.6, and 1032.5±146.5, $p<0.01$ for all). Although increased proliferation of PAECs was noted in response to hypoxia+CSE at 16 h compared with hypoxia and CSE alone ($p<0.05$), no significant difference was observed in cell proliferation after exposure to hypoxia+CSE at both 3 and 24 h compared with hypoxia and CSE alone (Figure 6.6A). CCK-8 assay measurement was consistent with the result obtained from the WST-1 assay, which confirmed that hypoxia+CSE caused an increase in proliferation of PAECs at 24 h compared with control (306.1±20.6, $p<0.0001$) and compared with hypoxia alone ($p<0.01$). The effect of hypoxia+CSE did not further induce proliferation of PAECs compared with CSE alone (Figure 6.6B).

Overall, our findings demonstrated that hypoxia can further enhance CSE effect on cell proliferation at early time point in PASMCs (24 h) and in PAECs (16 h), and it is mainly the effect of CSE at later time points (particularly in PASMCs). This suggests that CSE is a more potent inducer of PASMC and PAEC proliferation than hypoxia. In addition, these data also suggest that WST-1 assay is more sensitive than CCK-8 assay in our experimental setting. Therefore, WST-1 assay was used to assess cell proliferation for further experiments.

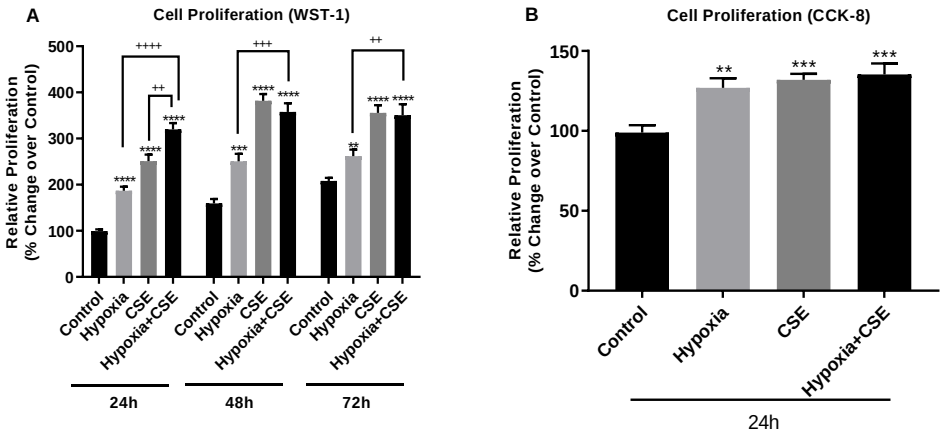


Figure 6.5 Effect of CSE, hypoxia and hypoxia+CSE on proliferation of human PASMCs.
Confluent human PASMCs were treated with or without CSE (5%) under normoxic (21% O_2) or hypoxic (1% O_2) conditions for 48 h with daily fresh DMEM+ and CSE and then with the same concentrations of CSE in DMEM- for 24 h. Cell proliferation was assessed at various time points (24, 48, and 72 h) using WST-1 and at 24 h using CCK-8 (B). Data were expressed as relative proliferation (% change over control). Each data point represents mean ± SEM from one experiment performed in eight different wells. **p<0.01, ***p<0.001, ****p<0.0001 compared with control at the corresponding time point. $^{++}$p<0.01, $^{+++}$p<0.001, $^{++++}$p<0.0001 compared with hypoxia or CSE at the corresponding time point.

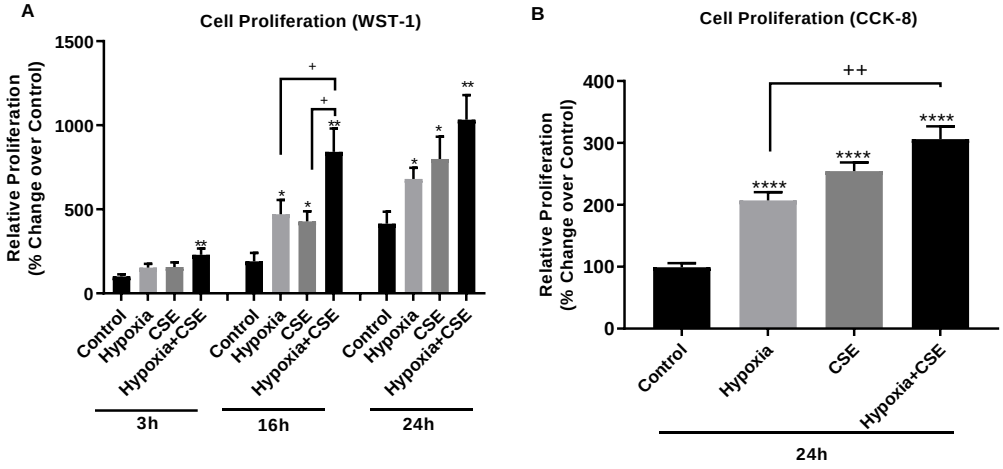


Figure 6.6 Effect of CSE, hypoxia and hypoxia+CSE on proliferation of human PAECs.
Confluent human PAECs were treated with or without CSE (3%) under normoxic (21% O_2) or hypoxic (1% O_2) conditions for 24 h. Cell proliferation was assessed at various time points (3, 16, and 24 h) using WST-1. Data were expressed as relative proliferation (% change over control). Each data point represents mean ± SEM from one experiment performed in six different wells. *p<0.05, **p<0.01, ****p<0.0001 compared with control at the corresponding time point. $^{+}$p<0.05, $^{++}$p<0.01 compared with hypoxia or CSE at the corresponding time point.

6.4.4 Effect of celecoxib on CSE-induced proliferation of human PASMCs and PAECs

We demonstrated in Chapter 3 that CSE can induce COX-2 expression in both PASMCs and PAECs. As shown in Figure 6.1 and Figure 6.2, CSE can also stimulate proliferation of PASMCs and PAECs. However, it is unknown whether CSE-induced COX-2 expression plays a role in the induction of PASMC and PAEC proliferation. Thus, we assessed the effect of celecoxib, a selective COX-2 inhibitor, on CSE-induced cell proliferation.

Human PASMCs were treated with increasing concentrations of celecoxib (0-100 nM) 1 hour prior to treatment with or without CSE (5%) for 24 h. WST-1 assay was then conducted to evaluate cell proliferation. The results showed that CSE induced cell proliferation (% change 236.4±22.2, $p<0.0001$) compared with control, and this induction of PASMC proliferation was inhibited by celecoxib in a concentration-dependent manner (Figure 6.7). Although treatment with 0.01 nM of celecoxib had no effect on CSE-induced cell proliferation, a slight but significant decrease of cell proliferation was observed at 0.1 nM of celecoxib (% change 168.4±11.9, $p<0.05$) compared with CSE alone. Celecoxib at 1 nM and 10 nM caused further reduction of cell proliferation (% change 118.5±10.0, $p<0.001$ and 136.5±23.7, $p<0.001$, respectively). A complete inhibition of cell proliferation was achieved at the highest concentration tested, 100 nM (% change 98.6±9.1, $p<0.0001$) compared with CSE alone (Figure 6.7).

Similar to results from PASMCs, we showed that PAEC proliferation was increased by CSE (% change 225.9±5.8, $p<0.0001$) compared with control. The use of celecoxib inhibited proliferation of PAECs in a concentration-dependent manner (Figure

6.8). Treatment with 0.1 nM of celecoxib did not have any effect on CSE-induced proliferation of PAECs compared with CSE alone. However, a gradual inhibition of cell proliferation was noted following cell treatment with celecoxib at 1 nM, 10 nM, and 100 nM (% change 164.2±16.2, $p<0.01$, 140.0±17.1, $p<0.001$ and 125.7±17.6, $p<0.001$, respectively) compared with CSE alone (Figure 6.8).

Our findings suggest that celecoxib can inhibit CSE-induced PASMC and PAEC proliferation, likely due to the inhibition of CSE-induced COX-2-derived TXA_2 production in both PASMCs and PAECs.

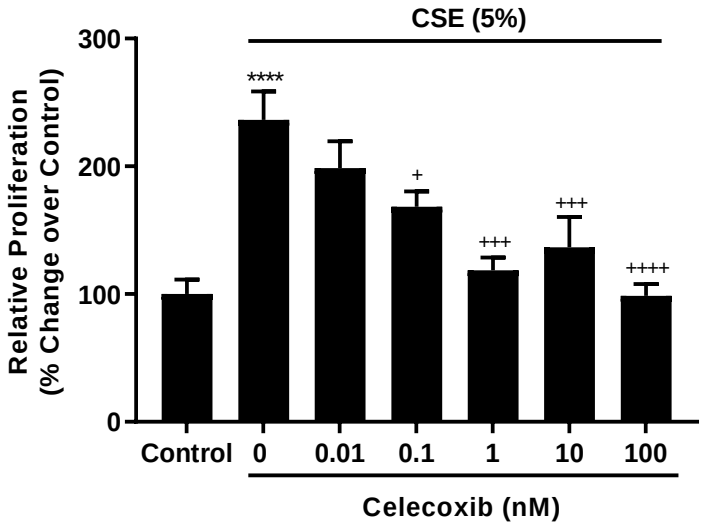


Figure 6.7 Effect of celecoxib on CSE-induced proliferation of human PASMCs.
Confluent human PASMCs were incubated with increasing concentrations of celecoxib (0-100 nM) 1 hour prior to treatment with or without CSE (5%) for 24 h. WST-1 was then conducted. Data were expressed as relative proliferation (% change over control). Each data point represents mean ± SEM from one experiment performed in eight different wells. ****$p<0.0001$ compared with control. $^{+}p<0.05$, $^{+++}p<0.001$, $^{++++}p<0.0001$ compared with CSE alone.

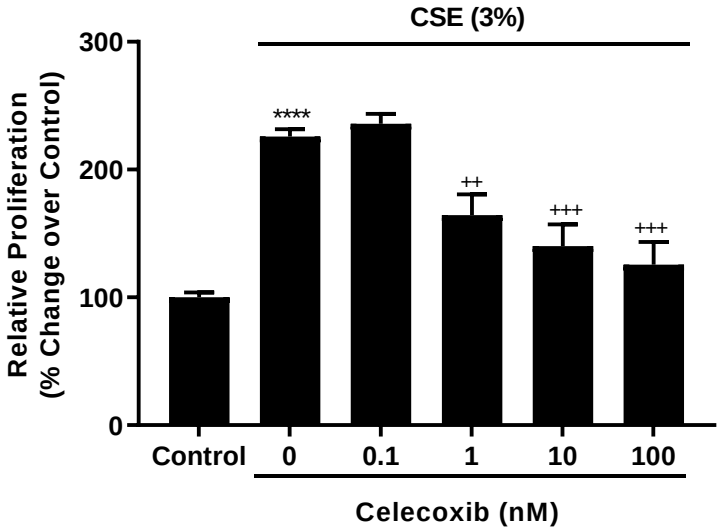


Figure 6.8 Effect of celecoxib on CSE-induced proliferation of human PAECs.
Confluent human PAECs were incubated with increasing concentrations of celecoxib (0-100 nM) 1 hour prior to treatment with or without CSE (3%) for 24 h. WST-1 was then conducted. Data were expressed as relative proliferation (% change over control). Each data point represents mean ± SEM from one experiment performed in six different wells. ****$p<0.0001$ compared with control. $^{++}p<0.01$, $^{+++}p<0.001$ compared with CSE alone.

6.4.5 Effect of celecoxib on hypoxia-induced proliferation of human PASMCs and PAECs

To evaluate the effect of celecoxib on hypoxia-induced PASMC and PAEC proliferation, cells were incubated with different concentrations of celecoxib (0-100 nM) 1 hour prior to cell incubation under normoxic or hypoxic conditions for 24 h. The WST-1 assay results showed that hypoxia stimulated PASMC proliferation (% change 148.8±4.5, $p<0.0001$) compared with control (Figure 6.9). Interestingly, treatment with 0.1 nM and 1 nM of celecoxib caused no significant effect on hypoxia-induced proliferation of PASMCs. Celecoxib at the highest two concentrations tested (10 nM and 100 nM) resulted in a significant inhibition of hypoxia-induced PASMC proliferation (% change 93.8±2.8, $p<0.0001$ and 88.0±6.7, $p<0.0001$, respectively) compared with hypoxia alone (Figure 6.9). Next, we showed that PAEC proliferation was induced by hypoxia (% change 300.6±14.2, $p<0.0001$) compared with control. Surprisingly, the use of celecoxib at all concentrations tested caused no significant effect on hypoxia-induced PAEC proliferation (Figure 6.10).

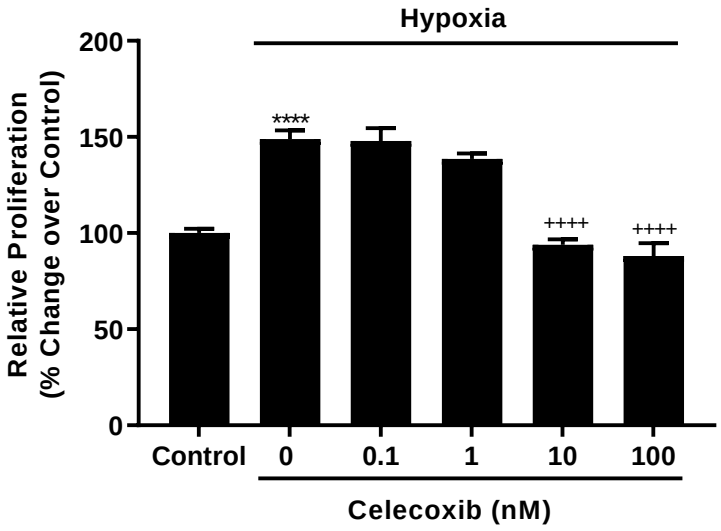


Figure 6.9 Effect of celecoxib on hypoxia-induced proliferation of human PASMCs.
Confluent human PASMCs were pre-treated with increasing concentrations of celecoxib (0-100 nM) 1 hour prior to cell incubation under normoxic (21% O_2) or hypoxic (1% O_2) conditions for 24 h. WST-1 was then conducted. Data were expressed as relative proliferation (% change over control). Each data point represents mean ± SEM from one experiment performed in six different wells. ****$p<0.0001$ compared with control. $^{++++}p<0.0001$ compared with hypoxia alone.

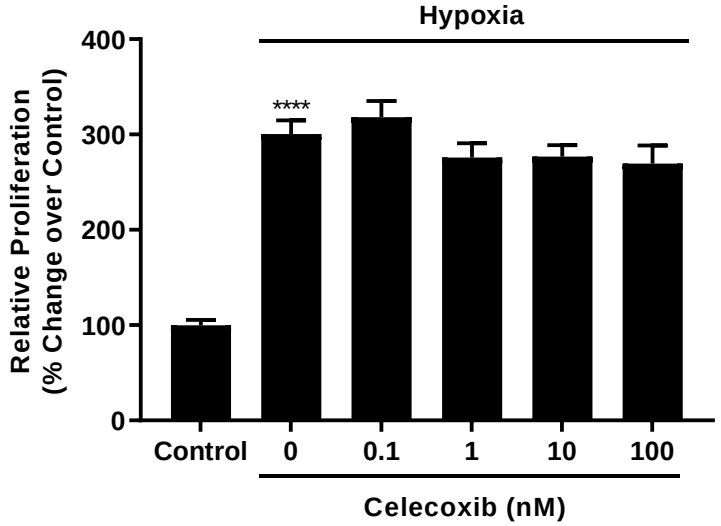


Figure 6.10 Effect of celecoxib on hypoxia-induced proliferation of human PAECs.
Confluent human PAECs were incubated with increasing concentrations of celecoxib (0-100 nM) 1 hour prior to cell incubation under normoxic (21% O_2) or hypoxic (1% O_2) conditions for 24 h. WST-1 was then conducted. Data were expressed as relative proliferation (% change over control). Each data point represents mean ± SEM from one experiment performed in eight different wells. ****$p<0.0001$ compared with control.

6.4.6 Effect of celecoxib on hypoxia in combination with CSE-induced proliferation of human PASMCs and PAECs

As shown in Figure 6.11, hypoxia+CSE stimulated proliferation of PASMCs (271.9±7.7, $p<0.0001$) compared with control. Similar to celecoxib effect on CSE- and hypoxia-induced PASMC proliferation, the induction of PASMC proliferation was inhibited in a concentration-dependent manner. Although treatment with celecoxib at the lowest two concentrations tested (0.1 nM and 1 nM) did not have any effect on hypoxia+CSE-induced proliferation of PASMCs, celecoxib at 10 nM and 100 nM caused a significant inhibition of hypoxia+CSE-induced PASMC proliferation (% change 193.5±9.5, $p<0.0001$ and 173.1±7.4, $p<0.0001$, respectively) compared with hypoxia+CSE alone (Figure 6.11). Consistent with celecoxib effect on hypoxia-induced PAEC proliferation, celecoxib at all concentrations tested showed no significant effect on hypoxia+CSE-induced PAEC proliferation (Figure 6.12).

Collectively, the ability of celecoxib to inhibit hypoxia- and hypoxia+CSE-induced proliferation of PASMCs (but not PAECs) indicates that COX-2 expression upregulation in response to hypoxia in PASMCs (but not in PAECs) may contribute to cell proliferation, likely by regulating mediator with proliferative properties (TXA_2).

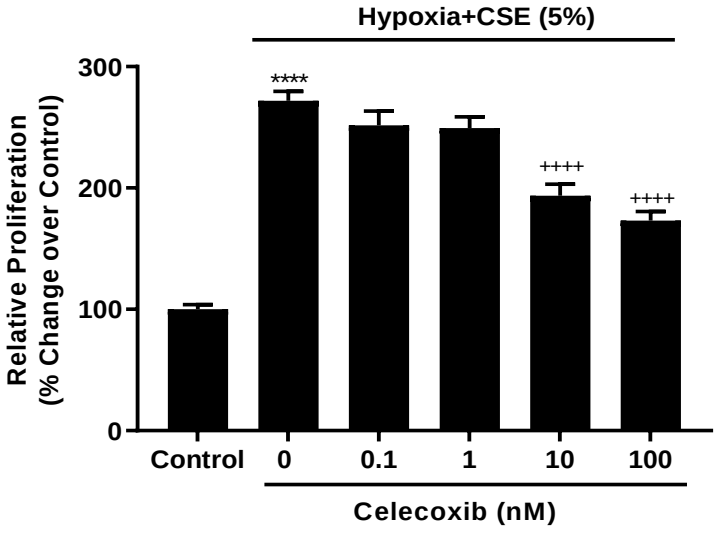


Figure 6.11 Effect of celecoxib on hypoxia+CSE-induced proliferation of human PASMCs.
Confluent human PASMCs were pre-treated with increasing concentrations of celecoxib (0-100 nM) 1 hour prior to treatment with or without CSE (5%) under normoxic (21% O_2) or hypoxic (1% O_2) conditions for 24 h. WST-1 was then conducted. Data were expressed as relative proliferation (% change over control). Each data point represents mean ± SEM from one experiment performed in six different wells. ****p<0.0001 compared with control. $^{++++}$p<0.0001 compared with hypoxia+CSE alone.

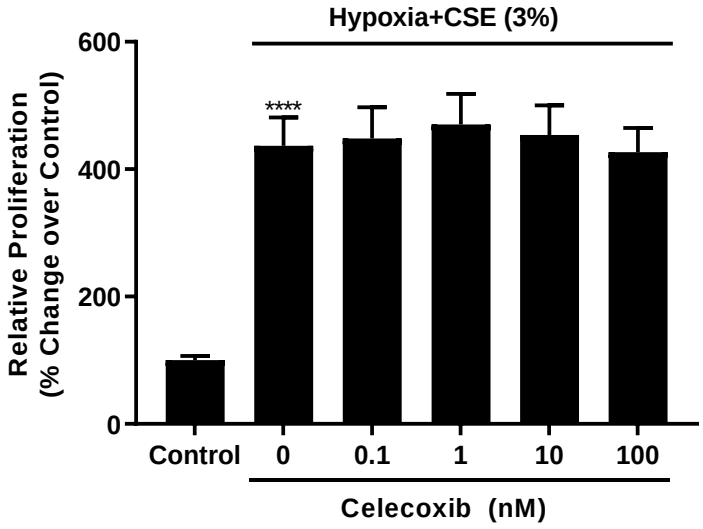


Figure 6.12 Effect of celecoxib on hypoxia+CSE-induced proliferation of human PAECs.
Confluent human PAECs were pre-treated with increasing concentrations of celecoxib (0-100 nM) 1 hour prior to treatment with or without CSE (3%) under normoxic (21% O_2) or hypoxic (1% O_2) conditions for 24 h. WST-1 was then conducted. Data were expressed as relative proliferation (% change over control). Each data point represents mean ± SEM from one experiment carried out in eight different wells. ****p<0.0001 compared with control.

6.4.7 Effect of beraprost sodium on CSE-induced proliferation of human PASMCs and PAECs

Because CSE reduced the production of PGI_2 as a result of the downregulated PGIS expression, we investigated whether stable PGI_2 analogue beraprost sodium can prevent CSE-induced PASMC proliferation. Our results showed that treatment with CSE increased PASMC proliferation (% change 268.2±20.8, $p<0.0001$) compared with control, and this increased PASMC proliferation was inhibited by beraprost sodium in a concentration-dependent manner (Figure 6.13). Beraprost sodium was found to significantly reduce CSE-induced PASMC proliferation at a concentration as low as 1 pM (% change 156.3±8.9, $p<0.001$) compared with CSE alone. A complete inhibition of cell proliferation was reached following the use of beraprost sodium at 10 pM (% change 100.5±3.0, $p<0.0001$) compared with CSE alone (Figure 6.13).

We next explored the effect of beraprost sodium on CSE-induced proliferation of PAECs. Consistent with our findings from PASMCs, although beraprost sodium at 0.01 pM did not have any effect on CSE-induced PAEC proliferation, a significant and concentration-dependent reduction of CSE-induced PAEC proliferation was observed following the use of beraprost sodium at 0.1, 1, and 10 pM (% change 162.2±14.3, $p<0.05$, 159.9±8.8, $p<0.01$ and 141.3±13.2, $p<0.01$, respectively) compared with CSE alone (Figure 6.14).

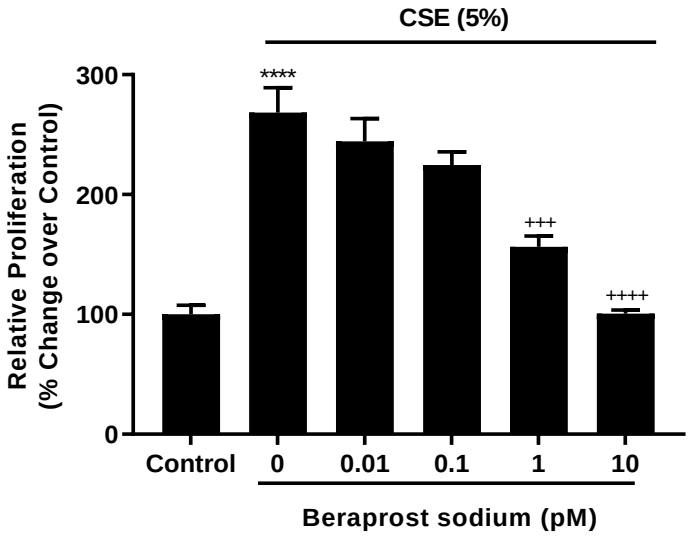


Figure 6.13 Effect of beraprost sodium on CSE-induced proliferation of human PASMCs.
Confluent human PASMCs were incubated with increasing concentrations of beraprost sodium (0-10 pM) 1 hour prior to treatment with or without CSE (5%) for 24 h. WST-1 was then conducted. Data were expressed as relative proliferation (% change over control). Each data point represents mean ± SEM from one experiment performed in six different wells. ****$p<0.0001$ compared with control. $^{+++}p<0.001$, $^{++++}p<0.0001$ compared with CSE alone.

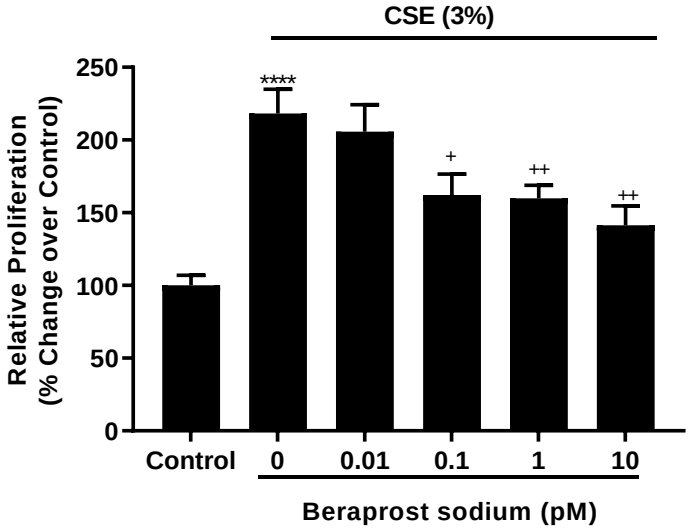


Figure 6.14 Effect of beraprost sodium on CSE-induced proliferation of human PAECs.
Confluent human PAECs were incubated with increasing concentrations of beraprost sodium (0-10 pM) 1 hour prior to treatment with or without CSE (3%) for 24 h. WST-1 was then conducted. Data were expressed as relative proliferation (% change over control). Each data point represents mean ± SEM from one experiment performed in eight different wells. ****$p<0.0001$ compared with control. $^{+}p<0.05$, $^{++}p<0.01$, $^{+++}p<0.001$ compared with CSE alone.

6.4.8 Effect of beraprost sodium on hypoxia-induced proliferation of human PASMCs and PAECs

We then investigated if the use of beraprost sodium is able to inhibit hypoxia-induced PASMC and PAEC proliferation. The data shown in Figure 6.15 revealed that hypoxia stimulated PASMC proliferation (% change 126.1±2.2, $p<0.0001$) compared with control. This effect of hypoxia on PASMC proliferation was inhibited by the use of beraprost sodium in a concentration-dependent manner. A slight but significant reduction of hypoxia-induced PASMC proliferation was noted in response to the lowest concentration of beraprost sodium (0.01pM) (% change 118.8±2.0, $p<0.05$) compared with hypoxia alone. This reduction of cell proliferation was further enhanced by beraprost sodium at 0.1pM and 1pM (% change 111.6±1.9, $p<0.001$ and 109.8±1.4, $p<0.001$, respectively). A complete inhibtion of hypoxia-induced PASMC proliferation was observed at 10 pM (% change 104.0±2.3, $p<0.0001$) (Figure 6.15). Unlike the effect of beraprost sodium on hypoxia-induced PASMC proliferation, the use of beraprost sodium (0-10 pM) showed no significant effect on hypoxia-induced PAEC proliferation compared with hypoxia alone (Figure 6.16).

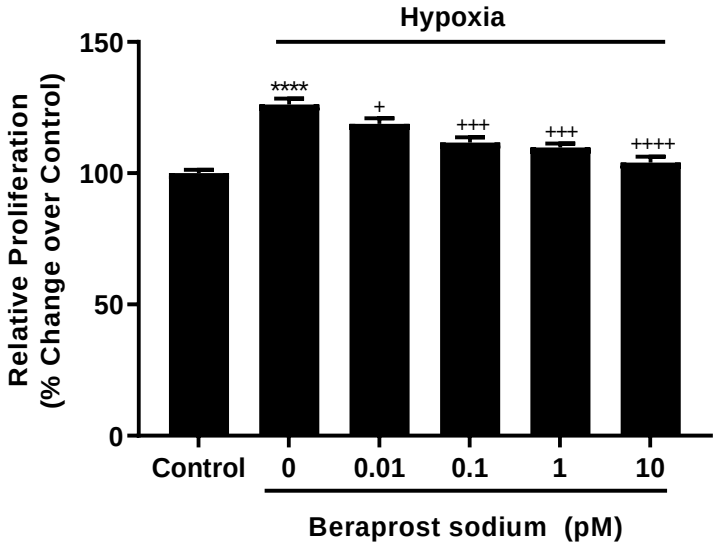


Figure 6.15 Effect of beraprost sodium on hypoxia-induced proliferation of human PASMCs.
Confluent human PASMCs were incubated with increasing concentrations of beraprost sodium (0-10 pM) 1 hour prior to cell incubation under normoxic (21% O_2) or hypoxic (1% O_2) conditions for 24 h. WST-1 was then conducted. Data were expressed as relative proliferation (% change over control). Each data point represents mean ± SEM from one experiment performed in six different wells. ****$p<0.0001$ compared with control. $^{+}p<0.05$, $^{+++}p<0.001$, $^{++++}p<0.0001$ compared with hypoxia alone.

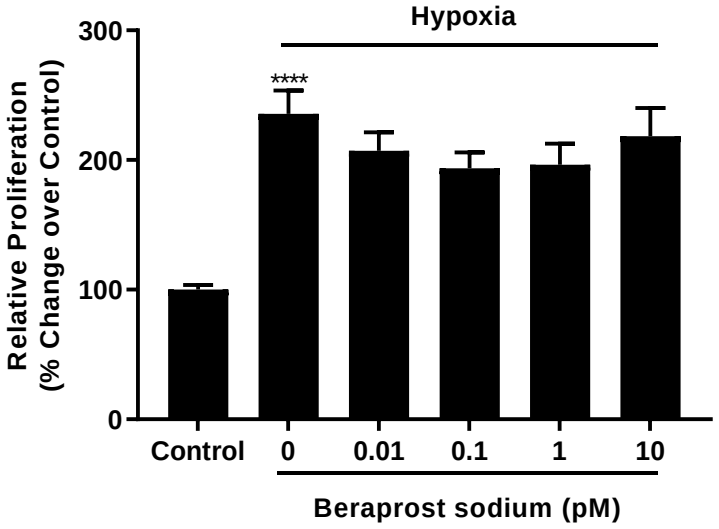


Figure 6.16 Effect of beraprost sodium on hypoxia-induced proliferation of human PAECs.
Confluent PAECs were pre-treated with increasing concentrations of beraprost sodium (0-10 pM) 1 hour prior to cell incubation under normoxic (21% O_2) or hypoxic (1% O_2) conditions for 24 h. WST-1 was then conducted. Data were expressed as relative proliferation (% change over control). Each data point represents mean ± SEM from one experiment performed in eight different wells. ****$p<0.0001$ compared with control.

6.4.9 Effect of beraprost sodium on hypoxia in combination with CSE-induced proliferation of human PASMCs and PAECs

As shown in Figure 6.17, hypoxia+CSE stimulated PASMC proliferation (% change 174.4±4.5, $p<0.0001$) compared with control. Although beraprost sodium at 0.01pM did not have any effect on proliferating PASMCs, higher concentration of beraprost sodium (0.1pM) slightly but significantly reduced hypoxia+CSE-induced cell proliferation (% change 157.6±3.6, $p<0.05$) compared with hypoxia+CSE alone (Figure 6.17). Beraprost sodium at the highest two concentrations tested 1pM and 10pM exerted further anti-proliferative effect (% change 145.1±4.4, $p<0.001$, 138.8±6.5, $p<0.01$, respectively) compared with hypoxia+CSE alone (Figure 6.17)

Next, we found that hypoxia+CSE induced PAEC proliferation (% change 234.4±11.9, $p<0.0001$) compared with control (Figure 6.18). Consistent with the effect of beraprost sodium on hypoxia-induced PAEC proliferation, the use beraprost sodium caused no significant effect on hypoxia+CSE-induced PAEC proliferation compared with hypoxia+CSE alone (Figure 6.18).

Although stable PGI_2 analogues are generally known as potent inhibitors of cell proliferation, our findings suggest that the anti-proliferative effect of beraprost sodium may, in part, result from the ability of stable PGI_2 analogue to restore the balance between PGI_2 and TXA_2.

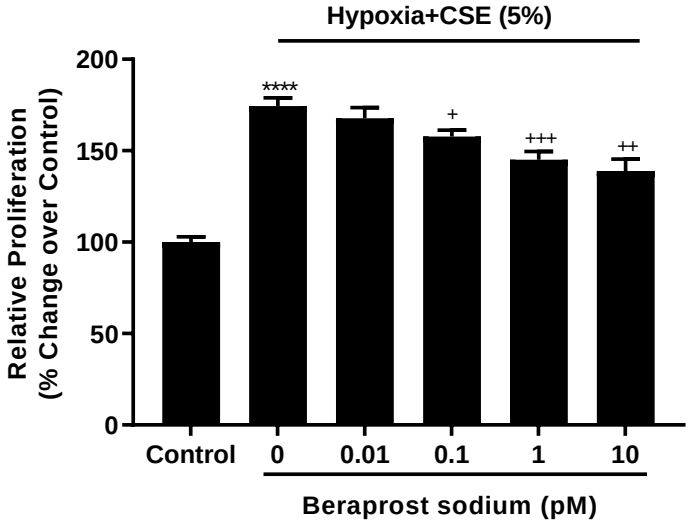


Figure 6.17 Effect of beraprost sodium on hypoxia+CSE-induced proliferation of human PASMCs. Confluent human PASMCs were incubated with increasing concentrations of beraprost sodium (0-10 pM) 1 hour prior to treatment with or without CSE (5%) under normoxic (21% O_2) or hypoxic (1% O_2) conditions for 24 h. WST-1 was then conducted. Data were expressed as relative proliferation (% change over control). Each data point represents mean ± SEM from one experiment performed in six different wells. ****$p<0.0001$ compared with control. $^{+}p<0.05$, $^{++}p<0.01$, $^{+++}p<0.001$ compared with hypoxia+CSE alone.

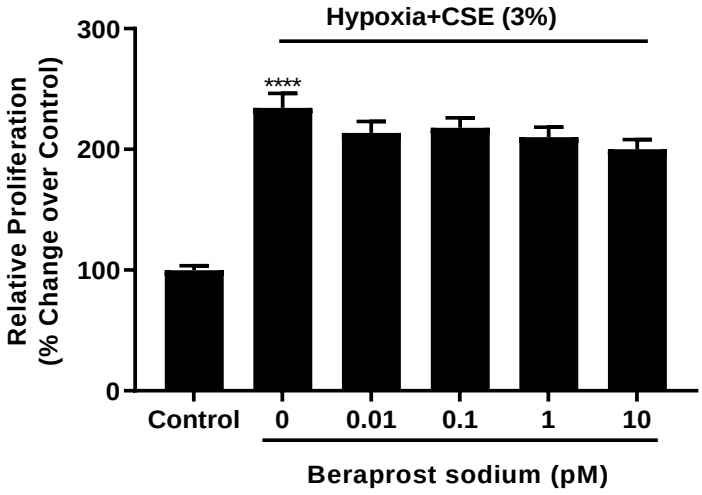


Figure 6.18 Effect of beraprost sodium on hypoxia+CSE-induced proliferation of human PAECs. Confluent human PAECs were incubated with increasing concentrations of beraprost sodium (0-10 pM) 1 hour prior to treatment with or without CSE (3%) under normoxic (21% O_2) or hypoxic (1% O_2) conditions for 24 h. WST-1 was then conducted. Data were expressed as relative proliferation (% change over control). Each data point represents mean ± SEM from one experiment performed in eight different wells. ****$p<0.0001$ compared with control.

6.4.10 Effect of daltroban on CSE-induced proliferation of human PASMCs and PAECs

Given the findings in Chapter 3 that CSE can potentiate TXA_2 production in PASMCs and PAECs, we here were interested to find out if blocking increased TXA_2 effects by the use of daltroban, TXA_2 receptor antagonist, can inhibit CSE-induced proliferation of PASMCs and PAECs. Our results showed that CSE caused an increase in PASMC proliferation (% change 257.5±17.6, $p<0.0001$) compared with control, and the use of daltroban inhibited CSE-mediated PASMC proliferation in a concentration-dependent manner compared with CSE alone (Figure 6.19). A significant reduction of proliferating PASMCs was noted following the use of daltroban at 0.1 nM (% change 186.1±11.9, $p<0.01$) compared with CSE alone. Further reduction of cell proliferation was also observed in response to daltroban at 1 nM (% change 138.4±17.6, $p<0.001$) compared with CSE alone. Daltroban at 10 nM and 100 nM completely inhibited CSE-induced PASMC proliferation (% change 90.6±19.7, $p<0.0001$, 113.1±17.0, $p<0.0001$, respectively) compared with CSE alone (Figure 6.19).

Similar to results from PASMCs, we showed that CSE induced PAEC proliferation compared with control (% change 248.3±15.4, $p<0.0001$) (Figure 6.20). This increase in proliferation of PAECs was inhibited by daltroban in a concentration-dependent manner compared with CSE alone (Figure 6.20). Although treatment with 0.01 nM and 0.1 nM of daltroban did not have any effect on CSE-induced proliferation of PAECs compared with CSE alone, significant inhibition of cell proliferation was noted in response to daltroban at 1 nM and 10 nM (% change 156.6±18.7, $p<0.01$, 131.6±9.2, $p<0.001$, respectively) compared with CSE alone (Figure 6.20).

Our findings demonstrated that TXA_2 receptor antagonist can inhibit CSE-induced proliferation of PASMCs and PAECs. This suggests that daltroban may exert anti-proliferative effect by blocking the effect of CSE-induced TXA_2 production in both PASMCs and PAECs.

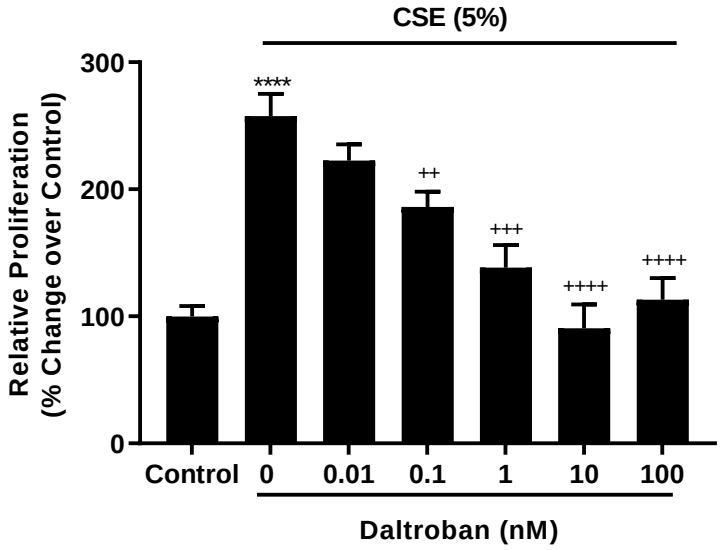


Figure 6.19 Effect of daltroban on CSE-induced proliferation of human PASMCs.
Confluent human PASMCs were incubated with increasing concentrations of daltroban (0-100 nM) 1 hour prior to treatment with or without CSE (5%) for 24 h. WST-1 was then conducted. Data were expressed as relative proliferation (% change over control). Each data point represents mean ± SEM from one experiment carried out in eight different wells. ****$p<0.0001$ compared with control. $^{++}p<0.01$, $^{+++}p<0.001$, $^{++++}p<0.0001$ compared with CSE alone.

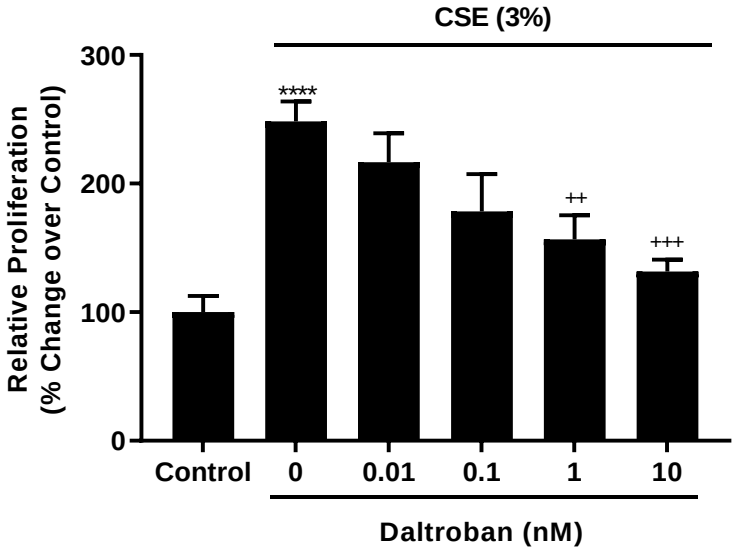


Figure 6.20 Effect of daltroban on CSE-induced proliferation of human PAECs.
Confluent human PAECs were incubated with increasing concentrations of daltroban (0-10 nM) 1 hour prior to treatment with or without CSE (3%) for 24 h. WST-1 was then conducted. Data were expressed as relative proliferation (% change over control). Each data point represents mean ± SEM from one experiment performed in eight different wells. ****$p<0.0001$ compared with control. $^{++}p<0.01$, $^{+++}p<0.001$ compared with CSE alone.

6.4.11 Effect of daltroban on hypoxia-induced proliferation of human PASMCs and PAECs

Having demonstrated that hypoxia induced TXA_2 production in both cell types, we sought to determine whether daltroban can also induce anti-proliferative effect on PASMCs and PAECs. As shown in Figure 6.21, hypoxia caused an increase in PASMC proliferation (% change 150.6±4.9, $p<0.0001$) compared with control. Cell stimulation with daltroban decreased PASMC proliferation and this decrease was a statistically significant at all concentrations tested compared with hypoxia alone. A slight reduction of PASMC growth was seen at 0.01 nM and 0.1 nM of daltroban (% change 133.0±4.2, $p<0.05$, 131.7±3.4, $p<0.05$, respectively) compared with hypoxia alone. This was followed by a greater reduction in PASMC proliferation by 1 nM of daltroban (% change 107.4±4.8, $p<0.001$). A complete inhibition of this abnormal cell proliferation was achieved by daltroban at 10 nM (% change 95.8±2.7, $p<0.0001$, respectively) compared with hypoxia alone (Figure 6.21). Interestingly, daltroban at all concentrations tested had no effect on hypoxia-induced proliferation of PAECs compared with hypoxia alone (Figure 6.22).

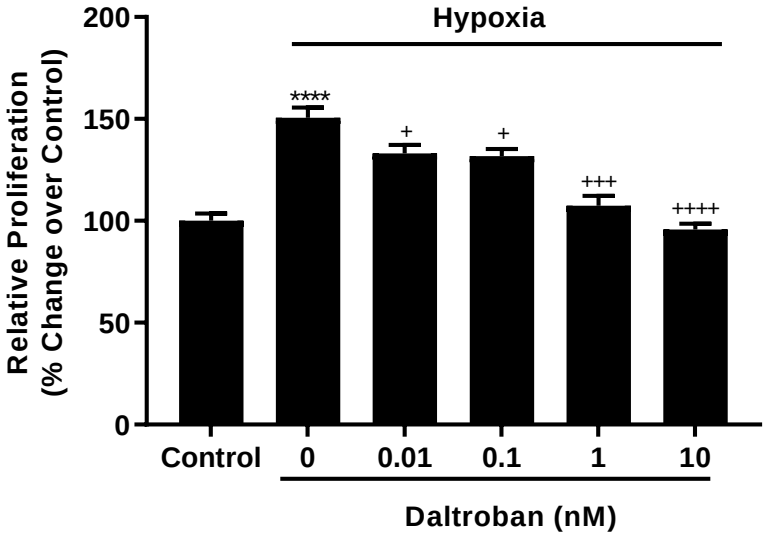


Figure 6.21 Effect of daltroban on hypoxia-induced proliferation of human PASMCs.
Confluent human PASMCs were incubated with increasing concentrations of daltroban (0-10 nM) 1 hour prior to cell incubation under normoxic (21% O_2) or hypoxic (1% O_2) conditions for 24 h. WST-1 was then conducted. Data were expressed as relative proliferation (% change over control). Each data point represents mean ± SEM from one experiment performed in six different wells. ****$p<0.0001$ compared with control. $^{+}p<0.05$, $^{+++}p<0.001$, $^{++++}p<0.0001$ compared with hypoxia alone.

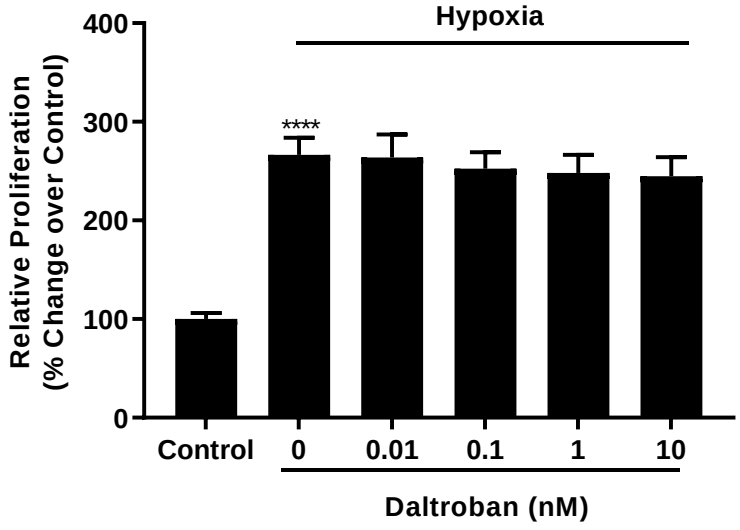


Figure 6.22 Effect of daltroban on hypoxia-induced proliferation of human PAECs.
Confluent PAECs were pre-treated with increasing concentrations of daltroban (0-10 nM) 1 hour prior to cell incubation under normoxic (21% O_2) or hypoxic (1% O_2) conditions for 24 h. WST-1 was then conducted. Data were expressed as relative proliferation (% change over control). Each data point represents mean ± SEM from one experiment performed in seven different wells. ****$p<0.0001$ compared with control.

6.4.12 Effect of daltroban on hypoxia in combination with CSE-induced proliferation of human PASMCs and PAECs

Exposure of PASMCs to hypoxia+CSE resulted in an induction of cell proliferation (% change 183.4±9.6, $p<0.0001$) compared with control (Figure 6.23). Although daltroban at the lowest concentration used (0.01 nM) did not affect cell proliferation, a gradual reduction of PASMC proliferation was observed at 0.1 nM and 1 nM of daltroban (% change 153.6±7.3, $p<0.05$, 130.7±9.0, $p<0.01$, respectively) compared with hypoxia+CSE alone. Nearly complete inhibition of PASMC proliferation was seen following the use of daltroban at 10 nM (% change 110.4±6.4, $p<0.0001$) compared with hypoxia+CSE alone (Figure 6.23). We also found that hypoxia+CSE induced PAEC proliferation (% change 369.2±23.0, $p<0.0001$) compared with control (Figure 6.24). Consistent with the effect of daltroban on hypoxia-stimulated PAEC proliferation, daltroban at all concentrations tested did not elicit a significant reduction of proliferating PAECs (Figure 6.24).

The observation that daltroban can inhibit hypoxia- and hypoxia+CSE-induced proliferation of PASMCs (but not PAECs) suggests that hypoxia- and hypoxia+CSE-induced TXA_2 production may contribute to proliferation of PASMCs (but not PAECs).

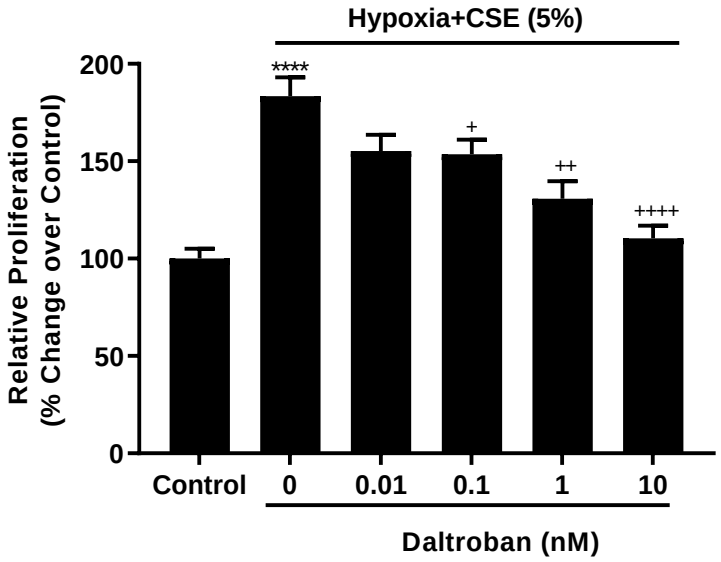


Figure 6.23 Effect of daltroban on hypoxia+CSE-induced proliferation of human PASMCs.
Confluent human PASMCs were incubated with increasing concentrations of daltroban (0-10 nM) 1 hour prior to treatment with or without CSE (5%) under normoxic (21% O_2) or hypoxic (1% O_2) conditions for 24 h. WST-1 was then conducted. Data were expressed as relative proliferation (% change over control). Each data point represents mean ± SEM from one experiment performed in six different wells. ****$p<0.0001$ compared with control. $^{+}p<0.05$, $^{++}p<0.01$, $^{++++}p<0.0001$ compared with hypoxia+CSE alone.

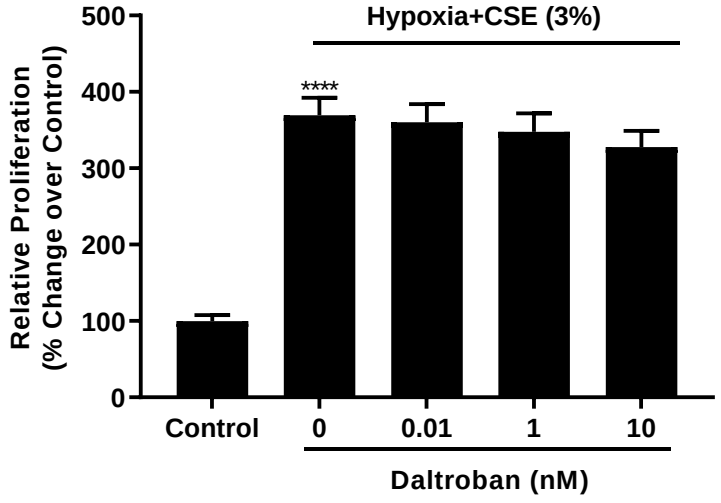


Figure 6.24 Effect of daltroban on hypoxia+CSE-induced proliferation of human PAECs.
Confluent human PAECs were incubated with increasing concentrations of daltroban (0-10 nM) 1 hour prior to treatment with or without CSE (3%) under normoxic (21% O_2) or hypoxic (1% O_2) conditions for 24 h. WST-1 was then conducted. Data were expressed as relative proliferation (% change over control). Each data point represents mean ± SEM from one experiment performed in eight different wells. ****$p<0.0001$ compared with control.

6.4.13 Effect of PF-03549184 on CSE-induced proliferation of human PASMCs and PAECs

PF-03549184, also known as PF-9184, is a potent inhibitor of mPGES-1. We have previously reported that CSE downregulates the protein expression of mPGES-1 and reduces PGE_2 release in PASMCs, but induces PGE_2 release as a result of upregulated mPGES-1 protein expression in PAECs. Thus, we wanted to assess whether PGE_2 production has a role in CSE-induced proliferation of human PASMCs and PAECs. Our results showed that treatment with CSE caused an increase in PASMC proliferation (% change 163.5±10.4, $p<0.0001$) compared with control (Figure 6.25). We did not see any significant differences in cell growth between CSE-treated cells plus PF-03549184 (0-100 nM) and CSE-treated cells alone. Perhaps also surprisingly, the use of PF-03549184 did not affect CSE-induced PAEC proliferation (Figure 6.26).

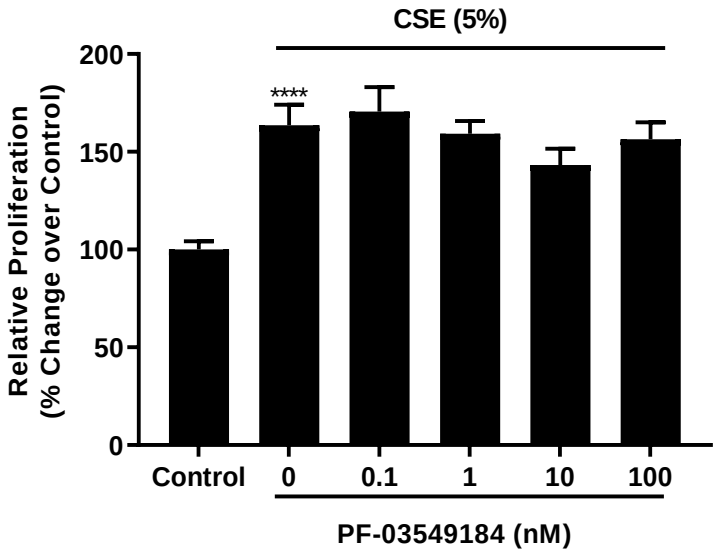


Figure 6.25 Effect of PF-03549184 on CSE-induced proliferation of human PASMCs.
Confluent human PASMCs were incubated with increasing concentrations of PF-03549184 (0-100 nM) 1 hour prior to treatment with or without CSE (5%) for 24 h. WST-1 was then conducted. Data were expressed as relative proliferation (% change over control). Each data point represents mean ± SEM from one experiment performed in eight different wells. ****p<0.0001 compared with control.

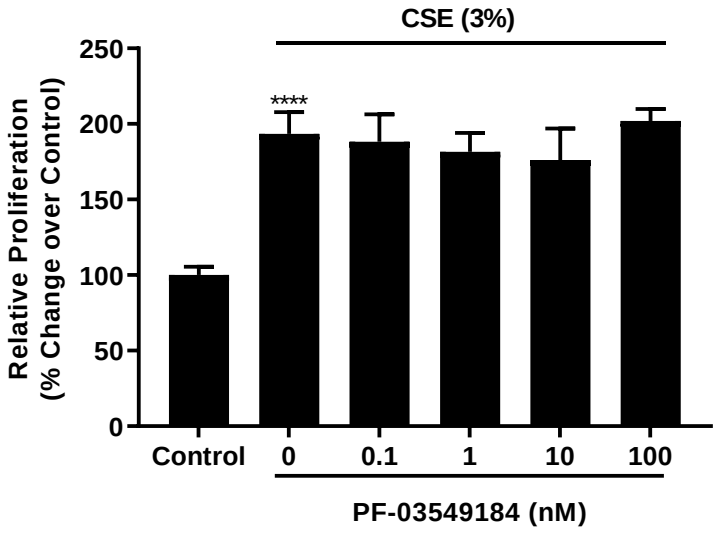


Figure 6.26 Effect of PF-03549184 on CSE-induced proliferation of human PAECs.
Confluent human PAECs were incubated with increasing concentrations of PF-03549184 (0-100 nM) 1 hour prior to treatment with or without CSE (3%) for 24 h. WST-1 was then conducted. Data were expressed as relative proliferation (% change over control). Each data point represents mean ± SEM from one experiment performed in eight different wells. ****p<0.0001 compared with control.

6.4.14 Effect of PF-03549184 on hypoxia-induced proliferation of human PASMCs and PAECs

Next, we went on to assess the effect of PF-03549184 on hypoxia-induced proliferation of human PASMCs and PAECs. Human PASMCs and PAECs were incubated with increasing concentrations (0-100 nM) 1 hour prior to cell incubation under normoxic or hypoxic conditions for 24 h. As shown in Figure 6.27 and Figure 6.28, hypoxia significantly induced proliferation of human PASMCs and PAECs (% change 144.6±2.6, 243.6±12.1, respectively, $p<0.0001$) compared with control. Surprisingly, PF-03549184, a potent inhibitor of mPGES-1, had no significant effect on proliferation of human PASMCs and PAECs compared with hypoxia alone (Figure 6.27 and Figure 6.28).

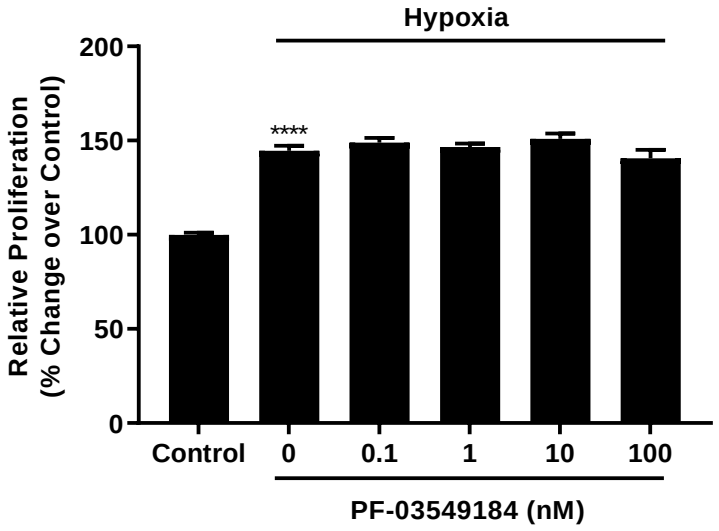


Figure 6.27 Effect of PF-03549184 on hypoxia-induced proliferation of human PASMCs.
Confluent human PASMCs were incubated with increasing concentrations of PF-03549184 (0-100 nM) 1 hour prior to cell incubation under normoxic (21% O_2) or hypoxic (1% O_2) conditions for 24 h. WST-1 was then conducted. Data were expressed as relative proliferation (% change over control). Each data point represents mean ± SEM from one experiment performed in eight different wells. ****p<0.0001 compared with control.

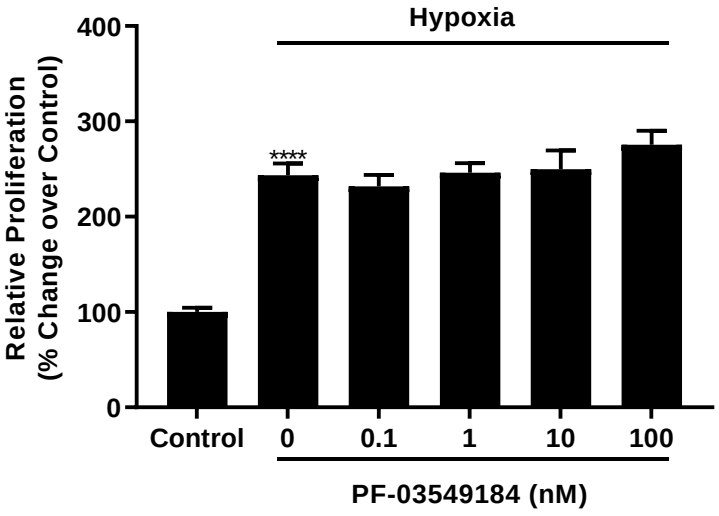


Figure 6.28 Effect of PF-03549184 on hypoxia-induced proliferation of human PAECs.
Confluent PAECs were pre-treated with increasing concentrations of PF-03549184 (0-100 nM) 1 hour prior to cell incubation under normoxic (21% O_2) or hypoxic (1% O_2) conditions for 24 h. WST-1 was then conducted. Data were expressed as relative proliferation (% change over control). Each data point represents mean ± SEM from one experiment performed in eight different wells. ****p<0.0001 compared with control.

6.4.15 Effect of PF-03549184 on hypoxia in combination with CSE-induced proliferation of human PASMCs and PAECs

To determine the effect of PF-03549184 on hypoxia in combination with CSE-induced proliferation of human PASMCs and PAECs, we incubated PASMCs and PAECs with PF-03549184 at 0, 0.1, 1, 10 and 100 nM 1 hour prior to treatment with or without CSE under normoxic or hypoxic conditions for 24 h. WST-1 assay was conducted and the results showed that PASMC and PAEC incubation with CSE under hypoxic condition resulted in an increase in proliferation of PASMCs and PAECs (% change 145.9±1.5, 343.6±11.4, respectively, $p<0.0001$) compared with control. Similar to mPGES-1 inhibitor effect on CSE- and hypoxia-induced proliferation, the use of PF-03549184 did not change hypoxia+CSE-induced proliferation of PASMCs and PAECs (Figure 6.29 and Figure 6.30).

Our data suggest that mPGES-1 inhibitor PF-03549184 does not have any effect on CSE-, hypoxia- and hypoxia+CSE-induced PASMC and PAEC proliferation.

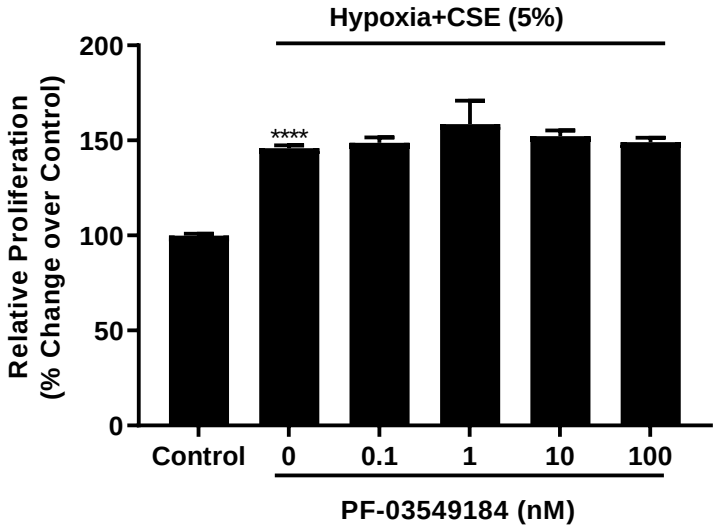


Figure 6.29 Effect of PF-03549184 on hypoxia+CSE-induced proliferation of human PASMCs.
Confluent human PASMCs were incubated with increasing concentrations of PF-03549184 (0-100 nM) 1 hour prior to treatment with or without CSE (5%) under normoxic (21% O_2) or hypoxic (1% O_2) conditions for 24 h. WST-1 was then conducted. Data were expressed as relative proliferation (% change over control). Each data point represents mean ± SEM from one experiment performed in eight different wells. ****p<0.0001 compared with control.

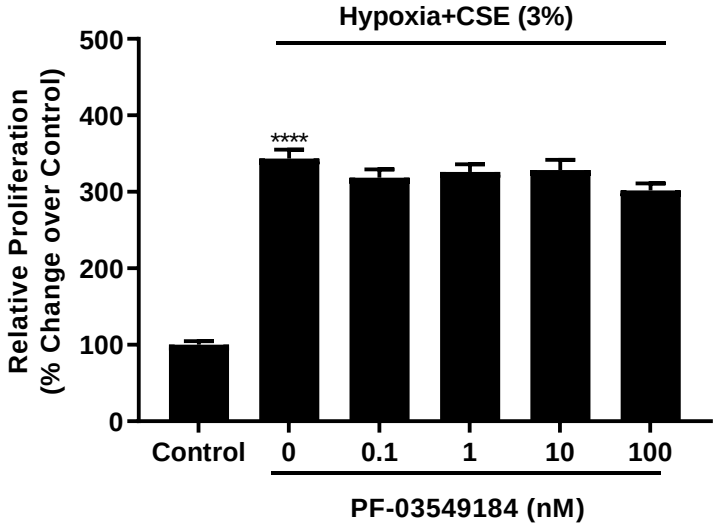


Figure 6.30 Effect of PF-03549184 on hypoxia+CSE-induced proliferation of human PAECs.
Confluent human PAECs were incubated with increasing concentrations of PF-03549184 (0-100 nM) 1 hour prior to treatment with or without CSE (3%) under normoxic (21% O_2) or hypoxic (1% O_2) conditions for 24 h. WST-1 was then conducted. Data were expressed as relative proliferation (% change over control). Each data point represents mean ± SEM from one experiment performed in eight different wells. ****p<0.0001 compared with control.

6.4.16 Effect of sodium nitroprusside on CSE-induced proliferation of human PASMCs and PAECs

Sodium nitroprusside, a nitric oxide donor, is known to have potent vasodilatory properties and is clinically used to lower blood pressure. Whether sodium nitroprusside has effect on CSE- and hypoxia-induced proliferation of human PASMCs and PAECs is unknown. Thus, we tested the effect of sodium nitroprusside on CSE-induced proliferation of human PASMCs and PAECs. Our results showed that CSE promoted PASMC proliferation (% change 130.9±1.9, $p<0.0001$) compared with control (Figure 6.31). Sodium nitroprusside reduced the proliferation of PASMCs in a concentration-dependent manner. Although sodium nitroprusside at the lowest concentration used (0.1 μM) did not have any effect on PASMC proliferation, a slight but significant reduction of CSE-induced PASMC proliferation was noted in response to sodium nitroprusside at 1 μM and 10 μM (% change 121.0±2.1, $p<0.01$ and 119.0±2.3, $p<0.01$, respectively) compared with CSE alone (Figure 6.31). Sodium nitroprusside at highest concentration tested (100 μM) completely inhibited CSE-induced PASMC proliferation (% change 104.6±3.5, $p<0.0001$) compared with CSE (Figure 6.31). We also found that CSE treatment induced PAEC proliferation (% change 196.2±18.0, $p<0.001$) compared with control (Figure 6.32). Compared with CSE alone, the use of sodium nitroprusside at 0.1 μM and 1 μM did not have any effect on PAEC proliferation, whereas sodium nitroprusside at 10 μM and 100 μM decreased CSE-induced PAEC proliferation (% change 124.5±9.4, $p<0.01$ and 123.6±10.2, $p<0.01$, respectively) (Figure 6.32).

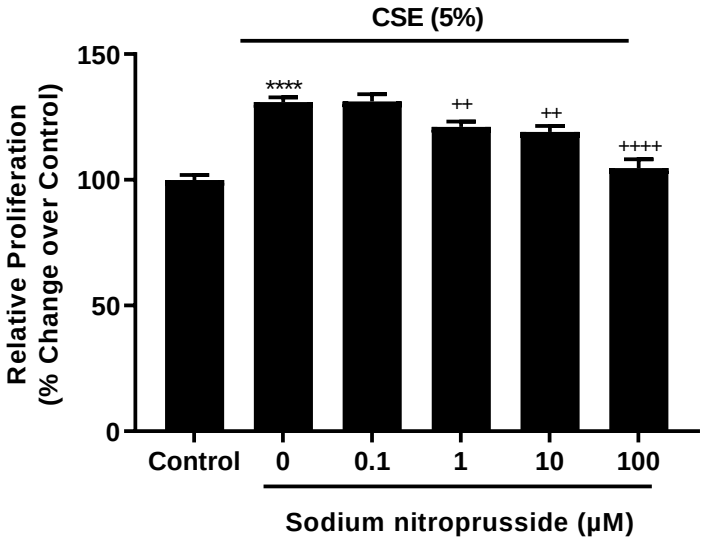


Figure 6.31 Effect of sodium nitroprusside on CSE-induced proliferation of human PASMCs.
Confluent human PASMCs were incubated with increasing concentrations of Sodium nitroprusside (0-100 μM) 1 hour prior to treatment with or without CSE (5%) for 24 h. WST-1 was then conducted. Data were expressed as relative proliferation (% change over control). Each data point represents mean ± SEM from one experiment performed in six different wells. ****$p<0.0001$ compared with control. $^{++}p<0.01$, $^{++++}p<0.0001$ compared with CSE alone.

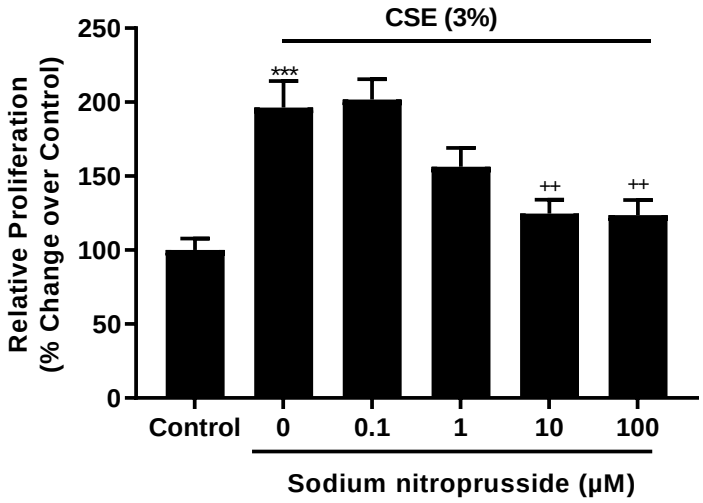


Figure 6.32 Effect of sodium nitroprusside on CSE-induced proliferation of human PAECs.
Confluent human PAECs were incubated with increasing concentrations of Sodium nitroprusside (0-100 μM) 1 hour prior to treatment with or without CSE (3%) for 24 h. WST-1 was then conducted. Data were expressed as relative proliferation (% change over control). Each data point represents mean ± SEM from one experiment performed in eight different wells. ***$p<0.001$ compared with control. $^{++}p<0.01$ compared with CSE alone.

6.4.17 Effect of sodium nitroprusside on hypoxia-induced proliferation of human PASMCs and PAECs

Next, we explored the effect of sodium nitroprusside on hypoxia-induced proliferation of human PASMCs and PAECs and found that hypoxia had the ability to increase proliferation of PASMCs (% change 125.8±5.4, $p<0.01$) compared with control (Figure 6.33). This increased proliferation of PASMCs was unchanged following the use of sodium nitroprusside at 0.1 μM and 1 μM, but was significantly reduced in response to 10 μM and 100 μM of sodium nitroprusside (% change 103.2±3.4, $p<0.01$ and 86.4±5.9, $p<0.001$, respectively) compared with hypoxia alone (Figure 6.33). We then went on to assess the effect of sodium nitroprusside on CSE-induced proliferation of PAECs. The results showed that PAECs proliferated in response to hypoxia. Sodium nitroprusside decreased this excessive proliferation of PAECs in a concentration-dependent manner compared with hypoxia alone with a signficant effect at the highest two concentration tested (10 μM and 100 μM) (% change 176.7±8.9, $p<0.01$ and 152.8±8.2, $p<0.0001$, respectively) compared with hypoxia alone (Figure 6.34).

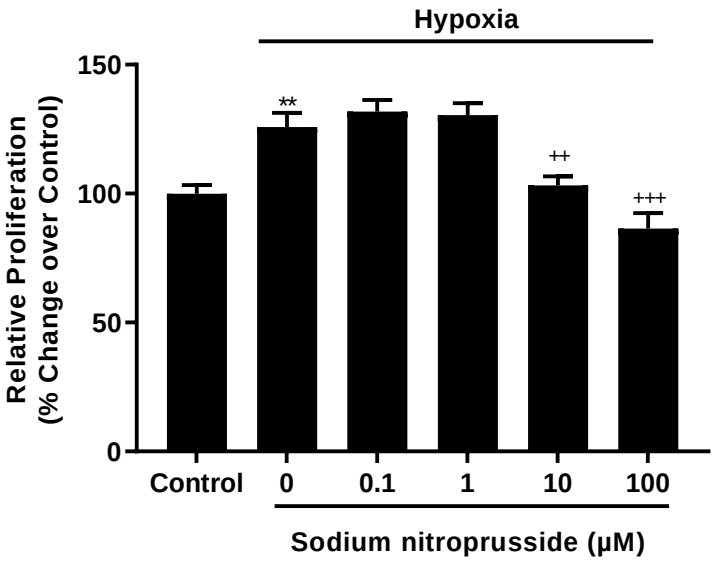


Figure 6.33 Effect of sodium nitroprusside on hypoxia-induced proliferation of human PASMCs. Confluent human PASMCs were incubated with increasing concentrations of sodium nitroprusside (0-100 μM) 1 hour prior to cell incubation under normoxic (21% O_2) or hypoxic (1% O_2) conditions for 24 h. WST-1 was then conducted. Data were expressed as relative proliferation (% change over control). Each data point represents mean ± SEM from one experiment performed in six different wells. **p<0.01 compared with control. $^{++}$p<0.01, $^{+++}$p<0.001 compared with hypoxia alone.

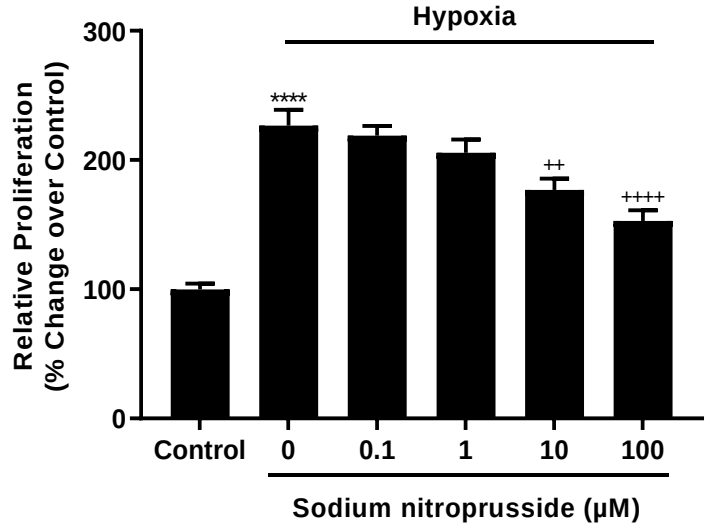


Figure 6.34 Effect of sodium nitroprusside on hypoxia-induced proliferation of human PAECs. Confluent PAECs were pre-treated with increasing concentrations of sodium nitroprusside (0-100 μM) 1 hour prior to cell incubation under normoxic (21% O_2) or hypoxic (1% O_2) conditions for 24 h. WST-1 was then conducted. Data were expressed as relative proliferation (% change over control). Each data point represents mean ± SEM from one experiment performed in eight different wells. ****p<0.0001 compared with control. $^{++}$p<0.01, $^{++++}$p<0.0001 compared with hypoxia alone.

6.4.18 Effect of sodium nitroprusside on hypoxia in combination with CSE-induced proliferation of human PASMCs and PAECs

Thus far, we have demonstrated the sodium nitroprusside can inhibit CSE- and hypoxia- induced proliferation of human PASMCs and PAECs. Here, we wanted to determine the effect of sodium nitroprusside on hypoxia+CSE-induced proliferation of human PASMCs and PAECs. Figure 6.35 revealed that the effect of hypoxia+CSE stimulated proliferation of PASMCs (% change 163.2±4.6, $p<0.0001$) compared with control. Inhibition of PASMC growth was observed after the use of sodium nitroprusside at 1, 10 and 100 μM (% change 137.6±7.5, $p<0.05$, 129.7±4.1, $p<0.0001$ and 98.8±2.8, $p<0.0001$, respectively) compared with hypoxia+CSE alone (Figure 6.35). Similar to these findings, PAECs proliferated in response to hypoxia+CSE exposure (% change 223.5±8.3, $p<0.0001$) compared with control, and this increase in PAEC proliferation was inhibited by sodium nitroprusside at 1, 10 and 100 μM (% change 178.7±7.1, $p<0.01$, 167.5±7.1, $p<0.001$ and 139.9±9.7, $p<0.0001$, respectively) compared with hypoxia+CSE alone (Figure 6.36).

Our results also suggest sodium nitroprusside is able to inhibit CSE-, hypoxia-, and hypoxia+CSE-induced PASMC proliferation, even though it is unlikely that PASMCs can produce nitric oxide. In addition, the results also suggest the nitric oxide donor may, in part, exert its anti-proliferative effect on PAECs by compensating for CSE- and hypoxia-induced reduction of nitric oxide production.

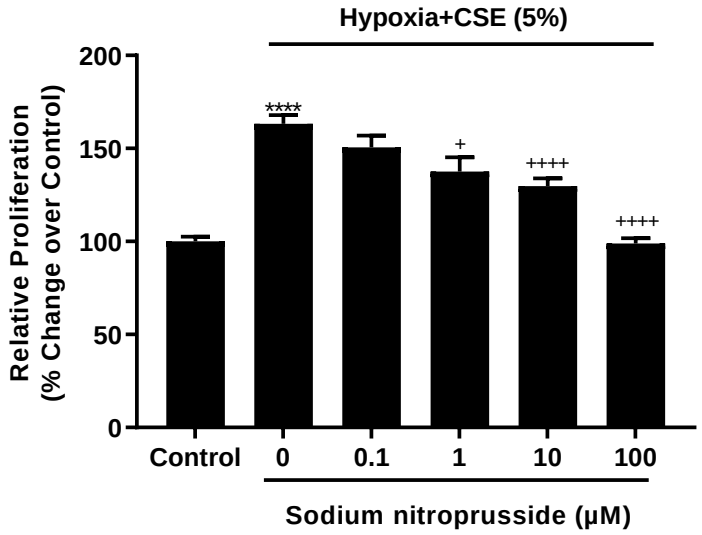


Figure 6.35 Effect of sodium nitroprusside on hypoxia+CSE-induced proliferation of human PASMCs.
Confluent human PASMCs were incubated with increasing concentrations of sodium nitroprusside (0-100 μM) 1 hour prior to treatment with or without CSE (5%) under normoxic (21% O_2) or hypoxic (1% O_2) conditions for 24 h. WST-1 was then conducted. Data were expressed as relative proliferation (% change over control). Each data point represents mean ± SEM from one experiment performed in eight different wells. ****$p<0.0001$ compared with control. $^{+}p<0.05$, $^{++++}p<0.0001$ compared with hypoxia+CSE alone.

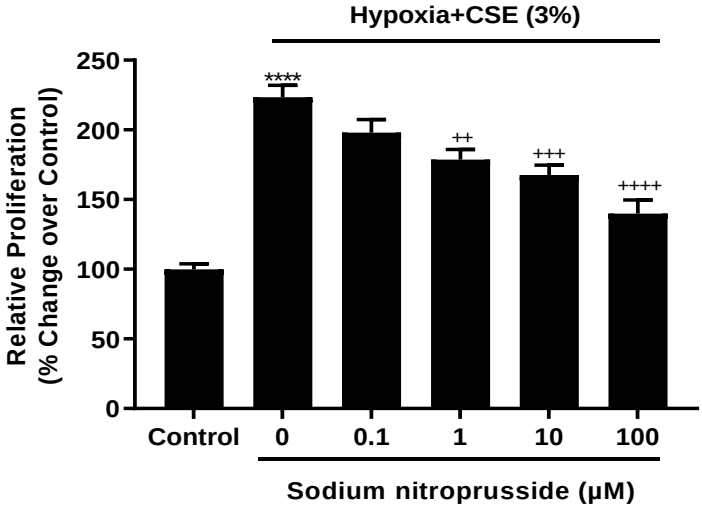


Figure 6.36 Effect of sodium nitroprusside on hypoxia+CSE-induced proliferation of human PAECs.
Confluent human PAECs were incubated with increasing concentrations of sodium nitroprusside (0-100 μM) 1 hour prior to treatment with or without CSE (3%) under normoxic (21% O_2) or hypoxic (1% O_2) conditions for 24 h. WST-1 was then conducted. Data were expressed as relative proliferation (% change over control). Each data point represents mean ± SEM from one experiment performed in eight different wells. ****$p<0.0001$ compared with control. $^{++}p<0.01$, $^{+++}p<0.001$, $^{++++}p<0.0001$ compared with hypoxia+CSE alone.

6.4.19 Effect of bosentan on CSE-, hypoxia- and hypoxia in combination with CSE-induced proliferation of human PAECs

To assess the effect of bosentan, an ET-A and ET-B receptor antagonist, on CSE-, hypoxia- and hypoxia+CSE-induced proliferation of human PAECs, we incubated PAECs with bosentan at different concentrations (0-10 μM) 1 hour prior to treatment with or without CSE (3%) under normoxic or hypoxic conditions for 24 h. We first found that CSE, hypoxia and hypoxia+CSE induced proliferation of PAECs (% change 254.0±17.4, 246.5±9.7 and 331.1±26.1, respectively, $p<0.0001$) (Figure 6.37, Figure 6.38 and Figure 6.39). Interestingly, the use of bosentan did not have significant effect on CSE-, hypoxia- and hypoxia+CSE-induced proliferation of PAECs (Figure 6.37, Figure 6.38 and Figure 6.39).

These findings support our observations in Chapters 3 and 4 that the production of endothelin was reduced and unchanged by CSE and hypoxia, respectively, and suggest that endothelin pathway may not play a critical role in the regulation of CSE- and hypoxia-induced PAEC dysfunction and proliferation.

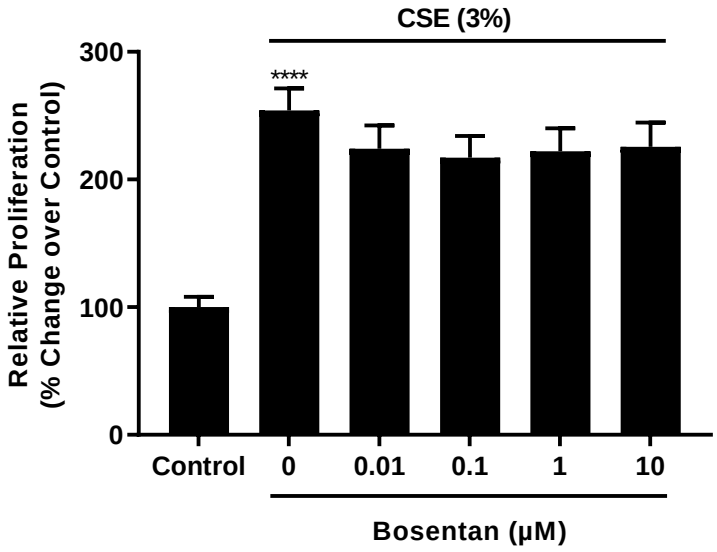


Figure 6.37 Effect of bosentan on CSE-induced proliferation of human PAECs.
Confluent human PAECs were incubated with increasing concentrations of bosentan (0-10 μM) 1 hour prior to treatment with or without CSE (3%) for 24 h. WST-1 was then conducted. Data were expressed as relative proliferation (% change over control). Each data point represents mean ± SEM from one experiment performed in six different wells. ****p<0.0001 compared with control.

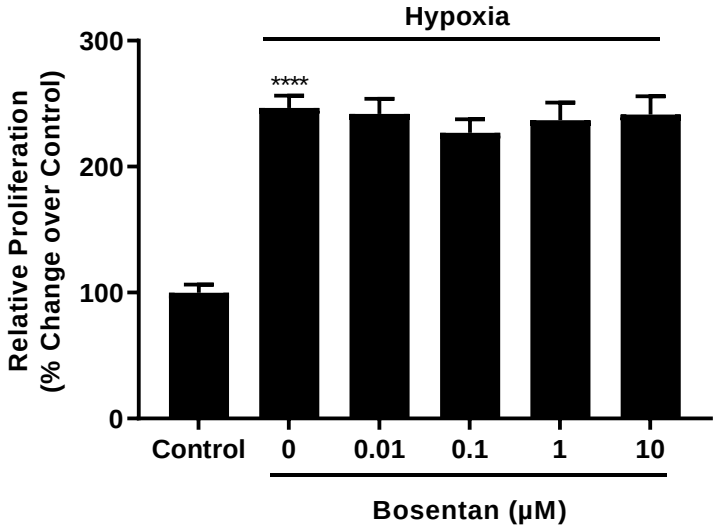


Figure 6.38 Effect of bosentan on hypoxia-induced proliferation of human PAECs.
Confluent PAECs were pre-treated with increasing concentrations of bosentan (0-10 μM) 1 hour prior to cell incubation under normoxic (21% O_2) or hypoxic (1% O_2) conditions for 24 h. WST-1 was then conducted. Data were expressed as relative proliferation (% change over control). Each data point represents mean ± SEM from one experiment performed in six different wells. ****p<0.0001 compared with control.

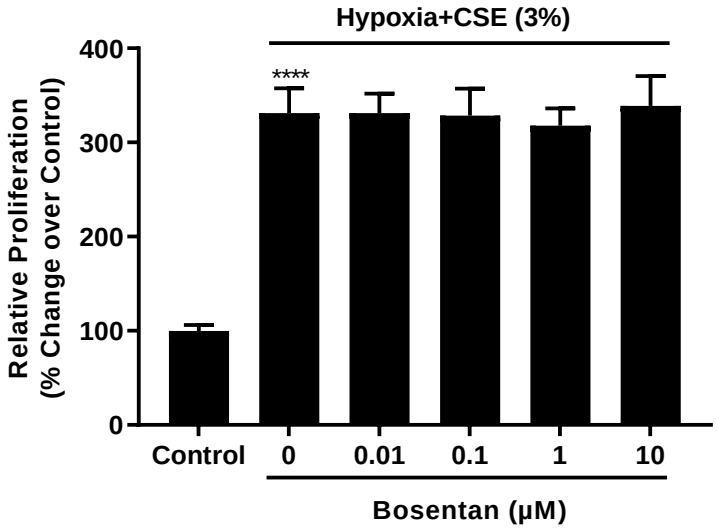


Figure 6.39 Effect of bosentan on hypoxia+CSE-induced proliferation of human PAECs.
Confluent human PAECs were incubated with increasing concentrations of bosentan (0-10 μM) 1 hour prior to treatment with or without CSE (3%) under normoxic (21% O_2) or hypoxic (1% O_2) conditions for 24 h. WST-1 was then conducted. Data were expressed as relative proliferation (% change over control). Each data point represents mean ± SEM from one experiment performed in six different wells. ****$p<0.0001$ compared with control.

6.4.20 Effect of CSE and hypoxia alone or in combination on pro/cleaved caspase 3 levels in human PASMCs and PAECs

As shown earlier, CSE and hypoxia either individually or in combination can stimulate proliferation of PASMCs and PAECs. However, it is unclear whether CSE and hypoxia can induce apoptosis of human PASMCs and PAECs. Western blotting was carried out to assess the effect of CSE and hypoxia on apoptosis marker pro/cleaved caspase 3 in PASMCs, as well as in PAECs. Total cell lysates from HeLa cells treated with staurosporine were used as a positive control. We found that pro-caspase 3 was detectable in both untreated PASMCs (Figure 6.40A) and PAECs (Figure 6.41A). In contrast, cleaved caspase 3 was undetectable in PASMCs and PAECs at basal levels. Surprisingly, treatment with or without CSE under normoxic or hypoxic conditions failed to cause any effect on pro/cleaved caspase 3 levels in both cell types compared with untreated cells and CSE or hypoxia alone (Figure 6.40B and C and Figure 6.41B and C).

The results suggest that cell treatment with CSE and hypoxia result in no effect on pro/cleaved caspase 3 in both cell types.

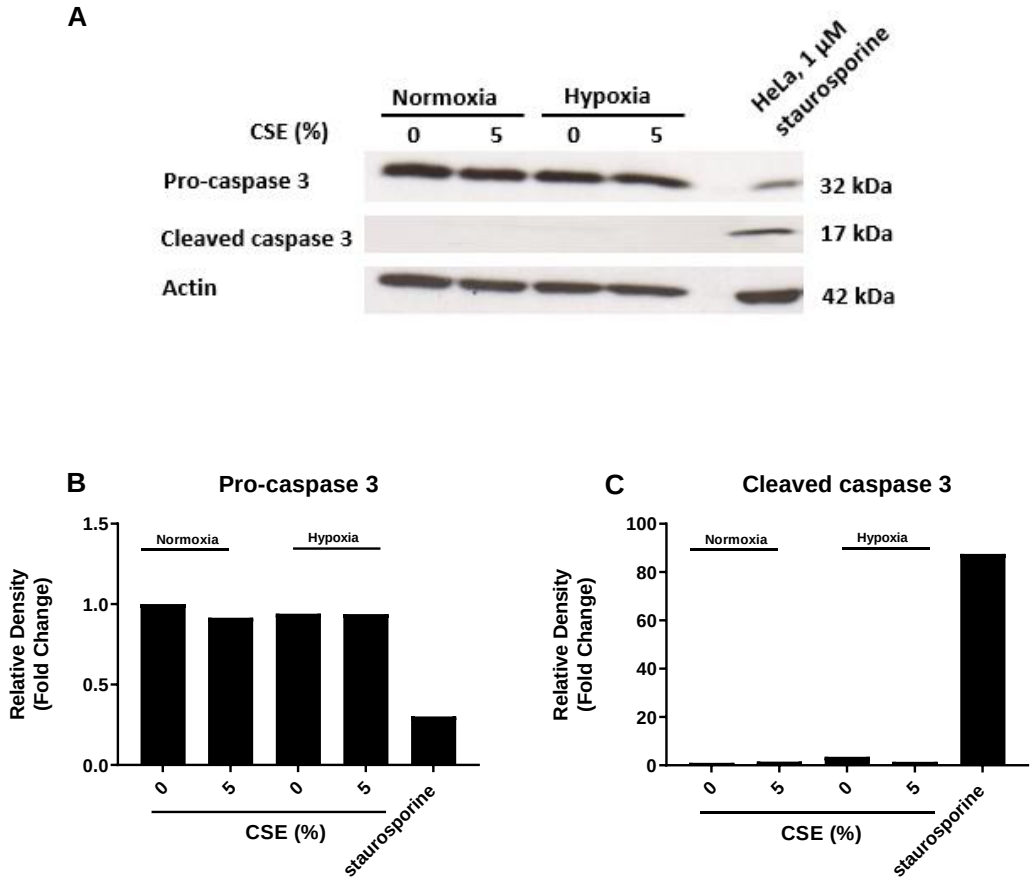


Figure 6.40 Effect of CSE, hypoxia and hypoxia+CSE on pro/cleaved caspase 3 in human PASMCs. Confluent human PASMCs were treated with CSE (0% and 5%) under normoxic (21% O_2) or hypoxic (1% O_2) conditions for 48 h with daily fresh DMEM+ and CSE and then with the same concentrations of CSE under normoxic or hypoxic conditions in DMEM- for 24 h. Total cell lysates were collected for Western blot analysis of pro/cleaved caspase 3 protein. Total cell lysates from HeLa cells treated with staurosporine were used as a positive control. A, Western blot showing the effect of CSE under normoxic or hypoxic conditions on pro/cleaved caspase 3 levels. B and C, optical densitometry analysis of Western blotting bands. Data were normalised with the loading control actin and were expressed as fold change over untreated cells (0% CSE). This figure shows data from one experiment.

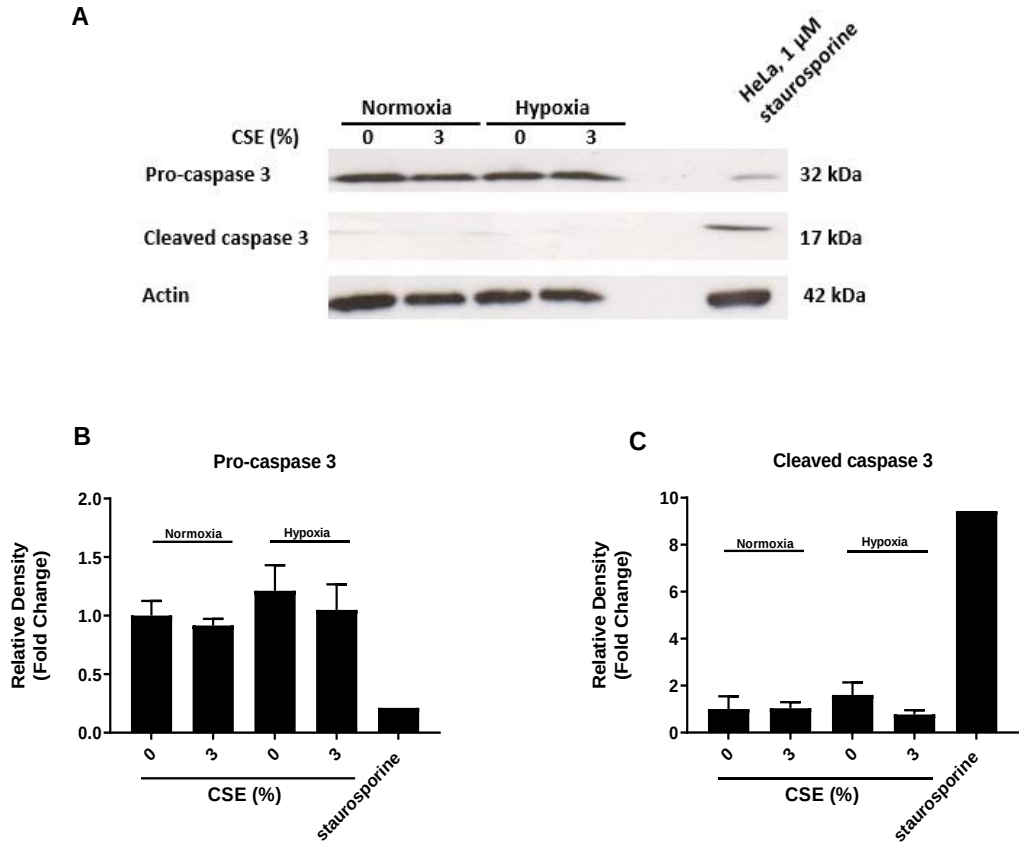


Figure 6.41 Effect of CSE, hypoxia and hypoxia+CSE on pro/cleaved caspase 3 in human PAECs. Confluent human PAECs were treated with CSE (0% and 3%) under normoxic (21% O_2) or hypoxic (1% O_2) conditions for 24 h prior to total cell lysates collection for Western blot analysis of pro/cleaved caspase 3. Total cell lysates from HeLa cells treated with staurosporine were used as a positive control. A, a representative Western blot showing the effect of CSE under normoxic or hypoxic conditions on pro/cleaved caspase 3 levels. B and C, optical densitometry analysis of Western blotting bands. Data were normalised with the loading control actin and were expressed as fold change over untreated cells (0% CSE). Each data point represents mean ± SEM from three independent experiments using one cell line.

6.4.21 Effect of CSE, hypoxia and hypoxia in combination with CSE on cleaved PARP1 levels in human PASMCs and PAECs

PARP1 plays a key role in the routine repair of DNA damage and is known to be cleaved by activated caspases 3 (Chaitanya et al., 2010). Increased cleaved caspases 3 and PARP1 are considered as a hallmark for apoptosis (Chaitanya et al., 2010). Here, we assessed the effect of CSE and hypoxia on cleaved PARP1 in PASMCs and PAECs. We first found that cleaved PARP1 was undetectable at basal levels in PASMCs (Figure 6.42A). Cell incubation with CSE (0% and 5%) under normoxic or hypoxic conditions showed no significant effect on cleaved PARP1 levels compared with untreated cells and CSE or hypoxia alone (Figure 6.42B). Next, we found that cleaved PARP1 was undetectable basally in PAECs. (Figure 6.43A). Although cell exposure to hypoxia alone did not have any effect on the levels of cleaved PARP1, CSE (3%) under normoxic or hypoxic conditions caused a significant increase in cleaved PARP1 levels compared with control (fold change 5.7±0.3, $p<0.001$, 5.3±0.4, $p<0.001$, respectively) (Figure 6.43B).

Increased cleaved PARP1 following CSE treatment under normoxic or hypoxic conditions in PAECs suggests that CSE can induce PAEC apoptosis.

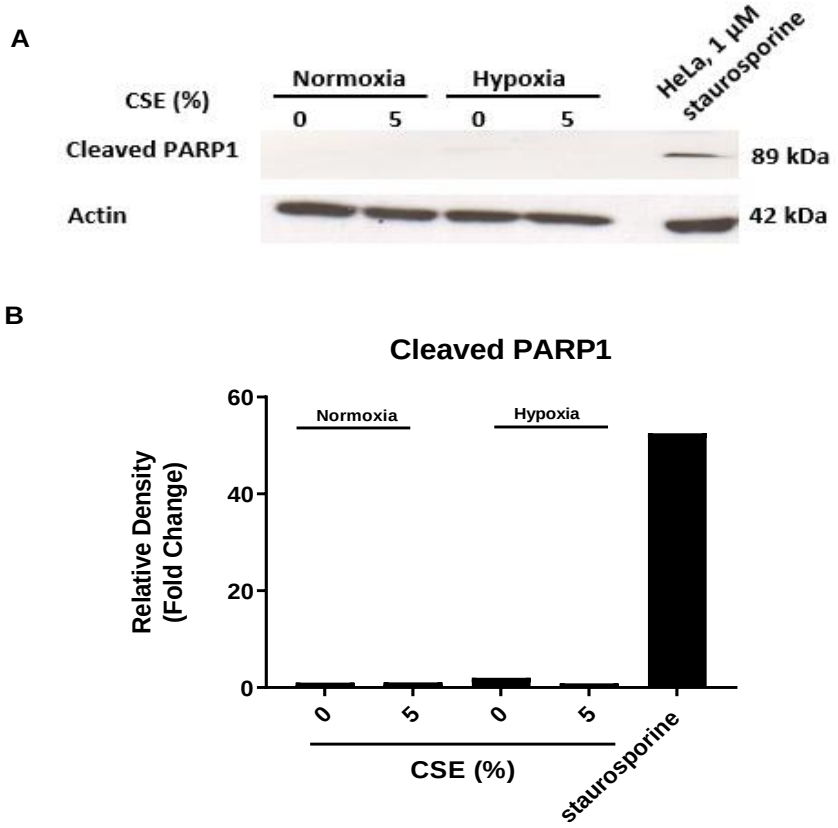


Figure 6.42 Effect of CSE, hypoxia and hypoxia+CSE on cleaved PARP1 in human PASMCs.
Confluent human PASMCs were treated with CSE (5%) under normoxic (21% O_2) or hypoxic (1% O_2) conditions for 48 h with daily fresh DMEM+ and CSE and then with the same concentrations of CSE under normoxic or hypoxic conditions in DMEM- for 24 h. Total cell lysates were collected for Western blot analysis of cleaved PARP1 protein. Total cell lysates from HeLa cells treated with staurosporine were used as a positive control. A, Western blot showing the effect of CSE under normoxic or hypoxic conditions on cleaved PARP1 levels. B and C, optical densitometry analysis of Western blotting bands. Data were normalised with the loading control actin and were expressed as fold change over untreated cells (0% CSE). This figure shows data from one experiment.

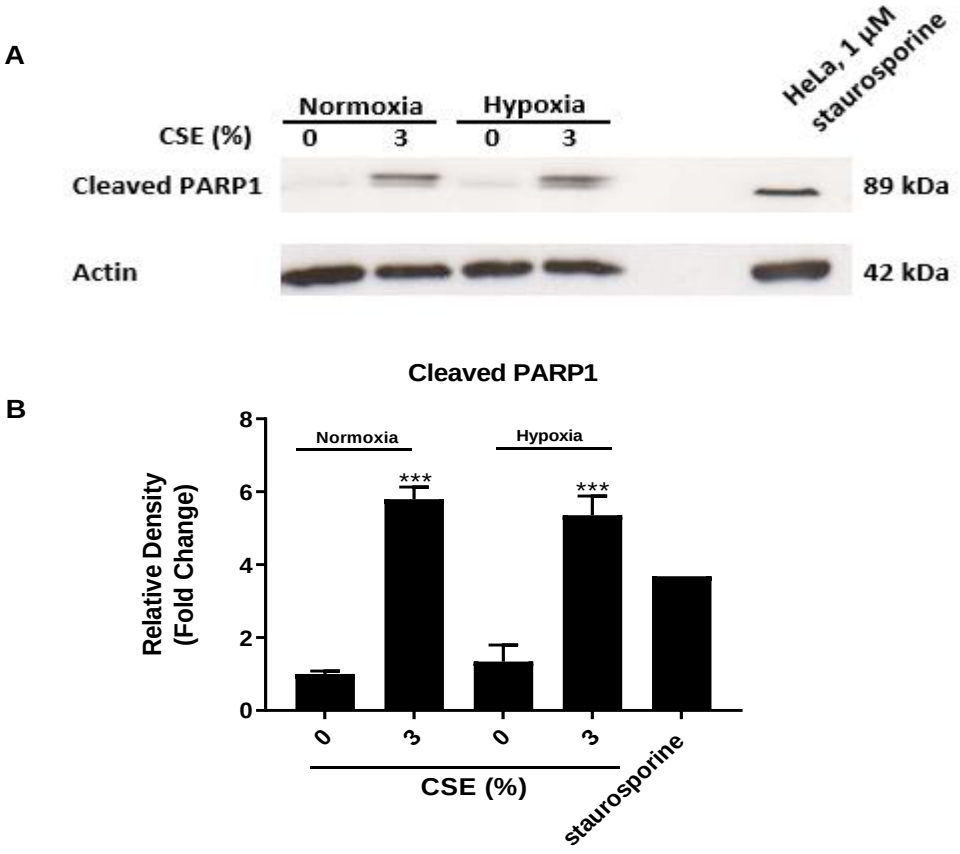


Figure 6.43 Effect of CSE, hypoxia and hypoxia+CSE on cleaved PARP1 in human PAECs.
Confluent human PAECs were treated with CSE (0% and 3%) under normoxic (21% O_2) or hypoxic (1% O_2) conditions for 24 h prior to total cell lysates collection for Western blot analysis of cleaved PARP1. Total cell lysates from HeLa cells treated with staurosporine were used as a positive control. A, a representative Western blot showing the effect of CSE under normoxic or hypoxic conditions on cleaved PARP1 levels. B and C, optical densitometry analysis of Western blotting bands. Data were normalised with the loading control actin and were expressed as fold change over untreated cells (0% CSE). Each data point represents mean ± SEM from three experiments using one cell line. ***$p<0.001$ compared with untreated cells.

6.4.22 Effect of drugs targeting prostanoid and sodium nitroprusside on CSE-induced cleaved PARP1 levels in human PAECs

Since cleaved PARP1 levels were induced in response to CSE under normoxic or hypoxic conditions, we next wanted to explore the role of the altered release of vasoactive mediators in CSE-induced cleaved PARP1 in PAECs. PAECs were stimulated with one concentration of beraprost sodium (10 pM), daltroban (10 nM), celecoxib (100 nM), PF-03549184 (100 nM), and sodium nitroprusside (100 μM) 1 hour prior to treatment without and with CSE (3%) for 24 h and then Western blotting was conducted. Our results showed that CSE induced cleaved PARP1 (Figure 6.44A and B). Cell incubation with beraprost sodium, daltroban, celecoxib, PF-03549184, and sodium nitroprusside resulted in no significant effect on CSE-induced cleaved PARP1 in human PAECs as shown in the densitometry analysis of Western blotting bands (Figure 6.44C and D).

These results suggest that stable PGI_2 analogue, TXA_2 receptor antagonist, selective COX-2 inhibitor, mPGES-1 inhibitor, and nitric oxide donor are unable to inhibit CSE-induced cleaved PARP1 levels in PAECs.

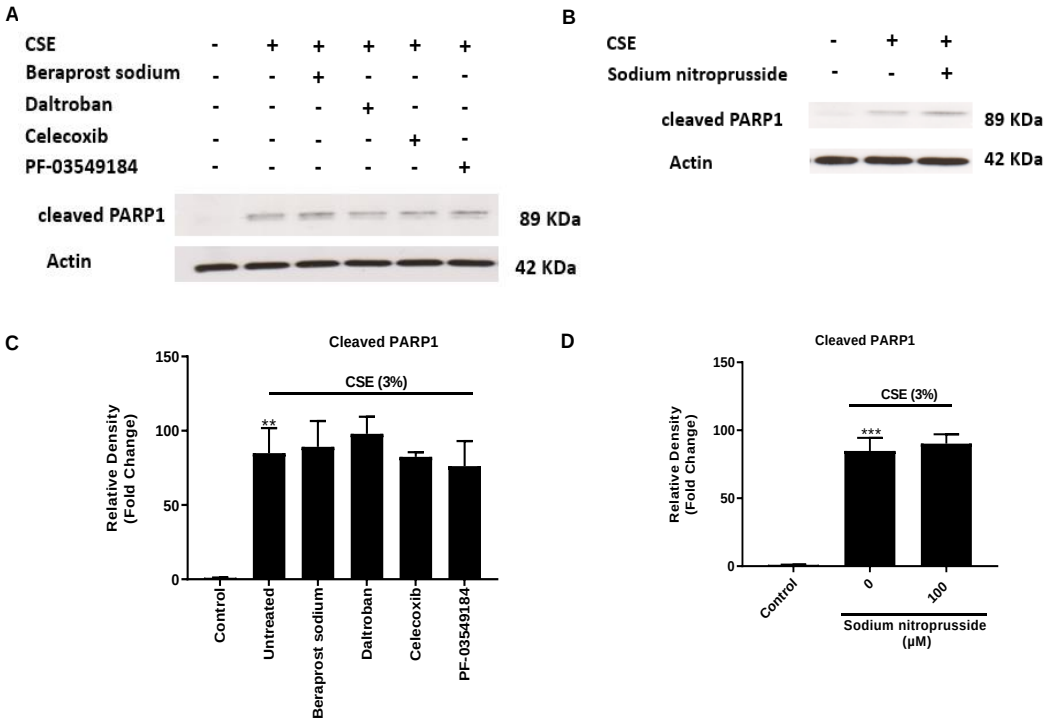


Figure 6.44 Effect of drugs targeting prostanoid and sodium nitroprusside on CSE-induced cleaved PARP1 in human PAECs.

Confluent PAECs were pre-treated with one concentration of beraprost sodium (10 pM), daltroban (10 nM), celecoxib (100 nM), PF-03549184 (100 nM) (A) and sodium nitroprusside (100 μM) (B) 1 hour prior to treatment without and with CSE (3%) for 24 h. Total cell lysates were collected for Western blot analysis of cleaved PARP1 protein. A and B, representative Western blots showing the effect of these drugs on CSE-induced cleaved PARP1 levels. C and D, optical densitometry analysis of Western blotting bands. Data were normalised with the loading control actin and were expressed as fold change over control. Each data point represents mean ± SEM from three experiments using one cell line. **p<0.01, ***p<0.001 compared with control.

6.4.23 Effect of CSE, hypoxia and hypoxia in combination with CSE on annexin v in human PAECs

Thus far, the results demonstrating enhanced cleaved PARP1 by CSE suggest that CSE can induce cell apoptosis in PAECs. To further confirm this finding, PAECs were treated with or without CSE under normoxic or hypoxic conditions for 24 h. The supernatants were collected at three different time points (3, 16, and 24 h), and then annexin v, an early marker of apoptosis, was assessed by ELISA. We found that annexin v was undetectable in the medium from untreated cells and was still undetectable after stimulation with CSE, hypoxia and hypoxia+CSE. Raw data for annexin v standards and samples are shown in Figure 6.45.

The results suggest that CSE and hypoxia either in combination or as single factors do not induce annexin v.

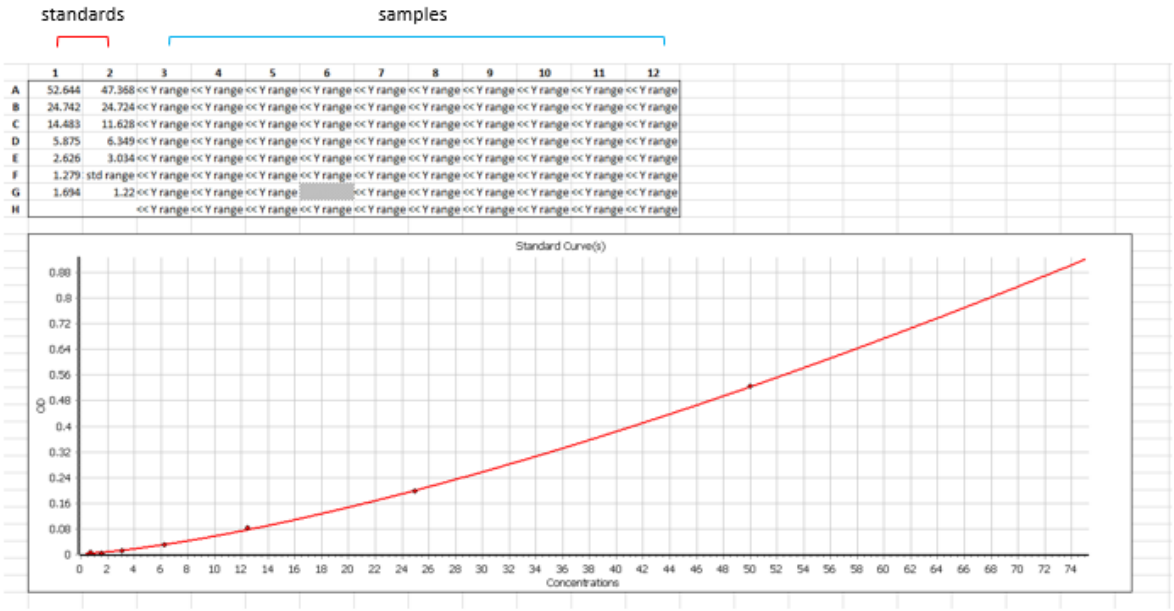


Figure: 6.45 Effect of CSE, hypoxia and hypoxia+CSE on annexin v in human PAECs.
Confluent human PAECs were treated with or without CSE (3%) under normoxic (21% O_2) or hypoxic (1% O_2) conditions for 24 h. Supernatants were collected at different time points (3, 16, and 24 h) and assayed for Annexin v using ELISA. A figure of raw data for annexin v standards and samples is shown.

6.5 Discussion

The key findings of this Chapter are that CSE and hypoxia stimulated PASMC and PAEC proliferation. Although CSE had no effect on pro/cleaved caspase 3 and annexin v in both cell types, CSE induced cleaved PARP1 levels in PAECs (but not in PASMCs). Hypoxia did not affect markers of apoptosis in both cell types. Our results also showed that beraprost sodium, daltroban, and celecoxib (but not bosentan and PF-03549184) inhibited CSE-induced PASMC and PAEC proliferation. In addition, we observed that beraprost sodium, daltroban, celecoxib, and sodium nitroprusside (but not PF-03549184) were able to reduce hypoxia-induced proliferation of PASMCs. Although drugs targeting prostanoids and bosentan caused no effect on hypoxia-induced PAEC proliferation, sodium nitroprusside had the ability to decrease hypoxia-induced proliferation of PAECs. Summary tables of the findings of Chapter 6 are shown in Tables 6.1 and 6.2.

To the best of our knowledge, this is the first report to show that altered prostanoid and nitric oxide signalling pathways may, in part, contribute to CS- and hypoxia-induced pulmonary vascular remodelling through the induction of PASMC and PAEC proliferation. These signalling pathways could serve as a potential therapeutic target for the treatment of patients with pulmonary hypertension in COPD.

Table 6.1 A summary table of the findings of Chapter 6.

Drugs	**Effect on CSE, hypoxia, and hypoxia+CSE-induced proliferation of PASMCs**		
Selective COX-2 inhibitor	**CSE**	**Hypoxia**	**Hypoxia+CSE**
Celecoxib	↓	↓	↓
PGI_2 analogue	**CSE**	**Hypoxia**	**Hypoxia+CSE**
Beraprost sodium	↓	↓	↓
TXA_2 receptor antagonist	**CSE**	**Hypoxia**	**Hypoxia+CSE**
Daltroban	↓	↓	↓
mPGES-1 inhibitor	**CSE**	**Hypoxia**	**Hypoxia+CSE**
PF-03549184	↔	↔	↔
Nitric oxide donor	**CSE**	**Hypoxia**	**Hypoxia+CSE**
Sodium nitroprusside	↓	↓	↓

CSE, Cigarette smoke extract; PASMCs, Pulmonary artery smooth muscle cells; COX-2, Cyclooxygenase-2; PGI_2, Prostaglandin I_2; TXA_2, Thromboxane A_2; mPGES-1, Microsomal prostaglandin E synthase-1; ↔, Unchanged; ↓, Decreased.

Table 6.2 A summary table of the findings of Chapter 6.

Drugs	Effect on CSE, hypoxia, and hypoxia+CSE-induced proliferation of PAECs		
Selective COX-2 inhibitor	**CSE**	**Hypoxia**	**Hypoxia+CSE**
Celecoxib	↓	↔	↔
PGI_2 analogue	**CSE**	**Hypoxia**	**Hypoxia+CSE**
Beraprost sodium	↓	↔	↔
TXA_2 receptor antagonist	**CSE**	**Hypoxia**	**Hypoxia+CSE**
Daltroban	↓	↔	↔
mPGES-1 inhibitor	**CSE**	**Hypoxia**	**Hypoxia+CSE**
PF-03549184	↔	↔	↔
Nitric oxide donor	**CSE**	**Hypoxia**	**Hypoxia+CSE**
Sodium nitroprusside	↓	↓	↓
ET-A and ET-B receptor antagonist	**CSE**	**Hypoxia**	**Hypoxia+CSE**
Bosentan	↔	↔	↔

CSE, Cigarette smoke extract; PAECs, Pulmonary artery endothelial cells; COX-2, Cyclooxygenase-2; PGI_2, Prostaglandin I_2; TXA_2, Thromboxane A_2; mPGES-1, Microsomal prostaglandin E synthase-1, ET-A and ET-B endothelin receptor-A and B; ↔, Unchanged; ↓, Decreased.

6.5.1 CSE and hypoxia effect on PASMC and PAEC proliferation

Cell proliferation is defined as an increase in the number of cells, and it can be measured either directly by cell counting or indirectly by assessing cells that have undergone DNA synthesis (e.g. Bromodeoxyuridine (BrdU) and 5-ethynyl-2′-deoxyuridine (EdU)), as well as the metabolic activity of cells in culture (e.g. cell proliferation reagent WST-1). Due to the variability associated with cell counting (Quent et al., 2010) and the potential DNA damage and complexity associated with BrdU and EdU (Chung et al., 2017, Kohlmeier et al., 2013), measuring the metabolic activity of cells in culture is currently the most widely used method as colorimetric assays are safe, convenient, accurate, sensitive and fast (Rampersad, 2012, Xie et al., 2018, Ginouves et al., 2014).

Based on the fact that WST-1 and WST-8 assays are the most common metabolic activity assays used to evaluate cell proliferation and anti-proliferative drug screening (Xie et al., 2018), a WST-1 assay was used as the primary method (and CCK-8 assay as the secondary method) of assessing cell proliferation in the current study. Although the WST-1 assay has a long history of being used to evaluate cell proliferation (Tukler Henriksson et al., 2015, Yin et al., 2013) and its consistency with respect to cell counting and BrdU methods has been previously reported (Mynampati et al., 2017, Yin et al., 2014), the sensitivity of the WST-1 assay was determined in the current study (Appendix, Figure 8.13). A direct correlation was demonstrated between the absorbance value and number of metabolically active PASMCs in the culture, which suggests that the cell proliferation reagent WST-1 assay is capable of estimating the number of viable cells in our experimental setting.

In the current study, the results confirmed the previous findings that demonstrated CSE (Xiang et al., 2010) and hypoxia (Wang et al., 2018, Liu et al., 2018) can stimulate the proliferation of human PASMCs, and hypoxia can expedite the proliferation of human PAECs (Porter et al., 2014, Dabral et al., 2016). The results also showed, for the first time, that CSE induced the proliferation of human PAECs. These observations suggest that hypoxia and CS are strong stimuli responsible for pulmonary vascular remodelling via the induction of PASMC and PAEC proliferation, which eventually leads to the development of pulmonary hypertension.

The additive effect of hypoxia+CSE on PASMC proliferation at 24 h suggests that hypoxia may amplify the detrimental effects of CS on pulmonary vascular remodelling at early time point by enhancing cell proliferation. However, the fact that this additive effect was disappeared at 48 and 72 h suggests that CSE effect on the induction of PASMC proliferation is more prominent than hypoxia, further supporting the finding in Chapter 4 that hypoxia did not enhance CSE-induced effects on vasoactive gene expression and mediator release. Since significant increase in cell proliferation was observed at the shortest time point, the present study explored the role of the imbalanced release of vasoactive mediators in CSE- and hypoxia-induced PASMC proliferation at 24 h.

6.5.1.1 The role of prostanoids in CSE- and hypoxia-induced PASMC proliferation

In Chapter 3, we demonstrated that CSE reduced PGI_2 levels and increased TXA_2 levels in PASMCs (all measured at 72 h, aiming to assess the chronic effect of CS). Despite not measuring prostanoid production (including PGI_2 and TXA_2) at 24 h, it is highly likely that the stable PGI_2 analogue and TXA_2 receptor antagonist completely

inhibited CSE-induced PASMC proliferation by compensating for the reduction of endogenous PGI_2 and blocking increased TXA_2 effect, respectively. This observation suggests that the balance between PGI_2 and TXA_2 in PASMCs is important for cardiovascular homeostasis and disturbance of this balance may eventually contribute to vascular remodelling.

In addition, it was shown, in the current Chapter, that the selective COX-2 inhibitor celecoxib had the capability to suppress PASMC proliferation. This suggests that CSE-induced COX-2 expression might have a detrimental effect, and it is likely this anti-proliferative effect occurs via the inhibition of CSE-induced COX-2-derived TXA_2 production. Although it is generally accepted that the inhibition of COX-2 activity would also lead to a reduction in other COX-2-derived prostanoids (e.g. PGI_2 and PGE_2), this is unlikely, in our current study, as PGI_2 and PGE_2 levels were already reduced by CSE as a result of the downregulated PGIS and mPGES-1 expression, respectively. The already reduced mPGES-1/PGE_2 by CSE may also explain why the mPGES-1 inhibitor failed to exert an effect on CSE-induced PASMC proliferation. These findings have not been previously reported and suggest that CSE-induced imbalance with a decrease in the levels of PGI_2 and an increase in the levels of TXA_2 may contribute significantly to PASMC proliferation, leading to pulmonary vascular remodelling in COPD-associated pulmonary hypertension.

In Chapter 4, the hypoxia-induced PGI_2, PGE_2, and TXA_2 production is likely to result from the increased COX-2 expression. As previously mentioned, celecoxib can inhibit all prostanoid production. However, under hypoxic condition, it is possible that celecoxib exerts its anti-proliferative effect by the inhibition of the proliferative mediator

TXA_2 without altering mediators with anti-proliferative properties (e.g. PGI_2 and PGE_2), but further experiments will be required to confirm this. Our observation is supported by the finding of animal experimental research in which the COX-2 selective inhibitor NS-398 was demonstrated to improve a piglet model of hypoxic pulmonary hypertension (Fike et al., 2005). It is suggested that this effect is due to the inhibition of the augmented TXA_2 production without adversely affecting PGI_2 levels in hypoxic arteries, unlike normal conditions where NS-398 reduced the production of prostanoids by similar amounts (Fike et al., 2005). Despite the increased PGI_2 production, the use of beraprost sodium was demonstrated to inhibit hypoxia-induced PASMC proliferation. This supports the idea that PGI_2 improves the survival prospects in patients with PAH via the inhibition of the growth of PASMC and is consistent with the finding of a previous study that showed beraprost sodium can suppress human PASMC proliferation under hypoxic conditions (Kadowaki et al., 2007). It is thought that this anti-proliferative effect was achieved through the downregulation of $p27^{kip1}$ expression ($p27^{kip1}$ is a cyclin-dependent kinase inhibitor).

It is interesting to note that the use of PGI_2 analogue, COX-2 inhibitor and TXA_2 receptor antagonist similarly exerted complete inhibition of CSE- and hypoxia-induced cell proliferation. However, when both CSE and hypoxia were combined, the anti-proliferative effect of PGI_2 analogue, COX-2 inhibitor and TXA_2 receptor antagonist in human PASMCs was reduced, despite the fact that hypoxia did not further enhance CSE-induced effects on prostanoid production. This suggests the combined effect of CSE and hypoxia may cause at least a partial resistance to inhibitory effects of these agents targeting prostanoid pathway on PASMC proliferation. Given the fact that hypoxia, in the

current study, was able to amplify the detrimental effects of CSE on cell proliferation, it is also possible that the reduced anti-proliferative effect of the PGI_2 analogue and other drugs targeting prostanoid pathway comes as a result of this enhancement of cell proliferation.

To the best of our knowledge, this is the first study to have suggested that altered release of vasoactive mediators plays a key role in CSE- and hypoxia-induced PASMC proliferation. Abnormal cell growth leads to pulmonary vascular remodelling and an increase in PVR and PAP, eventually contributing to COPD-associated pulmonary hypertension.

6.5.1.2 The role of prostanoids in CSE- and hypoxia-induced PAEC proliferation

Given that CSE reduced PGI_2/TXA_2 as a result of COX-2-derived TXA_2 production (Chapter 3), we postulated the inhibitory effect of beraprost sodium and celecoxib on CSE-induced PAEC proliferation, in our current study, is likely due to the capability of these agents to restore PGI_2/TXA_2 balance. Consistent with our findings reported above in PASMCs, blocking CSE-induced TXA_2 effect by TXA_2 receptor antagonist has also been shown to inhibit CSE-induced PAEC proliferation. This strongly suggests that altered release of prostanoids (particularly TXA_2) may contribute to CS-induced vascular dysfunction and remodelling in COPD. Furthermore, PGE_2 could both stimulate and suppress vascular cell proliferation depending on its binding receptors (Zhao et al., 2012, Patel et al., 2018). Since PGE_2 has been reported to contribute to human umbilical vein endothelial cell proliferation (Zhao et al., 2012), it was expected that the inhibition of PGE_2 by the use of mPGES-1 inhibitor may exert anti-proliferative effect. Surprisingly, PAEC proliferation was unchanged in response to the use of

mPGES-1 inhibitor, which suggests that CSE-induced PAEC proliferation is probably not modulated by increased PGE_2 production, but rather by the increase in TXA_2 production and the reduction of PGI_2/TXA_2 ratio.

Intriguingly, beraprost sodium, celecoxib, PF-03549184, and daltroban failed to inhibit hypoxia-induced PAEC proliferation. Despite the increase in TXA_2 production, this observation is probably due to the inability of hypoxia to induce the expression of COX-2 and its downstream products PGI_2 and PGE_2 (Chapter 4). The finding that the hypoxia+CSE-induced proliferation of PAECs remained also unchanged after the use of beraprost sodium, celecoxib, PF-03549184, and daltroban, indicates that hypoxia-induced PAEC proliferation is mainly mediated by hypoxia rather than CSE. Although the role of agents targeting prostanoid pathway on hypoxia-induced PAEC proliferation has not been previously studied, it has been suggested that COX-2-derived PGE_2 is involved in the modulation of hypoxia-induced human umbilical vein endothelial cell proliferation (Zhao et al., 2012). However, it is important to note that this does not exclude the possibility that other prostanoids (e.g. TXA_2) may also have been involved in this process, as PGE_2 was the only prostanoid assessed in that study (Zhao et al., 2012).

Our findings suggest that pathways, other than prostanoids, may be involved in hypoxia-induced PAEC proliferation. There is evidence to suggest that hypoxia-induced PAEC proliferation is regulated via Notch1 signalling by suppressing of the expression of p21, a tumour suppressor, and by increasing the expression of Bcl-2 and survivin, apoptosis inhibitors (Dabral et al., 2016). In part, this might explain our findings and suggests that Notch1 signalling is critical for hypoxia-induced PAEC proliferation. In addition, the observation that Notch1 signalling was not involved in the regulation of the

proliferative potential of PASMCs (Dabral et al., 2016) further supports the findings of the current study that hypoxia-induced proliferation of PASMCs may be mediated, at least in part, by the altered prostanoid signalling pathway.

Collectively, although it is likely that other signalling pathways are more important than prostanoids in the regulation of hypoxia-mediated PAEC proliferation, the ability of beraprost sodium, celecoxib and daltroban to inhibit CSE-induced PAEC proliferation suggests that imbalanced prostanoids could make a critical contribution to CSE-induced PAEC proliferation. These novel findings also suggest that targeting the prostanoid signalling pathway may have the potential to reduce CS-induced vascular remodelling through the suppression of PAEC proliferation.

6.5.1.3 The role of nitric oxide and endothelin in CSE- and hypoxia-induced PASMC and PAEC proliferation

We also provide evidence that sodium nitroprusside, a nitric oxide donor, significantly decreased CSE-, hypoxia- and hypoxia+CSE-induced PASMC proliferation, supporting the traditionally held view that nitric oxide regulates the growth of neighboring PASMCs, even though PAECs are the primary source of eNOS-derived nitric oxide generation in vascular cells. The use of nitric oxide donor to compensate the loss of nitric oxide production in PAECs has also resulted in suppression of CSE-, hypoxia- and hypoxia+CSE-induced proliferation of PAECs. These observations suggest that nitric oxide may extert paracrine and autocrine anti-proliferative effect, most likley via a cGMP-mediated mechanism. It is also worth noting that prostanoid vaoactive agents did not have a similar effect to that of the nitric oxide donor on the inhibition of hypoxia-induced PAEC proliferation, indicating that the exertion of anti-proliferative effect by

increasing nitric oxide through the cGMP pathway could play a more important role than prostanoid-cAMP pathway-mediated effects in the inhibitory effects on hypoxia-induced PAEC proliferation.

It is interesting to find that bosentan did not elicit anti-proliferative effect in CSE- and hypoxia-treated PAECs. This supports the finding of Chapters 3 and 4 that endothelin production may not be an important part of CSE- and hypoxia-induced PAEC dysfunction. Because PASMCs produced endothelin at low basal levels compared with PAECs and that endothelin levels were unchanged in response to CSE and hypoxia in PASMCs, the effect of bosentan on CSE- and hypoxia-induced cell proliferation was not assessed in PASMCs.

6.5.2 CSE and hypoxia effect on PASMC and PAEC apoptosis

It is important to ensure a balance between cell proliferation and apoptosis in PASMCs and PAECs to maintain normal vascular function. If this balalnce is disrupted, the lumen of the blood vessels narrows, resulting in vascular remodelling, an increase in pulmonary artery resistance and pressure and pulmonary hypertnsion. A further objective of this Chapter was to determine whether CSE and hypoxia could induce apoptosis in human PASMCs and PAECs.

Our results demonstrated that hypoxia did not induce PASMC and PAEC apoptosis. This is consistent with previous studies and is likely to occur due to the fact that hypoxia can induce PASMC and PAEC proliferation, but exhibit simultaneous resistance to apoptosis, by suppressing of the levels of p21 and promoting the anti-apoptotic factor survivin (Dabral et al., 2016, Zhang et al., 2016, Liu et al., 2018). Furthermore, the observation that CSE did not induce apoptosis markers in human

PASMCs is in agreement with a previous study showing that CSE is unable to induce rat PASMC apoptosis (Li et al., 2015).

Caspases 3 is a major ‘executor’ of apoptosis. Although it is generally accepted that activated caspase 3 cleaves PARP1 during apoptosis, a process of programmed cell death, this is unlikely, in our current study, as CSE-induced cleaved PARP1 was not associated with cleaved caspase 3 in human PAECs. This may be explained by the fact that PARP1 can be activated, even without the presence of activated caspase 3 (Janicke et al., 1998, Woo et al., 1998). It is suggested that PARP1 can be cleaved by other active forms of caspases (e.g. caspase 7) during apoptosis (Desroches and Denault, 2019). In addition, there is evidence to suggest cathepsins, a large family of lysosomal enzymes comprising 11 cysteinyl cathepsins, can also cleave PARP1 (Gobeil et al., 2001, Aldonyte et al., 2009). This cleaved PARP1 is essentiel for translocation of mitochondrial apoptosis-inducing factor, a key mediator of caspase-independent apoptosis, to nucleus, where it induces DNA fragmentation, leading to apoptosis (Zhang et al., 2017). Our findings are supported by a previous study demonstrating that activated caspase 3 is not responsible for induced cleaved PARP in CSE-treated cultured porcine PAECs (Aldonyte et al., 2009). It has also been shown that CSE can induce apoptosis in other human vascular endothelial cells, such as pulmonary microvascular endothelial cells and umbilical vein endothelial cells (Nana-Sinkam et al., 2007, Chen et al., 2012). This very interinguing finding together with the observation that PAECs can also proliferate in response to CSE suggests that the increased cleaved PARP1 levels may play a role in cell proliferation either autonomously or by the induction of cell growth factors (e.g. VEGF) (Golpon et al., 2004), which may have impact in neighboring cells. This supports the

concept that apoptotic cells can influence the behaviors of neighboring cells and stimulate cell proliferation (Perez-Garijo, 2018, Sakao et al., 2005).

Annexin v is used to detect apoptotic cells, as it has the ability to bind to phosphatidylserine or PS, which is translocated from the inner to the outer leaflet of the cell membrane during apoptosis. It is interesting to find that annexin v was undetetcable in response to CSE in PAECs, as assessed by ELISA. The fact that CSE induced cleaved PARP1 levels suggests that it is possible that CSE induced annexin v below the detection levels of the ELISA, considering the high sensitivity of the annexin v ELISA kit used in this study (0.33 ng/ml). Another possibility is that the quantitative measurement of free annexin v levels by ELISA may not be the most appropriate method to use. It has been demonstrated that CSE can induce cleaved PARP and annexin v binding to PS (assessed by flow cytometry) in cultured porcine PAECs (Aldonyte et al., 2009). This supports the idea that the detection of annexin v binding to PS by flow cytometry may be a more accurate method than that used in the current study.

Compensation for the reduced PGI_2 levels by the use of stable PGI_2 analogue has been reported to prevent CSE-induced apoptosis in human umbilical vein endothelial cells (Chen et al., 2012), as well as in human pulmonary microvascular endothelial cells (Nana-Sinkam et al., 2007). However, the role of CSE-induced imbalanced release of vasoactive mediators in the inhibition of PAEC apoptosis has not been previously studied in any cell system. To our surprise, restoring PGI_2/TXA_2 balance by beraprost sodium and celecoxib, compenstenting for nitric oxide reduction by sodium nitroprusside, and blocking increased TXA_2 effects by daltroban, failed to inhibit CSE-induced cleaved PARP1 levels. This suggests that it is unlikely the CSE-induced imbalanced release of

vasoactive mediators play a critical role in CSE-induced cleaved PARP1 in PAECs. In addition to the unaffected PGI_2 production by CSE, in our study, the fact that cell types and methods used to assess apoptosis are different could explain the disparity between our findings and those by Chen et al. (2012) and Nana-Sinkam et al. (2007). Together, the induction of cleaved PARP1 strongly suggests that CSE can induce apoptosis in PAECs, likely via caspase 3-independent form of apoptosis. However, further studies using other methods (e.g flow cytometry) will be needed to confirm our annexin v ELISA findings.

To conclude, the results presented in this final Chapter provide direct evidence for the first time that imbalanced vasoactive mediator release may, in part, contribute to CSE- and hypoxia-induced PASMC and PAEC proliferation. Our findings suggest that altered prostanoid and nitric oxide pathways play a more important role in hypoxia- and CS-induced modulation of vascular structure than endothelin pathway. These novel observations may yield further insights into the signalling pathways involved in CS- and hypoxia-induced vascular remodelling, thus leading to the development of new therapeutic targets for pulmonary hypertension in COPD.

Chapter 7. General discussion, limitations, future directions and conclusions

7.1 General discussion

The main aims of this thesis were to evaluate whether CSE and hypoxia can cause imbalanced vasoactive gene expression and mediator release in human PASMCs and PAECs and to find out whether $ECVE^{+/-n}$ has similar effects as CSE on the induction of the imbalance. We were also interested in investigating the role of the release of individual vasoactive mediators in CSE- and hypoxia-induced cell proliferation and apoptosis. The key findings of this thesis are that CSE (but not $ECVE^{+/-n}$) and hypoxia can cause imbalanced mediator release by inducing altered release of prostanoids (particularly reducing the PGI_2/TXA_2 ratio due to increased TXA_2) and nitric oxide. Our results indicate that the restoration of the balance between PGI_2 and TXA_2 by beraprost sodium and celecoxib (via the inhibition of COX-2-derived TXA_2 production) is likely to play a role in the inhibition of CSE- and hypoxia-induced cell proliferation. The anti-proliferative effect of daltroban is probably as a result of blocking the effect of CSE- and hypoxia-induced TXA_2 production. Furthermore, although hypoxia failed to induce apoptosis in both cell types, CSE induced apoptosis in PAECs (but not PASMCs). This induction is unlikely mediated by the altered release of vasoactive mediators.

The results presented in this thesis highlighted two important pathways that may have a critical role in CSE- and hypoxia-induced PASMC and PAEC dysfunction and proliferation. The first pathway is prostanoid, which mainly consists of PGE_2, PGI_2, and TXA_2, downstream products derived from the sequential enzymatic actions of COX-2 and their respective prostanoid synthases. Although $ECVE^{-/+n}$ had no effect on the release of prostanoids, our data suggest that CSE and hypoxia can induce imbalanced release of prostanoids, particularly by increasing the production of vasoconstrictive and

proliferative mediator TXA_2 in both cell types, which consequently leads to a reduction in the PGI_2/TXA_2 ratio. This indicates that the disrupted prostanoid pathway (particularly PGI_2/TXA_2 imbalance) plays a key role in PASMC and PAEC dysfunction and that the anti-proliferative effect of agents targeting prostanoids (e.g. beraprost sodium and celecoxib) observed in this study, at least in part, may result from restoring the altered balance of prostanoids. Clinical and preclinical animal studies using agents targeting prostanoids, by either compensating for PGI_2 reduction or blocking increased TXA_2 effects have been promising. The use of PGI_2 analogues demonstrated significant improvements in the symptoms of patients with PAH (Galie et al., 2016), likely by inhibiting cell proliferation via a cAMP-dependent pathway (Clapp et al., 2002). Although targeting TXA_2-TP receptor signalling is not currently used as a therapeutic target for patients with all forms of pulmonary hypertension (due to lack of evidence), the inhibition of COX-2-derived TXA_2 production and blocking TXA_2 effects using TXAS inhibitors or TP receptor antagonists, have been shown to prevent pulmonary hypertension in animal model studies (Delannoy et al., 2010, Hirenallur et al., 2012, Fike et al., 2005, Su and Jin, 1989). The novel findings presented in this thesis suggest that blocking increased TXA_2 effects by the use of TXA_2 receptor antagonist (daltroban) can exert anti-proliferative effects. Furthermore, the addition of PGI_2 analogue (beraprost sodium) and the inhibition of CSE- and hypoxia-induced COX-2-derived TXA_2 production by COX-2 inhibitor (celecoxib) can restore the balance of prostanoids and help reduce vascular remodelling in COPD-associated pulmonary hypertension via the inhibition of PASMC and PAEC proliferation.

The second pathway is nitric oxide, which is known as a potent pulmonary vasodilator and anti-proliferative mediator (Labonte et al., 2008). Within this thesis, we further showed that CSE and hypoxia (but not ECVE$^{-/+n}$) reduced nitric oxide, likely as a result of the downregulated eNOS protein expression in PAECs and the use of sodium nitroprusside (a nitric oxide donor) inhibited CSE- and hypoxia-indcued PAEC proliferation. Despite the fact that PASMCs do not express eNOS and produce nitric oxide, the addition of nitric oxide donor was able to inhibit CSE- and hypoxia-indcued PASMC proliferation. This supports the view that nitric oxide, produced in neighbouring PAECs, has the ability to diffuse into PASMCs, leading to inhibition of PASMC growth and vasodilation (Crosswhite and Sun, 2014). Although the exact mechanism by which nitric oxide donor caused anti-proliferative effects is unclear, it has been suggested that this anti-proliferative effect may be mediated through the cGMP pathway (Lehners et al., 2018). In addition, the ability of nitric oxide donor (but not agents targeting prostanoid) to inhibit hypoxia-induced PAEC proliferation suggests that nitric oxide-sGC-cGMP signalling pathway can be more important than prostanoids-induced cAMP formation (Clapp et al., 2002) at inhibiting PAEC proliferation, induced by hypoxia. Our findings support the recent retrospective analysis of patients with COPD-associated pulmonary hypertension demonstrating that treatment with riociguat (sGC stimulator) can significantly decrease PVR (Pichl et al., 2019). In addition, the use of the PDE5 inhibitor sildenafil was shown to prevent CS-induced pulmonary hypertension in a guinea-pig model (Dominguez-Fandos et al., 2015), and attenuate hypoxia-induced pulmonary hypertension in a rat model (Sebkhi et al., 2003). Altogether, the results reported in this

study suggest that restoring the altered nitric oxide bioavailability can be a potential therapeutic target for pulmonary hypertension in COPD.

Previous studies focused on PAEC dysfunction as the source of imbalanced vasoactive mediator release. However, not much is known regarding the role of PASMCs, as the traditional view of PASMCs in pulmonary hypertension is that they are a passive partner in the process of vascular remodelling and vasoconstriction, contracting and proliferating in response to altered release of vasoactive mediators in PAECs. This study presented evidence, for the first time, that PASMCs also have important synthetic functions and can serve as a rich source of vasoactive prostanoids with vasodilatory/anti-proliferative and vasoconstrictive/proliferative properties that may modulate vascular remodelling in pulmonary hypertension. More importantly, our work provides further evidence that the CSE- and hypoxia-induced imbalanced response is more profound in PASMCs than PAECs. This suggests that CSE- and hypoxia-induced altered PASMC dysfunction may play a more prominent role in the contribution to pulmonary artery remodelling and pulmonary hypertension in COPD than the traditionally recognised PAEC dysfunction, given the fact that PASMCs constitute a more prominent part in remodelled vasculature. A greater understanding of the autocrine mechanisms regulating PASMC function may lead to the development of new therapeutic drugs for the treatment of pulmonary hypertension in COPD.

7.2 Limitations of the current studies

In this study, there are several limitations that need to be addressed. Firstly, the data presented in this thesis are derived from *in vitro* experiments using human PASMCs and PAECs. We found that CSE and hypoxia induced imbalanced vasoactive gene

expression and mediator release. However, it is unknown whether the imbalance can also be observed in diseased PASMCs and PAECs. It is therefore necessary for our future investigations to use PASMCs and PAECs from non-smokers, smokers with COPD, and smokers without COPD to further strengthen and confirm our findings.

Secondly, although we incubated PASMCs for 72 hours, aiming to mimic chronic conditions, to assess the effect of CSE, hypoxia, and $ECVE^{-/+n}$ on vasoactive gene expression and mediator release, it remains critical to explore the chronic effect in PAECs. This is because when we tried to use a similar experimental condition as that used for PASMCs, cytotoxicity was observed in PAECs. Thus, a pilot study of an extended range of CSE concentration was conducted to determine the desired concentrations and duration of the treatment. As a result, we had to reduce the incubation time, as well as CSE concentrations.

Thirdly, we demonstrated that TXA_2 production was induced, possibly via COX-2 protein expression upregulation by CSE and hypoxia in PASMCs and by CSE in PAECs. In addition, the PASMC and PAEC proliferation was significantly and concentration-dependently inhibited by celecoxib and daltroban. These findings suggest that the anti-proliferative effect of celecoxib is most likely via the inhibition of CSE- and hypoxia-induced COX-2-derived proliferative mediator TXA_2 production. Although it is highly likely that the anti-proliferative effect of celecoxib was a result of the decrease in CSE-induced TXA_2 production, time restrictions prevented us from confirming our findings by assessing the effect of COX-2 inhibitor celecoxib on TXA_2 production and other prostanoid production.

Fourthly, although primary human PASMCs from three different healthy donors were used to explore the effect of CSE and hypoxia on vasoactive gene expression and mediator release, the role of altered release of individual vasoactive mediator in cell proliferation and apoptosis of human PASMCs was assessed using one line of primary PASMCs during the course of this project due to time restriction. In addition, only one line of primary PAECs, obtained from main pulmonary artery of one healthy donor, was used in this study. Thus, it is important to acknowledge that the effect could be limited to this cell line, as the responses of one cell line may be different from others. However, we were not able to further strengthen our findings in PAECs using a greater number of cell lines because cultured PAECs are difficult to grow and maintain. In addition, attempts to culture PAECs using DMEM+ (the same culture medium used for PASMCs) proved unsuccessful because of the fact that this type of cell must be maintained in a special culture medium. This makes obtaining a different line of PAECs from other suppliers difficult as it will result in using different culture mediums; consequently, leading to variations in the results.

Finally, we investigated the effect of $ECVE^{+/-n}$ on vasoactive gene expression and mediator release using unflavoured e-cig liquid to avoid confounders, and we found $ECVE^{+/-n}$ is unlikely to have similar effects as CSE does. However, we can not exclude the possibility that flavoured $ECVE^{+/-n}$ may have different effects as it has been suggested that most of the harmful effects of e-cig are likely caused by flavoured e-cig liquid (Kaur et al., 2018).

7.3 Future directions

- Previous histochemical and immunohistochemical studies suggest the interactions exist between PAECs and PASMCs in COPD-associated pulmonary hypertension. In future study, it would be of interest to explore the interactions between PASMCs and PAECs.
- Since the underlying molecular mechanism was not explored in this thesis, future studies focusing on investigating the mechanism responsible for the observations reported in the current study are needed.
- It would also be interesting to conduct further studies using PASMCs and PAECs from non-smokers, smokers with COPD, and smokers without COPD, as well as precision-cut lung slices to validate key findings in histological lung tissue samples from patients and animal model studies.

7.4 Concluding remarks

Pulmonary hypertension is a common and serious complication of COPD characterised by vascular remodelling as a result of proliferation of pulmonary artery cells. The findings outlined in this thesis provide evidence that CSE (but not $ECVE^{-/+n}$) and hypoxia to a lesser extent can alter the PGI_2/TXA_2 ratio (mainly as a result of the increased TXA_2 production) and the production of nitric oxide. In addition to the ability of TXA_2 receptor antagonist to inhibit cell proliferation via blocking enhanced TXA_2 production, the use of agents targeting prostanoids (e.g. stable PGI_2 analogue and selective COX-2 inhibitor) and nitric oxide donor can exert anti-proliferative effects, at least in part, by restoring the balance of vasoactive mediators. These findings suggest that targeting these disrupted pathways is likely to provide a potential therapeutic target for

pulmonary vascular remodelling in COPD-associated pulmonary hypertension. Data presented in this study also suggest that smoking cessation can be important therapeutic intervention for patients with COPD, as it may prevent further vascular alterations, caused by cigarette smoking.

Chapter 8. Appendix

8.1 Cell viability

8.1.1 Effect of CSE on the cell viability of human PASMCs and PAECs

As described in the materials and methods, section 2.4.1.1 that 10% CSE for PASMCs and 5% CSE for PAECs were excluded due to cytotoxicity. We selected the concentration range of CSE (0%, 1%, 2.5%, and 5% for PASMCs) and (0%, 1%, 2%, and 3% for PAECs). Cell viability assessed by MTT showed no significant difference between untreated and treated cells in response to different concentrations of CSE treatment in both PASMCs (Figure 8.1) and PAECs (Figure 8.2). Thus, CSE concentrations (0%-5% for PASMCs and 0%-3% for PAECs) were used for further experiments to assess the effect of CSE on the expression and mediator release of vasoactive genes.

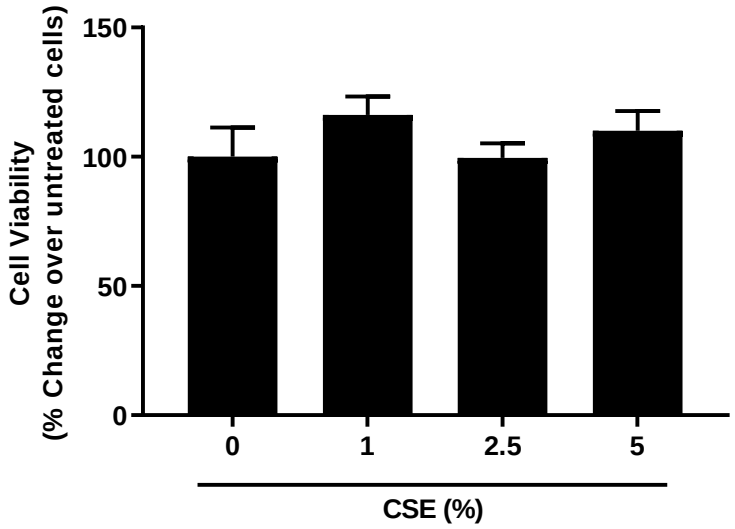


Figure 8.1 Effect of CSE on cell viability in human PASMCs.
Confluent human PASMCs were treated with different concentrations of CSE (0%, 1%, 2.5%, and 5%) for 48 h with daily fresh DMEM+ and CSE and then with the same concentrations of CSE in DMEM- for 24 h. Cell viability was assessed by MTT. Data were expressed as % change over untreated cells (0% CSE). Each data point represents mean ± SEM from three experiments using cells from three different donors.

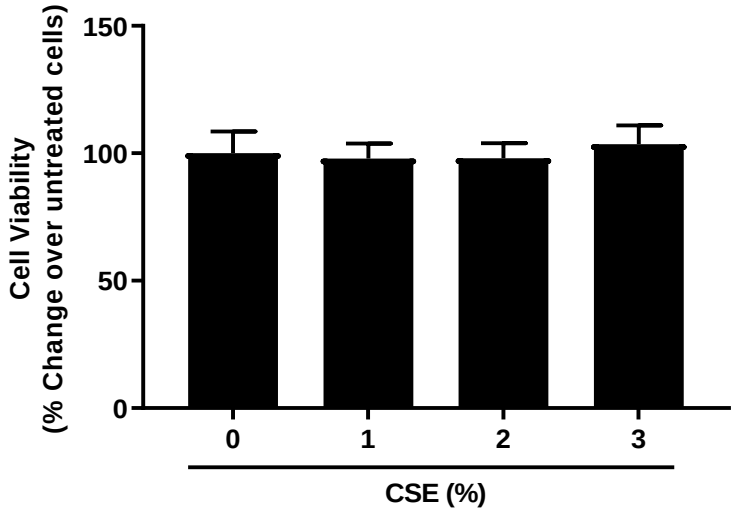


Figure 8.2 Effect of CSE on cell viability in human PAECs.
Confluent human PAECs were treated with different concentrations of CSE (0%, 1%, 2%, and 3%) for 24 h. Cell viability was assessed by MTT. Data were expressed as fold change over untreated cells (0% CSE). Each data point represents mean ± SEM from three experiments using one cell line.

8.1.2 Effect of hypoxia alone and in combination with CSE on the cell viability of human PASMCs and PAECs

As previously reported in Chapter 3, the CSE (0%-5% for PASMCs and 0%-3% for PAECs) were not toxic. PASMCs and PAECs were incubated with same concentrations of CSE under normoxic or hypoxic conditions for 72 h and 24 h, respectively. Cell viability was then assessed by MTT. The results showed that there was no significant difference between untreated and treated cells in response to CSE stimulation under both conditions in both human PASMCs (Figure 8.3) and PAECs (Figure 8.4). Thus, CSE concentrations (up to 5% for PASMCs and up to 3% for PAECs) under normoxic or hypoxic conditions were used to assess the effect of hypoxia alone and in combination with CSE on the expression and mediator release of vasoactive genes.

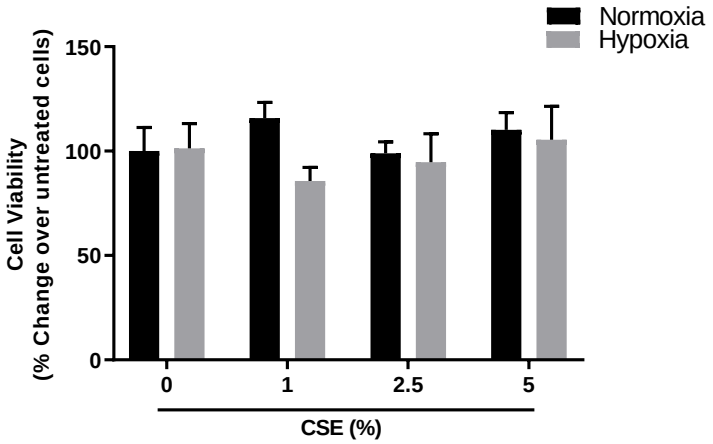


Figure 8.3 Effect of hypoxia and hypoxia+CSE on cell viability in human PASMCs.
Confluent human PASMCs were treated with different concentrations of CSE (0%, 1%, 2.5%, and 5%) under normoxic (21% O_2) or hypoxic (1% O_2) conditions for 48 h with daily fresh DMEM+ and CSE and then with the same concentrations of CSE under normoxic or hypoxic conditions in DMEM- for 24 h. Cell viability was assessed by MTT. Data were expressed as fold change over untreated cells (0% CSE). Each data point represents mean ± SEM from three experiments using cells from three different donors.

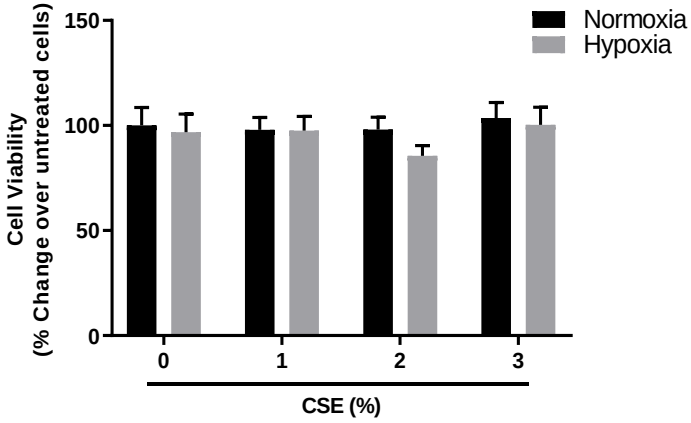


Figure 8.4 Effect of hypoxia and hypoxia+CSE on cell viability in human PAECs.
Confluent human PAECs were treated with different concentrations of CSE (0%, 1%, 2%, and 3%) under normoxic (21% O_2) or hypoxic (1% O_2) conditions for 24 h. Cell viability was assessed by MTT. Data were expressed as fold change over untreated cells (0% CSE). Each data point represents mean ± SEM from three experiments using one cell line.

8.1.3 Effect of ECVE$^{+/-n}$ on the cell viability of human PASMCs and PAECs

The effect of ECVE$^{+/-n}$ (0.1%, 0.25%, 0.5%, and 1%) treatment on cell viability was assessed by MTT assay. We found no significant difference between untreated and treated PASMCs with 0.1%, 0.25%, and 0.5% ECVE$^{+/-n}$. However, the cell viability was significantly reduced following treatment with 1% ECVE$^{+/-n}$ compared with control (Figure 8.5). PAEC stimulation with 0.1%, 0.25%, and 0.5% ECVE$^{+/-n}$ had no effect on the cell viability, whereas treatment with 1% ECVE$^{+/-n}$ markedly decreased the viability of PAECs compared with control (Figure 8.6). Then, 1% ECVE$^{+/-n}$ was excluded due to cell cytotoxicity and treatment with 0.1%, 0.25%, and 0.5% ECVE$^{+/-n}$ (for both PASMCs and PAECs) were used to explore the effect of ECVE$^{+/-n}$ on the expression and mediator release of vasoactive genes.

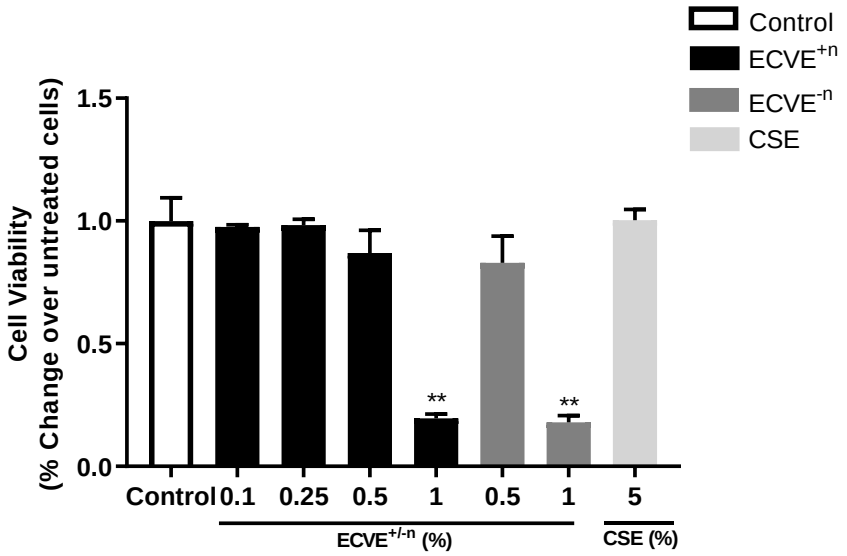


Figure 8.5 Effect of ECVE$^{+/-n}$ on cell viability in human PASMCs.
Confluent human PASMCs were treated with or without ECVE^{+n} (0.1%, 0.25%, 0.5%, and 1%), ECVE^{-n} (0.5% and 1%) and CSE (5%) for 48 h with daily fresh DMEM+ and ECVE$^{+/-n}$ or CSE and then with the same concentrations of ECVE$^{+/-n}$ or CSE in DMEM- for 24 h. Cell viability was assessed by MTT. Data were expressed as fold change over control. Each data point represents mean ± SEM from three experiments using cells from three different donors. **p<0.01 compared with control.

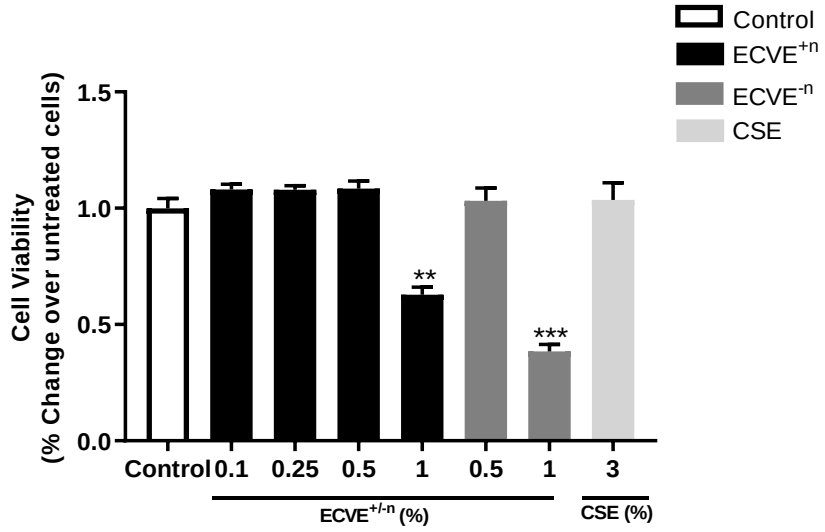


Figure 8.6 Effect of ECVE$^{+/-n}$ on cell viability in human PAECs.
Confluent human PAECs were treated with or without ECVE^{+n} (0.1%, 0.25%, 0.5%, and 1%), ECVE^{-n} (0.5% and 1%) and CSE (3%) for 24 h. Cell viability was then assessed by MTT. Data were expressed as fold change over control. Each data point represents mean ± SEM from three experiments using one cell line. **p<0.01, ***p<0.001 compared with control.

8.2 Housekeeping gene β2M

8.2.1 Effect of CSE on the mRNA of housekeeping gene β2M in human PASMCs and PAECs

We also tested the housekeeping gene β2M mRNA expression in response to CSE stimulation before the genes of interest were assessed. Our results showed that CSE treatment had no effect on the C_T value of β2M mRNA level compared with untreated cells in human PASMCs (Figure 8.7) and PAECs (Figure 8.8). The results indicate that β2M is a good housekeeping gene to be used for the current study. Therefore, β2M was used as a housekeeping gene for further experiments to assess the effect of CSE on the mRNA expression of vasoactive genes in both human PASMCs and PAECs.

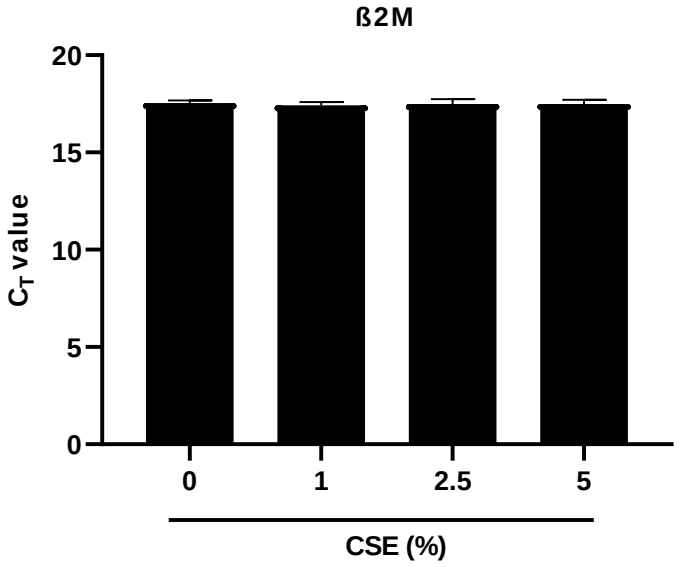


Figure 8.7 Effect of CSE on the mRNA expression of the housekeeping gene β2M in human PASMCs. Confluent human PASMCs were stimulated with different concentrations of CSE (0%, 1%, 2.5%, and 5%) for 48 h with daily fresh DMEM+ and CSE and then with the same concentrations of CSE in DMEM- for 24 h. Total RNA was isolated and the samples were then assayed for the mRNA expression of β2M using RT-qPCR. Data were expressed as a raw C_T value. Each data point represents mean ± SEM from three independent experiments using cells from three different donors.

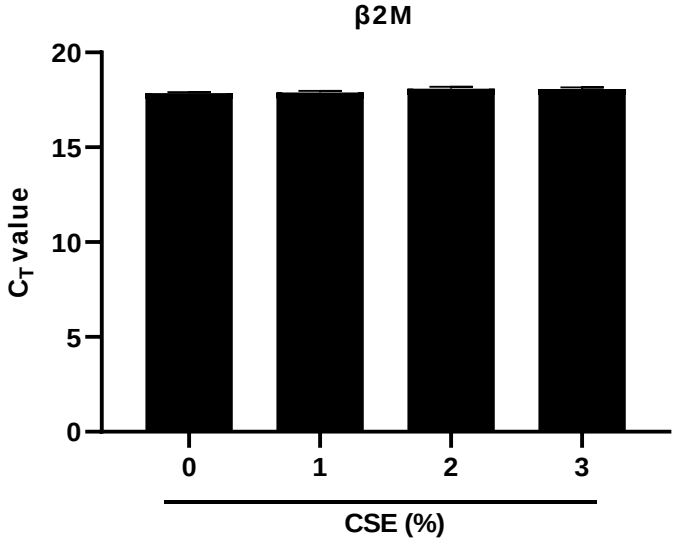


Figure 8.8 Effect of CSE on the mRNA expression of the housekeeping gene β2M in human PAECs. Confluent human PAECs were treated with different concentrations of CSE (0%, 1%, 2%, and 3%) for 24 h prior to total RNA isolation. The samples were assayed for the mRNA expression of β2M using RT-qPCR. Data were expressed as a raw C_T value. Each data point represents mean ± SEM from three independent experiments using one cell line.

8.2.2 Effect of hypoxia alone and in combination with CSE on the mRNA of housekeeping gene β2M in human PASMCs and PAECs

Next, the housekeeping gene β2M mRNA expression in response to CSE stimulation under normoxic or hypoxic conditions was evaluated in human PASMCs and PAECs before the genes of interest were tested. We found the mRNA expression of the reference gene β2M remained unaltered following cell stimulation with CSE under normoxic or hypoxic conditions in both human PASMCs (Figure 8.9) and PAECs (Figure 8.10) compared with untreated cells. Accordingly, β2M was used as a housekeeping gene to determine the effect of hypoxia alone and in combination with CSE on the mRNA expression of vasoactive genes in both human PASMCs and PAECs.

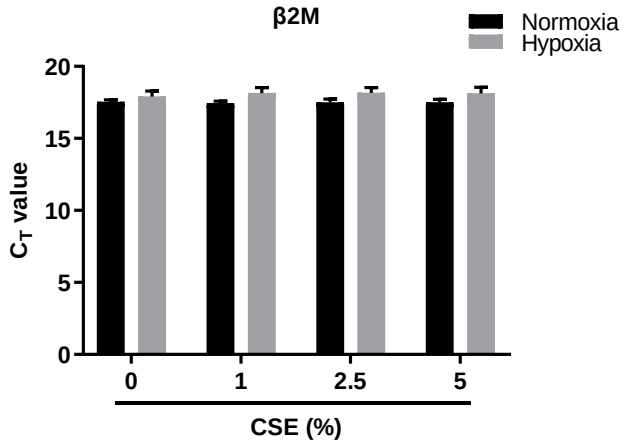


Figure 8.9 Effect of hypoxia and hypoxia+CSE on the mRNA expression of the housekeeping gene β2M in human PASMCs.
Confluent human PASMCs were stimulated with different concentrations of CSE (0%, 1%, 2.5%, and 5%) under normoxic (21% O_2) or hypoxic (1% O_2) conditions for 48 h with daily fresh DMEM+ and CSE daily, and then with the same concentrations of CSE under normoxic or hypoxic conditions in DMEM- for 24 h. Total RNA was isolated and the samples were then assayed for the mRNA expression of β2M using RT-qPCR. Data were expressed as a raw C_T value. Each data point represents mean ± SEM from three independent experiments using cells from three different donors.

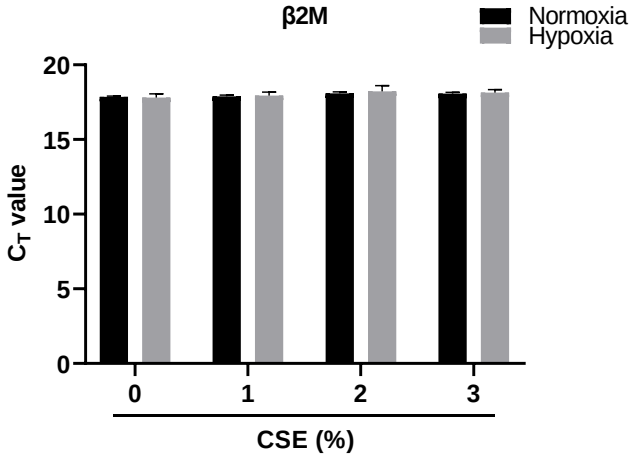


Figure 8.10 Effect of hypoxia and hypoxia+CSE on the mRNA expression of the housekeeping gene β2M in human PAECs.
Confluent human PAECs were treated with different concentrations of CSE (0%, 1%, 2%, and 3%) under normoxic (21% O_2) or hypoxic (1% O_2) conditions for 24 h prior to total RNA isolation. The samples were assayed for the mRNA expression of β2M using RT-qPCR. Data were expressed as a raw CT value. Each data point represents mean ± SEM from three independent experiments using one cell line.

8.2.3 Effect of ECVE$^{+/-n}$ on the mRNA of housekeeping gene β2M in human PASMCs and PAECs

The chosen ECVE$^{+/-n}$ concentrations were used to examine the housekeeping gene β2M mRNA expression following ECVE$^{+/-n}$ treatment before the genes of interest were assessed. It was found that cell stimulation with ECVE$^{+/-n}$ caused no significant changes on the C_T value of β2M mRNA levels compared with control in human PASMCs (Figure 8.11) and PAECs (Figure 8.12). Therefore, β2M was used as a housekeeping gene to assess the effect of ECVE$^{+/-n}$ on the mRNA expression of vasoactive genes in both human PASMCs and PAECs.

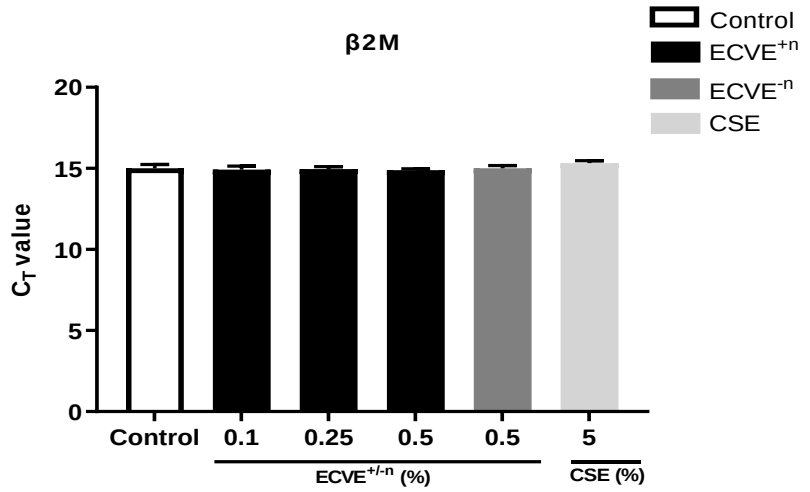


Figure 8.11 Effect of ECVE$^{+/-n}$ on the mRNA expression of the housekeeping gene β2M in human PASMCs.
Confluent human PASMCs were stimulated with or without ECVE^{+n} (0.1%, 0.25%, and 0.5%), ECVE^{-n} (0.5%) and CSE (5%) for 48 h with daily fresh DMEM+ and ECVE$^{+/-n}$ or CSE and then with the same concentrations of ECVE$^{+/-n}$ or CSE in DMEM- for 24 h. Total RNA was isolated and the samples were then assayed for the mRNA expression of β2M using RT-qPCR. Data were expressed as a raw C_T value. Each data point represents mean ± SEM from three independent experiments using cells from three different donors.

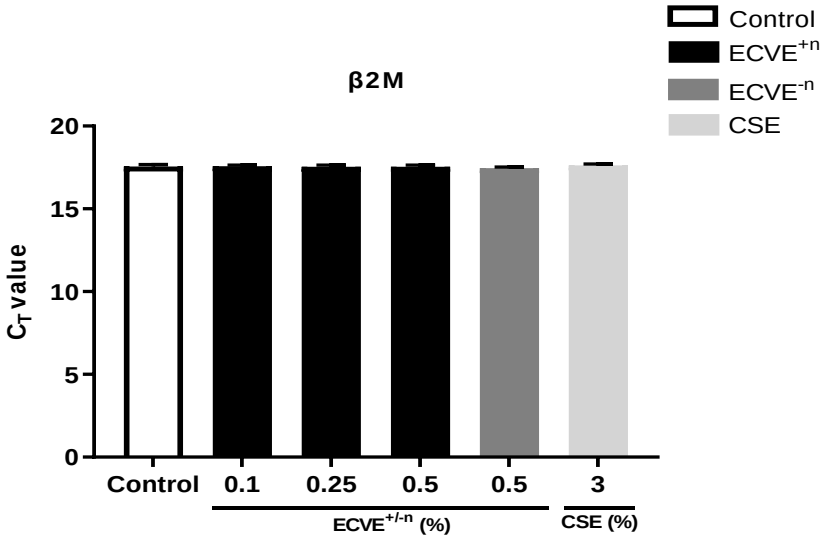


Figure 8.12 Effect of ECVE$^{+/-n}$ on the mRNA expression of the housekeeping gene β2M in human PAECs.
Confluent human PAECs were treated with or without ECVE^{+n} (0.1%, 0.25%, and 0.5%), ECVE^{-n} (0.5%) and CSE (3%) for 24 h prior to total RNA isolation. The samples were assayed for the mRNA expression of β2M using RT-qPCR. Data were expressed as a raw C_T value. Each data point represents mean ± SEM from three independent experiments using one cell line.

8.3 Direct correlation of human PASMCs with WST-1 assay

To assess the sensitivity of the WST-1 assay in our experimental setting, a cell titration experiment was conducted. Human PASMCs were seeded at various known densities (4000, 8000, 16000, 32000, and 64000 cell/well) in a 24-well plate and allowed to grow for 12 h. Then the WST-1 assay was used to determine cell viability as described in the materials and methods, section 2.11.1. The results showed that there is a direct correlation of the absorbance value to the number of metabolically active PASMCs in the culture ($R^2 = 0.9801$) as shown in Figure 8.13.

This observation suggests that cell proliferation reagent WST-1 can be used to estimate the number of viable cells in our experimental setting.

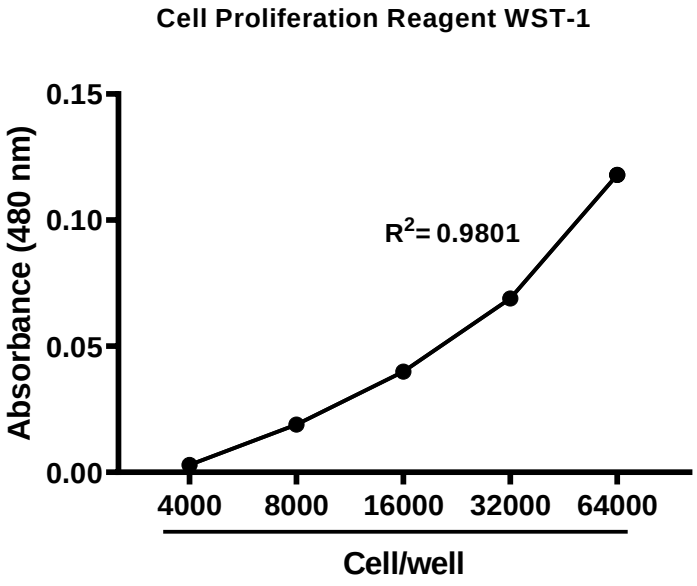


Figure 8.13 Correlation between known human PASMC density and WST-1 assay results.
Human PASMCs were seeded at various densities (4000, 8000, 16000, 32000, and 64000 cells/well) and allowed to grow in DMEM+ for 12 h. WST-1 was then conducted.

8.4 Materials

Hyperfilm ECL	Amersham Biosciences
PVDF membrane	BioRad

8.5 Reagents

Ammonium persulphate	Sigma-Aldrich
Amphotericin B	Sigma-Aldrich
Bis/Acrylamide	Sigma-Aldrich
Bovine serum albumin	Thermo Fisher Scientific
Bromophenol blue	Sigma-Aldrich
Deoxynucleotide triphosphates	Promega, USA
Dimethyl sulfoxide	Sigma-Aldrich
Dulbecco's modified eagle's medium	Sigma-Aldrich
ECL Western blotting detection reagent	Amersham Biosciences, UK
Ethanol	Sigma-Aldrich
Foetal bovine serum	Thermo Fisher Scientific
Glycerol	Sigma-Aldrich
Glycine	Sigma-Aldrich
Hydrochloric acid	Sigma-Aldrich
Hydrogen peroxide	Sigma-Aldrich
L-glutamine	Sigma-Aldrich
β-mercaptoethanol	Sigma-Aldrich
Methanol	Sigma-Aldrich
N,N,N′,N′-Tetramethylethylenediamine	Sigma-Aldrich
Non-fat dry milk	Santa Cruz Biotechnology, USA
NP40	Sigma-Aldrich
Penicillin/Streptomycin	Sigma-Aldrich
Phosphate buffered saline tablets	Sigma-Aldrich
Phenylmethanesulphonylfluoride	Sigma-Aldrich
Protease inhibitor cocktails	Sigma-Aldrich
Rainbow molecular weight marker	Amersham Biosciences
Sodium chloride	Sigma-Aldrich
Sodium dodecyl sulfate	Sigma-Aldrich
Sodium deoxycholate	Sigma-Aldrich
Sodium orthovanadate	Sigma-Aldrich
SYBR FAST qPCR Master Mix	Kapa Biosystems
Trizma base	Sigma-Aldrich
Trypsin-EDTA	Sigma-Aldrich
TWEEN 20	Sigma-Aldrich
Low-serum endothelial cell growth medium (LS-ECGM)	PromoCell

8.6 Antibodies

HRP Conjugated Secondary Antibody Cocktail	Abcam
Mouse anti-human COX-2 monoclonal antibody	Cayman Chemical
Prostaglandin E Synthase-1(microsomal) Monoclonal Antibody	Cayman Chemical
Mouse anti-human Prostaglandin I2 Synthase antibody	R&D Systems, UK
Mouse anti-human thromboxane synthase antibody	Novus Biologicals, USA
Mouse anti- human GAPDH monoclonal antibody	Santa Cruz, USA
Mouse anti-human NOS3 monoclonal Antibody	Santa Cruz
Polyclonal rabbit anti-mouse immunoglobulins/HRP antibody	Dako Group, USA
Primary Antibody Cocktail (pro/p17-caspase-3, cleaved PARP1, muscle actin)	Abcam

8.7 Kits

Annexin v Human ELISA Kit	Thermo Fisher Scientific
BCA Protein Assay Kit	Thermo Fisher Scientific
Endothelin ELISA Kit	Cayman Chemical
Cell Counting Kit-8	Sigma-Aldrich
Cell Proliferation Reagent WST-1	Sigma-Aldrich
Cayman's 6-keto $PGF_{1\alpha}$ ELISA Kit	Cayman Chemical
Nitrate/Nitrite Fluorometric Assay Kit	Cayman Chemical
Prostaglandin E_2 ELISA Kit -Monoclonal	Cayman Chemical
Thromboxane B_2 ELISA Kit	Cayman Chemical
High-Capacity cDNA Reverse Transcription Kit	Applied Biosystems
NucleoSpin RNA Extraction Kit	Macherey Nagel

8.8 Drugs

Beraprost sodium	Sigma-Aldrich Mass: 1 mg Molecular weight: 420.47 To make original stock of 0.05 M, dissolved in 47.56 µl DMSO
Bosentan hydrate	Sigma-Aldrich Mass: 10 mg Molecular weight: 569.63 To make original stock of 0.5 M,

	dissolved in 35.11 µl DMSO
Celecoxib	Sigma-Aldrich Mass: 5 mg Molecular weight: 381.37 To make original stock of 0.5 M, dissolved in 26.22 µl DMSO
Daltroban	Sigma-Aldrich Mass: 5 mg Molecular weight: 353.82 To make original stock of 0.5 M, dissolved in 28.26 µl DMSO
Sodium nitroprusside dihydrate	Sigma-Aldrich Mass: 25 g Molecular weight: 297.95 To make original stock of 0.5 M, dissolved in 671.25 µl cell culture medium
PF-03549184 (inhibitor of mPGES-1)	Sigma-Aldrich Mass: 5 mg Molecular weight: 461.32 To make original stock of 0.5 Molar, dissolved in 21.67 µl DMSO

8.9 Buffer recipes

Buffers	**Buffer Contents**
RIPA buffer	150 mM sodium chloride, 1.0% NP-40, 0.5% sodium deoxycholate, 0.1% Sodium dodecyl sulphate, 50 mM tris-HCL pH 8.0, and then the following additives were added to RIPA buffer for protein collection: 1mM sodium orthovanadate, 2 mM PMSF, 1mM protease inhibitor cocktail.
Buffer 1	1.5 M tris base, 0.4% SDS, and then pH was adjusted to 8.8 with concentrated hydrochloric acid in 100 ml dH_2O
Buffer 2	0.5 M tris base, 0.4% SDS, and then pH was adjusted to 6.8 with concentrated hydrochloric acid in 100 ml dH_2O
Blocking buffer	TBS-T (Tris-Buffered Saline with 0.1% Tween 20) with 5% non-fat dry milk.
10× Running buffer	0.2 M tris base, 1.91 M glycine, 1% SDS (sodium dodecyl sulfate) in 1 liters of dH_2O

	1× =900ml dH_2O+100ml of 10× Running buffer
10× Transfer buffer	0.2 M tris base, 1.91 M glycine. 1× =1400ml dH_2O+200ml of 10× Transfer buffer +400ml methanol
10× TBS-T buffer	0.2 M tris base, 87.6g sodium chloride, 10 ml Tween 20, and pH to be between 7.4-4.6 Finally, ddH_2O was added to make final volume of 1000 ml pH to be between 7.4-4.6 1× =900ml dH_2O+100ml of 10× TBS-T
10% Resolving gel	To make 4 gels: 13.32 ml of 30% bis/acrylamide 10.4 ml of buffer1 15.84 ml of ddH_2O 400 µl of 10% Ammonium persulfate 40 µl of Tetramethylethylenediamine (TEMED)
Stacking gel	To make 4 gels: 1.3 ml of 30% Bis/Acrylamide 2.5 ml of buffer1 6.1 ml of ddH_2O 50 µl of 10% Ammonium persulfate 10 µl of TEMED
4× Laemmli buffer	62.5 mM tris HCL PH 6.8 (prepared separately in 100 ml of ddH_2O), 4 ml 100% glycerol, 1% SDS, 0.01% bromophenol blue, and 7 ml ddH_2O
Carestream Kodak autoradiography GBX developer/fixer	Thermo Fisher Scientific Diluted in water ratio of 1:5
TXB_2, PGE_2, endothelin, and 6-keto $PGF_{1\alpha}$ ELISA washing buffers	ELISA washing buffers were prepared following the instructions of the manufacturer. 5 ml of concentrated (400×) wash buffer and 1 ml of polysorbate 20 were added to ddH_2O to final volume of 2 liters.
Annexin v human ELISA washing buffer	Following the instructions of the manufacturer, 50 ml of concentrated (20×) wash buffer was added to ddH_2O to final volume of 1000 ml to make wash buffer 1×.

8.10 Cell culture medium recipes

DMEM+	20% of FBS. 0.02% penicillin/streptomycin: (5000units of penicillin and 5mg of streptomycin/ml), sterile-filtered, BioReagent. 0.02% L-glutamine, (200mM solution), sterile-filtered, Bioxtra. 0.01% Amphotericin-B, 250 mg/ml, sterile-filtered, BioReagent.
DMEM-	0.5% of FBS. 0.02% penicillin/streptomycin: (5000units of penicillin and 5mg of streptomycin/ml), sterile-filtered. 0.02% L-glutamine, (200mM solution), sterile-filtered. 0.01% Amphotericin-B, 250 mg/ml, sterile-filtered.
LS-ECGM	0.02 ml /ml Foetal calf serum. 0.004 ml / ml Endothelial cell growth supplement. 0.1 ng/ml epidermal growth factor. 1 ng/ml basic fibroblast growth factor. 90 µg / ml heparin. 1 µg/ml hydrocortisone.

8.11 CSE and ECVE Materials

Kentucky Tobacco Research and Development Centre, University of Kentucky	3R4F research- grade cigarettes.
Vapor Vapes (Fully Licensed and FDA Compliant)	Unflavored e-cigarettes liquid 50%/50% mix of vegetable glycerine /propylene glycol 0 mg (nicotine free)

Vapor Vapes (Fully Licensed and FDA Compliant)	Unflavored e-cigarettes liquid 50/50 mix of vegetable glycerine /propylene glycol 24 mg of nicotine
SmokTech (Fully Licensed & FDA Compliant)	SMOK Alien 220 watts Mod Kit Voltage Range: 0.35-8.0V Power Range: 6-220W E-cigarettes liquid Capacity: 3ml
Charles Austen Pumps	DA7C pump

Chapter 9. References

ABMAN, S. H., HANSMANN, G., ARCHER, S. L., IVY, D. D., ADATIA, I., CHUNG, W. K., HANNA, B. D., ROSENZWEIG, E. B., RAJ, J. U., CORNFIELD, D., STENMARK, K. R., STEINHORN, R., THEBAUD, B., FINEMAN, J. R., KUEHNE, T., FEINSTEIN, J. A., FRIEDBERG, M. K., EARING, M., BARST, R. J., KELLER, R. L., KINSELLA, J. P., MULLEN, M., DETERDING, R., KULIK, T., MALLORY, G., HUMPL, T. & WESSEL, D. L. 2015. Pediatric Pulmonary Hypertension: Guidelines From the American Heart Association and American Thoracic Society. *Circulation,* 132**,** 2037-2099.

ADACHI, C., NARUSE, M., ISHIHARA, Y., TANABE, A., TAKAGI, S., YOSHIMOTO, T., NARUSE, K., KAGAWA, J. & TAKANO, K. 2000. Effects of acute and chronic cigarette smoking on the expression of endothelin-1 mRNA of the cardiovascular tissues in rats. *J Cardiovasc Pharmacol,* 36**,** S198-S200.

AGUSTI, A. G., BARBERA, J. A., ROCA, J., WAGNER, P. D., GUITART, R. & RODRIGUEZ-ROISIN, R. 1990. Hypoxic pulmonary vasoconstriction and gas exchange during exercise in chronic obstructive pulmonary disease. *Chest,* 97**,** 268-275.

ALDONYTE, R., BRANTLY, M., BLOCK, E., PATEL, J. & ZHANG, J. 2009. Nuclear localization of active matrix metalloproteinase-2 in cigarette smoke-exposed apoptotic endothelial cells. *Exp Lung Res,* 35**,** 59-75.

AN, J., LI, J. Q., WANG, T., LI, X. O., GUO, L. L., WAN, C., LIAO, Z. L., DONG, J. J., XU, D. & WEN, F. Q. 2013. Blocking of thromboxane A(2) receptor attenuates airway mucus hyperproduction induced by cigarette smoke. *Eur J Pharmacol,* 703**,** 11-17.

ANTONIEWICZ, L., BOSSON, J. A., KUHL, J., ABDEL-HALIM, S. M., KIESSLING, A., MOBARREZ, F. & LUNDBACK, M. 2016. Electronic cigarettes increase endothelial progenitor cells in the blood of healthy volunteers. *Atherosclerosis,* 255**,** 179-185.

ARCASOY, S. M., CHRISTIE, J. D., FERRARI, V. A., SUTTON, M. S., ZISMAN, D. A., BLUMENTHAL, N. P., POCHETTINO, A. & KOTLOFF, R. M. 2003. Echocardiographic assessment of pulmonary hypertension in patients with advanced lung disease. *Am J Respir Crit Care Med,* 167**,** 735-740.

ARCHER, S. L., MIKE, D., CROW, J., LONG, W. & WEIR, E. K. 1996. A placebo-controlled trial of prostacyclin in acute respiratory failure in COPD. *Chest,* 109**,** 750-755.

BADESCH, D. B., MCLAUGHLIN, V. V., DELCROIX, M., VIZZA, C. D., OLSCHEWSKI, H., SITBON, O. & BARST, R. J. 2004. Prostanoid therapy for pulmonary arterial hypertension. *J Am Coll Cardiol,* 43**,** 56S-61S.

BAI, Y., SUN, L., HU, S. & WEI, Y. 2011. Combination therapy in pulmonary arterial hypertension: a meta-analysis. *Cardiology,* 120**,** 157-165.

BARBERA, J. A. & BLANCO, I. 2009. Pulmonary hypertension in patients with chronic obstructive pulmonary disease: advances in pathophysiology and management. *Drugs,* 69**,** 1153-1171.

BARBERA, J. A., PEINADO, V. I. & SANTOS, S. 2003. Pulmonary hypertension in chronic obstructive pulmonary disease. *Eur Respir J,* 21**,** 892-905.

BARBERA, J. A., PEINADO, V. I., SANTOS, S., RAMIREZ, J., ROCA, J. & RODRIGUEZ-ROISIN, R. 2001. Reduced expression of endothelial nitric oxide

synthase in pulmonary arteries of smokers. *Am J Respir Crit Care Med,* 164**,** 709-713.

BARST, R. J. 2007. A review of pulmonary arterial hypertension: role of ambrisentan. *Vasc Health Risk Manag,* 3**,** 11-22.

BARST, R. J. 2008. Pulmonary hypertension: past, present and future. *Ann Thorac Med,* 3**,** 1-4.

BAZAN, I. S. & FARES, W. H. 2015. Pulmonary hypertension: diagnostic and therapeutic challenges. *Ther Clin Risk Manag,* 11**,** 1221-1233.

BLANCO, I., GIMENO, E., MUNOZ, P. A., PIZARRO, S., GISTAU, C., RODRIGUEZ-ROISIN, R., ROCA, J. & BARBERA, J. A. 2010. Hemodynamic and gas exchange effects of sildenafil in patients with chronic obstructive pulmonary disease and pulmonary hypertension. *Am J Respir Crit Care Med,* 181**,** 270-278.

BLANCO, I., SANTOS, S., GEA, J., GUELL, R., TORRES, F., GIMENO-SANTOS, E., RODRIGUEZ, D. A., VILARO, J., GOMEZ, B., ROCA, J. & BARBERA, J. A. 2013. Sildenafil to improve respiratory rehabilitation outcomes in COPD: a controlled trial. *Eur Respir J,* 42**,** 982-992.

BOGAARD, H. J. 2017. Hypoxic pulmonary vasoconstriction in COPD-associated pulmonary hypertension: been there, done that? *Eur Respir J,* 50**,** 1701191.

BONDURAND, N., DUFOUR, S. & PINGAULT, V. 2018. News from the endothelin-3/EDNRB signaling pathway: Role during enteric nervous system development and involvement in neural crest-associated disorders. *Dev Biol,* 444 Suppl 1**,** S156-S169.

BOURQUE, S. L., DAVIDGE, S. T. & ADAMS, M. A. 2011. The interaction between endothelin-1 and nitric oxide in the vasculature: new perspectives. *Am J Physiol Regul Integr Comp Physiol,* 300**,** R1288-R1295.

BOZIER, J., RUTTING, S., XENAKI, D., PETERS, M., ADCOCK, I. & OLIVER, B. G. 2019. Heightened response to e-cigarettes in COPD. *ERJ Open Res,* 5**,** 00192-2018.

BRADBURY, D. A., NEWTON, R., ZHU, Y. M., STOCKS, J., CORBETT, L., HOLLAND, E. D., PANG, L. H. & KNOX, A. J. 2002. Effect of bradykinin, TGF-beta1, IL-1beta, and hypoxia on COX-2 expression in pulmonary artery smooth muscle cells. *Am J Physiol Lung Cell Mol Physiol,* 283**,** L717-L725.

BURROWS, B., KETTEL, L. J., NIDEN, A. H., RABINOWITZ, M. & DIENER, C. F. 1972. Patterns of cardiovascular dysfunction in chronic obstructive lung disease. *N Engl J Med,* 286**,** 912-918.

CAMACHO, M., RODRIGUEZ, C., GUADALL, A., ALCOLEA, S., ORRIOLS, M., ESCUDERO, J. R., MARTINEZ-GONZALEZ, J. & VILA, L. 2011. Hypoxia upregulates PGI-synthase and increases PGI(2) release in human vascular cells exposed to inflammatory stimuli. *J Lipid Res,* 52**,** 720-731.

CAPORALE, A., LANGHAM, M. C., GUO, W., JOHNCOLA, A., CHATTERJEE, S. & WEHRLI, F. W. 2019. Acute Effects of Electronic Cigarette Aerosol Inhalation on Vascular Function Detected at Quantitative MRI. *Radiology,* 293**,** 97-106.

CARNEVALE, R., SCIARRETTA, S., VIOLI, F., NOCELLA, C., LOFFREDO, L., PERRI, L., PERUZZI, M., MARULLO, A. G., DE FALCO, E., CHIMENTI, I., VALENTI, V., BIONDI-ZOCCAI, G. & FRATI, G. 2016. Acute Impact of

Tobacco vs Electronic Cigarette Smoking on Oxidative Stress and Vascular Function. *Chest,* 150**,** 606-612.

CELLI, B. R., DECRAMER, M., WEDZICHA, J. A., WILSON, K. C., AGUSTI, A., CRINER, G. J., MACNEE, W., MAKE, B. J., RENNARD, S. I., STOCKLEY, R. A., VOGELMEIER, C., ANZUETO, A., AU, D. H., BARNES, P. J., BURGEL, P. R., CALVERLEY, P. M., CASANOVA, C., CLINI, E. M., COOPER, C. B., COXSON, H. O., DUSSER, D. J., FABBRI, L. M., FAHY, B., FERGUSON, G. T., FISHER, A., FLETCHER, M. J., HAYOT, M., HURST, J. R., JONES, P. W., MAHLER, D. A., MALTAIS, F., MANNINO, D. M., MARTINEZ, F. J., MIRAVITLLES, M., MEEK, P. M., PAPI, A., RABE, K. F., ROCHE, N., SCIURBA, F. C., SETHI, S., SIAFAKAS, N., SIN, D. D., SORIANO, J. B., STOLLER, J. K., TASHKIN, D. P., TROOSTERS, T., VERLEDEN, G. M., VERSCHAKELEN, J., VESTBO, J., WALSH, J. W., WASHKO, G. R., WISE, R. A., WOUTERS, E. F., ZUWALLACK, R. L. & RESEARCH, A. E. T. F. F. C. 2015. An Official American Thoracic Society/European Respiratory Society Statement: Research questions in chronic obstructive pulmonary disease. *Am J Respir Crit Care Med,* 191**,** e4-e27.

CHAITANYA, G. V., STEVEN, A. J. & BABU, P. P. 2010. PARP-1 cleavage fragments: signatures of cell-death proteases in neurodegeneration. *Cell Commun Signal,* 8**,** 31.

CHANNICK, R. N., SIMONNEAU, G., SITBON, O., ROBBINS, I. M., FROST, A., TAPSON, V. F., BADESCH, D. B., ROUX, S., RAINISIO, M., BODIN, F. & RUBIN, L. J. 2001. Effects of the dual endothelin-receptor antagonist bosentan in patients with pulmonary hypertension: a randomised placebo-controlled study. *Lancet,* 358**,** 1119-1123.

CHAOUAT, A., BUGNET, A. S., KADAOUI, N., SCHOTT, R., ENACHE, I., DUCOLONE, A., EHRHART, M., KESSLER, R. & WEITZENBLUM, E. 2005. Severe pulmonary hypertension and chronic obstructive pulmonary disease. *Am J Respir Crit Care Med,* 172**,** 189-194.

CHAOUAT, A., NAEIJE, R. & WEITZENBLUM, E. 2008. Pulmonary hypertension in COPD. *Eur Respir J,* 32**,** 1371-1385.

CHAOUAT, A., SAVALE, L., CHOUAID, C., TU, L., SZTRYMF, B., CANUET, M., MAITRE, B., HOUSSET, B., BRANDT, C., LE CORVOISIER, P., WEITZENBLUM, E., EDDAHIBI, S. & ADNOT, S. 2009. Role for interleukin-6 in COPD-related pulmonary hypertension. *Chest,* 136**,** 678-687.

CHATTERJEE, S., TAO, J. Q., JOHNCOLA, A., GUO, W., CAPORALE, A., LANGHAM, M. C. & WEHRLI, F. W. 2019. Acute exposure to e-cigarettes causes inflammation and pulmonary endothelial oxidative stress in nonsmoking, healthy young subjects. *Am J Physiol Lung Cell Mol Physiol,* 317**,** L155-L166.

CHEN, H. 2018. Role of thromboxane A2 signaling in endothelium-dependent contractions of arteries. *Prostaglandins Other Lipid Mediat,* 134**,** 32-37.

CHEN, L., YANG, G., XU, X., GRANT, G., LAWSON, J. A., BOHLOOLY, Y. M. & FITZGERALD, G. A. 2013. Cell selective cardiovascular biology of microsomal prostaglandin E synthase-1. *Circulation,* 127**,** 233-243.

CHEN, Y., CHEN, P., HANAOKA, M., DROMA, Y. & KUBO, K. 2008. Enhanced levels of prostaglandin E2 and matrix metalloproteinase-2 correlate with the severity of airflow limitation in stable COPD. *Respirology,* 13**,** 1014-1021.

CHEN, Y., HANAOKA, M., CHEN, P., DROMA, Y., VOELKEL, N. F. & KUBO, K. 2009. Protective effect of beraprost sodium, a stable prostacyclin analog, in the development of cigarette smoke extract-induced emphysema. *Am J Physiol Lung Cell Mol Physiol,* 296**,** L648-L656.

CHEN, Y., LUO, H., KANG, N., GUAN, C., LONG, Y., CAO, J., SHEN, Q., LI, J., YANG, M., PENG, H. & CHEN, P. 2012. Beraprost sodium attenuates cigarette smoke extract-induced apoptosis in vascular endothelial cells. *Mol Biol Rep,* 39**,** 10447-10457.

CHESTER, A. H. & YACOUB, M. H. 2014. The role of endothelin-1 in pulmonary arterial hypertension. *Glob Cardiol Sci Pract,* 2014**,** 62-78.

CHIDA, M. & VOELKEL, N. F. 1996. Effects of acute and chronic hypoxia on rat lung cyclooxygenase. *Am J Physiol,* 270**,** L872-L878.

CHRISTMAN, B. W., MCPHERSON, C. D., NEWMAN, J. H., KING, G. A., BERNARD, G. R., GROVES, B. M. & LOYD, J. E. 1992. An imbalance between the excretion of thromboxane and prostacyclin metabolites in pulmonary hypertension. *N Engl J Med,* 327**,** 70-75.

CHUNG, S., KIM, S. H., SEO, Y., KIM, S. K. & LEE, J. Y. 2017. Quantitative analysis of cell proliferation by a dye dilution assay: Application to cell lines and cocultures. *Cytometry A,* 91**,** 704-712.

CLAPP, L. H., FINNEY, P., TURCATO, S., TRAN, S., RUBIN, L. J. & TINKER, A. 2002. Differential effects of stable prostacyclin analogs on smooth muscle proliferation and cyclic AMP generation in human pulmonary artery. *Am J Respir Cell Mol Biol,* 26**,** 194-201.

COGGINS, M. P. & BLOCH, K. D. 2007. Nitric oxide in the pulmonary vasculature. *Arterioscler Thromb Vasc Biol,* 27**,** 1877-1885.

COMPEER, M. G., SUYLEN, D. P. L., HACKENG, T. M. & DE MEY, J. G. R. 2012. Endothelin-1 and -2: Two amino acids matter. *Life Sciences,* 91**,** 607-612.

COSENTINO, F., ETO, M., DE PAOLIS, P., VAN DER LOO, B., BACHSCHMID, M., ULLRICH, V., KOUROEDOV, A., DELLI GATTI, C., JOCH, H., VOLPE, M. & LUSCHER, T. F. 2003. High glucose causes upregulation of cyclooxygenase-2 and alters prostanoid profile in human endothelial cells: role of protein kinase C and reactive oxygen species. *Circulation,* 107**,** 1017-1023.

CROSSWHITE, P. & SUN, Z. 2014. Molecular mechanisms of pulmonary arterial remodeling. *Mol Med,* 20**,** 191-201.

DABRAL, S., TIAN, X., KOJONAZAROV, B., SAVAI, R., GHOFRANI, H. A., WEISSMANN, N., FLORIO, M., SUN, J., JONIGK, D., MAEGEL, L., GRIMMINGER, F., SEEGER, W., SAVAI PULLAMSETTI, S. & SCHERMULY, R. T. 2016. Notch1 signalling regulates endothelial proliferation and apoptosis in pulmonary arterial hypertension. *Eur Respir J,* 48**,** 1137-1149.

DAGOUASSAT, M., GAGLIOLO, J. M., CHRUSCIEL, S., BOURIN, M. C., DUPREZ, C., CARAMELLE, P., BOYER, L., HUE, S., STERN, J. B., VALIDIRE, P., LONGROIS, D., NOREL, X., DUBOIS-RANDE, J. L., LE GOUVELLO, S., ADNOT, S. & BOCZKOWSKI, J. 2013. The cyclooxygenase-2-prostaglandin E2

pathway maintains senescence of chronic obstructive pulmonary disease fibroblasts. *Am J Respir Crit Care Med,* 187**,** 703-714.

DAVI, G., BASILI, S., VIERI, M., CIPOLLONE, F., SANTARONE, S., ALESSANDRI, C., GAZZANIGA, P., CORDOVA, C. & VIOLI, F. 1997. Enhanced thromboxane biosynthesis in patients with chronic obstructive pulmonary disease. The Chronic Obstructive Bronchitis and Haemostasis Study Group. *Am J Respir Crit Care Med,* 156**,** 1794-1799.

DAVIE, N., HALEEN, S. J., UPTON, P. D., POLAK, J. M., YACOUB, M. H., MORRELL, N. W. & WHARTON, J. 2002. ET(A) and ET(B) receptors modulate the proliferation of human pulmonary artery smooth muscle cells. *Am J Respir Crit Care Med,* 165**,** 398-405.

DELANNOY, E., COURTOIS, A., FREUND-MICHEL, V., LEBLAIS, V., MARTHAN, R. & MULLER, B. 2010. Hypoxia-induced hyperreactivity of pulmonary arteries: role of cyclooxygenase-2, isoprostanes, and thromboxane receptors. *Cardiovasc Res,* 85**,** 582-592.

DESROCHES, A. & DENAULT, J. B. 2019. Caspase-7 uses RNA to enhance proteolysis of poly(ADP-ribose) polymerase 1 and other RNA-binding proteins. *Proc Natl Acad Sci U S A,* 116**,** 21521-21528.

DOMINGUEZ-FANDOS, D., VALDES, C., FERRER, E., PUIG-PEY, R., BLANCO, I., TURA-CEIDE, O., PAUL, T., PEINADO, V. I. & BARBERA, J. A. 2015. Sildenafil in a cigarette smoke-induced model of COPD in the guinea-pig. *Eur Respir J,* 46**,** 346-354.

DUBOIS, R. N., AWAD, J., MORROW, J., ROBERTS, L. J. & BISHOP, P. R. 1994. Regulation of eicosanoid production and mitogenesis in rat intestinal epithelial cells by transforming growth factor-alpha and phorbol ester. *Journal of Clinical Investigation,* 93**,** 493-498.

DUNLAP, B. & WEYER, G. 2016. Pulmonary Hypertension: Diagnosis and Treatment. *Am Fam Physician,* 94**,** 463-469.

EDDAHIBI, S., CHAOUAT, A., TU, L., CHOUAID, C., WEITZENBLUM, E., HOUSSET, B., MAITRE, B. & ADNOT, S. 2006. Interleukin-6 gene polymorphism confers susceptibility to pulmonary hypertension in chronic obstructive pulmonary disease. *Proc Am Thorac Soc,* 3**,** 475-476.

ELLIS, E. F., OELZ, O., ROBERTS, L. J., 2ND, PAYNE, N. A., SWEETMAN, B. J., NIES, A. S. & OATES, J. A. 1976. Coronary arterial smooth muscle contraction by a substance released from platelets: evidence that it is thromboxane A2. *Science,* 193**,** 1135-1137.

FAGAN, K. A., MCMURTRY, I. F. & RODMAN, D. M. 2001. Role of endothelin-1 in lung disease. *Respir Res,* 2**,** 90-101.

FAN, F., TIAN, H., GENG, J., DENG, J., LIU, Y., CHEN, C., ZHANG, S., ZHANG, Y., LI, J., TIAN, H., DART, A. M. & ZOU, Y. 2018. Mechanism of Beraprost Effects on Pulmonary Hypertension: Contribution of Cross-Binding to PGE2 Receptor 4 and Modulation of O2 Sensitive Voltage-Gated K(+) Channels. *Front Pharmacol,* 9**,** 1518.

FERRER, E., PEINADO, V. I., CASTANEDA, J., PRIETO-LLORET, J., OLEA, E., GONZALEZ-MARTIN, M. C., VEGA-AGAPITO, M. V., DIEZ, M., DOMINGUEZ-FANDOS, D., OBESO, A., GONZALEZ, C. & BARBERA, J. A.

2011. Effects of cigarette smoke and hypoxia on pulmonary circulation in the guinea pig. *Eur Respir J,* 38**,** 617-627.

FERRER, E., PEINADO, V. I., DIEZ, M., CARRASCO, J. L., MUSRI, M. M., MARTINEZ, A., RODRIGUEZ-ROISIN, R. & BARBERA, J. A. 2009. Effects of cigarette smoke on endothelial function of pulmonary arteries in the guinea pig. *Respir Res,* 10**,** 76.

FIKE, C. D., KAPLOWITZ, M. R., THOMAS, C. J. & NELIN, L. D. 1998. Chronic hypoxia decreases nitric oxide production and endothelial nitric oxide synthase in newborn pig lungs. *Am J Physiol,* 274**,** L517-L526.

FIKE, C. D., KAPLOWITZ, M. R., ZHANG, Y. & PFISTER, S. L. 2005. Cyclooxygenase-2 and an early stage of chronic hypoxia-induced pulmonary hypertension in newborn pigs. *J Appl Physiol* 98**,** 1111-1118.

FISHER, M. R., CRINER, G. J., FISHMAN, A. P., HASSOUN, P. M., MINAI, O. A., SCHARF, S. M., FESSLER, H. E. & GROUP, N. R. 2007. Estimating pulmonary artery pressures by echocardiography in patients with emphysema. *Eur Respir J,* 30**,** 914-921.

FISHER, M. R., FORFIA, P. R., CHAMERA, E., HOUSTEN-HARRIS, T., CHAMPION, H. C., GIRGIS, R. E., CORRETTI, M. C. & HASSOUN, P. M. 2009. Accuracy of Doppler echocardiography in the hemodynamic assessment of pulmonary hypertension. *Am J Respir Crit Care Med,* 179**,** 615-621.

FISHMAN, A. P. 2001. Clinical classification of pulmonary hypertension. *Clin Chest Med,* 22**,** 385-391.

FOSHAT, M. & BOROUMAND, N. 2017. The Evolving Classification of Pulmonary Hypertension. *Arch Pathol Lab Med,* 141**,** 696-703.

FUKURODA, T., KOBAYASHI, M., OZAKI, S., YANO, M., MIYAUCHI, T., ONIZUKA, M., SUGISHITA, Y., GOTO, K. & NISHIKIBE, M. 1994. Endothelin receptor subtypes in human versus rabbit pulmonary arteries. *J Appl Physiol (1985),* 76**,** 1976-1982.

GALIE, N., HINDERLITER, A. L., TORBICKI, A., FOURME, T., SIMONNEAU, G., PULIDO, T., ESPINOLA-ZAVALETA, N., ROCCHI, G., MANES, A., FRANTZ, R., KURZYNA, M., NAGUEH, S. F., BARST, R., CHANNICK, R., DUJARDIN, K., KRONENBERG, A., LECONTE, I., RAINISIO, M. & RUBIN, L. 2003. Effects of the oral endothelin-receptor antagonist bosentan on echocardiographic and doppler measures in patients with pulmonary arterial hypertension. *J Am Coll Cardiol,* 41**,** 1380-1386.

GALIE, N., HUMBERT, M., VACHIERY, J. L., GIBBS, S., LANG, I., TORBICKI, A., SIMONNEAU, G., PEACOCK, A., VONK NOORDEGRAAF, A., BEGHETTI, M., GHOFRANI, A., GOMEZ SANCHEZ, M. A., HANSMANN, G., KLEPETKO, W., LANCELLOTTI, P., MATUCCI, M., MCDONAGH, T., PIERARD, L. A., TRINDADE, P. T., ZOMPATORI, M., HOEPER, M. & GROUP, E. S. C. S. D. 2016. 2015 ESC/ERS Guidelines for the diagnosis and treatment of pulmonary hypertension: The Joint Task Force for the Diagnosis and Treatment of Pulmonary Hypertension of the European Society of Cardiology (ESC) and the European Respiratory Society (ERS): Endorsed by: Association for European Paediatric and Congenital Cardiology (AEPC), International Society for Heart and Lung Transplantation (ISHLT). *Eur Heart J,* 37**,** 67-119.

GALIE, N., HUMBERT, M., VACHIERY, J. L., VIZZA, C. D., KNEUSSL, M., MANES, A., SITBON, O., TORBICKI, A., DELCROIX, M., NAEIJE, R., HOEPER, M., CHAOUAT, A., MORAND, S., BESSE, B., SIMONNEAU, G., ARTERIAL PULMONARY, H. & BERAPROST EUROPEAN STUDY, G. 2002. Effects of beraprost sodium, an oral prostacyclin analogue, in patients with pulmonary arterial hypertension: a randomized, double-blind, placebo-controlled trial. *J Am Coll Cardiol,* 39**,** 1496-1502.

GALIE, N., MANES, A. & BRANZI, A. 2004. The endothelin system in pulmonary arterial hypertension. *Cardiovasc Res,* 61**,** 227-237.

GALIE, N., RUBIN, L., HOEPER, M., JANSA, P., AL-HITI, H., MEYER, G., CHIOSSI, E., KUSIC-PAJIC, A. & SIMONNEAU, G. 2008. Treatment of patients with mildly symptomatic pulmonary arterial hypertension with bosentan (EARLY study): a double-blind, randomised controlled trial. *Lancet,* 371**,** 2093-2100.

GERACI, M. W., GAO, B., SHEPHERD, D. C., MOORE, M. D., WESTCOTT, J. Y., FAGAN, K. A., ALGER, L. A., TUDER, R. M. & VOELKEL, N. F. 1999. Pulmonary prostacyclin synthase overexpression in transgenic mice protects against development of hypoxic pulmonary hypertension. *Journal of Clinical Investigation,* 103**,** 1509-1515.

GIAID, A. & SALEH, D. 1995. Reduced expression of endothelial nitric oxide synthase in the lungs of patients with pulmonary hypertension. *N Engl J Med,* 333**,** 214-221.

GIAID, A., YANAGISAWA, M., LANGLEBEN, D., MICHEL, R. P., LEVY, R., SHENNIB, H., KIMURA, S., MASAKI, T., DUGUID, W. P. & STEWART, D. J. 1993. Expression of endothelin-1 in the lungs of patients with pulmonary hypertension. *N Engl J Med,* 328**,** 1732-1739.

GINOUVES, M., CARME, B., COUPPIE, P. & PREVOT, G. 2014. Comparison of tetrazolium salt assays for evaluation of drug activity against Leishmania spp. *J Clin Microbiol,* 52**,** 2131-2138.

GOBEIL, S., BOUCHER, C. C., NADEAU, D. & POIRIER, G. G. 2001. Characterization of the necrotic cleavage of poly(ADP-ribose) polymerase (PARP-1): implication of lysosomal proteases. *Cell Death Differ,* 8**,** 588-594.

GOLOGANU, D., STANESCU, C., URSICA, T., BALEA, M. I., IONITA, D. & BOGDAN, M. A. 2013. Prevalence and Characteristics of Pulmonary Hypertension Associated with COPD - A Pilot Study in Patients Referred to a Pulmonary Rehabilitation Program Clinic. *Maedica (Buchar),* 8**,** 243-248.

GOLPON, H. A., FADOK, V. A., TARASEVICIENE-STEWART, L., SCERBAVICIUS, R., SAUER, C., WELTE, T., HENSON, P. M. & VOELKEL, N. F. 2004. Life after corpse engulfment: phagocytosis of apoptotic cells leads to VEGF secretion and cell growth. *FASEB J,* 18**,** 1716-1718.

GOMBERG-MAITLAND, M. & OLSCHEWSKI, H. 2008. Prostacyclin therapies for the treatment of pulmonary arterial hypertension. *Eur Respir J,* 31**,** 891-901.

GOMEZ, I., FOUDI, N., LONGROIS, D. & NOREL, X. 2013. The role of prostaglandin E2 in human vascular inflammation. *Prostaglandins Leukot Essent Fatty Acids,* 89**,** 55-63.

GRIMMINGER, J., GHOFRANI, H. A., WEISSMANN, N., KLOSE, H. & GRIMMINGER, F. 2016. COPD-associated pulmonary hypertension: clinical implications and current methods for treatment. *Expert Rev Respir Med,* 7**,** 755-766.

HAMPL, V., BIBOVA, J., BANASOVA, A., UHLIK, J., MIKOVA, D., HNILICKOVA, O., LACHMANOVA, V. & HERGET, J. 2006. Pulmonary vascular iNOS induction participates in the onset of chronic hypoxic pulmonary hypertension. *Am J Physiol Lung Cell Mol Physiol,* 290**,** L11-L20.

HERSH, C. P., DEMEO, D. L., AL-ANSARI, E., CAREY, V. J., REILLY, J. J., GINNS, L. C. & SILVERMAN, E. K. 2004. Predictors of survival in severe, early onset COPD. *Chest,* 126**,** 1443-1451.

HIGHAM, A., BOSTOCK, D., BOOTH, G., DUNGWA, J. V. & SINGH, D. 2018. The effect of electronic cigarette and tobacco smoke exposure on COPD bronchial epithelial cell inflammatory responses. *Int J Chron Obstruct Pulmon Dis,* 13**,** 989-1000.

HIGHAM, A., RATTRAY, N. J., DEWHURST, J. A., TRIVEDI, D. K., FOWLER, S. J., GOODACRE, R. & SINGH, D. 2016. Electronic cigarette exposure triggers neutrophil inflammatory responses. *Respir Res,* 17**,** 56.

HIRATA, Y., EMORI, T., EGUCHI, S., KANNO, K., IMAI, T., OHTA, K. & MARUMO, F. 1993. Endothelin receptor subtype B mediates synthesis of nitric oxide by cultured bovine endothelial cells. *J Clin Invest,* 91**,** 1367-1373.

HIREMATH, J., THANIKACHALAM, S., PARIKH, K., SHANMUGASUNDARAM, S., BANGERA, S., SHAPIRO, L., POTT, G. B., VNENCAK-JONES, C. L., ARNESON, C., WADE, M., WHITE, R. J. & GROUP, T. S. 2010. Exercise improvement and plasma biomarker changes with intravenous treprostinil therapy for pulmonary arterial hypertension: a placebo-controlled trial. *J Heart Lung Transplant,* 29**,** 137-149.

HIRENALLUR, S. D., DETWEILER, N. D., HAWORTH, S. T., LEMING, J. T., GORDON, J. B. & RUSCH, N. J. 2012. Furegrelate, a thromboxane synthase inhibitor, blunts the development of pulmonary arterial hypertension in neonatal piglets. *Pulm Circ,* 2**,** 193-200.

HIROKAWA, K., O'SHAUGHNESSY, K. M., RAMRAKHA, P. & WILKINS, M. R. 1994. Inhibition of nitric oxide synthesis in vascular smooth muscle by retinoids. *Br J Pharmacol,* 113**,** 1448-1454.

HISADA, T., AYAORI, M., OHRUI, N., NAKASHIMA, H., NAKAYA, K., UTO-KONDO, H., YAKUSHIJI, E., TAKIGUCHI, S., TERAO, Y., MIYAMOTO, Y., ADACHI, T., NAKAMURA, H., OHSUZU, F., IKEWAKI, K. & SAKURAI, Y. 2012. Statin inhibits hypoxia-induced endothelin-1 via accelerated degradation of HIF-1alpha in vascular smooth muscle cells. *Cardiovasc Res,* 95**,** 251-259.

HO, T., CUSACK, R. P., CHAUDHARY, N., SATIA, I. & KURMI, O. P. 2019. Under- and over-diagnosis of COPD: a global perspective. *Breathe (Sheff),* 15**,** 24-35.

HOEPER, M. M. 2008. Treating pulmonary hypertension in COPD: where do we start? *Eur Respir J,* 32**,** 541-542.

HUMBERT, M., LAU, E. M., MONTANI, D., JAIS, X., SITBON, O. & SIMONNEAU, G. 2014. Advances in therapeutic interventions for patients with pulmonary arterial hypertension. *Circulation,* 130**,** 2189-2208.

HUMBERT, M., MONTI, G., BRENOT, F., SITBON, O., PORTIER, A., GRANGEOT-KEROS, L., DUROUX, P., GALANAUD, P., SIMONNEAU, G. & EMILIE, D. 1995. Increased interleukin-1 and interleukin-6 serum concentrations in severe primary pulmonary hypertension. *Am J Respir Crit Care Med,* 151**,** 1628-1631.

IGLARZ, M., STEINER, P., WANNER, D., REY, M., HESS, P. & CLOZEL, M. 2015. Vascular Effects of Endothelin Receptor Antagonists Depends on Their Selectivity for ETA Versus ETB Receptors and on the Functionality of Endothelial ETB Receptors. *J Cardiovasc Pharmacol,* 66**,** 332-337.

ITOH, A., NISHIHIRA, J., MAKITA, H., MIYAMOTO, K., YAMAGUCHI, E. & NISHIMURA, M. 2003. Effects of IL-1beta, TNF-alpha, and macrophage migration inhibitory factor on prostacyclin synthesis in rat pulmonary artery smooth muscle cells. *Respirology,* 8**,** 467-472.

JAEN, R. I., PRIETO, P., CASADO, M., MARTIN-SANZ, P. & BOSCA, L. 2018. Post-translational modifications of prostaglandin-endoperoxide synthase 2 in colorectal cancer: An update. *World J Gastroenterol,* 24**,** 5454-5461.

JANICKE, R. U., NG, P., SPRENGART, M. L. & PORTER, A. G. 1998. Caspase-3 is required for alpha-fodrin cleavage but dispensable for cleavage of other death substrates in apoptosis. *J Biol Chem,* 273**,** 15540-15545.

JEREMY, J. Y., ROWE, D., EMSLEY, A. M. & NEWBY, A. C. 1999. Nitric oxide and the proliferation of vascular smooth muscle cells. *Cardiovasc Res,* 43**,** 580-594.

JOHN, M., MCKEEVER, T. M., HADDAD, M. A., HALL, I. P., SAYERS, I., COCKCROFT, J. R. & BOLTON, C. E. 2016. Traditional and emerging indicators of cardiovascular risk in chronic obstructive pulmonary disease. *Chron Respir Dis,* 13**,** 247-255.

JONES, D. A., BENJAMIN, C. W. & LINSEMAN, D. A. 1995. Activation of thromboxane and prostacyclin receptors elicits opposing effects on vascular smooth muscle cell growth and mitogen-activated protein kinase signaling cascades. *Mol Pharmacol,* 48**,** 890-896.

JYOTHULA, S. & SAFDAR, Z. 2009. Update on pulmonary hypertension complicating chronic obstructive pulmonary disease. *International Journal of Chronic Obstructive Pulmonary Disease,* 4**,** 351-363.

KADOWAKI, M., MIZUNO, S., DEMURA, Y., AMESHIMA, S., MIYAMORI, I. & ISHIZAKI, T. 2007. Effect of hypoxia and Beraprost sodium on human pulmonary arterial smooth muscle cell proliferation: the role of p27kip1. *Respir Res,* 8**,** 77.

KAMAL, R., SRIVASTAVA, A. K. & KESAVACHANDRAN, C. N. 2015. Meta-analysis approach to study the prevalence of chronic obstructive pulmonary disease among current, former and non-smokers. *Toxicol Rep,* 2**,** 1064-1074.

KATIYAR, V. & KHARE, R. 2018. Prevalence of pulmonary hypertension in COPD. *International Journal of Advances in Medicine,* 5**,** 356-360.

KAUR, G., MUTHUMALAGE, T. & RAHMAN, I. 2018. Mechanisms of toxicity and biomarkers of flavoring and flavor enhancing chemicals in emerging tobacco and non-tobacco products. *Toxicol Lett,* 288**,** 143-155.

KAWABE, J., USHIKUBI, F. & HASEBE, N. 2010. Prostacyclin in vascular diseases. - Recent insights and future perspectives. *Circ J,* 74**,** 836-843.

KAWAKAMI, T., KANAZAWA, H., SATOH, T., IEDA, M., IEDA, Y., KIMURA, K., MOCHIZUKI, H., SHIMADA, T., YOKOYAMA, C., OGAWA, S., TANABE, T. & FUKUDA, K. 2007. AAV-PGIS gene transfer improves hypoxia-induced pulmonary hypertension in mice. *Biochemical and biophysical research communications,* 363**,** 656-661.

KAWUT, S. M., BAGIELLA, E., SHIMBO, D., LEDERER, D. J., AL-NAAMANI, N., ROBERTS, K. E., BARR, R. G., POST, W., HORN, E. M., TRACY, R., HASSOUN, P., GIRGIS, R. & GROUP, A.-S. S. 2011. Rationale and design of a phase II clinical trial of aspirin and simvastatin for the treatment of pulmonary arterial hypertension: ASA-STAT. *Contemp Clin Trials,* 32**,** 280-287.

KLINGER, J. R., ABMAN, S. H. & GLADWIN, M. T. 2013. Nitric oxide deficiency and endothelial dysfunction in pulmonary arterial hypertension. *Am J Respir Crit Care Med,* 188**,** 639-646.

KOBLIZEK, V., NOVOTNA, B., ZBOZINKOVA, Z. & HEJDUK, K. 2016. Diagnosing COPD: advances in training and practice - a systematic review. *Adv Med Educ Pract,* 7**,** 219-231.

KOHLMEIER, F., MAYA-MENDOZA, A. & JACKSON, D. A. 2013. EdU induces DNA damage response and cell death in mESC in culture. *Chromosome Res,* 21**,** 87-100.

KOWALCZYK, A., KLENIEWSKA, P., KOLODZIEJCZYK, M., SKIBSKA, B. & GORACA, A. 2015. The role of endothelin-1 and endothelin receptor antagonists in inflammatory response and sepsis. *Arch Immunol Ther Exp (Warsz),* 63**,** 41-52.

KUNICHIKA, N., LANDSBERG, J. W., YU, Y., KUNICHIKA, H., THISTLETHWAITE, P. A., RUBIN, L. J. & YUAN, J. X. 2004. Bosentan inhibits transient receptor potential channel expression in pulmonary vascular myocytes. *Am J Respir Crit Care Med,* 170**,** 1101-1107.

KUNTIC, M., OELZE, M., STEVEN, S., KROLLER-SCHON, S., STAMM, P., KALINOVIC, S., FRENIS, K., VUJACIC-MIRSKI, K., BAYO JIMENEZ, M. T., KVANDOVA, M., FILIPPOU, K., AL ZUABI, A., BRUCKL, V., HAHAD, O., DAUB, S., VARVERI, F., GORI, T., HUESMANN, R., HOFFMANN, T., SCHMIDT, F. P., KEANEY, J. F., DAIBER, A. & MUNZEL, T. 2019. Short-term e-cigarette vapour exposure causes vascular oxidative stress and dysfunction: evidence for a close connection to brain damage and a key role of the phagocytic NADPH oxidase (NOX-2). *Eur Heart J***,** pii: ehz772.

KYLHAMMAR, D. & RADEGRAN, G. 2012. Cyclooxygenase-2 inhibition and thromboxane A(2) receptor antagonism attenuate hypoxic pulmonary vasoconstriction in a porcine model. *Acta Physiol (Oxf),* 205**,** 507-519.

LABONTE, J., BROCHU, I., SIMARD, E. & D'ORLEANS-JUSTE, P. 2008. Distinct modulation of the endothelin-1 pathway in iNOS-/- and eNOS-/- mice. *Can J Physiol Pharmacol,* 86**,** 516-525.

LANG, I. M. & GAINE, S. P. 2015. Recent advances in targeting the prostacyclin pathway in pulmonary arterial hypertension. *Eur Respir Rev,* 24**,** 630-641.

LAYDEN, J. E., GHINAI, I., PRAY, I., KIMBALL, A., LAYER, M., TENFORDE, M., NAVON, L., HOOTS, B., SALVATORE, P. P., ELDERBROOK, M., HAUPT, T., KANNE, J., PATEL, M. T., SAATHOFF-HUBER, L., KING, B. A., SCHIER, J. G., MIKOSZ, C. A. & MEIMAN, J. 2019. Pulmonary Illness Related

to E-Cigarette Use in Illinois and Wisconsin - Preliminary Report. *N Engl J Med,* 10**,** 903-916.

LEDERER, D. J., BARTELS, M. N., SCHLUGER, N. W., BROGAN, F., JELLEN, P., THOMASHOW, B. M. & KAWUT, S. M. 2012. Sildenafil for chronic obstructive pulmonary disease: a randomized crossover trial. *COPD,* 9**,** 268-275.

LEE, S. D., LEE, D. S., CHUN, Y. G., SHIM, T. S., LIM, C. M., KOH, Y., KIM, W. S., KIM, D. S. & KIM, W. D. 2001. Cigarette smoke extract induces endothelin-1 via protein kinase C in pulmonary artery endothelial cells. *Am J Physiol Lung Cell Mol Physiol,* 281**,** L403-L411.

LEHNERS, M., DOBROWINSKI, H., FEIL, S. & FEIL, R. 2018. cGMP Signaling and Vascular Smooth Muscle Cell Plasticity. *J Cardiovasc Dev Dis,* 5**,** 20.

LI, X., PENG, K., ZHOU, Y., DENG, F. & MA, J. 2016. Inhibitory effect of Bailing capsule on hypoxia-induced proliferation of rat pulmonary arterial smooth muscle cells. *Saudi Med J,* 37**,** 498-505.

LI, Y., PU, G., CHEN, C. & YANG, L. 2015. Inhibition of FHL1 inhibits cigarette smoke extract-induced proliferation in pulmonary arterial smooth muscle cells. *Mol Med Rep,* 12**,** 3801-3808.

LIOU, J. Y., SHYUE, S. K., TSAI, M. J., CHUNG, C. L., CHU, K. Y. & WU, K. K. 2000. Colocalization of prostacyclin synthase with prostaglandin H synthase-1 (PGHS-1) but not phorbol ester-induced PGHS-2 in cultured endothelial cells. *J Biol Chem,* 275**,** 15314-15320.

LIU, G., HAO, P., XU, J., WANG, L., WANG, Y., HAN, R., YING, M., SUI, S., LIU, J. & LI, X. 2018. Upregulation of microRNA-17-5p contributes to hypoxia-induced proliferation in human pulmonary artery smooth muscle cells through modulation of p21 and PTEN. *Respir Res,* 19**,** 200.

LUNDEQUIST, A., NALLAMSHETTY, S. N., XING, W., FENG, C., LAIDLAW, T. M., UEMATSU, S., AKIRA, S. & BOYCE, J. A. 2010. Prostaglandin E(2) exerts homeostatic regulation of pulmonary vascular remodeling in allergic airway inflammation. *J Immunol,* 184**,** 433-441.

MACNEE, W. 2005. Pathogenesis of chronic obstructive pulmonary disease. *Proc Am Thorac Soc,* 2**,** 258-266.

MAHMOOD, T. & YANG, P. C. 2012. Western blot: technique, theory, and trouble shooting. *N Am J Med Sci,* 4**,** 429-434.

MAJED, B. H. & KHALIL, R. A. 2012. Molecular mechanisms regulating the vascular prostacyclin pathways and their adaptation during pregnancy and in the newborn. *Pharmacol Rev,* 64**,** 540-582.

MAKINO, A., FIRTH, A. L. & YUAN, J. X. 2011. Endothelial and smooth muscle cell ion channels in pulmonary vasoconstriction and vascular remodeling. *Compr Physiol,* 1**,** 1555-1602.

MANNINO, D. M. 2006. Underdiagnosed chronic obstructive pulmonary disease in England: new country, same story. *Thorax,* 61**,** 1032-1034.

MANNINO, D. M., HIGUCHI, K., YU, T. C., ZHOU, H., LI, Y., TIAN, H. & SUH, K. 2015. Economic Burden of COPD in the Presence of Comorbidities. *Chest,* 148**,** 138-150.

MARKEWITZ, B. A., FARRUKH, I. S., CHEN, Y., LI, Y. & MICHAEL, J. R. 2001. Regulation of endothelin-1 synthesis in human pulmonary arterial smooth muscle

cells. Effects of transforming growth factor-beta and hypoxia. *Cardiovasc Res,* 49**,** 200-206.

MARKEWITZ, B. A., KOHAN, D. E. & MICHAEL, J. R. 1995. Hypoxia decreases endothelin-1 synthesis by rat lung endothelial cells. *Am J Physiol,* 269**,** L215-L220.

MARTIN, E. M. & JONES, S. L. 2017. Inhibition of microsomal prostaglandin E-synthase-1 (mPGES-1) selectively suppresses PGE2 in an in vitro equine inflammation model. *Vet Immunol Immunopathol,* 192**,** 33-40.

MASRI, F. A., XU, W., COMHAIR, S. A., ASOSINGH, K., KOO, M., VASANJI, A., DRAZBA, J., ANAND-APTE, B. & ERZURUM, S. C. 2007. Hyperproliferative apoptosis-resistant endothelial cells in idiopathic pulmonary arterial hypertension. *Am J Physiol Lung Cell Mol Physiol,* 293**,** L548-L554.

MILARA, J., GABARDA, E., JUAN, G., ORTIZ, J. L., GUIJARRO, R., MARTORELL, M., MORCILLO, E. J. & CORTIJO, J. 2012. Bosentan inhibits cigarette smoke-induced endothelin receptor expression in pulmonary arteries. *Eur Respir J,* 39**,** 927-938.

MILARA, J., ORTIZ, J. L., JUAN, G., GUIJARRO, R., ALMUDEVER, P., MARTORELL, M., MORCILLO, E. J. & CORTIJO, J. 2010. Cigarette smoke exposure up-regulates endothelin receptor B in human pulmonary artery endothelial cells: molecular and functional consequences. *Br J Pharmacol,* 161**,** 1599-1615.

MINCHENKO, A. & CARO, J. 2000. Regulation of endothelin-1 gene expression in human microvascular endothelial cells by hypoxia and cobalt: role of hypoxia responsive element. *Mol Cell Biochem,* 208**,** 53-62.

MORJARIA, J. B., MONDATI, E. & POLOSA, R. 2017. E-cigarettes in patients with COPD: current perspectives. *Int J Chron Obstruct Pulmon Dis,* 12**,** 3203-3210.

MURAKAMI, M., NAKASHIMA, K., KAMEI, D., MASUDA, S., ISHIKAWA, Y., ISHII, T., OHMIYA, Y., WATANABE, K. & KUDO, I. 2003. Cellular prostaglandin E2 production by membrane-bound prostaglandin E synthase-2 via both cyclooxygenases-1 and -2. *J Biol Chem,* 278**,** 37937-37947.

MYNAMPATI, B. K., SAMBHAV, K., GROVER, S. & CHALAM, K. V. 2017. Inhibition of proliferation of retinal vascular endothelial cells more effectively than choroidal vascular endothelial cell proliferation by bevacizumab. *Int J Ophthalmol,* 10**,** 15-22.

NAEIJE, R. & BARBERA, J. A. 2001. Pulmonary hypertension associated with COPD. *Crit Care,* 5**,** 286-289.

NANA-SINKAM, S. P., LEE, J. D., SOTTO-SANTIAGO, S., STEARMAN, R. S., KEITH, R. L., CHOUDHURY, Q., COOL, C., PARR, J., MOORE, M. D., BULL, T. M., VOELKEL, N. F. & GERACI, M. W. 2007. Prostacyclin prevents pulmonary endothelial cell apoptosis induced by cigarette smoke. *Am J Respir Crit Care Med,* 175**,** 676-685.

NATHAN, S. D., BARBERA, J. A., GAINE, S. P., HARARI, S., MARTINEZ, F. J., OLSCHEWSKI, H., OLSSON, K. M., PEACOCK, A. J., PEPKE-ZABA, J., PROVENCHER, S., WEISSMANN, N. & SEEGER, W. 2019. Pulmonary hypertension in chronic lung disease and hypoxia. *Eur Respir J,* 53**,** 1801914.

NEEDLEMAN, P., MONCADA, S., BUNTING, S., VANE, J. R., HAMBERG, M. & SAMUELSSON, B. 1976. Identification of an enzyme in platelet microsomes which generates thromboxane A2 from prostaglandin endoperoxides. *Nature,* 261**,** 558-560.

NEWBY, A. C., SOUTHGATE, K. M. & ASSENDER, J. W. 1992. Inhibition of vascular smooth muscle cell proliferation by endothelium-dependent vasodilators. *Herz,* 17**,** 291-299.

NOREL, X. 2007. Prostanoid receptors in the human vascular wall. *ScientificWorldJournal,* 7**,** 1359-1374.

OLSCHEWSKI, H., SIMONNEAU, G., GALIE, N., HIGENBOTTAM, T., NAEIJE, R., RUBIN, L. J., NIKKHO, S., SPEICH, R., HOEPER, M. M., BEHR, J., WINKLER, J., SITBON, O., POPOV, W., GHOFRANI, H. A., MANES, A., KIELY, D. G., EWERT, R., MEYER, A., CORRIS, P. A., DELCROIX, M., GOMEZ-SANCHEZ, M., SIEDENTOP, H., SEEGER, W. & AEROSOLIZED ILOPROST RANDOMIZED STUDY, G. 2002. Inhaled iloprost for severe pulmonary hypertension. *N Engl J Med,* 347**,** 322-329.

ONGENA, K., DAS, C., SMITH, J. L., GIL, S. & JOHNSTON, G. 2010. Determining cell number during cell culture using the Scepter cell counter. *J Vis Exp***,** 2204.

OPITZ, I. & ULRICH, S. 2018. Pulmonary hypertension in chronic obstructive pulmonary disease and emphysema patients: prevalence, therapeutic options and pulmonary circulatory effects of lung volume reduction surgery. *J Thorac Dis,* 10**,** S2763-S2774.

OSWALD-MAMMOSSER, M., APPRILL, M., BACHEZ, P., EHRHART, M. & WEITZENBLUM, E. 1991. Pulmonary hemodynamics in chronic obstructive pulmonary disease of the emphysematous type. *Respiration,* 58**,** 304-310.

PAK, O., ALDASHEV, A., WELSH, D. & PEACOCK, A. 2007. The effects of hypoxia on the cells of the pulmonary vasculature. *Eur Respir J,* 30**,** 364-372.

PATEL, J. A., SHEN, L., HALL, S. M., BENYAHIA, C., NOREL, X., MCANULTY, R. J., MOLEDINA, S., SILVERSTEIN, A. M., WHITTLE, B. J. & CLAPP, L. H. 2018. Prostanoid EP(2) Receptors Are Up-Regulated in Human Pulmonary Arterial Hypertension: A Key Anti-Proliferative Target for Treprostinil in Smooth Muscle Cells. *Int J Mol Sci,* 19**,** 2372.

PEINADO, V. I., BARBERA, J. A., RAMIREZ, J., GOMEZ, F. P., ROCA, J., JOVER, L., GIMFERRER, J. M. & RODRIGUEZ-ROISIN, R. 1998. Endothelial dysfunction in pulmonary arteries of patients with mild COPD. *Am J Physiol,* 274**,** L908-L913.

PEINADO, V. I., PIZARRO, S. & BARBERA, J. A. 2008. Pulmonary vascular involvement in COPD. *Chest,* 134**,** 808-814.

PEINADO, V. I., SANTOS, S., RAMIREZ, J., ROCA, J., RODRIGUEZ-ROISIN, R. & BARBERA, J. A. 2002. Response to hypoxia of pulmonary arteries in chronic obstructive pulmonary disease: an in vitro study. *Eur Respir J,* 20**,** 332-338.

PEREZ-GARIJO, A. 2018. When dying is not the end: Apoptotic caspases as drivers of proliferation. *Semin Cell Dev Biol,* 82**,** 86-95.

PEREZ-PADILLA, R., VOLLMER, W. M., VAZQUEZ-GARCIA, J. C., ENRIGHT, P. L., MENEZES, A. M. & BUIST, A. S. 2009. Can a normal peak expiratory flow

exclude severe chronic obstructive pulmonary disease? *Int J Tuberc Lung Dis,* 13**,** 387-393.

PICHL, A., SOMMER, N., BEDNORZ, M., SEIMETZ, M., HADZIC, S., KUHNERT, S., KRAUT, S., ROXLAU, E. T., KOJONAZAROV, B., WILHELM, J., GREDIC, M., GALL, H., TELLO, K., RICHTER, M. J., PAK, O., PETROVIC, A., HECKER, M., SCHERMULY, R. T., GRIMMINGER, F., SEEGER, W., GHOFRANI, H. A. & WEISSMANN, N. 2019. Riociguat for treatment of pulmonary hypertension in COPD - a translational study. *Eur Respir J,* 53**,** 1802445.

POLOSA, R., MORJARIA, J. B., CAPONNETTO, P., PROSPERINI, U., RUSSO, C., PENNISI, A. & BRUNO, C. M. 2016. Evidence for harm reduction in COPD smokers who switch to electronic cigarettes. *Respir Res,* 17**,** 166.

PORTER, K. M., KANG, B. Y., ADESINA, S. E., MURPHY, T. C., HART, C. M. & SUTLIFF, R. L. 2014. Chronic hypoxia promotes pulmonary artery endothelial cell proliferation through H2O2-induced 5-lipoxygenase. *PLoS One,* 9**,** e98532.

PROFIT, L. & CHRISP, P. 2007. Lumiracoxib: the evidence of its clinical impact on the treatment of osteoarthritis. *Core Evid,* 2**,** 131-150.

QUENT, V. M., LOESSNER, D., FRIIS, T., REICHERT, J. C. & HUTMACHER, D. W. 2010. Discrepancies between metabolic activity and DNA content as tool to assess cell proliferation in cancer research. *J Cell Mol Med,* 14**,** 1003-1013.

RAGHAVAN, A., ZHOU, G., ZHOU, Q., IBE, J. C., RAMCHANDRAN, R., YANG, Q., RACHERLA, H., RAYCHAUDHURI, P. & RAJ, J. U. 2012. Hypoxia-induced pulmonary arterial smooth muscle cell proliferation is controlled by forkhead box M1. *Am J Respir Cell Mol Biol,* 46**,** 431-436.

RAKOTONIAINA, Z., GUERARD, P., LIRUSSI, F., ROCHETTE, L., DUMAS, M., GOIRAND, F. & BARDOU, M. 2008. Celecoxib but not the combination of celecoxib+atorvastatin prevents the development of monocrotaline-induced pulmonary hypertension in the rat. *Naunyn Schmiedebergs Arch Pharmacol,* 378**,** 241-251.

RAMPERSAD, S. N. 2012. Multiple applications of Alamar Blue as an indicator of metabolic function and cellular health in cell viability bioassays. *Sensors (Basel),* 12**,** 12347-12360.

RIETEMA, H., HOLVERDA, S., BOGAARD, H. J., MARCUS, J. T., SMIT, H. J., WESTERHOF, N., POSTMUS, P. E., BOONSTRA, A. & VONK-NOORDEGRAAF, A. 2008. Sildenafil treatment in COPD does not affect stroke volume or exercise capacity. *Eur Respir J,* 31**,** 759-764.

ROBBINS, I. M., KAWUT, S. M., YUNG, D., REILLY, M. P., LLOYD, W., CUNNINGHAM, G., LOSCALZO, J., KIMMEL, S. E., CHRISTMAN, B. W. & BARST, R. J. 2006. A study of aspirin and clopidogrel in idiopathic pulmonary arterial hypertension. *Eur Respir J,* 27**,** 578-584.

RODRIGUEZ-ROISIN, R., RABE, K. F., VESTBO, J., VOGELMEIER, C., AGUSTI, A., ALL, P., CURRENT MEMBERS OF THE SCIENCE, C. & THE BOARD OF DIRECTORS OF, G. 2017. Global Initiative for Chronic Obstructive Lung Disease (GOLD) 20th Anniversary: a brief history of time. *Eur Respir J,* 50**,** 1700671.

ROMAGNA, G., ALLIFRANCHINI, E., BOCCHIETTO, E., TODESCHI, S., ESPOSITO, M. & FARSALINOS, K. E. 2013. Cytotoxicity evaluation of electronic cigarette vapor extract on cultured mammalian fibroblasts (ClearStream-LIFE): comparison with tobacco cigarette smoke extract. *Inhal Toxicol,* 25**,** 354-361.

RUAN, C.-H., DIXON, R. A. F., WILLERSON, J. T. & RUAN, K.-H. 2010. Prostacyclin Therapy for Pulmonary Arterial Hypertension. *Texas Heart Institute Journal,* 37**,** 391-399.

RUBIN, L. J. & BADESCH, D. B. 2005. Evaluation and management of the patient with pulmonary arterial hypertension. *Ann Intern Med,* 143**,** 282-292.

RUBIN, L. J., BADESCH, D. B., BARST, R. J., GALIE, N., BLACK, C. M., KEOGH, A., PULIDO, T., FROST, A., ROUX, S., LECONTE, I., LANDZBERG, M. & SIMONNEAU, G. 2002. Bosentan therapy for pulmonary arterial hypertension. *N Engl J Med,* 346**,** 896-903.

SAKAO, S., TARASEVICIENE-STEWART, L., LEE, J. D., WOOD, K., COOL, C. D. & VOELKEL, N. F. 2005. Initial apoptosis is followed by increased proliferation of apoptosis-resistant endothelial cells. *FASEB J,* 19**,** 1178-1180.

SAKAO, S., TATSUMI, K. & VOELKEL, N. F. 2010. Reversible or irreversible remodeling in pulmonary arterial hypertension. *Am J Respir Cell Mol Biol,* 43**,** 629-634.

SAKAO, S., VOELKEL, N. F. & TATSUMI, K. 2014. The vascular bed in COPD: pulmonary hypertension and pulmonary vascular alterations. *Eur Respir Rev,* 23**,** 350-355.

SANTOS, S., PEINADO, V. I., RAMIREZ, J., MELGOSA, T., ROCA, J., RODRIGUEZ-ROISIN, R. & BARBERA, J. A. 2002. Characterization of pulmonary vascular remodelling in smokers and patients with mild COPD. *Eur Respir J,* 19**,** 632-638.

SASAKI, Y., KAMIYAMA, S., KAMIYAMA, A., MATSUMOTO, K., AKATSU, M., NAKATANI, Y., KUWATA, H., ISHIKAWA, Y., ISHII, T., YOKOYAMA, C. & HARA, S. 2015. Genetic-deletion of Cyclooxygenase-2 Downstream Prostacyclin Synthase Suppresses Inflammatory Reactions but Facilitates Carcinogenesis, unlike Deletion of Microsomal Prostaglandin E Synthase-1. *Sci Rep,* 5**,** 17376.

SCHARF, S. M., IQBAL, M., KELLER, C., CRINER, G., LEE, S., FESSLER, H. E. & NATIONAL EMPHYSEMA TREATMENT TRIAL, G. 2002. Hemodynamic characterization of patients with severe emphysema. *Am J Respir Crit Care Med,* 166**,** 314-322.

SCHMEDTJE, J. F., JR., JI, Y. S., LIU, W. L., DUBOIS, R. N. & RUNGE, M. S. 1997. Hypoxia induces cyclooxygenase-2 via the NF-kappaB p65 transcription factor in human vascular endothelial cells. *J Biol Chem,* 272**,** 601-608.

SCOTT, A., LUGG, S. T., ALDRIDGE, K., LEWIS, K. E., BOWDEN, A., MAHIDA, R. Y., GRUDZINSKA, F. S., DOSANJH, D., PAREKH, D., FORONJY, R., SAPEY, E., NAIDU, B. & THICKETT, D. R. 2018. Pro-inflammatory effects of e-cigarette vapour condensate on human alveolar macrophages. *Thorax,* 73**,** 1161-1169.

SEBKHI, A., STRANGE, J. W., PHILLIPS, S. C., WHARTON, J. & WILKINS, M. R. 2003. Phosphodiesterase type 5 as a target for the treatment of hypoxia-induced pulmonary hypertension. *Circulation,* 107**,** 3230-3235.

SELIMOVIC, N., BERGH, C. H., ANDERSSON, B., SAKINIENE, E., CARLSTEN, H. & RUNDQVIST, B. 2009. Growth factors and interleukin-6 across the lung circulation in pulmonary hypertension. *Eur Respir J,* 34**,** 662-668.

SHENG, H., WILLIAMS, C. S., SHAO, J., LIANG, P., DUBOIS, R. N. & BEAUCHAMP, R. D. 1998. Induction of cyclooxygenase-2 by activated Ha-ras oncogene in Rat-1 fibroblasts and the role of mitogen-activated protein kinase pathway. *J Biol Chem,* 273**,** 22120-22127.

SHI, Z., CHEN, Y., PEI, Y., LONG, Y., LIU, C., CAO, J. & CHEN, P. 2017. The role of cyclooxygenase-2 in the protection against apoptosis in vascular endothelial cells induced by cigarette smoking. *J Thorac Dis,* 9**,** 30-41.

SHUJAAT, A., BAJWA, A. A. & CURY, J. D. 2012. Pulmonary Hypertension Secondary to COPD. *Pulm Med,* 2012**,** 203952.

SIEGEL, D. A., JATLAOUI, T. C., KOUMANS, E. H., KIERNAN, E. A., LAYER, M., CATES, J. E., KIMBALL, A., WEISSMAN, D. N., PETERSEN, E. E., REAGAN-STEINER, S., GODFRED-CATO, S., MOULIA, D., MORITZ, E., LEHNERT, J. D., MITCHKO, J., LONDON, J., ZAKI, S. R., KING, B. A., JONES, C. M., PATEL, A., DELMAN, D. M., KOPPAKA, R., LUNG INJURY RESPONSE CLINICAL WORKING, G. & LUNG INJURY RESPONSE EPIDEMIOLOGY/SURVEILLANCE, G. 2019. Update: Interim Guidance for Health Care Providers Evaluating and Caring for Patients with Suspected E-cigarette, or Vaping, Product Use Associated Lung Injury - United States, October 2019. *MMWR Morb Mortal Wkly Rep,* 68**,** 919-927.

SIMONNEAU, G. 2009. [A new clinical classification of pulmonary hypertension]. *Bull Acad Natl Med,* 193**,** 1897-1909.

SIMONNEAU, G., BARST, R. J., GALIE, N., NAEIJE, R., RICH, S., BOURGE, R. C., KEOGH, A., OUDIZ, R., FROST, A., BLACKBURN, S. D., CROW, J. W., RUBIN, L. J. & TREPROSTINIL STUDY, G. 2002. Continuous subcutaneous infusion of treprostinil, a prostacyclin analogue, in patients with pulmonary arterial hypertension: a double-blind, randomized, placebo-controlled trial. *Am J Respir Crit Care Med,* 165**,** 800-804.

SIMONNEAU, G., GALIE, N., RUBIN, L. J., LANGLEBEN, D., SEEGER, W., DOMENIGHETTI, G., GIBBS, S., LEBREC, D., SPEICH, R., BEGHETTI, M., RICH, S. & FISHMAN, A. 2004. Clinical classification of pulmonary hypertension. *J Am Coll Cardiol,* 43**,** 5S-12S.

SIMONNEAU, G., GATZOULIS, M. A., ADATIA, I., CELERMAJER, D., DENTON, C., GHOFRANI, A., GOMEZ SANCHEZ, M. A., KRISHNA KUMAR, R., LANDZBERG, M., MACHADO, R. F., OLSCHEWSKI, H., ROBBINS, I. M. & SOUZA, R. 2013. Updated clinical classification of pulmonary hypertension. *J Am Coll Cardiol,* 62**,** D34-D41.

SIMONNEAU, G., TORBICKI, A., HOEPER, M. M., DELCROIX, M., KARLOCAI, K., GALIE, N., DEGANO, B., BONDERMAN, D., KURZYNA, M., EFFICACE, M., GIORGINO, R. & LANG, I. M. 2012. Selexipag: an oral, selective

prostacyclin receptor agonist for the treatment of pulmonary arterial hypertension. *Eur Respir J,* 40**,** 874-880.

SITBON, O., DELCROIX, M., BERGOT, E., BOONSTRA, A. B., GRANTON, J., LANGLEBEN, D., SUBIAS, P. E., GALIE, N., PFISTER, T., LEMARIE, J. C. & SIMONNEAU, G. 2014. EPITOME-2: An open-label study assessing the transition to a new formulation of intravenous epoprostenol in patients with pulmonary arterial hypertension. *Am Heart J,* 167**,** 210-217.

SMITH, M. C. & WROBEL, J. P. 2014. Epidemiology and clinical impact of major comorbidities in patients with COPD. *Int J Chron Obstruct Pulmon Dis,* 9**,** 871-888.

SMITH, W. L., DEWITT, D. L. & GARAVITO, R. M. 2000. Cyclooxygenases: structural, cellular, and molecular biology. *Annu Rev Biochem,* 69**,** 145-182.

SOON, E., HOLMES, A. M., TREACY, C. M., DOUGHTY, N. J., SOUTHGATE, L., MACHADO, R. D., TREMBATH, R. C., JENNINGS, S., BARKER, L., NICKLIN, P., WALKER, C., BUDD, D. C., PEPKE-ZABA, J. & MORRELL, N. W. 2010. Elevated levels of inflammatory cytokines predict survival in idiopathic and familial pulmonary arterial hypertension. *Circulation,* 122**,** 920-927.

STEINER, M. K., SYRKINA, O. L., KOLLIPUTI, N., MARK, E. J., HALES, C. A. & WAXMAN, A. B. 2009. Interleukin-6 overexpression induces pulmonary hypertension. *Circ Res,* 104**,** 236-244.

STENMARK, K. R., FRID, M. G., GRAHAM, B. B. & TUDER, R. M. 2018. Dynamic and diverse changes in the functional properties of vascular smooth muscle cells in pulmonary hypertension. *Cardiovasc Res,* 114**,** 551-564.

STEWART, D. J., LEVY, R. D., CERNACEK, P. & LANGLEBEN, D. 1991. Increased plasma endothelin-1 in pulmonary hypertension: marker or mediator of disease? *Ann Intern Med,* 114**,** 464-469.

STOLZ, D., RASCH, H., LINKA, A., DI VALENTINO, M., MEYER, A., BRUTSCHE, M. & TAMM, M. 2008. A randomised, controlled trial of bosentan in severe COPD. *Eur Respir J,* 32**,** 619-628.

SU, Y., HAN, W., GIRALDO, C., DE LI, Y. & BLOCK, E. R. 1998. Effect of cigarette smoke extract on nitric oxide synthase in pulmonary artery endothelial cells. *Am J Respir Cell Mol Biol,* 19**,** 819-825.

SU, Y. C. & JIN, X. R. 1989. Relation of TXA2 and PGI2 to the difference in hypoxic pulmonary vasoconstriction between different strains of rats. *J Tongji Med Univ,* 9**,** 148-152.

SUBBARAMAIAH, K., TELANG, N., RAMONETTI, J. T., ARAKI, R., DEVITO, B., WEKSLER, B. B. & DANNENBERG, A. J. 1996. Transcription of cyclooxygenase-2 is enhanced in transformed mammary epithelial cells. *Cancer Res,* 56**,** 4424-4429.

SUZUKI, K., NISHI, K., TAKABUCHI, S., KAI, S., MATSUYAMA, T., KUROSAWA, S., ADACHI, T., MARUYAMA, T., FUKUDA, K. & HIROTA, K. 2013. Differential roles of prostaglandin E-type receptors in activation of hypoxia-inducible factor 1 by prostaglandin E1 in vascular-derived cells under non-hypoxic conditions. *PeerJ,* 1**,** e220.

SWAN, C. E. & BREYER, R. M. 2011. Prostaglandin E2 modulation of blood pressure homeostasis: studies in rodent models. *Prostaglandins Other Lipid Mediat,* 96**,** 10-13.

TAKEMOTO, M., SUN, J., HIROKI, J., SHIMOKAWA, H. & LIAO, J. K. 2002. Rho-kinase mediates hypoxia-induced downregulation of endothelial nitric oxide synthase. *Circulation,* 106**,** 57-62.

TAN, X., FENG, L., HUANG, X., YANG, Y., YANG, C. & GAO, Y. 2017. Histone deacetylase inhibitors promote eNOS expression in vascular smooth muscle cells and suppress hypoxia-induced cell growth. *J Cell Mol Med,* 21**,** 2022-2035.

TAN, X., POULOSE, E. M., RAVEENDRAN, V. V., ZHU, B. T., STECHSCHULTE, D. J. & DILEEPAN, K. N. 2011. Regulation of the expression of cyclooxygenases and production of prostaglandin I(2) and E(2) in human coronary artery endothelial cells by curcumin. *J Physiol Pharmacol,* 62**,** 21-28.

TARASEVICIENE-STEWART, L., KASAHARA, Y., ALGER, L., HIRTH, P., MC MAHON, G., WALTENBERGER, J., VOELKEL, N. F. & TUDER, R. M. 2001. Inhibition of the VEGF receptor 2 combined with chronic hypoxia causes cell death-dependent pulmonary endothelial cell proliferation and severe pulmonary hypertension. *FASEB J,* 15**,** 427-438.

TAYLOR, M., CARR, T., OKE, O., JAUNKY, T., BREHENY, D., LOWE, F. & GACA, M. 2016. E-cigarette aerosols induce lower oxidative stress in vitro when compared to tobacco smoke. *Toxicol Mech Methods,* 26**,** 465-476.

THABUT, G., DAURIAT, G., STERN, J. B., LOGEART, D., LEVY, A., MARRASH-CHAHLA, R. & MAL, H. 2005. Pulmonary hemodynamics in advanced COPD candidates for lung volume reduction surgery or lung transplantation. *Chest,* 127**,** 1531-1536.

TONELLI, A. R., HASERODT, S., AYTEKIN, M. & DWEIK, R. A. 2013. Nitric oxide deficiency in pulmonary hypertension: Pathobiology and implications for therapy. *Pulm Circ,* 3**,** 20-30.

TOUYZ, R. M., ALVES-LOPES, R., RIOS, F. J., CAMARGO, L. L., ANAGNOSTOPOULOU, A., ARNER, A. & MONTEZANO, A. C. 2018. Vascular smooth muscle contraction in hypertension. *Cardiovasc Res,* 114**,** 529-539.

TUDER, R. M., CHACON, M., ALGER, L., WANG, J., TARASEVICIENE-STEWART, L., KASAHARA, Y., COOL, C. D., BISHOP, A. E., GERACI, M., SEMENZA, G. L., YACOUB, M., POLAK, J. M. & VOELKEL, N. F. 2001. Expression of angiogenesis-related molecules in plexiform lesions in severe pulmonary hypertension: evidence for a process of disordered angiogenesis. *J Pathol,* 195**,** 367-374.

TUDER, R. M., COOL, C. D., GERACI, M. W., WANG, J., ABMAN, S. H., WRIGHT, L., BADESCH, D. & VOELKEL, N. F. 1999. Prostacyclin synthase expression is decreased in lungs from patients with severe pulmonary hypertension. *Am J Respir Crit Care Med,* 159**,** 1925-1932.

TUDER, R. M., FLOOK, B. E. & VOELKEL, N. F. 1995. Increased gene expression for VEGF and the VEGF receptors KDR/Flk and Flt in lungs exposed to acute or to chronic hypoxia. Modulation of gene expression by nitric oxide. *J Clin Invest,* 95**,** 1798-1807.

TUKLER HENRIKSSON, J., COURSEY, T. G., CORRY, D. B., DE PAIVA, C. S. & PFLUGFELDER, S. C. 2015. IL-13 Stimulates Proliferation and Expression of Mucin and Immunomodulatory Genes in Cultured Conjunctival Goblet Cells. *Invest Ophthalmol Vis Sci,* 56**,** 4186-4197.

UMAR, S. & VAN DER LAARSE, A. 2010. Nitric oxide and nitric oxide synthase isoforms in the normal, hypertrophic, and failing heart. *Mol Cell Biochem,* 333**,** 191-201.

VALERIO, G., BRACCIALE, P. & GRAZIA D'AGOSTINO, A. 2009. Effect of bosentan upon pulmonary hypertension in chronic obstructive pulmonary disease. *Ther Adv Respir Dis,* 3**,** 15-21.

VIEGI, G., PISTELLI, F., SHERRILL, D. L., MAIO, S., BALDACCI, S. & CARROZZI, L. 2007. Definition, epidemiology and natural history of COPD. *Eur Respir J,* 30**,** 993-1013.

VLACHOPOULOS, C., IOAKEIMIDIS, N., ABDELRASOUL, M., TERENTES-PRINTZIOS, D., GEORGAKOPOULOS, C., PIETRI, P., STEFANADIS, C. & TOUSOULIS, D. 2016. Electronic Cigarette Smoking Increases Aortic Stiffness and Blood Pressure in Young Smokers. *J Am Coll Cardiol,* 67**,** 2802-2803.

VOLPI, G., FACCHINETTI, F., MORETTO, N., CIVELLI, M. & PATACCHINI, R. 2011. Cigarette smoke and alpha,beta-unsaturated aldehydes elicit VEGF release through the p38 MAPK pathway in human airway smooth muscle cells and lung fibroblasts. *Br J Pharmacol,* 163**,** 649-661.

WALKER, J., UNDEM, C., YUN, X., LADE, J., JIANG, H. & SHIMODA, L. A. 2016. Role of Rho kinase and Na+/H+ exchange in hypoxia-induced pulmonary arterial smooth muscle cell proliferation and migration. *Physiol Rep,* 4**,** e12702.

WANG, C. G., LI, C., LEI, W., JIANG, J. H., HUANG, J. A. & ZENG, D. X. 2018. The association of neuron-derived orphan receptor 1 with pulmonary vascular remodeling in COPD patients. *Int J Chron Obstruct Pulmon Dis,* 13**,** 1177-1186.

WANG, J. R., ZHOU, Y., SANG, K. & LI, M. X. 2013. [Association between pulmonary vascular remodeling and expression of hypoxia-inducible factor-1alpha, endothelin-1 and inducible nitric oxide synthase in pulmonary vessels in neonatal rats with hypoxic pulmonary hypertension]. *Zhongguo Dang Dai Er Ke Za Zhi,* 15**,** 138-144.

WEITZENBLUM, E., CHAOUAT, A. & KESSLER, R. 2013. Pulmonary hypertension in chronic obstructive pulmonary disease. *Pneumonol Alergol Pol,* 81**,** 390-398.

WEITZENBLUM, E., HIRTH, C., DUCOLONE, A., MIRHOM, R., RASAHOLINJANAHARY, J. & EHRHART, M. 1981. Prognostic value of pulmonary artery pressure in chronic obstructive pulmonary disease. *Thorax,* 36**,** 752-758.

WEITZENBLUM, E., SAUTEGEAU, A., EHRHART, M., MAMMOSSER, M., HIRTH, C. & ROEGEL, E. 1984. Long-term course of pulmonary arterial pressure in chronic obstructive pulmonary disease. *Am Rev Respir Dis,* 130**,** 993-998.

WILSON, S. J., ROCHE, A. M., KOSTETSKAIA, E. & SMYTH, E. M. 2004. Dimerization of the human receptors for prostacyclin and thromboxane facilitates thromboxane receptor-mediated cAMP generation. *J Biol Chem,* 279**,** 53036-53047.

WOO, M., HAKEM, R., SOENGAS, M. S., DUNCAN, G. S., SHAHINIAN, A., KAGI, D., HAKEM, A., MCCURRACH, M., KHOO, W., KAUFMAN, S. A., SENALDI, G., HOWARD, T., LOWE, S. W. & MAK, T. W. 1998. Essential contribution of caspase 3/CPP32 to apoptosis and its associated nuclear changes. *Genes Dev,* 12**,** 806-819.

WORT, S. J., WOODS, M., WARNER, T. D., EVANS, T. W. & MITCHELL, J. A. 2002. Cyclooxygenase-2 acts as an endogenous brake on endothelin-1 release by human pulmonary artery smooth muscle cells: implications for pulmonary hypertension. *Mol Pharmacol,* 62**,** 1147-1153.

WRIGHT, J. L. & CHURG, A. 1991. Effect of long-term cigarette smoke exposure on pulmonary vascular structure and function in the guinea pig. *Exp Lung Res,* 17**,** 997-1009.

WRIGHT, J. L., LAWSON, L., PARE, P. D., HOOPER, R. O., PERETZ, D. I., NELEMS, J. M., SCHULZER, M. & HOGG, J. C. 1983. The structure and function of the pulmonary vasculature in mild chronic obstructive pulmonary disease. The effect of oxygen and exercise. *Am Rev Respir Dis,* 128**,** 702-707.

WRIGHT, J. L., LEVY, R. D. & CHURG, A. 2005. Pulmonary hypertension in chronic obstructive pulmonary disease: current theories of pathogenesis and their implications for treatment. *Thorax,* 60**,** 605-609.

WRIGHT, J. L., PETTY, T. & THURLBECK, W. M. 1992. Analysis of the structure of the muscular pulmonary arteries in patients with pulmonary hypertension and COPD: National Institutes of Health nocturnal oxygen therapy trial. *Lung,* 170**,** 109-124.

WRIGHT, J. L., TAI, H. & CHURG, A. 2006. Vasoactive mediators and pulmonary hypertension after cigarette smoke exposure in the guinea pig. *J Appl Physiol (1985),* 100**,** 672-678.

WU, K. K. & LIOU, J. Y. 2005. Cellular and molecular biology of prostacyclin synthase. *Biochem Biophys Res Commun,* 338**,** 45-52.

XIANG, M., XU, Y. J., LIU, X. S. & ZENG, D. X. 2010. Cigarette smoke extract promotes human pulmonary artery smooth muscle cells proliferation through protein kinase C alpha-dependent induction of cyclin D1. *Chin Med J (Engl),* 123**,** 3663-3670.

XIE, L., DAI, Z., PANG, C., LIN, D. & ZHENG, M. 2018. Cellular glucose metabolism is essential for the reduction of cell-impermeable water-soluble tetrazolium (WST) dyes. *Int J Biol Sci,* 14**,** 1535-1544.

XING, A. P., DU, Y. C., HU, X. Y., XU, J. Y., ZHANG, H. P., LI, Y. & NIE, X. 2012. Cigarette smoke extract stimulates rat pulmonary artery smooth muscle cell proliferation via PKC-PDGFB signaling. *J Biomed Biotechnol,* 2012**,** 534384.

XIONG, P. Y., POTUS, F., CHAN, W. & ARCHER, S. L. 2018. Models and Molecular Mechanisms of World Health Organization Group 2 to 4 Pulmonary Hypertension. *Hypertension,* 71**,** 34-55.

YANAGISAWA, M., KURIHARA, H., KIMURA, S., TOMOBE, Y., KOBAYASHI, M., MITSUI, Y., YAZAKI, Y., GOTO, K. & MASAKI, T. 1988. A novel potent vasoconstrictor peptide produced by vascular endothelial cells. *Nature,* 332**,** 411-415.

YANG, G. & CHEN, L. 2016. An Update of Microsomal Prostaglandin E Synthase-1 and PGE2 Receptors in Cardiovascular Health and Diseases. *Oxid Med Cell Longev,* 2016**,** 5249086.

YANG, X., SHEARES, K. K., DAVIE, N., UPTON, P. D., TAYLOR, G. W., HORSLEY, J., WHARTON, J. & MORRELL, N. W. 2002. Hypoxic induction of cox-2 regulates proliferation of human pulmonary artery smooth muscle cells. *Am J Respir Cell Mol Biol,* 27**,** 688-696.

YERLY, P., PRELLA, M. & AUBERT, J. D. 2016. Current management of pulmonary arterial hypertension. *Swiss Med Wkly,* 146**,** w14305.

YIN, J., XIA, W., LI, Y., GUO, C., ZHANG, Y., HUANG, S., JIA, Z. & ZHANG, A. 2017. COX-2 mediates PM2.5-induced apoptosis and inflammation in vascular endothelial cells. *Am J Transl Res,* 9**,** 3967-3976.

YIN, J., XIA, W., ZHANG, Y., DING, G., CHEN, L., YANG, G., HUANG, S., JIA, Z. & ZHANG, A. 2018. Role of dihydroartemisinin in regulating prostaglandin E2 synthesis cascade and inflammation in endothelial cells. *Heart Vessels,* 33**,** 1411-1422.

YIN, L. M., WEI, Y., WANG, W. Q., WANG, Y., XU, Y. D. & YANG, Y. Q. 2014. Simultaneous application of BrdU and WST-1 measurements for detection of the proliferation and viability of airway smooth muscle cells. *Biol Res,* 47**,** 75.

YIN, L. M., WEI, Y., WANG, Y., XU, Y. D. & YANG, Y. Q. 2013. Long term and standard incubations of WST-1 reagent reflect the same inhibitory trend of cell viability in rat airway smooth muscle cells. *Int J Med Sci,* 10**,** 68-72.

YU, L. & HALES, C. A. 2011. Hypoxia does neither stimulate pulmonary artery endothelial cell proliferation in mice and rats with pulmonary hypertension and vascular remodeling nor in human pulmonary artery endothelial cells. *J Vasc Res,* 48**,** 465-475.

ZAKYNTHINOS, E., DANIIL, Z., PAPANIKOLAOU, J. & MAKRIS, D. 2011. Pulmonary hypertension in COPD: pathophysiology and therapeutic targets. *Curr Drug Targets,* 12**,** 501-513.

ZHANG, J., NARAYAN, V. M., JUEDES, N. & PATEL, J. M. 2009. Hypoxic upregulation of preproendothelin-1 gene expression is associated with protein tyrosine kinase-PI3K signaling in cultured lung vascular endothelial cells. *Int J Clin Exp Med,* 2**,** 87-94.

ZHANG, L., YAN, J., LIU, Y., ZHAO, Q., DI, C., CHAO, S., JIE, L., LIU, Y. & ZHANG, H. 2017. Contribution of caspase-independent pathway to apoptosis in malignant glioma induced by carbon ion beams. *Oncol Rep,* 37**,** 2994-3000.

ZHANG, S., LIU, B., FAN, Z., WANG, D., LIU, Y., LI, J., WANG, N., LIU, Y. & ZHANG, B. 2016. Targeted inhibition of survivin with YM155 promotes apoptosis of hypoxic human pulmonary arterial smooth muscle cells via the upregulation of voltage-dependent K(+) channels. *Mol Med Rep,* 13**,** 3415-3422.

ZHAO, L., MASON, N. A., MORRELL, N. W., KOJONAZAROV, B., SADYKOV, A., MARIPOV, A., MIRRAKHIMOV, M. M., ALDASHEV, A. & WILKINS, M. R. 2001. Sildenafil inhibits hypoxia-induced pulmonary hypertension. *Circulation,* 104**,** 424-428.

ZHAO, L., WU, Y., XU, Z., WANG, H., ZHAO, Z., LI, Y., YANG, P. & WEI, X. 2012. Involvement of COX-2/PGE2 signalling in hypoxia-induced angiogenic response in endothelial cells. *J Cell Mol Med,* 16**,** 1840-1855.

ZHOU, D. & SPECTOR, S. A. 2008. Human immunodeficiency virus type-1 infection inhibits autophagy. *AIDS,* 22**,** 695-699.